Yucca Mtn
Ground Motion Data Package

Vol. 1

2/97

9809180100 980911
PDR WASTE
WM-11 PDR

- Part 2

Yucca Mtn
Ground Motion Data Package

Vol. 1

2/97

Table of Contents

Ground Motion Data Package

Section 1 : Introduction

1.1 Schedule and Required Estimates 1.1-1

1.2 Distances for 16 cases 1.2-1

1.3 Site Velocity Profile 1.3-1

1.4 Yucca Mtn Velocities 1.4-1

Section 2: Ground Motion Models - General Information

2.1 Available Proponent Models 2.1-1

2.2 Summary of Available Ground Motion Models 2.2-1

2.3 Summary of Available Proponent Models for Adjustments 2.3-1

Section 3: Finite Fault Numerical Simulation for YM_{300}

3.1 Somerville (16 YM cases) 3.1-1

3.1.1 Documentation 3.1.1-1

3.1.2 Tabulated Results: Horizontal component 3.1.2-1

3.1.3 Tabulated Results : Vertical component 3.1.3-1

3.1.4 Plots of horizontal results 3.1.4-1

3.2 Silva (scenario earthquake exercises) 3.2.-1

3.3 Silva (41 YM cases) 3.3

3.3.1 Tabulated Results: Horizontal component 3.3.1-1

3.3.2 Modeling Uncertainty for Silva Finite Fault Simulations 3.3.2-1

3.4 Anderson & Zeng (16 YM cases) 3.4

3.4.1 Revised Synthetics for Yucca Mountain Earthquake Scenarios 3.4.1-1

3.4.2 Tabulated Results: Horizontal component 3.4.2-1

3.4.3 Tabulated Results: Vertical component 3.4.3-1

Section 4: Empirical Models

4.1 Additional Documentation 4.1-1

4.1.1 Abrahamson & Silva update for normal faulting 4.1.1-1

4.1.2 Boore et al. 1993 Horizontal Component Variability 4.1.2-1

4.1.3 Idriss 1997 update 4.1.3-1

4.1.4 McGarr (1984) Estimates 4.1.4-4

4.2 Electronic versions

*electronic file

4.2.1 Fortran code x
4.2.2 Excel spread sheets x
4.3 Plots For Empirical Models (w/o adjustments) 4.3-1

Section 5: Blast Experience Models
5.1 Model Names 5.1-1
5.2 Model Description 5.2-1
5.3 Excerpt from "Prediction of Ground Motion Characteristics of Underground Nuclear Detonations 5.3-1

Section 6: Hybrid Empirical (Campbell)
6.1 Spreadsheet Documentation 6.1-1

Section 7: Stochastic Point Source (Silva)
7.1 Regression Model 7.1-1
7.2 Uncertainties 7.2-1
7.3 Stress Drop scaling 7.3-1

Section 8: Proponent Conversions
8.1 YM_{300} / $YM_{surface}$ 8.1.1-1
8.1.1 Silva 8.1.1-1
8.2 $YM_{surface}$ / $CA_{surface}$ (w/o stress drop) 8.2.1-1
8.2.1 Silva point source stochastic model 8.2.1-1
8.3 YM_{300} / $CA_{surface}$ 8.3-1
8.3.1 Silva 8.3.1-1
8.3.2 Campbell 8.3.2-1
8.3.3 Comparison of Silva and Campbell models 8.3.3-1
8.4 $YM_{surface}$ / $CA_{surface}$ (stress drop only) 8.4-1
8.4.1 Silva point source 8.4.1-1
8.4.2 Campbell 8.4.2-1
8.4.3 Spudich Adjustment Factors 8.4.3-1
8.4.4 Comparison of models 8.4.4-1
8.5 Vertical-to-Horizontal Regression Results 8.5.1-1
8.6 PGA-PGV Regression Results 8.6.1-1

Section 9: Stress-drops for Normal Faulting Events

*electronic file

9.1 Updated stress-drop information 9.1-1

Section 10.1 Lucerne Recording
10.1.1 WCC processing of Lucerne x
10.1.2 PGE report on Lucerne x

Section 11: Precarious Rocks
11.1 Data on Precarious Rocks 11.1-1
11.2 Regression analysis for normal faulting using precarious rock constraints x

Section 12: Somerville Simulation Methodology

Section 13: Silva Simulation Methodology
13.1 Point source 13.1
13.1.1 Stochastic Ground Motion Model Descriptions 13.1.1-1
13.1.2 Model Validation 13.1.2-1
13.2 Finite fault

*electronic file

Section 1:

Introduction

1.1 Schedule and Required Estimates

Woodward-Clyde **Memorandum**

To: Ground Motion Experts

From: Norm Abrahamson
Ann Becker

Office: SLC

Date: February 25, 1997

Subject: Point Estimate Points

To avoid confusion, the following summarizes the data and due dates for your point estimates for the Yucca Mountain ground motion project. The Magnitude-Distance pairs for each submittal are summarized on the attached tables. At the interim meeting there was discussion of eliminating 1 Hz considering that 0.33 Hz had been included (May 2 deliverable). Although the 1 Hz values are still required at this time, their elimination is being negotiated.

Date	Components	Frequencies	M-D Pairs
March 7	Horiz	0.5, 20 Hz	16 Sets
March 14	Horiz, Vert	0.5, 5, 20 Hz pgv	16 Sets
May 2	Horiz, Vert	0.33, 0.5, 1, 2, 5, 10, 20 Hz pga, pgv	28 Sets

The elicitations will be on the information provided in the March 14 submittal. The elicitation schedule is: Anderson: Wed 3/19, 8 am - 12 noon
Boore: Thurs 3/20, 8 am - 12 noon
Campbell: Tues 3/18, 8 am - 12 noon
McGarr: Wed 3/19, 1 pm - 5 pm
Silva: Mon 3/17, 10 am - mid/late afternoon
Somerville: Thurs 3/20, 1 pm - 5 pm
Walck: Tues 3/18, 1 pm - 5 pm

A Campbell code to compute scale factors using his hybrid empirical model is available through ftp at: users.aol.com (anonymous user login), then cd to eqecolo, then cd to campbell. Ftp kwcy.exe, run it, and it unpacks into several files including a fortran code.

Data still pending are:	Probable delivery date
Silva finite fault runs (300 m velocity)	3/3
Anderson finite fault runs (300 m velocity)	3/3
Brune precarious rock constraints	3/3
Silva point source vertical	2/27
Revised data package (the 'Interim Meeting package'; revised as of 2/26)	2/27

C:\TEXTS\YUCCA\INTERIM\MEMO3.DOC\25-Feb-97

16 M-D Pairs, Due March 7

Distance[1]	Deep Focus[2]		Shallow Focus[2]					
(km)	M5.0	5.8	5.0	5.8	6.5	7.0	7.5	8.0
1			SS, HW		SS, HW, FW			
3								
5	SS, HW				HW, FW			
10		SS				SS		
20		HW						
50					SS, HW		SS, HW	
100								
160								

[1] Horizontal distance from surface expression of fault (up-dip extension).

[2] See handout from interim meeting for definition of Shallow and Deep foci. Shallow focus is centered at 5 km depth (and cannot extend into air). Bottom of deep focus rupture is at 14 km depth. Rupture width from Wells and Coppersmith (1994), 'all mechanisms'.

Deliverables are

- **values of μ, σ, σ_μ, σ_σ**
- **horizontal component only**
- **strike slip faulting ('SS') and/or normal faulting (hanging wall denoted 'HW', foot wall denoted 'FW'), as shown**
- **0.5 and 20 Hz**

16 M-D Pairs, Due March 14

Distance[1]	Deep Focus[2]		Shallow Focus[2]					
(km)	M5.0	5.8	5.0	5.8	6.5	7.0	7.5	8.0
1			SS, HW		SS, HW, FW			
3								
5	SS, HW				HW, FW			
10		SS				SS		
20		HW						
50					SS, HW		SS, HW	
100								
160								

[1] Horizontal distance from surface expression of fault (up-dip extension).

[2] See handout from interim meeting for definition of Shallow and Deep foci. Shallow focus is centered at 5 km depth (and cannot extend into air). Bottom of deep focus rupture is at 14 km depth. Rupture width from Wells and Coppersmith (1994), 'all mechanisms'.

Deliverables are

- **values of μ, σ, σ_μ, σ_σ**
- **horizontal and vertical components**
- **strike slip faulting ('SS') and/or normal faulting (hanging wall denoted 'HW', foot wall denoted 'FW'), as shown**
- **0.5, 5, 20 Hz, pgv**

1.1-3

28 M-D Pairs, Due May 2

Distance[1]	Deep Focus[2]		Shallow Focus[2]					
(km)	M5.0	5.8	5.0	5.8	6.5	7.0	7.5	8.0
1	SS		SS, HW	SS	SS, HW, FW	SS	SS	
3								
5	SS, HW	HW,FW		HW, FW	SS, HW, FW			
10		SS	SS, HW	SS, HW, FW	SS, HW, FW	SS, HW, FW	SS, HW	
20		HW			SS, HW, FW			
50			SS, HW	S, HW	SS, HW	SS, HW	SS, HW	SS
100					SS			
160			SS		SS			SS

[1] Horizontal distance from surface expression of fault (up-dip extension).

[2] See handout from interim meeting for definition of Shallow and Deep foci. Shallow focus is centered at 5 km depth (and cannot extend into air). Bottom of deep focus rupture is at 14 km depth. Rupture width from Wells and Coppersmith (1994), 'all mechanisms'.

Deliverables are

- **values of μ, σ, σ_μ, σ_σ**
- **horizontal and vertical components**
- **strike slip faulting ('SS') and/or normal faulting (hanging wall denoted 'HW', foot wall denoted 'FW'), as shown**
- **0.33, 0.5, 1, 2, 5, 10, 20 Hz, pga, pgv**

1.2 Geometries for 16 Preliminary Cases

Subset for Preliminary Analysis
(16 cases)

Case	M	depth	x*	SS	R_{rup}	R_{JB}	R_{seis}
1	5.0	shallow**	1	SS	3.2	1.0	3.2
2	5.0	shallow	1	HW	3.4	.9	3.4
3	5.0	deep***	5	SS	11.3	5.0	11.3
4	5.0	deep	5	HW	10.7	1.1	10.7
5	5.8	deep	10	SS	12.2	10.0	12.2
6	5.8	deep	20	HW	17.3	11.9	17.3
7	6.5	shallow	1	SS	1.0	1.0	3.2
8	6.5	shallow	1	HW	.9	0.0	3.1
9	6.5	shallow	-1	FW	1.0	1.0	4.1
10	6.5	shallow	5	HW	4.3	0.0	4.4
11	6.5	shallow	-5	FW	5.0	5.0	7.4
12	6.5	shallow	50	SS	50.0	50.0	50.1
13	6.5	shallow	50	HW	44.1	45.3	45.3
14	7.0	shallow	10	SS	10.0	10.0	10.4
15	7.5	shallow	50	SS	50.0	50.0	50.1
16	7.5	shallow	50	HW	44.2	41.9	44.2

*x = horizontal distance (km) from surface trace of "fault"

** centered at a depth of 5 km

*** bottom edge of rupture at 14 km depth

1.3 Site Velocity Profile

The site velocity profile is the profile used in the scenario earthquake study, with the top 300m removed. This is the "repository outcrop" velocity profile. The ground motion estimated for this profile will be referred to as "YM_{300}".

The kappa used for this site is based on removing the kappa from the top 300m. Using a reference kappa of 0.02 sec with the low strain damping estimated by Stoke, the kappa in the top 300 m is 0.0014 sec. The resulting kappa for this model is then 0.0186 sec.

Site Velocity Profile							
Layer #	Depth to top (km)	Thickness (km)	V_s (km/s)	V_p (km/s)	Density (g/cm^3)	Q_s	Q_p
1	0	.70	1.9	3.2	2.4	70	150
2	.70	.60	2.1	3.6	2.4	100	200
3	1.3	1.50	2.9	5.0	2.5	150	300
4	2.8	2.20	3.4	5.8	2.7	400	800
5	5.0	10.70	3.5	6.2	2.75	400	800
6	15.7	16.00	3.8	6.5	2.9	400	800
7	31.7	---	4.6	7.8	3.3	400	800

Mar 17

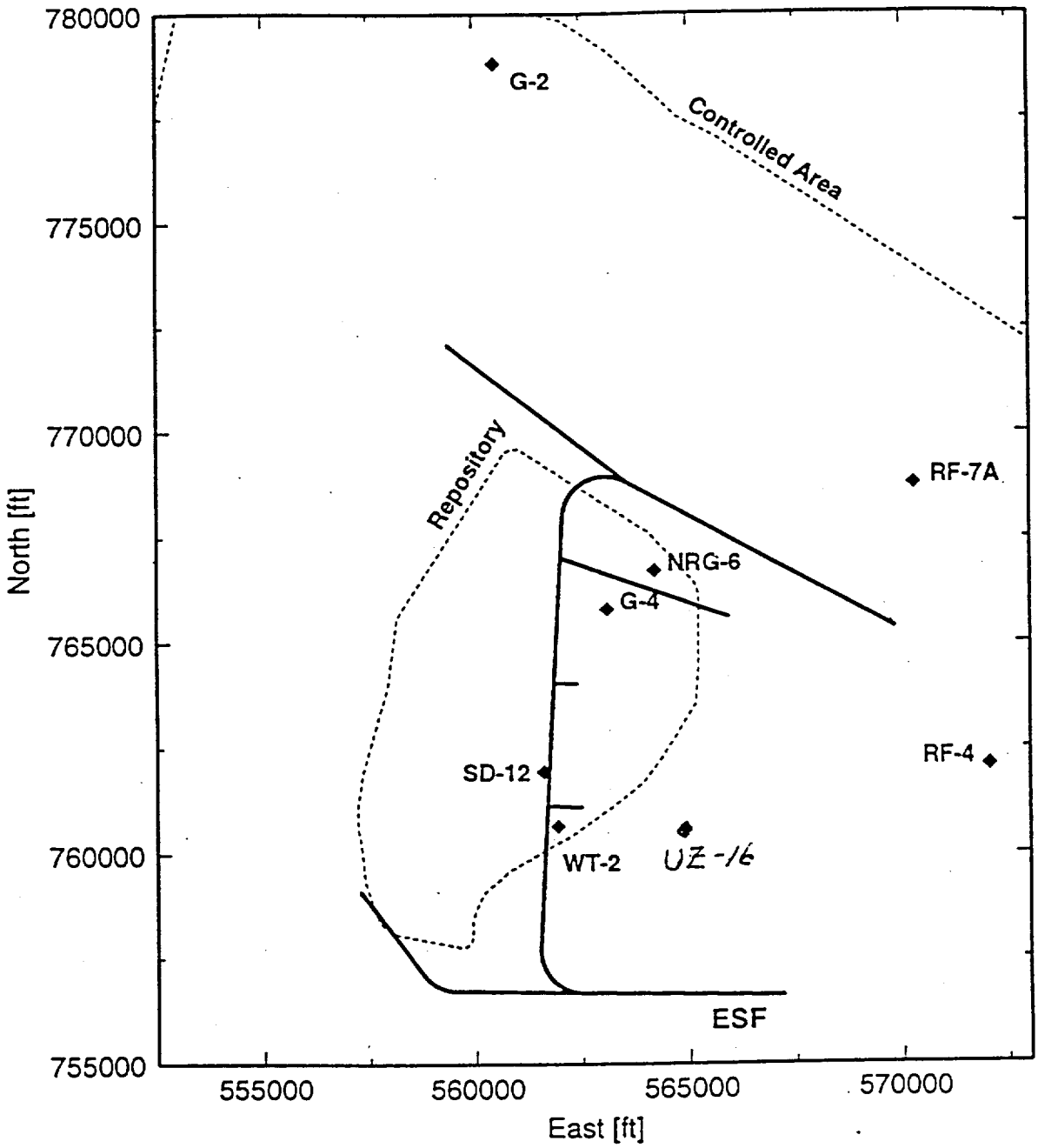

Figure V1. Location of new VSP surveys in wells: RF-4, RF-7A, SD-12, G-2, and G-4. Previous wells with VSP are WT-2 and NRG-6. Coordinates are Nevada State Plane.

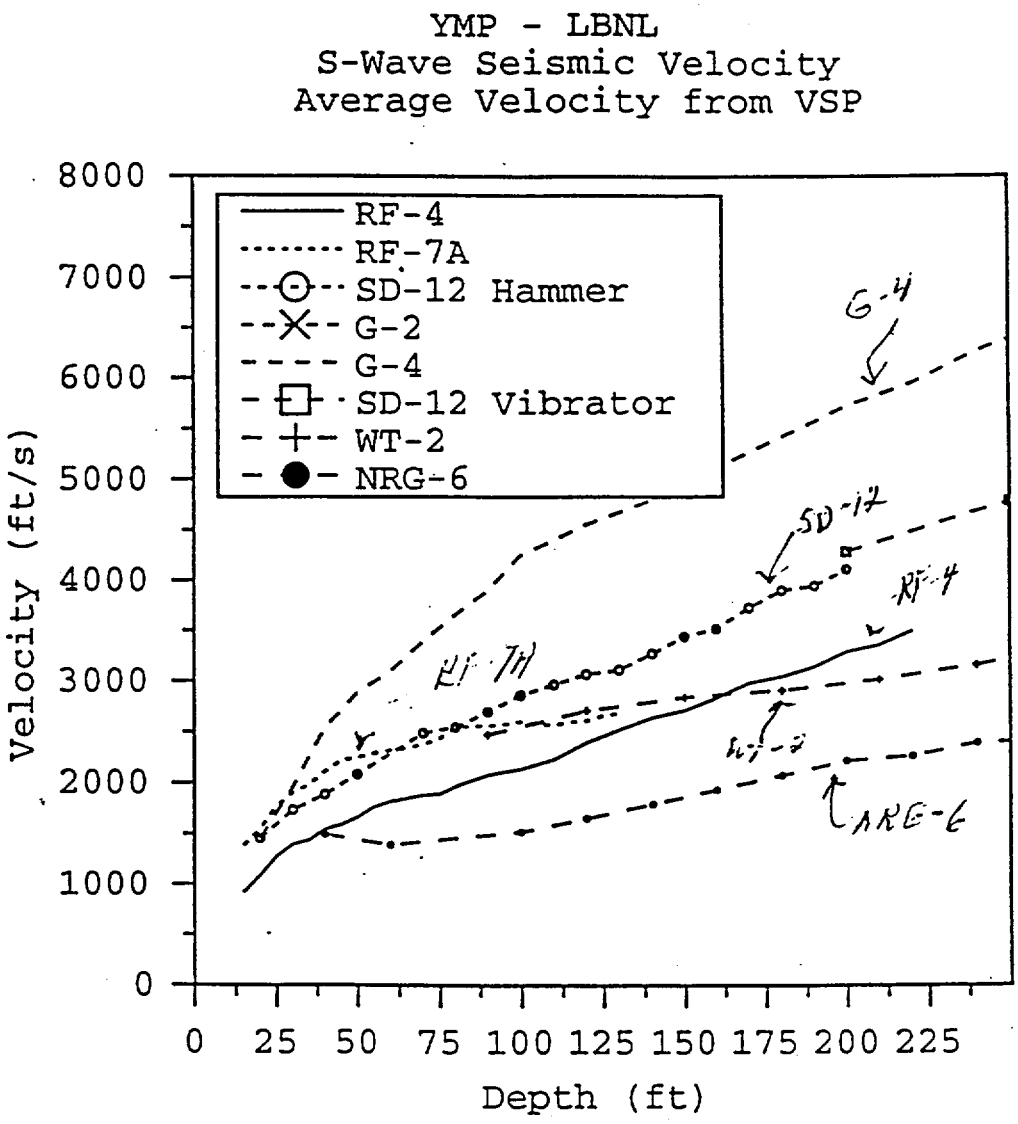

Figure V48. Shallow (0 -200 ft.) average S-wave velocity for all wells surveyed by LBNL. Note that the same geologic formations are not at the same depths in each well.

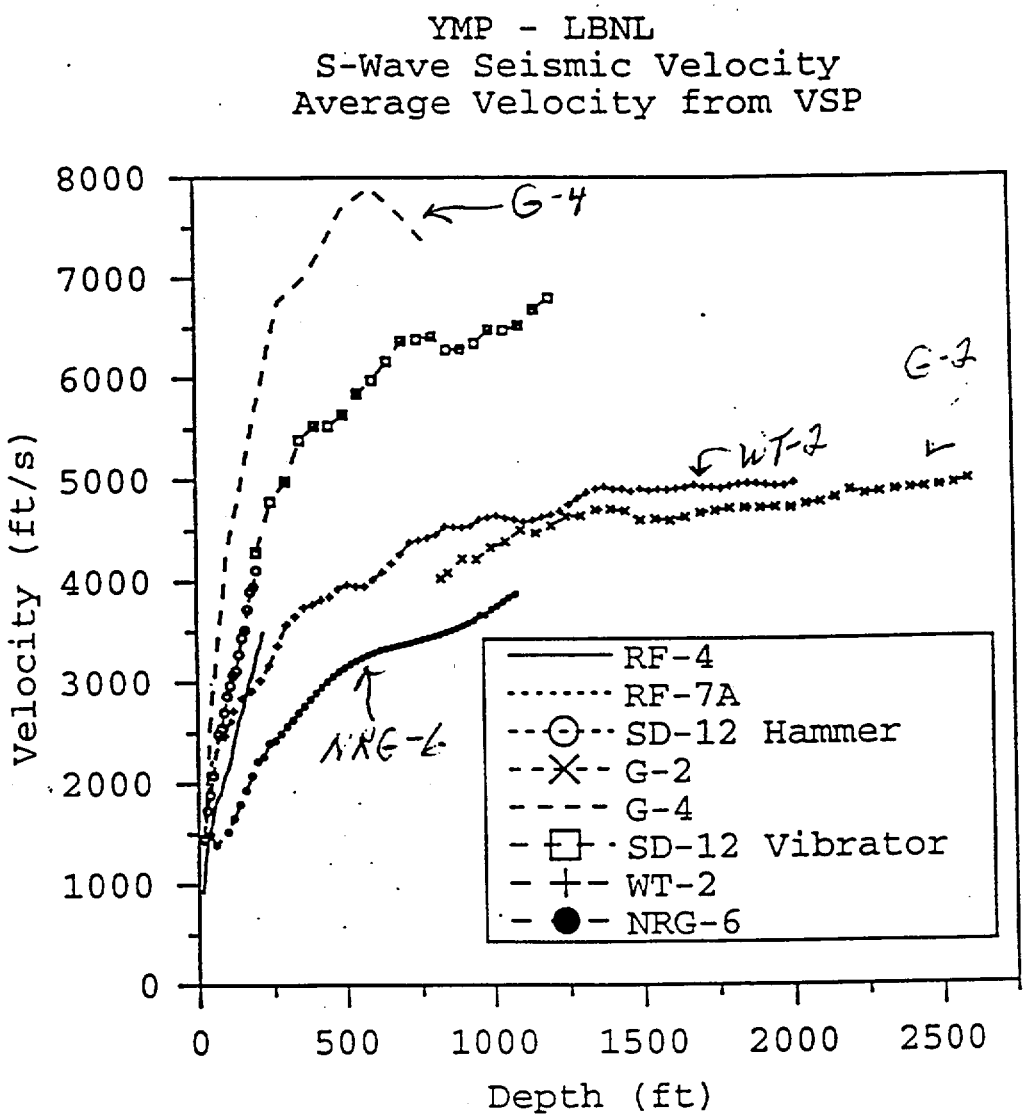

Figure V51. Deep (0-2750 ft.) average S-wave velocity for all wells surveyed by LBNL. Note that the same geologic formations are not at the same depths in each well.

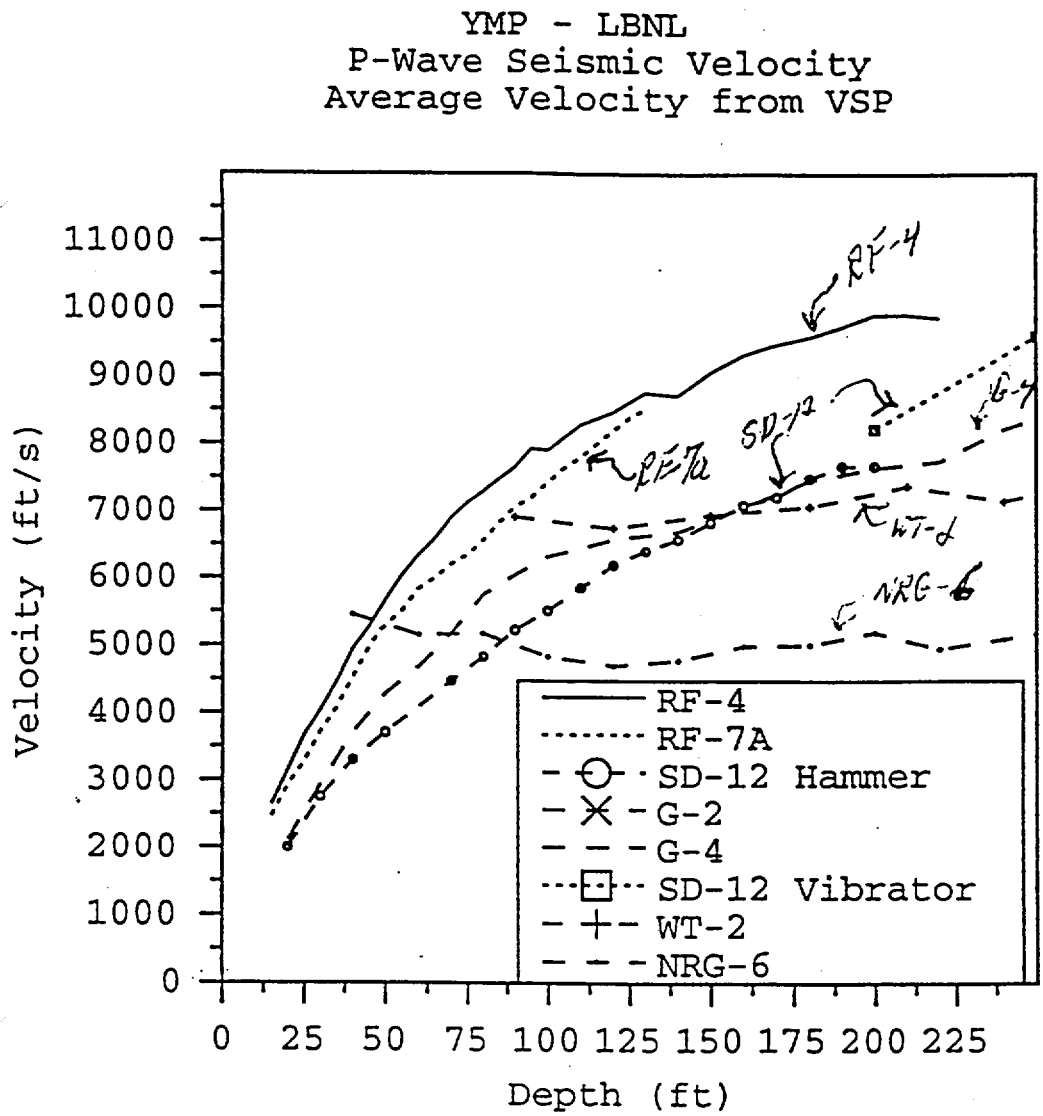

Figure V47. Shallow (0 -200 ft.) average P-wave velocity for all wells surveyed by LBNL. Note that the same geologic formations are not at the same depths in each well.

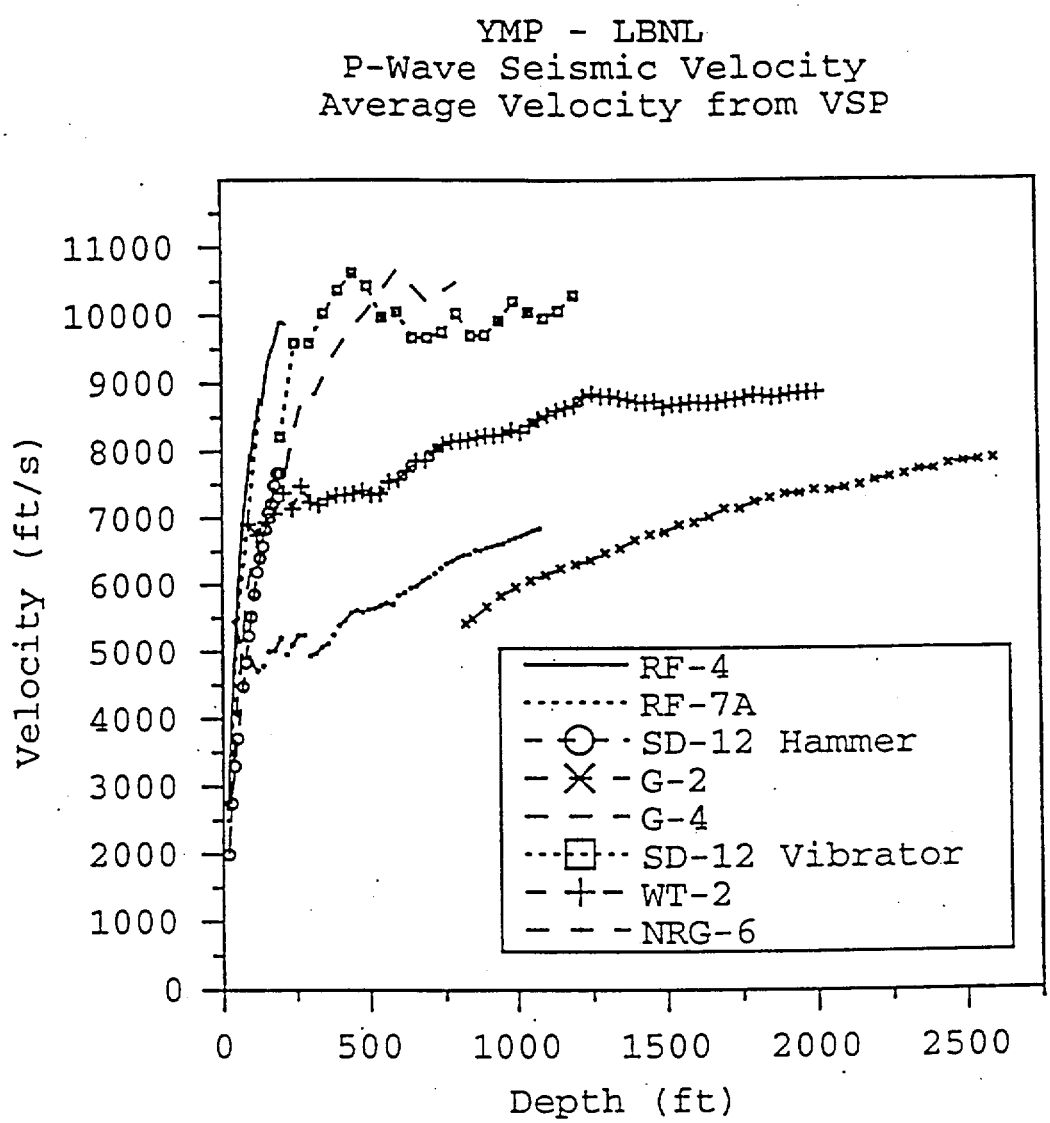

Figure V50. Deep (0-2750 ft.) average P-wave velocity for all wells surveyed by LBNL. Note that the same geologic formations are not at the same depths in each well.

Section 2:

Ground Motion Models - General Information

1. Empirical Models: These models and frequencies are provided in program yucatten

Modeler	Components Available[1]	PGV Available?	Frequencies Available[2]	Spudich Adjustment Available?
Abrahamson & Silva '97 (rock)	H, Z	No	0.33, 0.5, 1., 2., 5., 10., 20., pga	No
Boore, Joyner, Fumal '97 (V_s)	H	No	0.5, 1., 2., 5., 10., pga	Yes
Boore, Joyner, Fumal '94 (class A)	H	No	0.5, 1., 2., 5., 10., pga	No
Boore, Joyner, Fumal '94 (class B)	H	No	0.5, 1., 2., 5., 10., pga	No
Campbell '97 (soft rock)	H, Z	Yes	0.33, 0.5, 1., 2., 5., 10., 20., pga	No
Campbell '97 (hard rock)	H, Z	Yes	0.33, 0.5, 1., 2., 5., 10., 20., pga	No
Campbell '93-'94[3] (hard rock)	H	No	0.5, 1., 2., 5., 10., 20., pga	Yes
Campbell '90-'94[3] (soft rock)	H, Z[4]	No	0.5, 1., 2., 5., 10., 20., pga	Yes
Campbell '90[3] (soil/soft rock)	H, Z	No	0.5, 1., 2., 5., 10., 20., pga	Yes
Idriss '93[5] (rock/stiff soil)	H	No	0.33, 0.5, 1., 2., 5., 10., 20., pga	Yes
Idriss '97	H	No	pga	No
Joyner-Boore '88 (rock)	H	Yes	None (used for pgv only)	Yes
Sadigh et al. '97 (rock)	H, Z	No	0.33, 0.5, 1., 2., 5., 10., 20., pga	Yes
Sabetta and Pugliese '96 (rock)	H, Z	Yes	0.33, 0.5, 1., 2., 5., 10., pga	Yes
Spudich et al. '96 (rock)	H	No	0.5, 1., 2., 5., 10., pga	N/A
McGarr 84 (rock) (see page 4.1.4-1)	H	Yes	PGV only	No

Notes for Table 1.

[1] H indicates available for horizontal component, Z indicates available for vertical component

[2] Required frequencies are 0.33, 0.5, 1, 2, 5, 10 and 20 Hz

[3] Older Campbell models included because Spudich et al. provided correction factors

[4] Vertical motions provided in Campbell (1990), rock conditions, with no discrimination between hard or soft rock

[5] Idriss '93 is identical to Idriss '91

2. Numerical Models

Modeler	Components Available[1]	PGV Available?	Frequencies Available[2]	Cases Run
Anderson	H, Z	Yes	0.3[3], 0.5, 1, 2, 5, 10, 20, pga	16 (Preliminary Cases 1-16)
Silva Finite Fault	H	Yes	0.3[3], 0.5, 1, 2, 5, 10, 20, pga	41 (All Final Cases with M≥5.8)
Silva Point Source	H, Z	Yes	0.33, 0.5, 1, 2, 5, 10, 20, pga	16 (Preliminary Cases 1-16)
Somerville	H, Z	Yes	0.5, 1, 2, 5, 10 20, pga [4]	14 (Preliminary Cases 5-16)

Notes:
[1] H indicates available for horizontal component, Z indicates available for vertical component
[2] Required frequencies are 0.33, 0.5, 1, 2, 5, 10 and 20 Hz
[3] 0.30 Hz instead of 0.33 Hz
[4] No 0.33 Hz available at this time

Data Package Reference (Vol 1):

Modeler	Median Estimate μ	Aleatory Variability σ_{Model}	Aleatory Variability $\sigma_{Parametric}$	Total Aleatory Variability σ	Epistemic Variability σ_{μ}	Epistemic Variability σ_{σ}
Zeng & Anderson	3.4.4-1, 3.4.5-1 to -3	3.4.8-2 to 3.4.8-4	3.4.4-1, 3.4.5-1 to -3			
Silva Finite Fault	3.3-2, -3, -4	3.3.5-1 to 3.3.5-3	3.3-5, -6, -7			
Silva Point Source	7.1-2 (eq) & program	7.2-1	7.2-1			
Somerville	3.1.2-2, 3.1.3-1	3.1.2-4	3.1.2-5	3.1.2-3	3.1.2-6	3.1.2-7

3. Blast Models: These models and frequencies are provided in program yucatten

	Components Available[1]	PGV Available?	Frequencies Available[2]
Bennett Model 1	H	Yes	0.5, 1., 2., 5., 10., 20., pga
Bennett Model 2	H	No	0.5, 1., 2., 5., 10., 20., pga
Bennett Model 3	H	No	0.5, 1., 2., 5., 10., 20., pga

Notes:
[1] H indicates available for horizontal component
[2] Required frequencies are 0.33, 0.5, 1, 2, 5, 10 and 20 Hz

4. Hybrid Empirical

The hybrid empirical model are provided in the excel spreadsheets "HYBRD_SH.XLS" and "HYBRD_DP.XLS" for the shallow and deep cases, respectively. A description of this model is given in section 6.

The adjustment factors have been parameterized in the FORTRAN program "campFac.for". The factors from this program can be used to scale the ground motion estimates from the empirical attenuation relation.

	Components Available[1]	PGV Available?	Frequencies Available[2]
Hybrid Empirical	H, Z	Yes	0.33, 0.5, 1., 2., 5., 10., 20., pga

5. Adjustment Factors

Factors Adjust for:	Frequencies Available[1]	Issue	Modeler	Black Binder Ref.
Source, Crust, Site	0.33, 0.5, 1, 2, 5, 10, 20	CA → YM_{300} ($\Delta\sigma$ input)	Campbell	
Source, Crust, Site	0.33, 0.5, 1, 2, 5, 10, 20	CA → YM_{300} ($\Delta\sigma$ input)	Silva	
Source	0.33, 0.5, 1, 2, 5, 10, 20	CA → YM ($\Delta\sigma$ input)	Campbell	8.4.2-1
Source	0.5, 1, 2, 5, 10, 20	CA → YM ($\Delta\sigma$ input)	Silva	8.4.1-1
Source	N/A	CA Atten Relations → Extensional Regimes	Spudich et al.	8.4.3-1
Crust, Site	0.33, 0.5, 1, 2, 5, 10, 20	CA → YM_{300}	Campbell	8.3.2-1
Crust, Site	0.33, 0.5, 1, 2, 5, 10, 20	CA → YM_{300}	Silva	8.3.1-1
Crust, Site	0.33, 0.5, 1, 2, 5, 10, 20	CA → YM	Silva	8.2.1-2
YM Site	0.33, 0.5, 1, 2, 5, 10, 20	YM → YM_{300}	Silva	8.1.1-2
Vertical/Horizontal Ratio	0.33, 0.5, 1, 2, 5, 10, 20	N/A	Silva	8.5-1
PGV/PGA Ratio	N/A	YM300	Campbell	Spreadsheet
PGV/PGA Ratio	N/A	YM300	Silva	8.6-1

Notes:
[1] Required frequencies are 0.33, 0.5, 1, 2, 5, 10 and 20 Hz

5. Constraints on Models: Precarious rocks

See black binder Section 11.

2.2 Summary of Available Ground Motion Models

1. Finite Fault Numerical Simulation for YM_{300}	
Result:	Yucca Mountain ground motion at repository outcrop
Proponents:	Somerville (16 cases) Silva Anderson & Zeng
Issues:	Random component effect

2. Empirical

(a) Western US models

Result:	WUS (CA) ground motion at surface
Proponents:	Abrahamson & Silva (1997) Boore, Joyner, Fumal (Vs) (1997) Boore, Joyner, Fumal (class A) (1994) Boore, Joyner, Fumal (class B) (1994) Campbell (soft rock) (1997) Campbell (hard rock) (1997) Campbell (soft rock) (1993-94) Campbell (hard rock) (1993-94) Campbell (soft rock) (1990-94) Campbell (hard rock) (1990-94) Idriss (1991) Idriss (1997) Sadigh et al. (1997)
Issues:	CA---> $YM_{surface}$: Q, crust, kappa $CA_{\Delta\sigma}$ ---> $YM_{\Delta\sigma}$: (source) $YM_{surface}$---> YM_{300m}

(b) Extenstional regime empirical models

Result:	Extensional ground motion
Proponents:	Spudich et al. (1996) McGarr (Extensional regime) (1984)
Issues:	Extensional---> $YM_{surface}$: kappa, crust, Q $YM_{surface}$---> YM_{300m}

(c) Attenuation relations from other regions

Proponent:	Sabetta & Pugliese (1996) - Italian data
Issues:	Italy---> $YM_{surface}$: Q, crust, kappa $Italy_{\Delta\sigma}$ ---> $YM_{\Delta\sigma}$ $YM_{surface}$---> YM_{300m}

3. Blast Experience Models	
(a) NTS source & NTS attenuation	
Result:	NTS ground motion from blast
Proponents:	Bennett
Issues:	Blast source vs. earthquake source Shallow depth of blast $YM_{surface}$---> YM_{300m}
(b) NTS attenuation with Sadigh (1993) spectral shape	
Result:	WUS ground motion with blast attenuation rate
Proponents:	Bennett
Issues:	$WUS_{surface}$--->$YM_{surface}$ $YM_{surface}$---> YM_{300}
(c) Little Skull Mtn spectral shape and Sadigh magnitude scaling	
Result:	Little Skull Mtn ground motion with blast attenuation rate
Proponents:	Bennett
Issues:	$YM_{surface}$---> YM_{300m}

4. Hybrid Empirical	
Result:	Yucca Mountain ground motion at YM_{300} (YM-specific source, Q, crust, kappa)
Proponents:	Campbell
Issues:	Stress-drop for YM

5. Point Source Stochastic Model	
Result:	Yucca Mountain ground motion at YM_{300} (linear site response) (YM-specific source, crust, kappa)
Proponents:	Silva
Issues:	Median and variability of stress-drop for YM, Definition of equivalent point source distance

6. Scenario Earthquake Calculations (for models not being updated for YM_{300})	
Result:	Yucca Mountain ground motion at surface (with non linear site response) M6.4 (normal), M6.7(SS), M7.0(SS)
Proponents:	Chin Joyner
Issues:	$YM_{surface}$ ---> YM_{300m} magnitude scaling

Mar 17

2.3 Summary of Proponent Models for Adjustments

1. $YM_{surface}$ ---> YM_{300} Surface at Yucca Mountain to Repository Outcrop (300 m)	
Model 1:	
Conversion factor:	Ratio of YM_{300} / $YM_{surface}$
Source of factor:	1D vertical wave propagation (Silva)
Component:	horizontal
Tool provided in packet:	Plot of ratio. Tabulated values are also provided.
Accounts for:	differences in crustal velocity, kappa, Q

2. CA ---> $YM_{surface}$ California to Yucca Mountain (surface) (crust and kappa)	
Model 1: Conversion factor:	Ratio of $YM_{surface}$/ $CA_{surface}$
Source of factor:	Point source stochastic model (Silva)
Component:	horizontal
Tool provided in packet:	Plot of ratio. Tabulated values are also provided.
Accounts for:	crustal velocity, kappa, Q

3. CA ---> YM_{300} California to Yucca Mountain (surface) (crust and kappa)	
Model 1:	
Conversion factor:	$YM_{surface}$/ $CA_{surface}$ * YM_{300}/ $YM_{surface}$ (from cases 1 and 2 above)
Source of factor:	Point source stochastic model (Silva)
Component:	horizontal
Tool provided in packet:	Plot of ratio. Tabulated values are also provided.
Accounts for:	crustal velocity, kappa, Q
Method 2:	
Conversion factor:	Ratio of YM_{300}/ $CA_{surface}$
Source of factor:	Point source stochastic model (Campbell)
Component:	horizontal
Tool provided in packet:	Excel file plots of scale factors
Effects included:	crustal velocity, kappa, Q

4. $CA_{surface}$ ---> $YM_{surface}$ California to Yucca Mountain (surface) (stress drop only)	
Model 1:	
Conversion factor:	adjustment factors
Source of factor:	Empirical (Spudich)
Component:	horizontal, vertical
Tool provided in packet:	None. See Spudich report.
Accounts for:	observed differences between extensional regime and California models (implicitly also includes possible differences in crust and kappa)
Model 2:	
Conversion factor:	equation
Source of factor:	point source stochastic model (Silva)
Component:	horizontal
Tool provided in packet:	equation
Accounts for:	differences in median $\Delta\sigma$ between California and Yucca Mountain
Model 3:	
Conversion factor:	equation
Source of factor:	point source stochastic model (Campbell) (Implied from hybrid empirical factors)
Component:	horizontal
Tool provided in packet:	equation
Accounts for:	differences in median $\Delta\sigma$ between California and Yucca Mountain

Section 3.

Finite Fault Numerical Simulations for YM300

Section 3.1

Somerville Finite Fault Simulations

3.1.1 Somerville - 16 cases

YUCCA MOUNTAIN PROBABILISTIC SEISMIC HAZARD ANALYSIS

Documentation of Ground Motions for Specified Geometries

Paul Somerville, Woodward-Clyde

Ground motions generated Jan. 31, 1997; documented Feb. 13, 1997

Broadband Simulation Procedure

See Appendix 1.

Velocity Model

Velocity model has shear wave velocity at the surface of 1.9 km/sec. "Amplification factors" are contained exactly in the Green's functions used in the simulations.

Rupture Area

Relation between seismic moment and rupture area, based on slip models of 11 crustal earthquakes in tectonically active regions:

$A = 2.05 \times 10^{-15} \times Mo^{2/3}$ (Somerville et. al., 1993).

This relation is practically identical to Wells and Coppersmith (1994), and corresponds to an average static stress drop of 35 bars. Variations in slip on the fault produce variable local stress drop.

Rise Time

The relation between rise time and seismic moment, derived from the same set of 11 earthquakes, is:

$Tr = 1.72 \times 10^{-9} \times Mo^{1/3}$ (Somerville et. al., 1993).

Slip Models

Slip models were generated using a method developed by Abrahamson based on these 11 earthquakes and described in Somerville et al. (1993). The five slip models used for each magnitude are shown in the attached figures. The slip models were tapered with a cosine bell as follows: over the top 50% of the downdip width; over the bottom 10% of the downdip width; and over 5% of the length at each end.

Kappa - 0.02

Q - not included - only affects R=50 km, 5 Hz and above - we may recalculate these

Fault and Station Geometry and Correction for Rupture Directivity

The stations are located 0.25 of the fault length from the end of the fault. The three hypocenters used for each slip model are located as follows: one at the middle of the fault and one 0.17 of the fault length from either end. The three hypocenters sample quite a large range of directivity effects. At periods of 1 and 2 seconds, the spectra are corrected for directivity effects using the model of Somerville et al., Figure 8 (Seismological Research Letters, 68, p. 199-222, 1997) to give a value that represents the average over directivity effects. The aleatory variability in the median estimate of the response spectrum is increased at periods of 1 and 2 seconds to include larger parametric variability; one of these contributions is from directivity effects, as documented in Somerville et al., Figure 8.

Estimation of Aleatory Variability

Aleatory-Category	Sub-category	pga, 20, 10, 5, 2Hz	1 Hz and pgv		0.5 Hz	
			strike-slip	dip-slip	strike-slip	dip-slip
Parametric	Stressdrop*	0.28	0.28	0.28	0.28	0.28
	Directivity	0.0	0.18	0.05	0.34	0.10
	Other	0.20	0.40	0.40	0.40	0.40
	Total	0.35	0.52	0.49	0.60	0.50
Modeling		0.35	0.35	0.35	0.35	0.35
Total		0.49	0.63	0.60	0.69	0.61

* static stress drop, varied by varying the rupture area for a given seismic moment

TopShear1.9-M5.8-Dip90

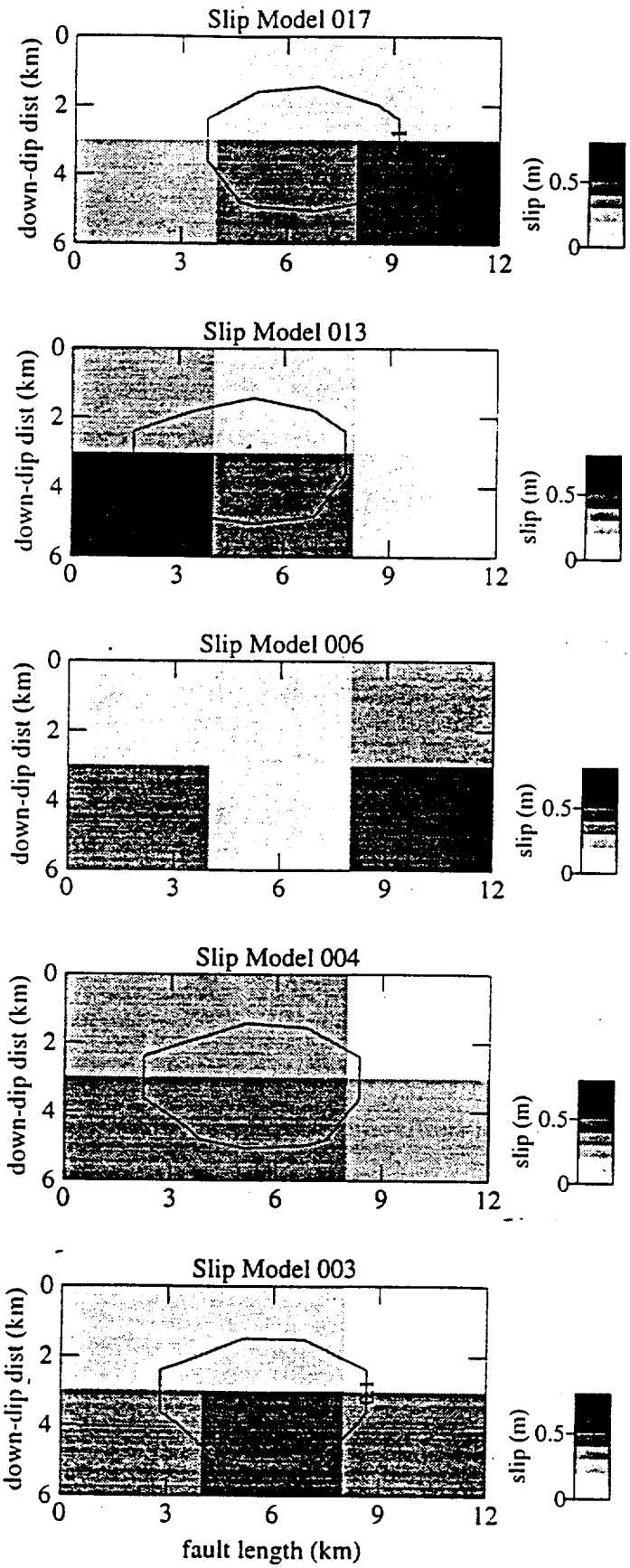

rwgrave0: Thu Feb 13 13:47:02 PST 1997
/tmp/tmp/SlipPlots

TopShear1.9-M6.5-Dip90

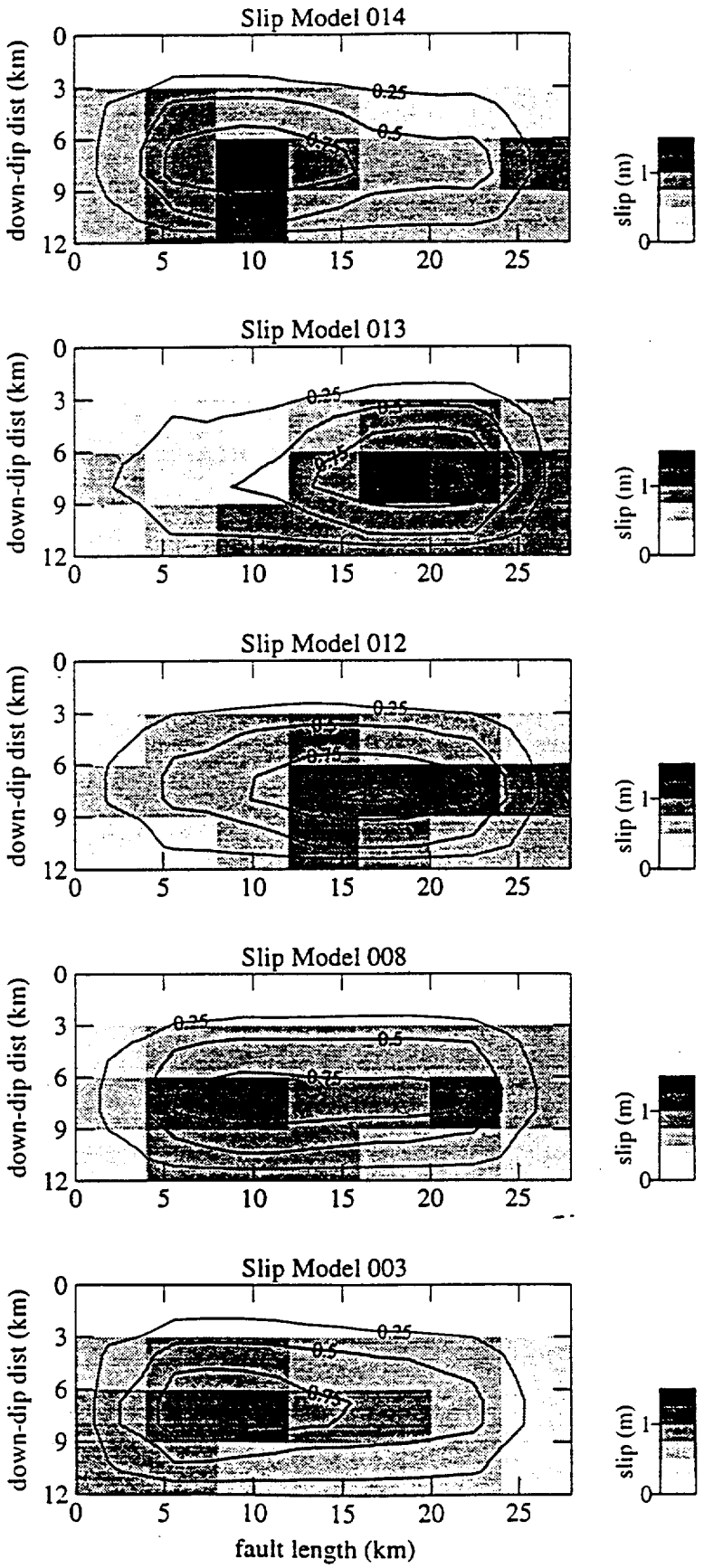

TopShear1.9-M7.0-Dip90

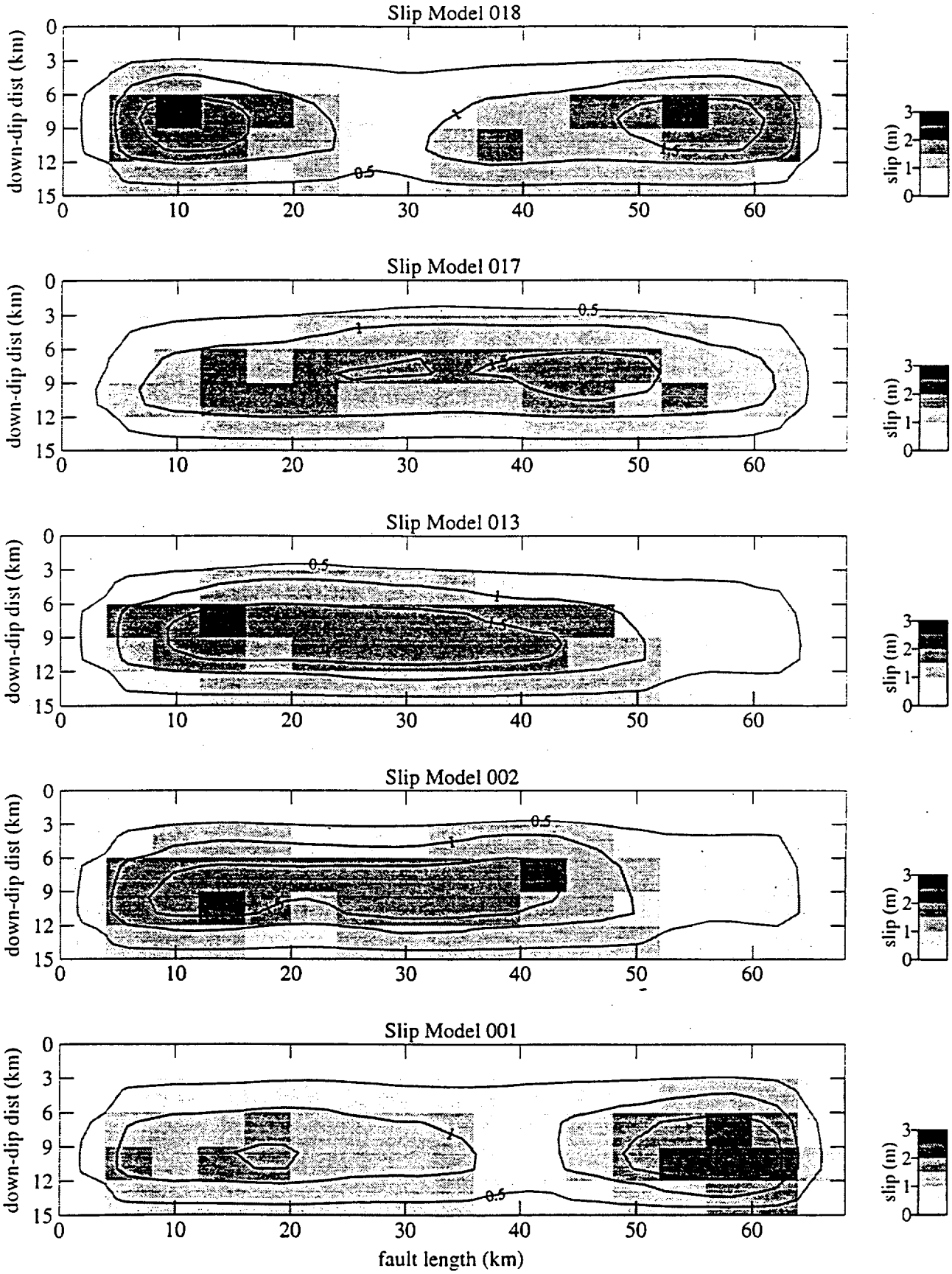

3.1.1-5

TopShear1.9-M7.5-Dip90

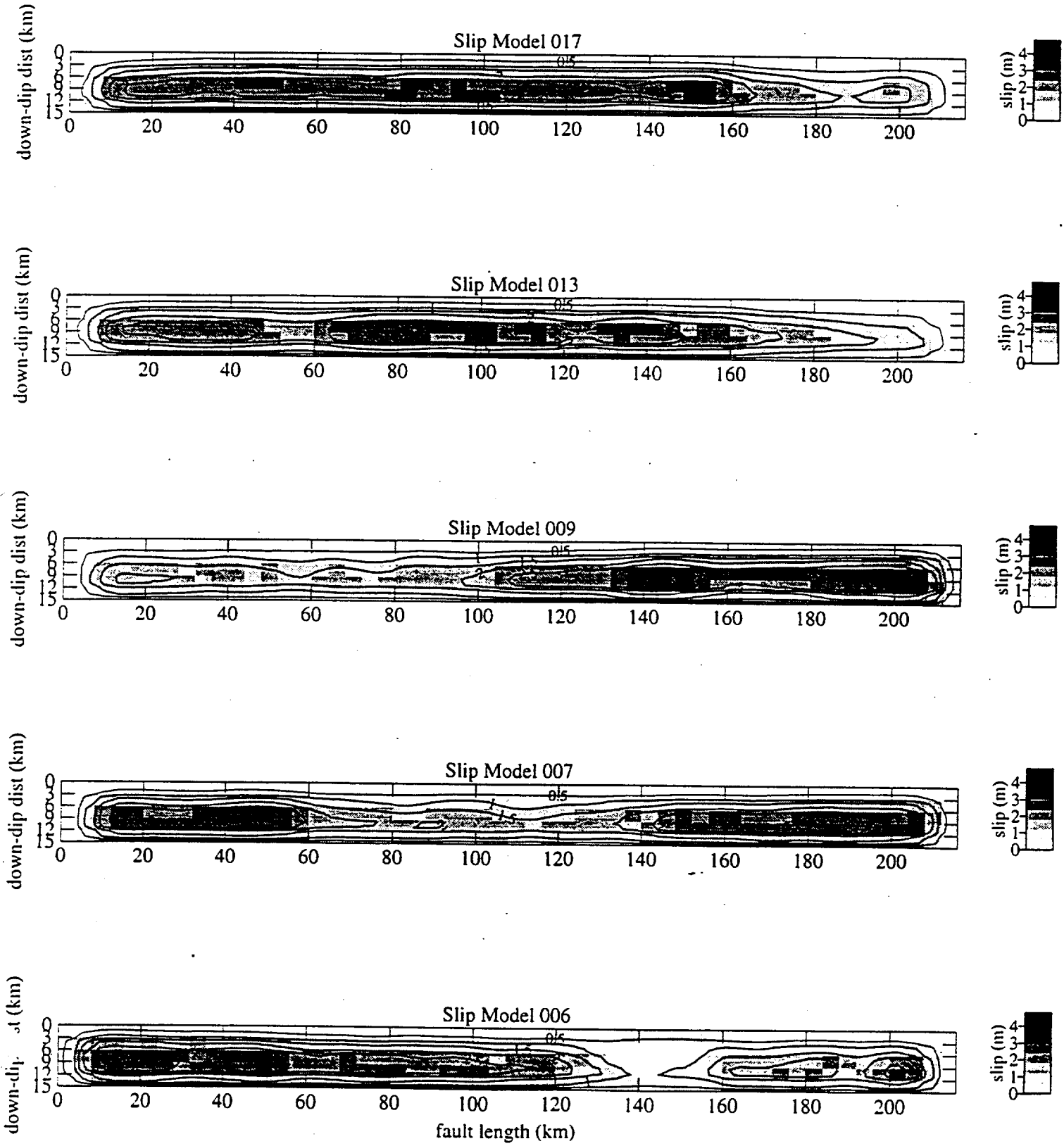

Fault Parameters used in Broadband Simulations

Due Date	1/31/97		1/31/97		1/31/97		1/31/97		1/31/97		1/31/97	
M	5 (not run)		5.8		6.5		7		7.5		8 (not run)	
Mo	3.55×10^{23}		5.62×10^{24}		6.31×10^{25}		3.55×10^{26}		2.0×10^{27}		1.12×10^{28}	
Rise Time	0.12		0.31		0.68		1.22		2.17		3.85	
Area	13		65 (72)		324 (336)		1023 (1020)		3236 (3240)		10233 (10200)	
Length - km/ elements	4 / 1		12 / 3		28 / 7		68 /17		216 / 54		680 /170	
Width - km / elements	3 / 1		6 / 2		12 / 4		15 / 5		15 / 5		15 / 5	
Downdip distance of hypocenter	1.5		4.5		9		11.25		11.25		11.25	
Horizontal distance of hypocenter from center	-1.33,0,+1.33		-4.0, 0, +4.0		-9.3,0,+9.3		-22.67, 0, +22.67		-72, 0,+72		-226.8, 0,+226.8	
Distance along stk of hypo			2., 6. 10.		4.7, 14.0, 23.3		11.33, 34., 56.67		36, 108, 180			
Dip/Rake	60 / 90	90 / 0	60 / 90	90 / 0	60 / 90	90 / 0	60 / 90	90 / 0	60 / 90	90 / 0	60 / 90	90 / 0
Depth of top			2.6 7.79	3.0 9.0	0	0	0	0	0	0	0	0
Depth to bottom			7.79 13	9 15	10.39	12	13	15	13	15		
Depth of hypocenter			6.50 11.69	7.5 13.5	7.79	9.0	9.74	11.25	9.74	11.25	9.74	11.25
Shear Velocity			3.5	3.5	3.5	3.5	3.5	3.5	3.5	3.5	3.5	3.5
Rupture Velocity			2.8	2.8	2.8	2.8	2.8	2.8	2.8	2.8	2.8	2.8
Station Locations	Station distances east of the projection of the fault plane at the surface: -50,-20,-10,-5,-1,1,5,10,20,50											
N of top center			3	3	7	7	17	17	54	54	170	170
E of top center												

Section 3.1.2

Tabluated Results for the Horizontal Component (Somerville Simulations, Cases 1-16)

Tabulation of Ground Motion Parameters

The following ground motion parameters are provided in the following tables:

Median Sa - Horizontal Component

Median Sa - Vertical Component

Combined Modeling and Parametric Components of Aleatory Variability about Median Sa- H

Modeling Component of Aleatory Variability about Median Sa- Horizontal

Parametric Component of Aleatory Variability about Median Sa- Horizontal

Epistemic Uncertainty in Median Sa- Horizontal

Epistemic Uncertainty in Combined Aleatory Variability about Median Sa- Horizontal

Woodward-Clyde: Somerville

Median Sa - Horizontal Component												
Frequency Hz	M_w 5.8 Deep		M_w 6.5							M_w 7.0	M_w 7.5	
	SS	HW	SS	HW	FW	HW	FW	SS	HW	SS	SS	HW
	10 km	20 km	1 km	1 km	1 km	5 km	5 km	50 km	50 km	10 km	50 km	50 km
0.5	.01730	0.0088	0.1530	0.0708	0.0819	0.0899	0.0605	0.0103	0.0059	0.0859	0.0174	0.0115
1.0	0.0563	0.0373	0.4130	0.2343	0.2348	0.3833	0.1983	0.0276	0.0176	0.2290	0.0688	0.0594
2.0	0.1309	0.0966	0.7771	0.5994	0.5993	0.7874	0.4337	0.0420	0.0499	0.6374	0.1699	0.1710
5.0	0.1764	0.1549	1.0876	0.9442	0.9421	1.2219	0.6278	0.0610	0.0788	0.7569	0.2602	0.2727
10.0	0.1776	0.1529	1.1180	1.0291	1.0311	1.2583	0.5670	0.0717	0.0726	0.8162	0.2240	0.2339
20.0	0.1385	0.1236	0.8230	0.6709	0.6678	1.0379	0.4871	0.0565	0.0534	0.5944	0.1814	0.1629
PGA	0.0889	0.0775	0.5636	0.4647	0.4598	0.6417	0.2873	0.0328	0.0336	0.3958	0.1007	0.0966
PGV	5.9900	4.1394	46.760	26.3591	27.4479	35.8396	20.1576	2.8650	2.2562	25.430	6.5440	4.8642

Woodward-Clyde: Somerville

Combined Modeling and Parametric Components of Aleatory Variability about Median Sa - Horizontal Component												
Frequency Hz	M_w 5.8 Deep		M_w 6.5							M_w 7.0	M_w 7.5	
	SS	HW	SS	HW	FW	HW	FW	SS	HW	SS	SS	HW
	10 km	20 km	1 km	1 km	1 km	5 km	5 km	50 km	50 km	10 km	50 km	50 km
0.5	0.69	0.61	0.69	0.61	0.61	0.61	0.61	0.61	0.61	0.69	0.61	0.61
1.0	0.63	0.60	0.63	0.60	0.60	0.60	0.60	0.60	0.60	0.63	0.60	0.60
2.0	0.49	0.49	0.49	0.49	0.49	0.49	0.49	0.49	0.49	0.49	0.49	0.49
5.0	0.49	0.49	0.49	0.49	0.49	0.49	0.49	0.49	0.49	0.49	0.49	0.49
10.0	0.49	0.49	0.49	0.49	0.49	0.49	0.49	0.49	0.49	0.49	0.49	0.49
20.0	0.49	0.49	0.49	0.49	0.49	0.49	0.49	0.49	0.49	0.49	0.49	0.49
PGA	0.49	0.49	0.49	0.49	0.49	0.49	0.49	0.49	0.49	0.49	0.49	0.49
PGV	0.63	0.60	0.63	0.60	0.60	0.60	0.60	0.60	0.60	0.63	0.60	.060

Woodward-Clyde: Somerville

Modeling Component of Aleatory Variability about Median Sa - Horizontal Component												
Frequency Hz	M_w 5.8 Deep		M_w 6.5							M_w 7.0	M_w 7.5	
	SS	HW	SS	HW	FW	HW	FW	SS	HW	SS	SS	HW
	10 km	20 km	1 km	1 km	1 km	5 km	5 km	50 km	50 km	10 km	50 km	50 km
0.5	0.35	0.35	0.35	0.35	0.35	0.35	0.35	0.35	0.35	0.35	0.35	0.35
1.0	0.35	0.35	0.35	0.35	0.35	0.35	0.35	0.35	0.35	0.35	0.35	0.35
2.0	0.35	0.35	0.35	0.35	0.35	0.35	0.35	0.35	0.35	0.35	0.35	0.35
5.0	0.35	0.35	0.35	0.35	0.35	0.35	0.35	0.35	0.35	0.35	0.35	0.35
10.0	0.35	0.35	0.35	0.35	0.35	0.35	0.35	0.35	0.35	0.35	0.35	0.35
20.0	0.35	0.35	0.35	0.35	0.35	0.35	0.35	0.35	0.35	0.35	0.35	0.35
PGA	0.35	0.35	0.35	0.35	0.35	0.35	0.35	0.35	0.35	0.35	0.35	0.35
PGV	0.35	0.35	0.35	0.35	0.35	0.35	0.35	0.35	0.35	0.35	0.35	0.35

Woodward-Clyde: Somerville

Parametric Component of Aleatory Variability about Median Sa - Horizontal Component												
Frequency Hz	M_w 5.8 Deep		M_w 6.5							M_w 7.0	M_w 7.5	
	SS	HW	SS	HW	FW	HW	FW	SS	HW	SS	SS	HW
	10 km	20 km	1 km	1 km	1 km	5 km	5 km	50 km	50 km	10 km	50 km	50 km
0.5	0.60	0.50	0.60	0.50	0.50	0.50	0.50	0.50	0.50	0.60	0.50	0.50
1.0	0.52	0.49	0.52	0.49	0.49	0.49	0.49	0.49	0.49	0.52	0.49	0.49
2.0	0.35	0.35	0.35	0.35	0.35	0.35	0.35	0.35	0.35	0.35	0.35	0.35
5.0	0.35	0.35	0.35	0.35	0.35	0.35	0.35	0.35	0.35	0.35	0.35	0.35
10.0	0.35	0.35	0.35	0.35	0.35	0.35	0.35	0.35	0.35	0.35	0.35	0.35
20.0	0.35	0.35	0.35	0.35	0.35	0.35	0.35	0.35	0.35	0.35	0.35	0.35
PGA	0.35	0.35	0.35	0.35	0.35	0.35	0.35	0.35	0.35	0.35	0.35	0.35
PGV	0.52	0.49	0.52	0.49	0.49	0.49	0.49	0.49	0.49	0.52	0.49	0.49

Woodward-Clyde: Somerville

Epistemic Uncertainty in Median Sa - Horizontal Component												
Frequency Hz	M_w 5.8 Deep		M_w 6.5							M_w 7.0	M_w 7.5	
	SS	HW	SS	HW	FW	HW	FW	SS	HW	SS	SS	HW
	10 km	20 km	1 km	1 km	1 km	5 km	5 km	50 km	50 km	10 km	50 km	50 km
0.5	0.2	0.2	0.2	0.2	0.2	0.2	0.2	0.2	0.2	0.2	0.2	0.2
1.0	0.2	0.2	0.2	0.2	0.2	0.2	0.2	0.2	0.2	0.2	0.2	0.2
2.0	0.2	0.2	0.2	0.2	0.2	0.2	0.2	0.2	0.2	0.2	0.2	0.2
5.0	0.2	0.2	0.2	0.2	0.2	0.2	0.2	0.2	0.2	0.2	0.2	0.2
10.0	0.2	0.2	0.2	0.2	0.2	0.2	0.2	0.2	0.2	0.2	0.2	0.2
20.0	0.2	0.2	0.2	0.2	0.2	0.2	0.2	0.2	0.2	0.2	0.2	0.2
PGA	0.2	0.2	0.2	0.2	0.2	0.2	0.2	0.2	0.2	0.2	0.2	0.2
PGV	0.2	0.2	0.2	0.2	0.2	0.2	0.2	0.2	0.2	0.2	0.2	0.2

Woodward-Clyde: Somerville

Epistemic Uncertainty in Aleatory Variability about Median Sa (+/-) - Horizontal Component												
Frequency Hz	M_w 5.8 Deep		M_w 6.5							M_w 7.0	M_w 7.5	
	SS	HW	SS	HW	FW	HW	FW	SS	HW	SS	SS	HW
	10 km	20 km	1 km	1 km	1 km	5 km	5 km	50 km	50 km	10 km	50 km	50 km
0.5	0.15	0.15	0.15	0.15	0.15	0.15	0.15	0.15	0.15	0.15	0.15	0.15
1.0	0.15	0.15	0.15	0.15	0.15	0.15	0.15	0.15	0.15	0.15	0.15	0.15
2.0	0.15	0.15	0.15	0.15	0.15	0.15	0.15	0.15	0.15	0.15	0.15	0.15
5.0	0.15	0.15	0.15	0.15	0.15	0.15	0.15	0.15	0.15	0.15	0.15	0.15
10.0	0.15	0.15	0.15	0.15	0.15	0.15	0.15	0.15	0.15	0.15	0.15	0.15
20.0	0.15	0.15	0.15	0.15	0.15	0.15	0.15	0.15	0.15	0.15	0.15	0.15
PGA	0.15	0.15	0.15	0.15	0.15	0.15	0.15	0.15	0.15	0.15	0.15	0.15
PGV	0.15	0.15	0.15	0.15	0.15	0.15	0.15	0.15	0.15	0.15	0.15	0.15

Section 3.1.3

Tabluated Results for the Vertical Component (Somerville Simulations, Cases 1-16)

Woodward-Clyde: Somerville

Median Sa - Vertical Component												
Frequency Hz	M_w 5.8 Deep		M_w 6.5							M_w 7.0	M_w 7.5	
	SS	HW	SS	HW	FW	HW	FW	SS	HW	SS	SS	HW
	10 km	20 km	1 km	1 km	1 km	5 km	5 km	50 km	50 km	10 km	50 km	50 km
0.5	0.0075	0.0048	0.0534	0.0661	0.0552	0.0515	0.0505	0.0035	0.0052	0.0282	0.0056	0.0076
1.0	0.0178	0.0179	0.1153	0.1309	0.1293	0.1449	0.1371	0.0059	0.0122	0.0890	0.0317	0.0283
2.0	0.0679	0.0512	0.2876	0.3819	0.3808	0.3927	0.2999	0.0228	0.0428	0.3420	0.0912	0.0797
5.0	0.0828	0.0769	0.5503	0.5391	0.5393	0.5936	0.3246	0.0270	0.0306	0.4553	0.1261	0.1176
10.0	0.1036	0.0990	0.8969	0.8949	0.8947	0.5713	0.4779	0.0345	0.0444	0.4909	0.1325	0.1313
20.0	0.0741	0.0790	0.5877	0.5470	0.5509	0.5943	0.3181	0.0269	0.0335	0.3969	0.0934	0.0977
PGA	0.0425	0.0472	0.3306	0.3299	0.3251	0.3075	0.1985	0.0172	0.0218	0.2186	0.0530	0.0554
PGV	2.5437	2.4366	12.8034	21.0499	18.6963	20.279	13.0190	0.7055	1.8854	10.838	2.3347	2.4583

Section 3.1.4

Plots of Results for the Horizontal Component (Somerville Simulations, Cases 1-16)

Display of Response Spectra

- o Unlike tabulated values, we have not corrected these spectra for rupture directivity

- o Station code: letter e or w indicates hanging wall or foot wall
  three digit number indicates horizontal distance to fault outcrop.

Yucca Broadband Results, All Magnitudes,Dip 60.0
Station e001, Component h

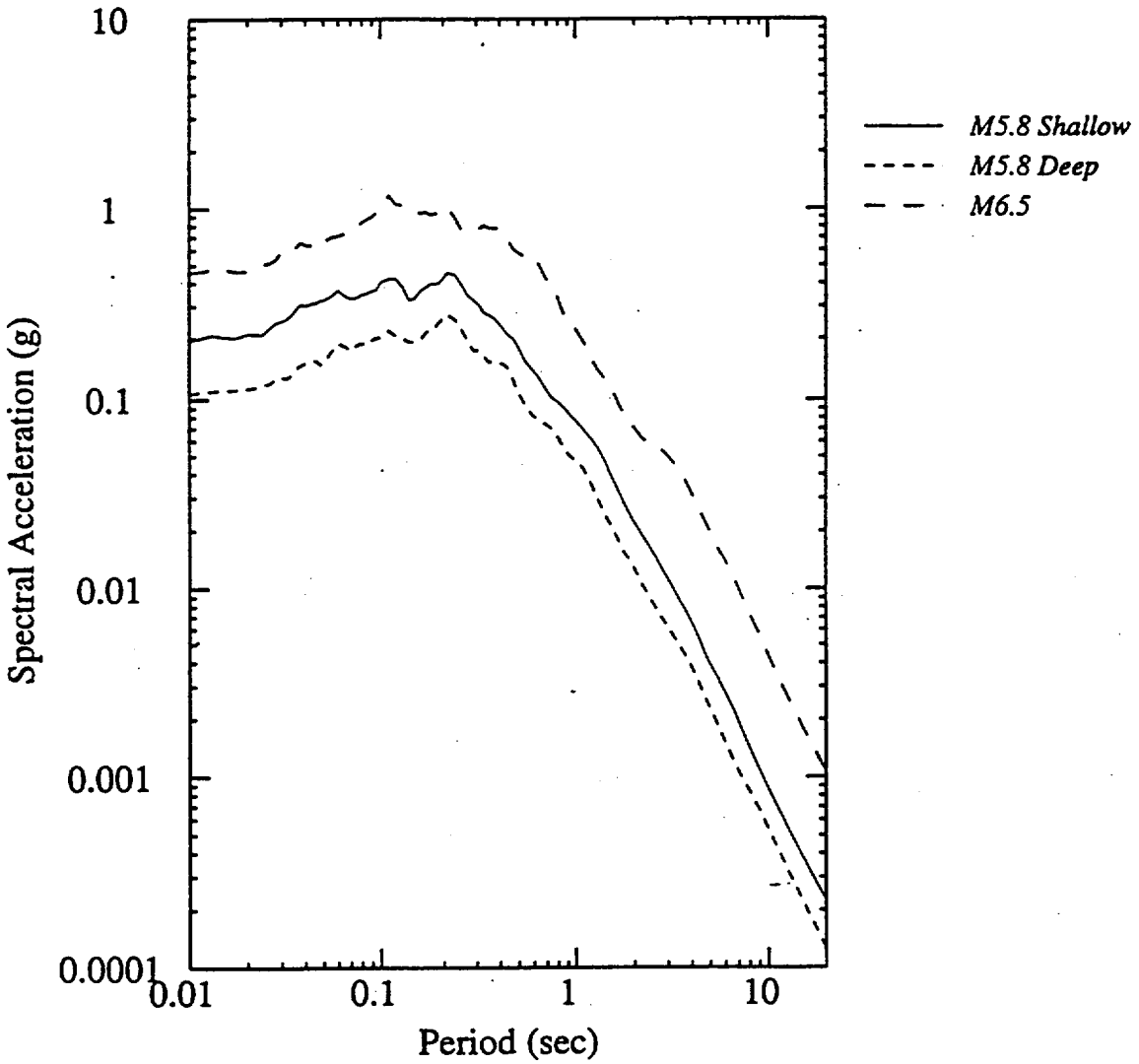

nfsmith0: Thu Jan 30 14:40:01 PST 1997
/tmp/nancy/Yucca/BroadBand/mplot_spectra_sum2.csh

Yucca Broadband Results, All Magnitudes,Dip 60.0
Station e005, Component h

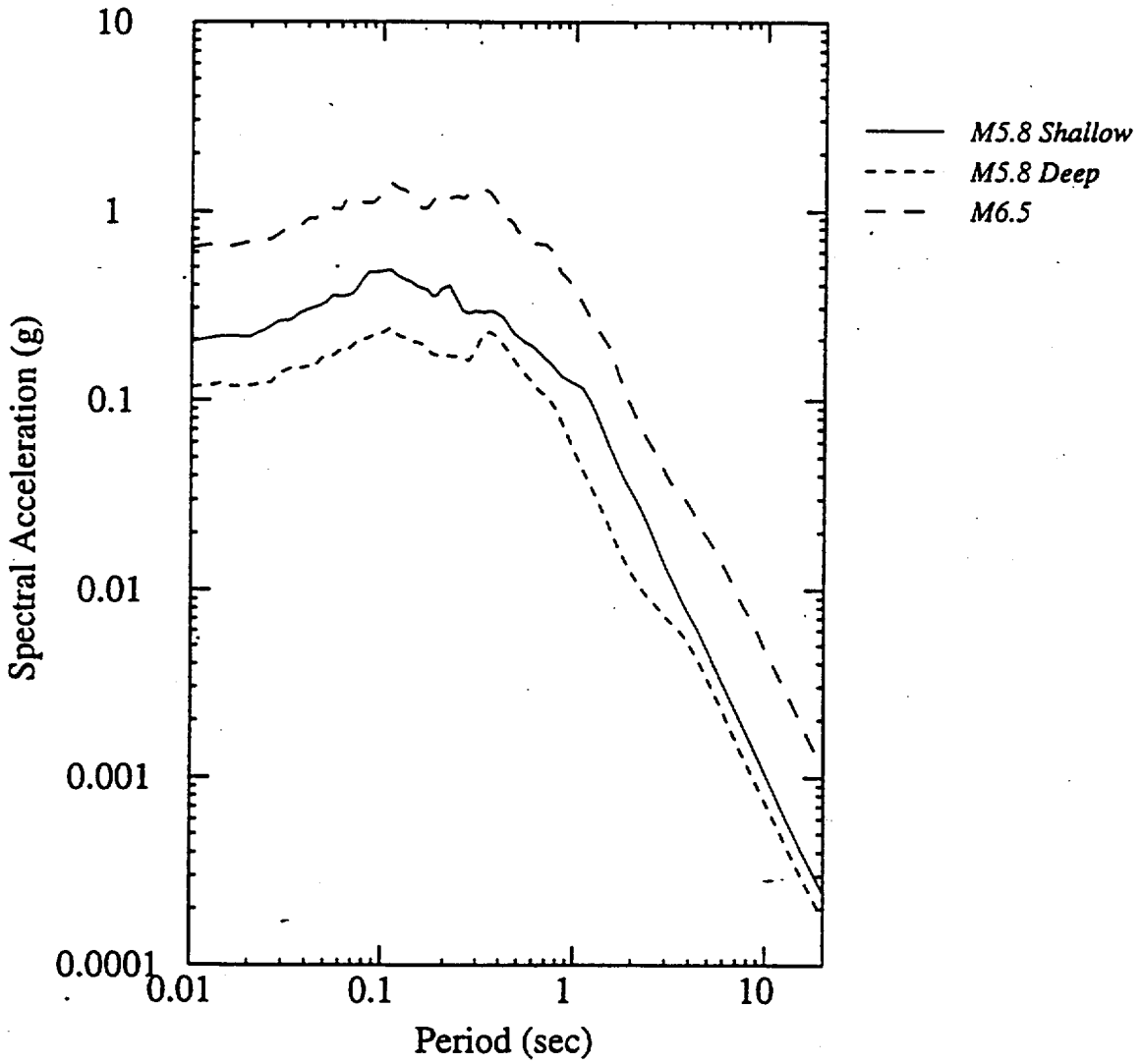

Yucca Broadband Results, All Magnitudes,Dip 60.0
Station e010, Component h

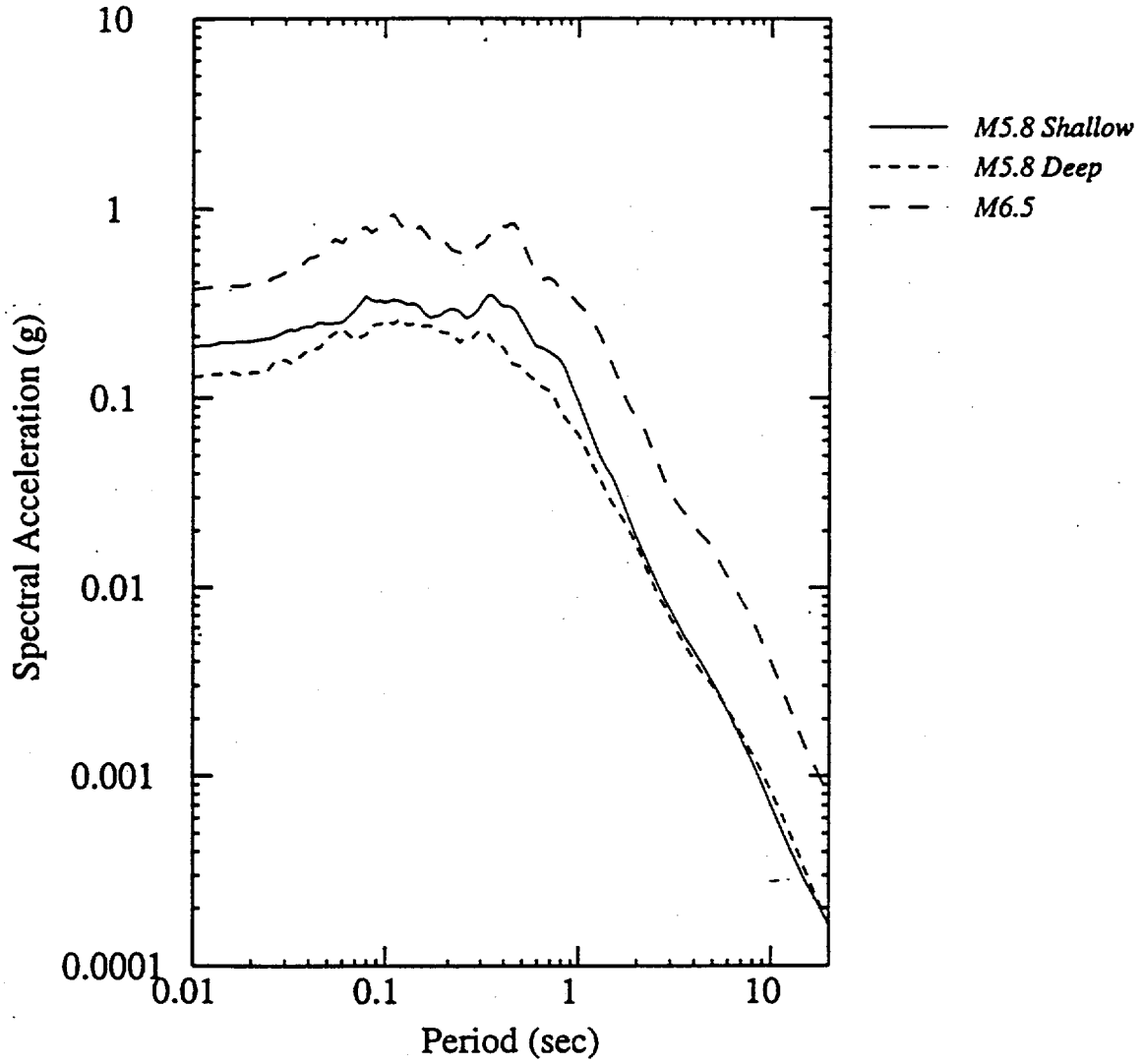

Yucca Broadband Results, All Magnitudes,Dip 60.0
Station e020, Component h

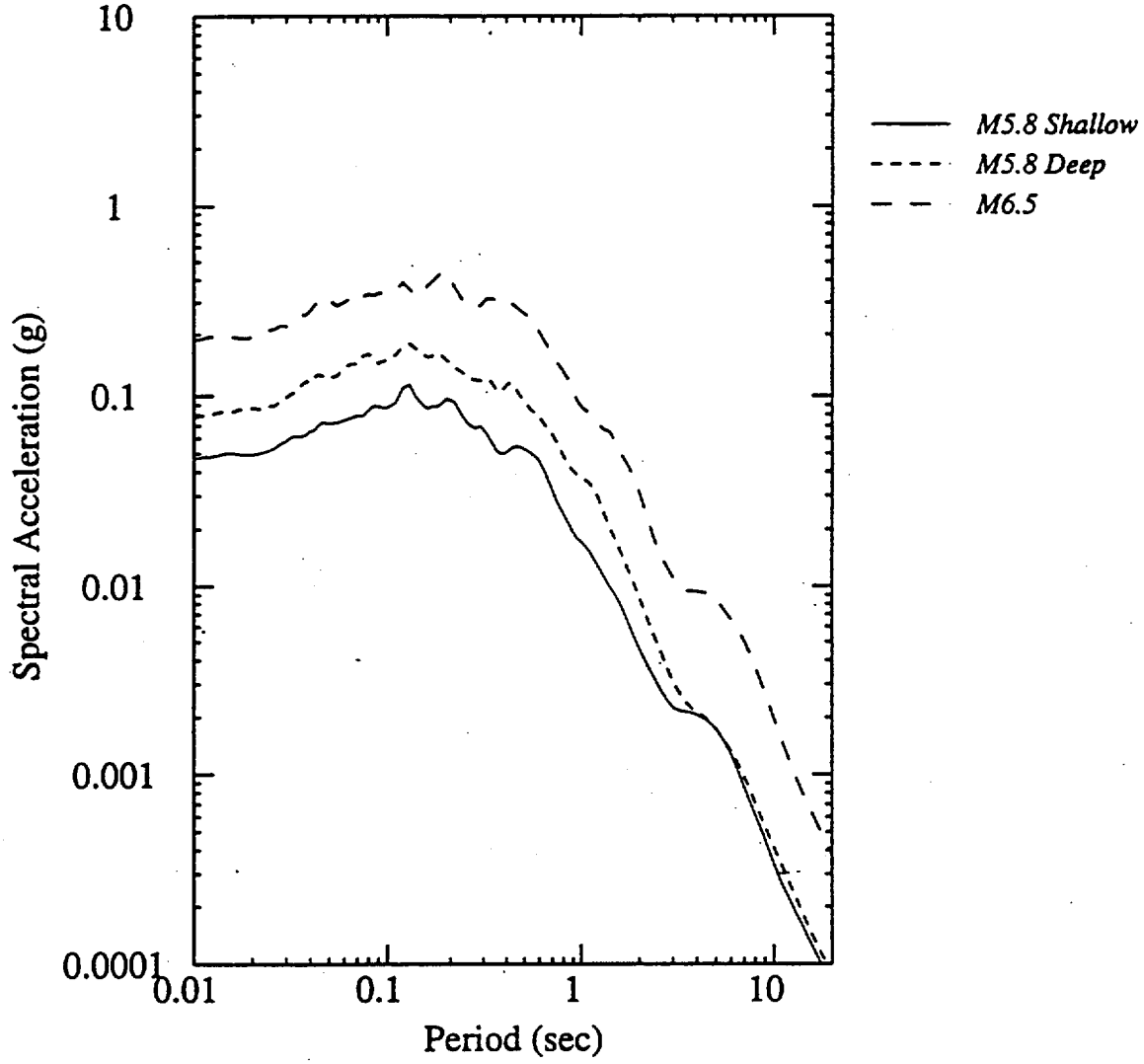

Yucca Broadband Results, All Magnitudes,Dip 60.0
Station e050, Component h

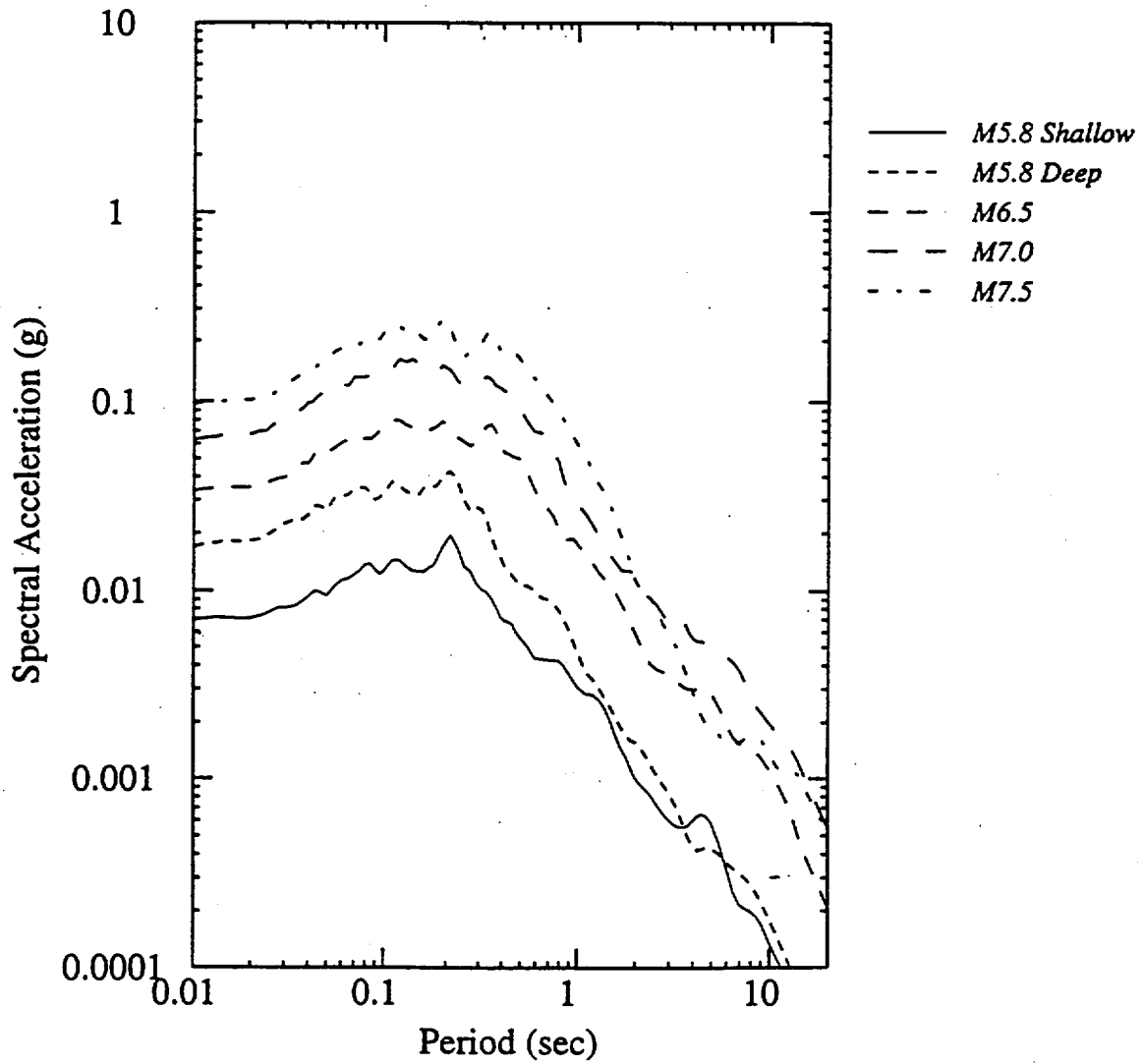

Yucca Broadband Results, All Magnitudes,Dip 60.0
Station w001, Component h

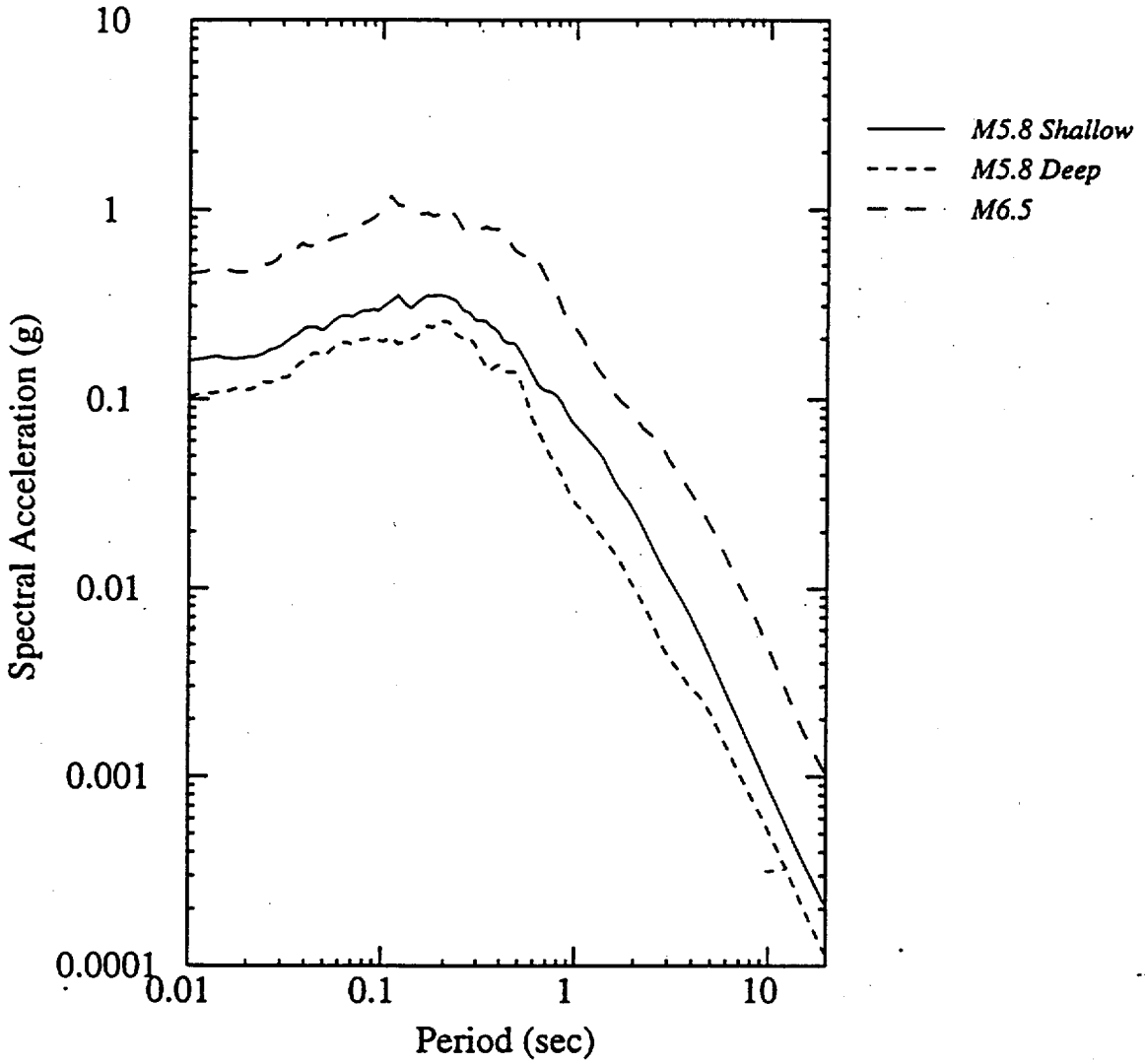

Yucca Broadband Results, All Magnitudes,Dip 60.0
Station w005, Component h

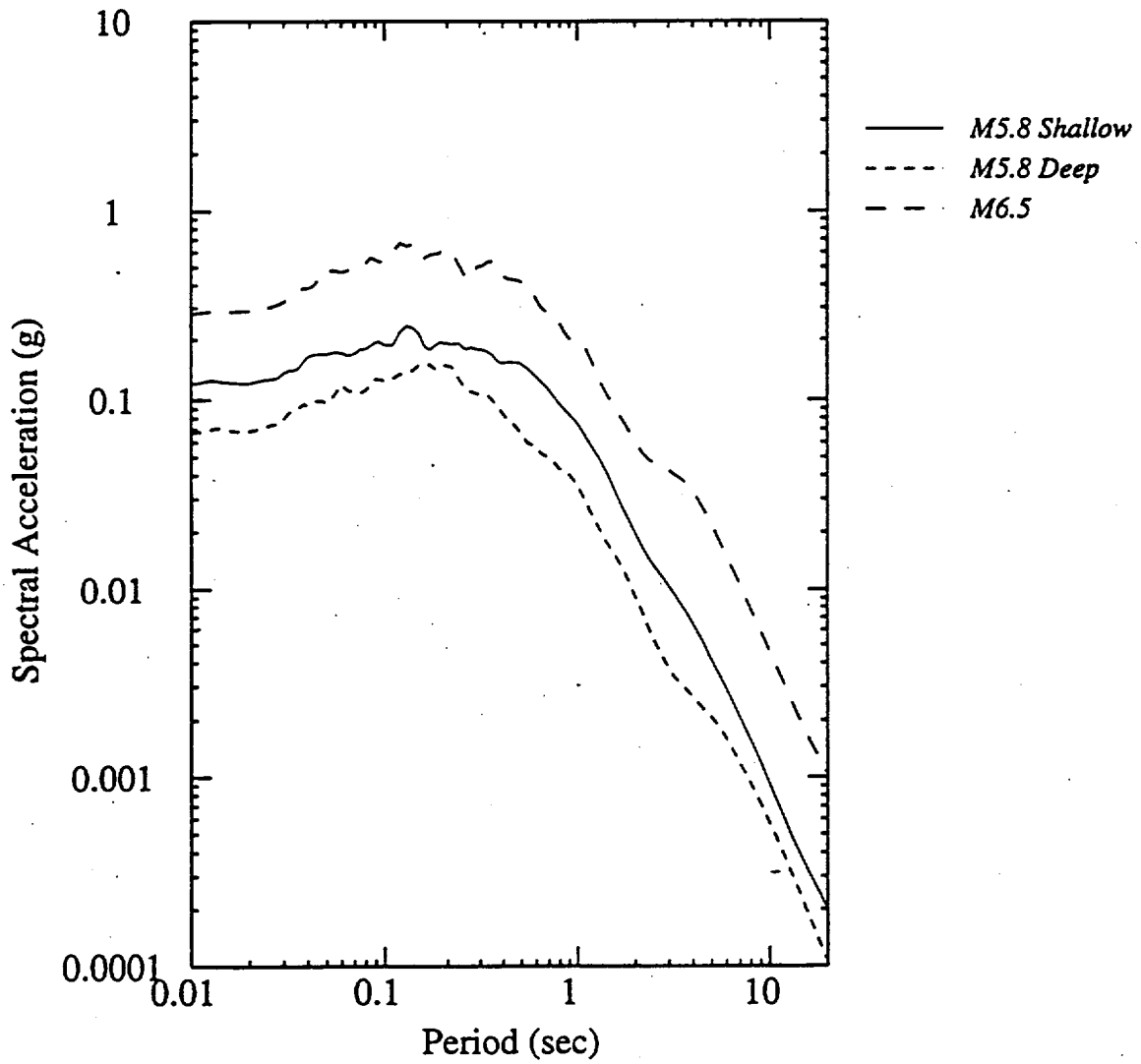

nfsmith0: Thu Jan 30 14:41:43 PST 1997
/tmp/nancy/Yucca/BroadBand/mplot_specra_sum2.csh

Yucca Broadband Results, All Magnitudes,Dip 60.0
Station w010, Component h

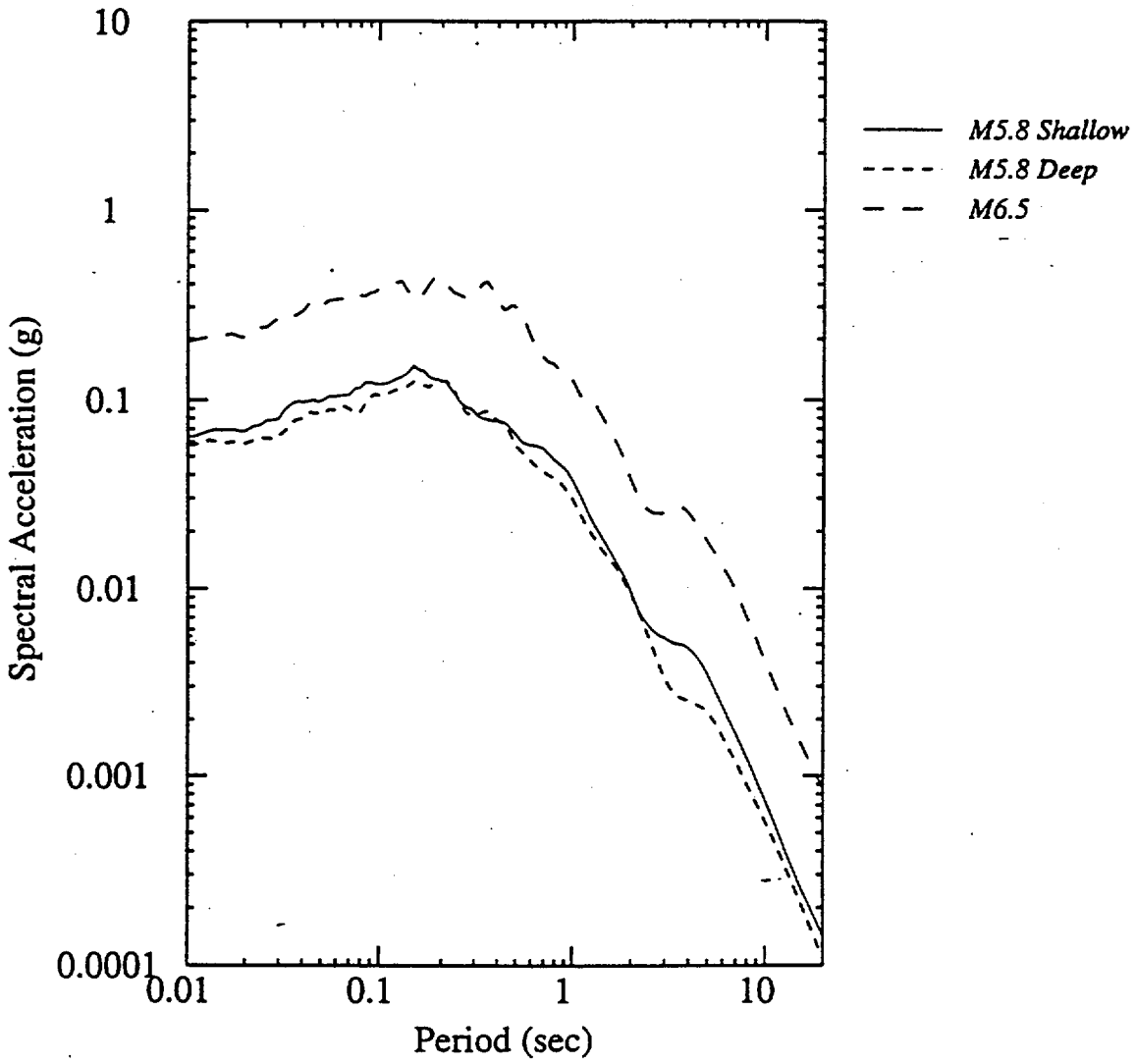

Yucca Broadband Results, All Magnitudes,Dip 60.0
Station w020, Component h

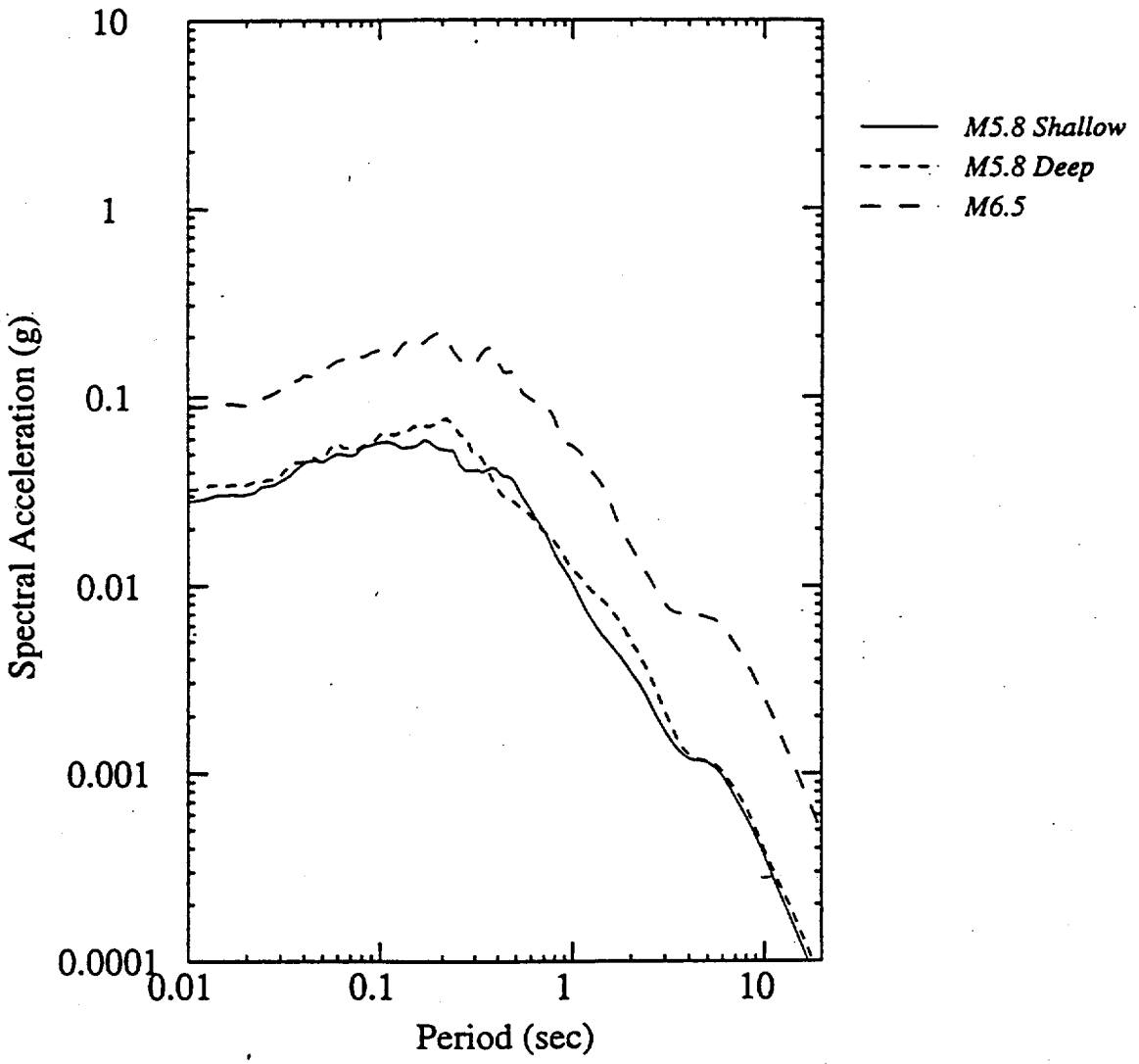

3.1.4-10

Yucca Broadband Results, All Magnitudes,Dip 60.0
Station w050, Component h

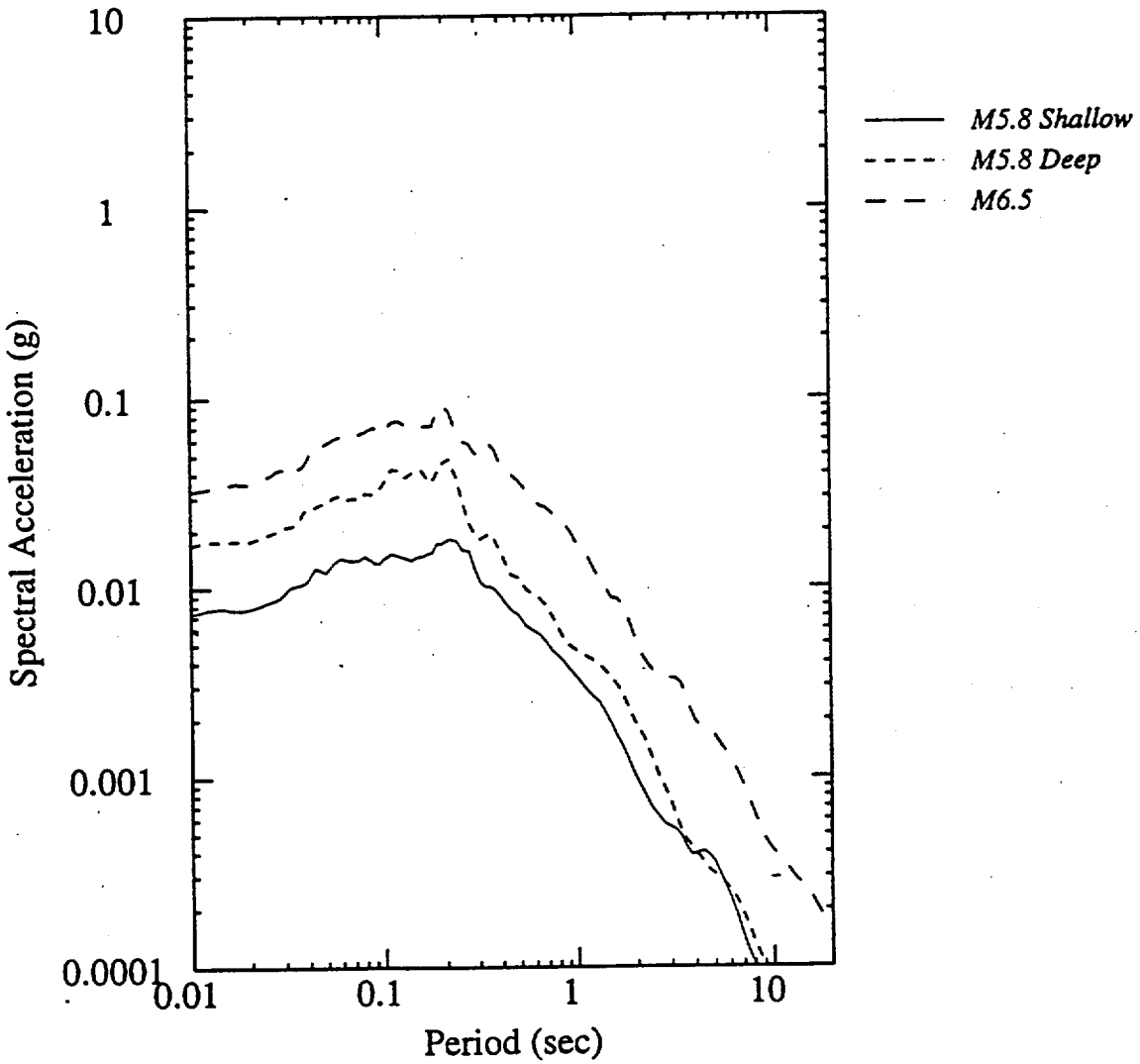

n/smith0: Thu Jan 30 14:42:34 PST 1997
/tmpb/nancy/Yucca/BroadBand/mplot_spectra_sum2.csh

3.14-11

Display of Attenuation for M 5.8 and M 6.5 for Discrete Periods

- o Unlike tabulated values, we have not corrected these spectra for rupture directivity
- o M5.8d means magnitude 5.8 deep; M5.8s means magnitude 5.8 shallow
- o Two dip angles, 60 and 90 degrees, are shown.
- o Many more results are shown than required for the exercise
- o Values required for exercise, shown as horizontal bars, are averages over 15 simulations whose complete range is shown as vertical lines of circles.
- o Hanging wall and foot wall values are not distinguished.

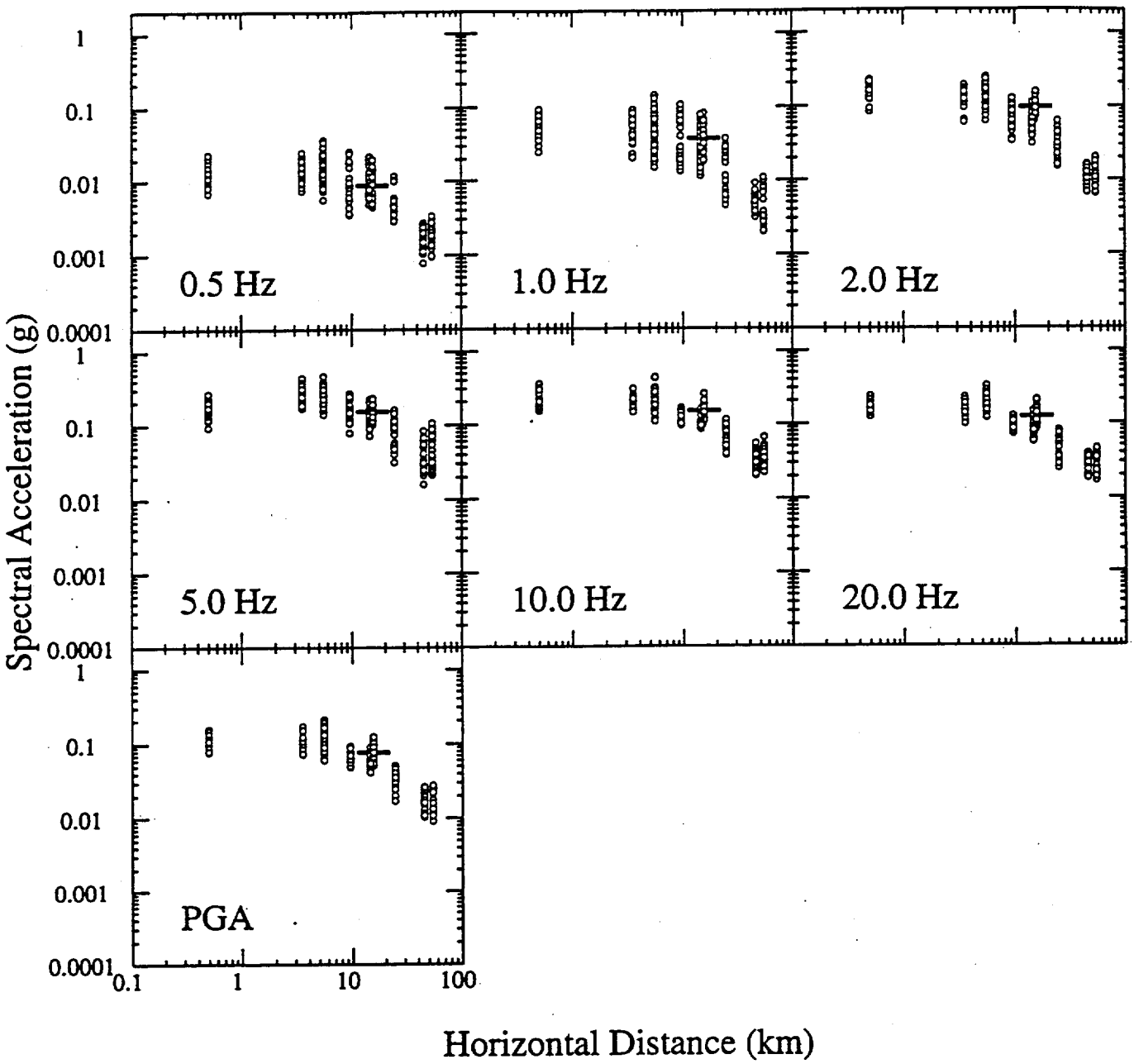

M5.8d, Dip 60.0, Horizontal Components

afsmith0: Fri Jan 31 16:38:38 PST 1997
/tmpb/nancy/Yucca/BroadBand/Atten/./mplot_m5.8d_60_h.cah

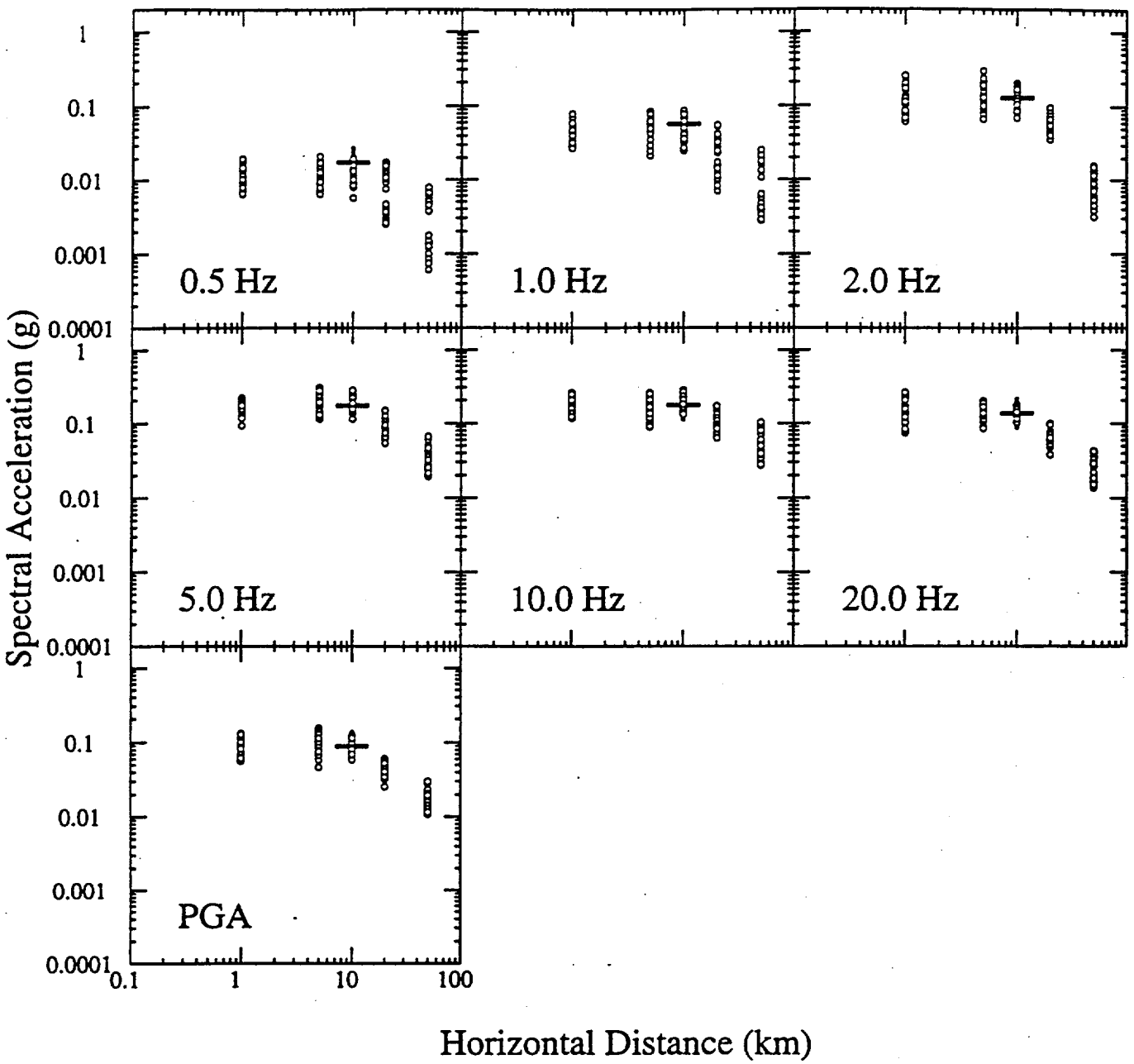

M5.8d, Dip 90.0, Horizontal Components

nfsmith0: Fri Jan 31 16:40:04 PST 1997
/usgs/nancy/Yucca/BroadBand/Asten/./mplot_m5.8d_90_h.csh

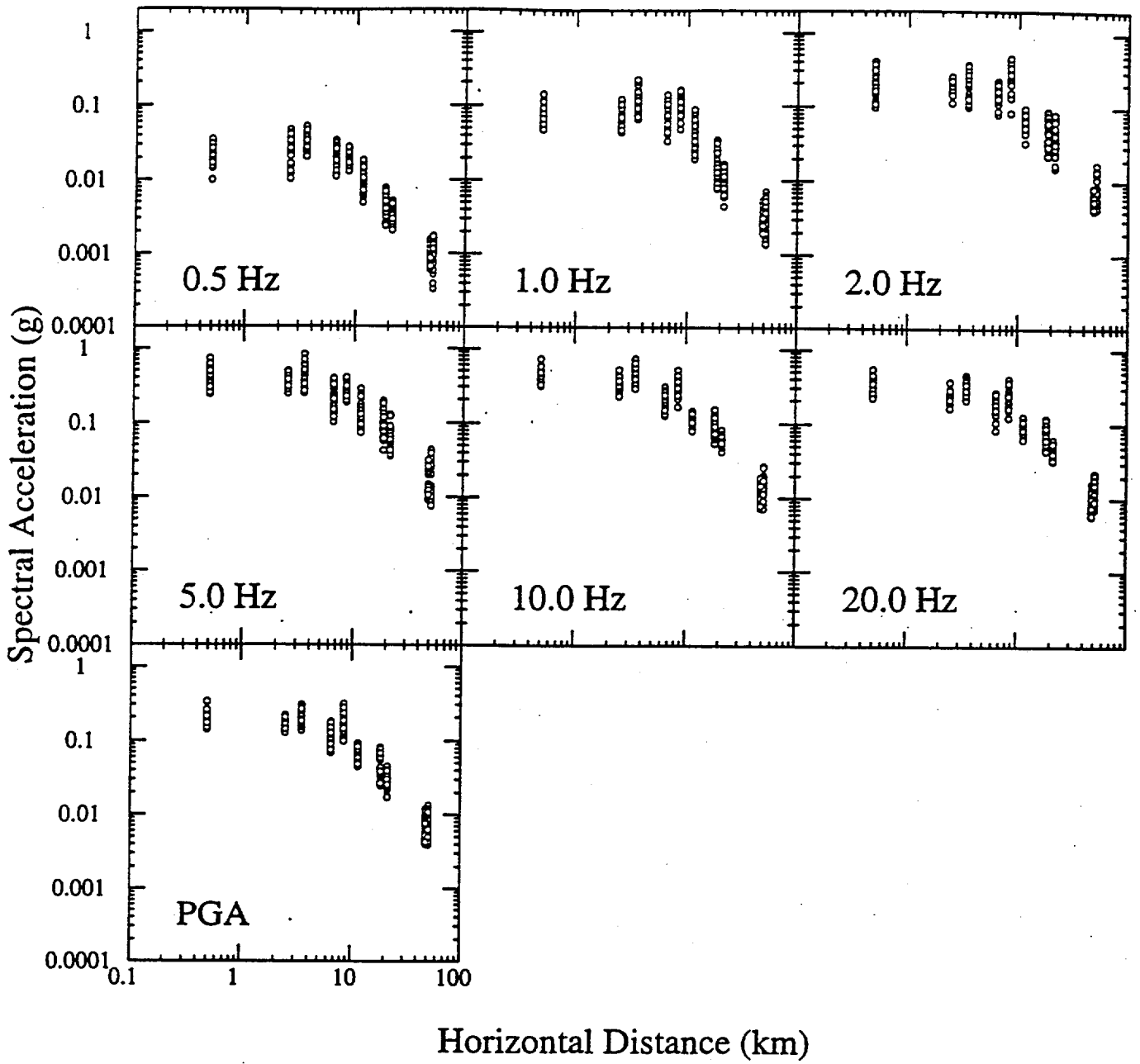

M5.8s, Dip 60.0, Horizontal Components

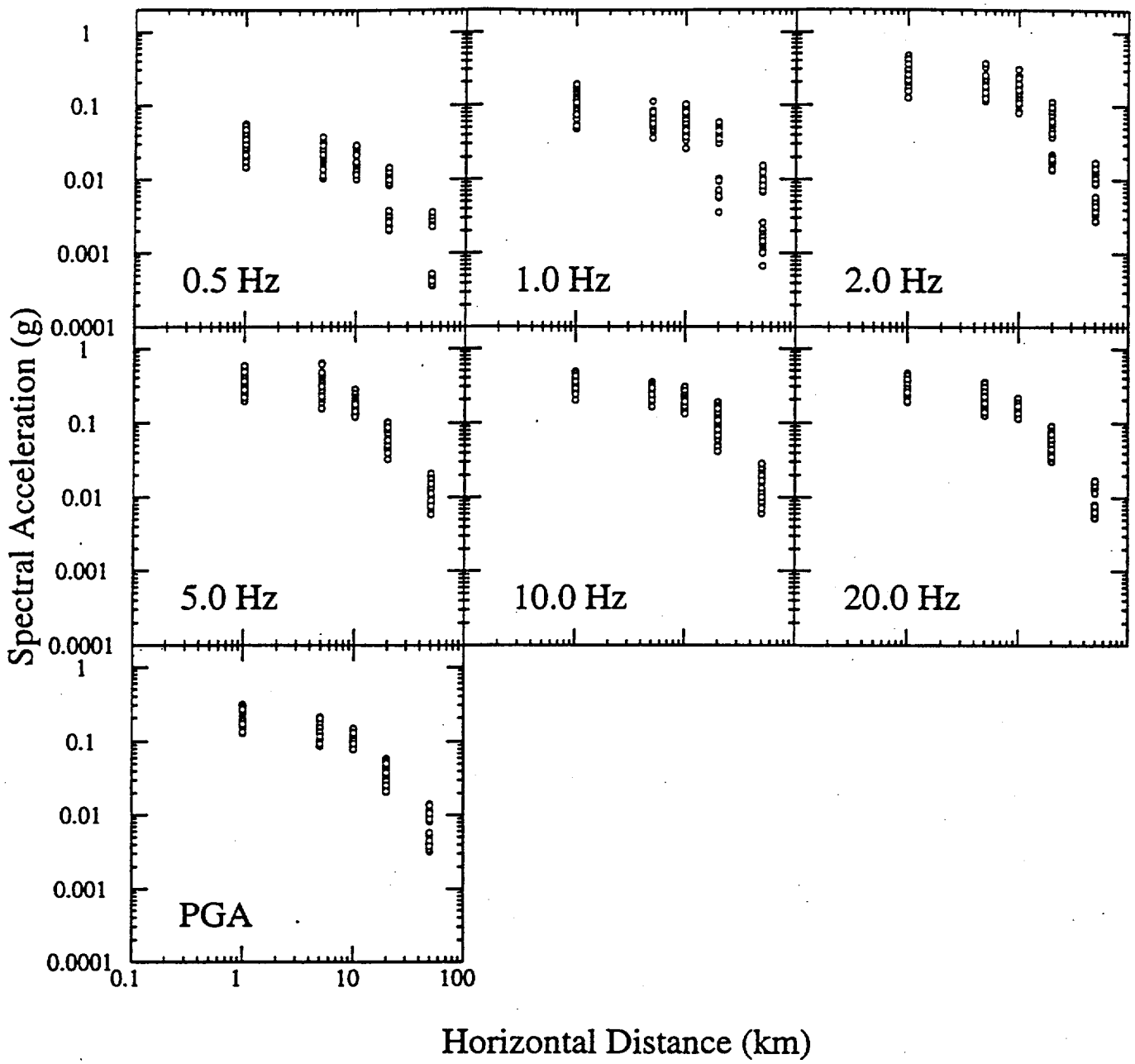

M5.8s, Dip 90.0, Horizontal Components

nfsmith0: Fri Jan 31 16:44:51 PST 1997
/tmpb/nancy/Yucca/BroadBand/Atten/./mplot_m5.8s_90_h.cah

3.1.4-16

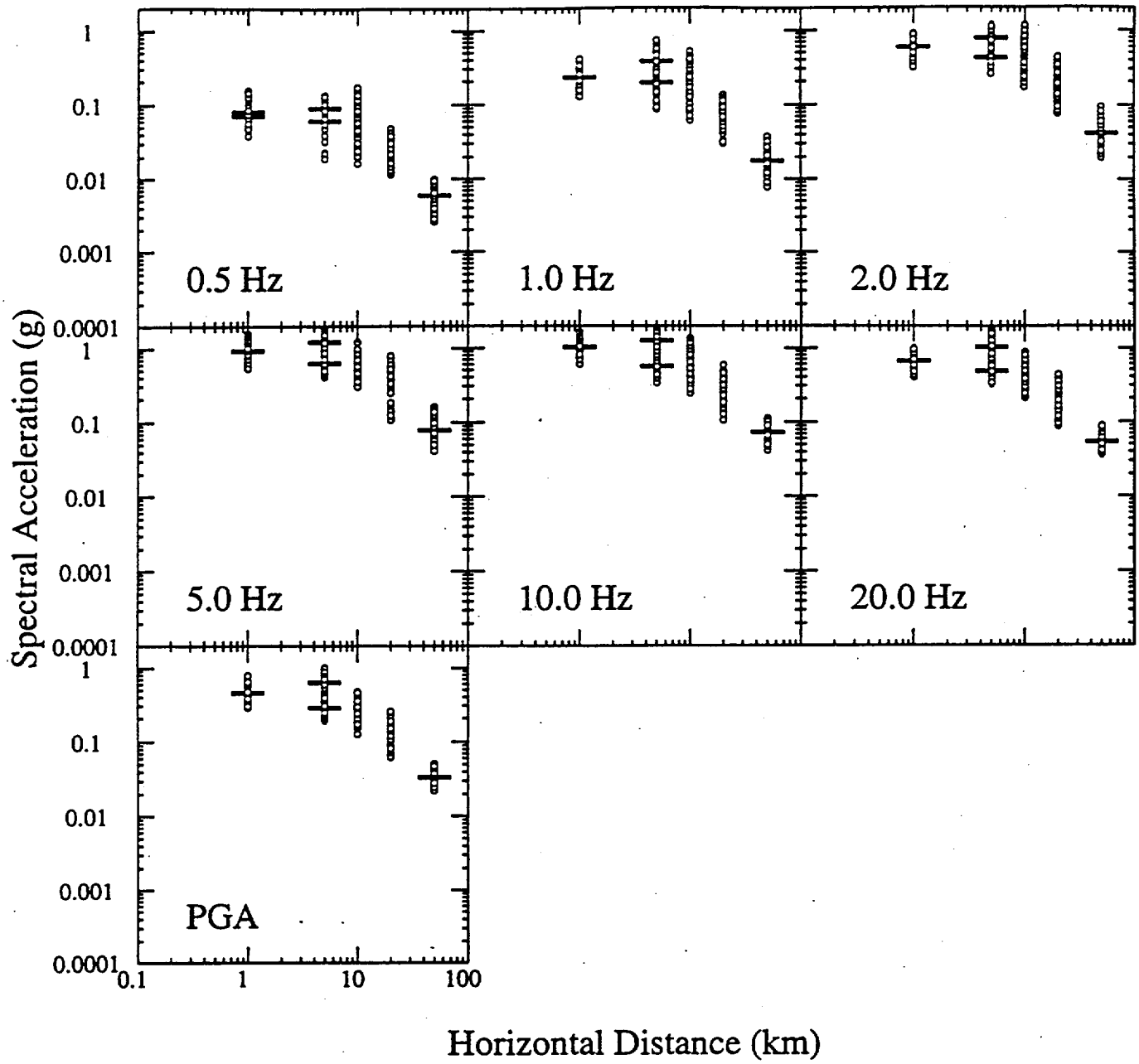

M6.5, Dip 60.0, Horizontal Components

nfsmuh0: Fri Jan 31 17:17:43 PST 1997
/tmpb/nancy/Yucca/BroadBand/Aucs/mplot_m6.5_60_h.csh

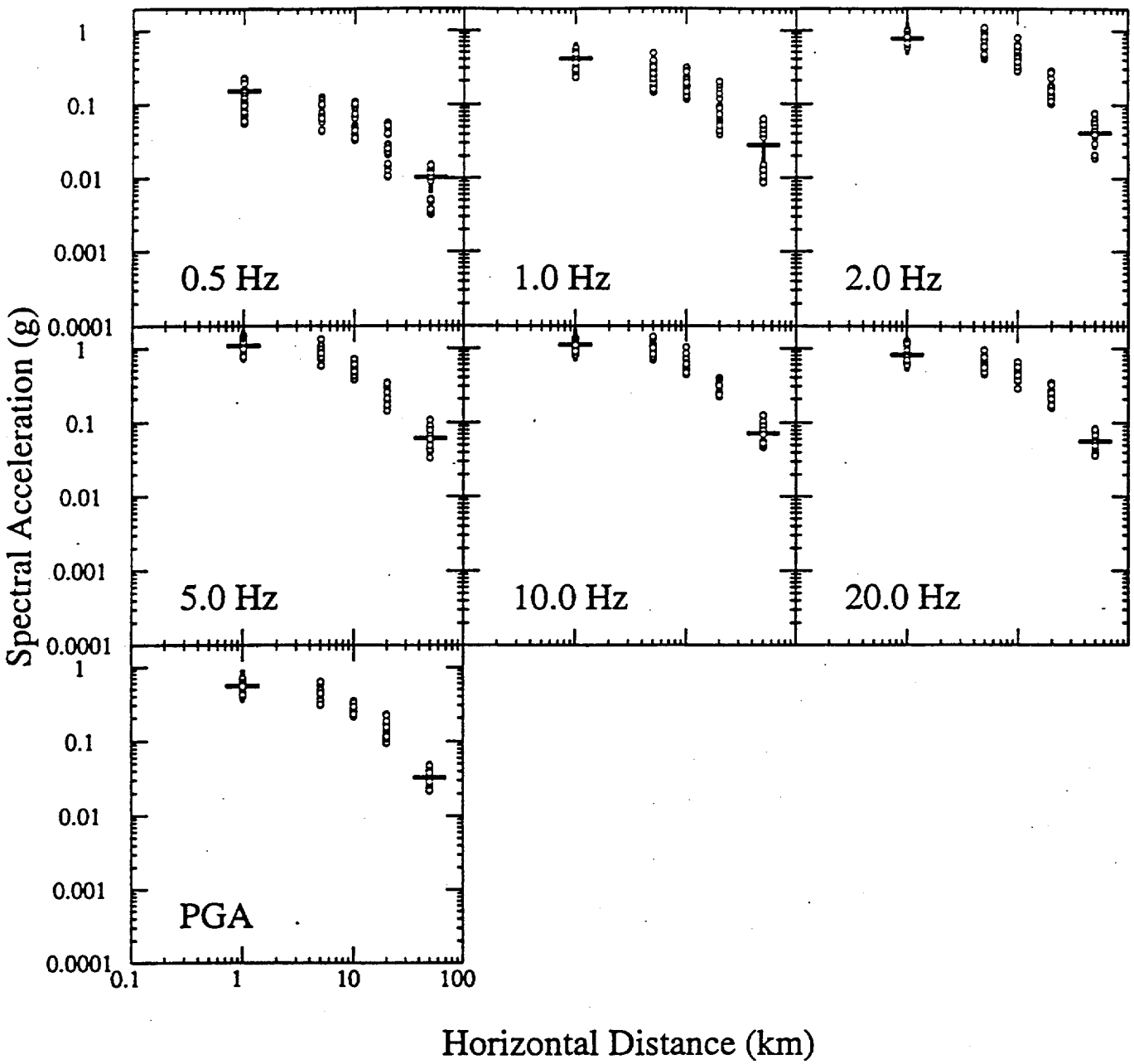

M6.5, Dip 90.0, Horizontal Components

nfsmith0: Fri Jan 31 17:18:24 PST 1997
/usgb/nancy/Yucca/BroadBand/Allen/mplot_m6.5_90_h.csh

Section 3.2

Silva Finite Fault Simulations for "Scenario Eqk Report" Events

3.2 Silva - Scenario earthquake simulations

Silva has repeated the scenario earthquake simulations for the normal faulting cases (N01, N03, N04, N07, N08) using the velocity structure for YM_{300}. These cases and site locations are given in the scenario earthquake report (see Tables 8.4, 8.5, and 8.6 and Figure 8-2 in the scenario earthquake report). N01 is the reference M6.4 event. N03 and N04 are for variations in the dip. N07 and N08 are for variations in the static stress drop. These variations of the simulations are parameterized in terms of the parameteric variability in the following tables.

Numerical Simulation (Silva) (Model 1)
(.5, 1, 2, 5, 10, 20 hz)

Numerical Simulation (Silva) (Model 1) Freq = .5 hz					
			Parametric Aleatory		
Site	N01 Median	Modeling Aleatory	dip	static Δσ	hypo, slip
1	0.13913	.71	.17		0.54743
2	0.14643	.71	.17		0.55421
3	0.10953	.71	.17		0.47319
4	0.12778	.71	.17		0.42962
5	0.07350	.71	.17		0.40146
6	0.02415	.71	.17		0.39609
7	0.11957	.71	.17		0.53078
8	0.10452	.71	.17		0.46069
9	0.08191	.71	.17		0.35055
10	0.08023	.71	.17		0.38889
11	0.02690	.71	.17		0.40705
12	0.01280	.71	.17		0.43094
13	0.10086	.71	.17		0.29140
14	0.04954	.71	.17		0.48379

Numerical Simulation (Silva) (Model 1) Freq = 1 hz					
			Parametric Aleatory		
Site	N01 Median	Modeling Aleatory	dip	static Δσ	hypo, slip
1	0.35004	.80	.16		0.34571
2	0.39094	.80	.16		0.33591
3	0.23563	.80	.16		0.43233
4	0.31213	.80	.16		0.37923
5	0.17045	.80	.16		0.30868
6	0.06655	.80	.16		0.32547
7	0.30388	.80	.16		0.36033
8	0.25819	.80	.16		0.30185
9	0.16677	.80	.16		0.36872
10	0.19120	.80	.16		0.31216
11	0.08736	.80	.16		0.33607
12	0.03648	.80	.16		0.30931
13	0.28418	.80	.16		0.32199
14	0.14260	.80	.16		0.33259

Numerical Simulation (Silva) (Model 1) Freq = 2 hz					
			Parametric Aleatory		
Site	N01 Median	Modeling Aleatory	dip	static $\Delta\sigma$	hypo, slip
1	0.73426	.63	.15		0.39386
2	0.74013	.63	.15		0.32529
3	0.51328	.63	.15		0.27372
4	0.70924	.63	.15		0.33703
5	0.36160	.63	.15		0.33499
6	0.11393	.63	.15		0.27005
7	0.62649	.63	.15		0.31392
8	0.47390	.63	.15		0.27505
9	0.36578	.63	.15		0.26138
10	0.36964	.63	.15		0.27023
11	0.13274	.63	.15		0.23224
12	0.06164	.63	.15		0.32265
13	0.48597	.63	.15		0.27715
14	0.21157	.63	.15		0.27634

Numerical Simulation (Silva) (Model 1) Freq = 5 hz					
			Parametric Aleatory		
Site	N01 Median	Modeling Aleatory	dip	static $\Delta\sigma$	hypo, slip
1	1.46383	.35	.13		0.35173
2	1.51426	.35	.13		0.27804
3	0.89306	.35	.13		0.30130
4	1.42467	.35	.13		0.31540
5	0.63101	.35	.13		0.23787
6	0.18603	.35	.13		0.26232
7	1.18949	.35	.13		0.28787
8	1.01035	.35	.13		0.29464
9	0.72373	.35	.13		0.29915
10	0.73908	.35	.13		0.26408
11	0.22513	.35	.13		0.22378
12	0.11319	.35	.13		0.19990
13	0.92230	.35	.13		0.30005
14	0.38599	.35	.13		0.21240

Numerical Simulation (Silva) (Model 1) Freq = 10 hz					
			Parametric Aleatory		
Site	N01 Median	Modeling Aleatory	dip	static Δσ	hypo, slip
1	1.79633	.38	.12		0.31252
2	1.88558	.38	.12		0.29524
3	1.18375	.38	.12		0.34209
4	1.72773	.38	.12		0.28160
5	0.71683	.38	.12		0.26558
6	0.19186	.38	.12		0.24728
7	1.38717	.38	.12		0.26503
8	1.18530	.38	.12		0.24705
9	0.84814	.38	.12		0.30985
10	0.87158	.38	.12		0.26473
11	0.24765	.38	.12		0.18644
12	0.11744	.38	.12		0.14901
13	1.08335	.38	.12		0.20530
14	0.41901	.38	.12		0.22381

Numerical Simulation (Silva) (Model 1) Freq = 20 hz					
			Parametric Aleatory		
Site	N01 Median	Modeling Aleatory	dip	static Δσ	hypo, slip
1	1.68699	.33	.10		0.36341
2	1.74833	.33	.10		0.27719
3	1.04367	.33	.10		0.29164
4	1.58250	.33	.10		0.26958
5	0.60689	.33	.10		0.24424
6	0.16858	.33	.10		0.20560
7	1.33397	.33	.10		0.29648
8	1.07103	.33	.10		0.25996
9	0.69699	.33	.10		0.27289
10	0.77563	.33	.10		0.21505
11	0.22336	.33	.10		0.15381
12	0.09404	.33	.10		0.14757
13	0.96551	.33	.10		0.20608
14	0.38247	.33	.10		0.17374

Numerical Simulation (Silva) (Model 1) Freq = 100 hz					
			Parametric Aleatory		
Site	N01 Median	Modeling Aleatory	dip	static $\Delta\sigma$	hypo, slip
1	0.83123	.33	.10		0.32954
2	0.87771	.33	.10		0.29222
3	0.51831	.33	.10		0.28893
4	0.78583	.33	.10		0.26911
5	0.32327	.33	.10		0.24932
6	0.09135	.33	.10		0.21946
7	0.66525	.33	.10		0.29090
8	0.54228	.33	.10		0.24685
9	0.36586	.33	.10		0.29009
10	0.39493	.33	.10		0.22810
11	0.11671	.33	.10		0.15827
12	0.05264	.33	.10		0.15167
13	0.49546	.33	.10		0.22342
14	0.19915	.33	.10		0.17691

Section 3.3

Silva Finite Fault Simulations

3.3 Silva - 41 YM Cases

Silva computed all cases required for the project with magnitude ≥ 5.8. These cases are all those shown on page 1.1-4 excepting the magnitude 5.0 cases.

Pacific Engineering: Silva Finite Fault

March 14, 1997

Median Sa-Horizontal Component (g):

REV. 0

Frequency* (Hz)	M_W 5.8								M_W 5.8 Deep			
	SS	HW	FW	SS	HW	FW	SS	HW	HW	FW	SS	HW
	1km	5km	5km	10km	10km	10km	50km	50km	5km	5km	10km	20km
0.30	0.032	0.026	0.014	0.010	0.013	0.007	0.001	0.001	0.018	0.012	0.011	0.007
0.50	0.078	0.075	0.046	0.031	0.046	0.025	0.005	0.004	0.061	0.040	0.030	0.022
1.00	0.303	0.275	0.155	0.135	0.224	0.075	0.017	0.015	0.192	0.121	0.120	0.106
2.00	0.702	0.679	0.305	0.300	0.442	0.174	0.028	0.022	0.392	0.259	0.249	0.233
5.00	1.095	1.040	0.489	0.489	0.710	0.270	0.040	0.039	0.593	0.375	0.412	0.343
10.00	1.308	1.146	0.529	0.471	0.692	0.275	0.034	0.027	0.632	0.393	0.409	0.340
20.00	0.909	0.810	0.379	0.364	0.517	0.200	0.023	0.020	0.448	0.275	0.296	0.236
100.00	0.598	0.537	0.255	0.244	0.348	0.137	0.018	0.015	0.307	0.193	0.203	0.165
PGV** (cm/sec)	35.62	32.23	16.46	14.69	8.75	8.75	1.42	1.93	20.31	13.10	12.71	10.43

*5% damped pseudo absolute response spectra

**Equivalent to PGA

3.3.1-1

Pacific Engineering: Silva Finite Fault

March 14, 1997

Median Sa-Horizontal Component (g):

REV. 0

Frequency* (Hz)	M_W 6.5															
	SS	HW	FW	SS	HW	FW	SS	HW	FW	SS	HW	FW	SS	HW	SS	SS
	1km	1km	1km	5km	5km	5km	10km	10km	10km	20km	20km	20km	50km	50km	100km	160km
0.30	0.056	0.058	0.048	0.045	0.055	0.032	0.031	0.043	0.020	0.014	0.018	0.009	0.008	0.004	0.005	0.004
0.50	0.174	0.150	0.129	0.135	0.144	0.084	0.086	0.129	0.053	0.048	0.062	0.031	0.019	0.013	0.014	0.008
1.00	0.508	0.477	0.402	0.404	0.450	0.266	0.258	0.378	0.159	0.133	0.188	0.090	0.066	0.046	0.043	0.020
2.00	0.875	0.905	0.728	0.690	0.836	0.463	0.469	0.677	0.297	0.265	0.358	0.169	0.102	0.082	0.063	0.029
5.00	1.316	1.492	1.217	1.093	1.425	0.775	0.709	1.090	0.485	0.423	0.568	0.277	0.160	0.120	0.074	0.032
10.00	1.337	1.491	1.157	1.060	1.379	0.730	0.699	1.075	0.466	0.386	0.521	0.239	0.134	0.108	0.056	0.020
20.00	0.980	1.036	0.835	0.761	0.990	0.517	0.492	0.753	0.320	0.249	0.344	0.158	0.085	0.067	0.037	0.015
100.00	0.619	0.668	0.535	0.494	0.633	0.338	0.323	0.491	0.213	0.173	0.238	0.113	0.065	0.050	0.032	0.013
PGV** (cm/sec)	45.51	45.25	37.23	36.17	43.39	25.01	23.48	34.82	14.96	12.06	16.48	8.12	5.19	3.67	3.23	1.61

*5% damped pseudo absolute response spectra

**Equivalent to PGA

Pacific Engineering: Silva Finite Fault

March 14, 1997

Median Sa-Horizontal Component (g):

REV. 0

Frequency* (Hz)	M_W 7.0						M_W 7.5					M 8.0	
	SS	SS	HW	FW	SS	HW	SS	SS	HW	SS	HW	SS	SS
	1 km	10 km	10 km	10 km	50 km	50 km	1 km	10 km	10 km	50 km	50 km	50 km	160 km
0.30	0.085	0.060	0.066	0.036	0.017	0.018	0.096	0.072	0.066	0.031	0.030	0.036	0.022
0.50	0.217	0.145	0.166	0.096	0.040	0.040	0.203	0.160	0.160	0.061	0.061	0.062	0.034
1.00	0.484	0.336	0.413	0.222	0.090	0.106	0.454	0.326	0.356	0.123	0.130	0.115	0.057
2.00	0.873	0.615	0.710	0.389	0.151	0.171	0.847	0.575	0.587	0.200	0.210	0.202	0.082
5.00	1.541	1.035	1.269	0.642	0.223	0.251	1.395	0.966	0.992	0.272	0.290	0.265	0.075
10.00	1.575	1.001	1.261	0.617	0.185	0.216	1.348	0.903	0.932	0.216	0.232	0.195	0.046
20.00	1.030	0.644	0.838	0.396	0.114	0.132	0.862	0.565	0.585	0.133	0.143	0.123	0.035
100.00	0.663	0.426	0.534	0.266	0.088	0.100	0.567	0.383	0.393	0.106	0.113	0.101	0.033
PGV** (cm/sec)	47.24	31.14	38.04	19.97	7.57	8.21	40.50	28.93	29.52	10.09	10.39	9.96	5.01

*5% damped pseudo absolute response spectra

**Equivalent to PGA

3.3.1-3

Pacific Engineering: Silva Finite Fault

March 14, 1997

Total Parametric Variability about Median Sa - Horizontal Component:

REV. 0

Frequency* (Hz)	M_W 5.8								M_W 5.8 Deep			
	SS	HW	FW	SS	HW	FW	SS	HW	HW	FW	SS	HW
	1km	5km	5km	10km	10km	10km	50km	50km	5km	5km	10km	20km
0.30	0.303	0.387	0.354	0.339	0.261	0.373	0.276	0.351	0.347	0.374	0.301	0.333
0.50	0.490	0.474	0.398	0.479	0.437	0.322	0.280	0.344	0.406	0.377	0.389	0.466
1.00	0.453	0.437	0.414	0.418	0.352	0.401	0.303	0.337	0.447	0.421	0.337	0.366
2.00	0.375	0.323	0.296	0.299	0.262	0.345	0.288	0.227	0.337	0.353	0.283	0.286
5.00	0.219	0.214	0.188	0.225	0.211	0.194	0.230	0.185	0.192	0.218	0.218	0.164
10.00	0.259	0.254	0.238	0.218	0.183	0.199	0.172	0.137	0.206	0.180	0.171	0.132
20.00	0.226	0.233	0.210	0.238	0.207	0.201	0.166	0.134	0.188	0.166	0.159	0.117
100.00**	0.223	0.227	0.202	0.232	0.200	0.203	0.175	0.136	0.198	0.181	0.149	0.122
PGV (cm/sec)	0.232	0.243	0.236	0.234	0.208	0.208	0.212	0.248	0.213	0.204	0.134	0.143

*5% damped pseudo absolute response spectra

**Equivalent to PGA

***Total Modeling Sigma: Computed over 15 earthquakes of M 5.8 to 7.4 at 487 sites and a fault distance range of about 1 to 500 km

3.3.1-4

Pacific Engineering: Silva Finite Fault

March 14, 1997

Total Parametric Variability about Median Sa - Horizontal Component:

REV. 0

Frequency* (Hz)	M_W 6.5															
	SS	HW	FW	SS	HW	FW	SS	HW	FW	SS	HW	FW	SS	HW	SS	SS
	1km	1km	1km	5km	5km	5km	10km	10km	10km	20km	20km	20km	50km	50km	100km	160km
0.30	0.414	0.460	0.460	0.415	0.476	0.433	0.428	0.467	0.407	0.326	0.305	0.361	0.354	0.359	0.313	0.393
0.50	0.378	0.382	0.394	0.419	0.394	0.427	0.442	0.480	0.371	0.382	0.403	0.429	0.305	0.300	0.221	0.209
1.00	0.389	0.477	0.464	0.414	0.425	0.434	0.448	0.463	0.400	0.322	0.306	0.350	0.380	0.242	0.239	0.223
2.00	0.375	0.431	0.428	0.373	0.427	0.429	0.378	0.380	0.335	0.304	0.346	0.326	0.299	0.215	0.161	0.196
5.00	0.337	0.433	0.415	0.339	0.415	0.365	0.328	0.350	0.314	0.307	0.318	0.322	0.240	0.172	0.134	0.136
10.00	0.324	0.436	0.421	0.350	0.425	0.388	0.312	0.349	0.270	0.271	0.265	0.288	0.230	0.143	0.125	0.112
20.00	0.320	0.436	0.427	0.336	0.415	0.382	0.323	0.369	0.292	0.288	0.278	0.287	0.230	0.104	0.110	0.113
100.00**	0.311	0.434	0.424	0.333	0.413	0.378	0.322	0.356	0.290	0.277	0.290	0.294	0.222	0.106	0.111	0.112
PGV (cm/sec)	0.309	0.401	0.392	0.334	0.387	0.355	0.343	0.381	0.310	0.262	0.271	0.295	0.214	0.140	0.142	0.164

*5% damped pseudo absolute response spectra

**Equivalent to PGA

***Total Modeling Sigma: Computed over 15 earthquakes of M 5.8 to 7.4 at 487 sites and a fault distance range of about 1 to 500 km

3.3.1-5

Pacific Engineering: Silva Finite Fault

March 14, 1997

Total Parametric Variability about Median Sa - Horizontal Component:

REV. 0

Frequency* (Hz)	M_W 7.0						M_W 7.5					M 8.0		
	SS	SS	HW	FW	SS	HW	SS	SS	HW	SS	HW	SS	SS	***
	1km	10km	10km	10km	50km	50km	1km	10km	10km	50km	50km	50km	160km	
0.30	0.497	0.407	0.508	0.438	0.317	0.338	0.633	0.531	0.609	0.343	0.303	0.377	0.350	0.86
0.50	0.442	0.415	0.469	0.399	0.300	0.299	0.676	0.586	0.644	0.344	0.266	0.422	0.365	0.79
1.00	0.482	0.440	0.482	0.416	0.261	0.265	0.731	0.604	0.718	0.325	0.291	0.462	0.440	0.69
2.00	0.456	0.406	0.399	0.394	0.247	0.256	0.742	0.641	0.723	0.305	0.265	0.565	0.505	0.66
5.00	0.454	0.394	0.382	0.351	0.233	0.222	0.766	0.722	0.756	0.361	0.311	0.675	0.596	0.60
10.00	0.452	0.411	0.418	0.385	0.249	0.223	0.823	0.761	0.818	0.400	0.352	0.718	0.578	0.57
20.00	0.452	0.408	0.414	0.387	0.250	0.227	0.843	0.772	0.826	0.382	0.339	0.668	0.525	0.53
100.00**	0.436	0.395	0.399	0.371	0.236	0.218	0.790	0.712	0.769	0.351	0.308	0.621	0.513	0.52
PGV (cm/sec)	0.415	0.340	0.382	0.355	0.236	0.217	0.694	0.599	0.676	0.306	0.265	0.443	0.384	0.69

*5% damped pseudo absolute response spectra

**Equivalent to PGA

***Total Modeling Sigma: Computed over 15 earthquakes of M 5.8 to 7.4 at 487 sites and a fault distance range of about 1 to 500 km

3.3.1-6

Section 3.3.2

Modeling Uncertainty for Silva Finite Fault Simulations

(see Section 13 for additional discussion)

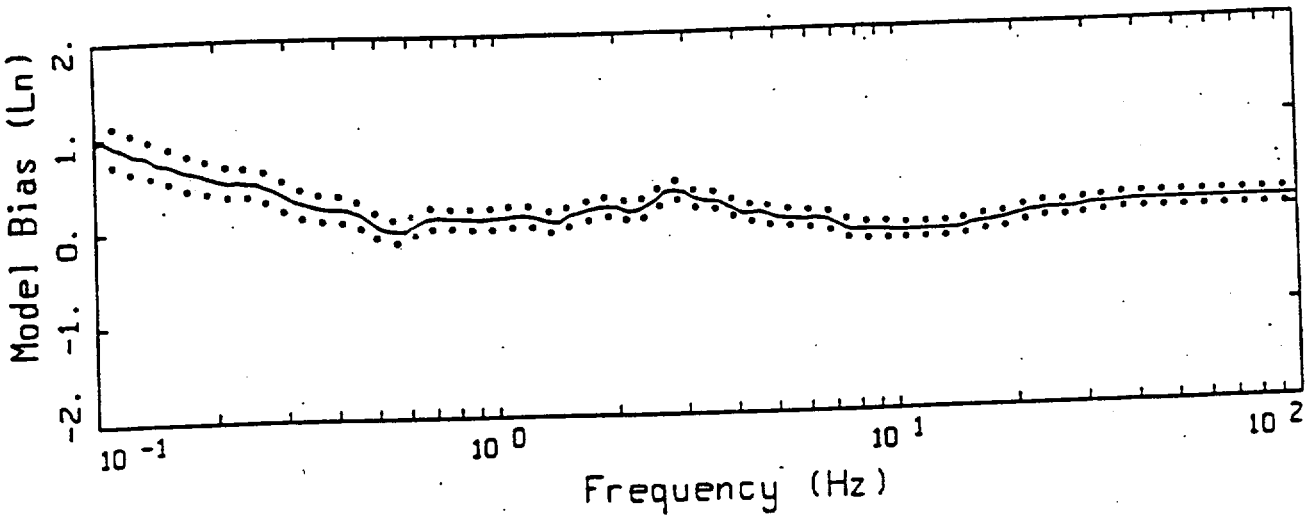

LEGEND

——— MODELING BIAS

..... 90% CONFIDENCE INTERVAL OF MODELING BIAS

..... 90% CONFIDENCE INTERVAL OF MODELING BIAS

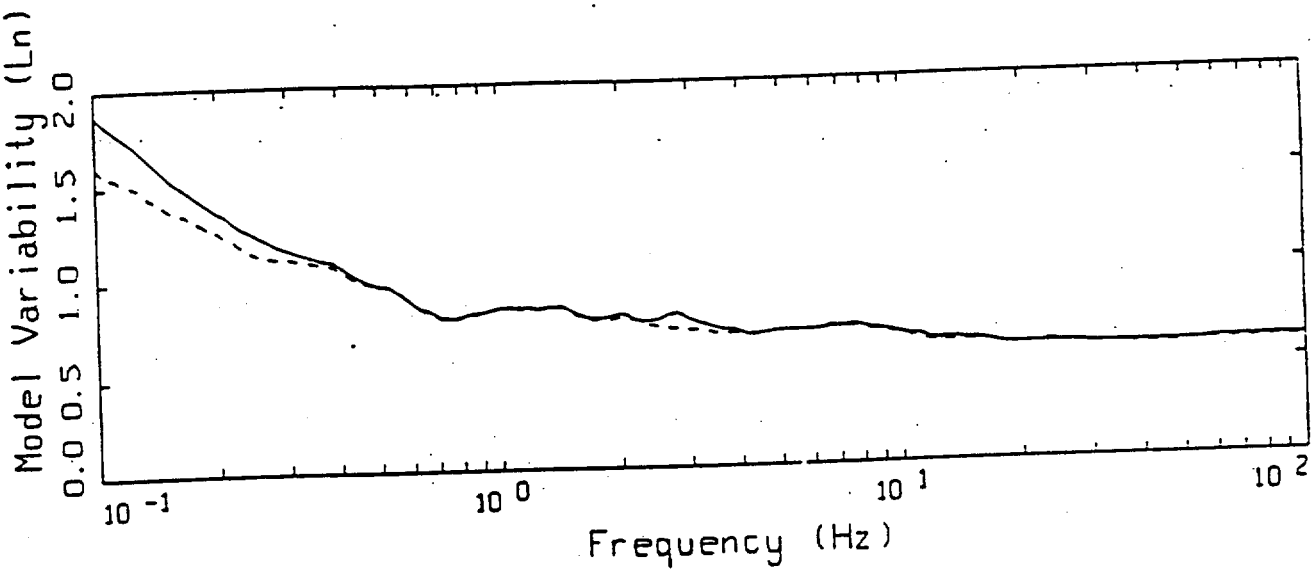

LEGEND

——— MEAN=0.0

------ BIAS CORRECTED

15 EARTHQUAKES FINITE-SOURCE
NONLINEAR, ALL 159 ROCK SITES

Figure 5.157

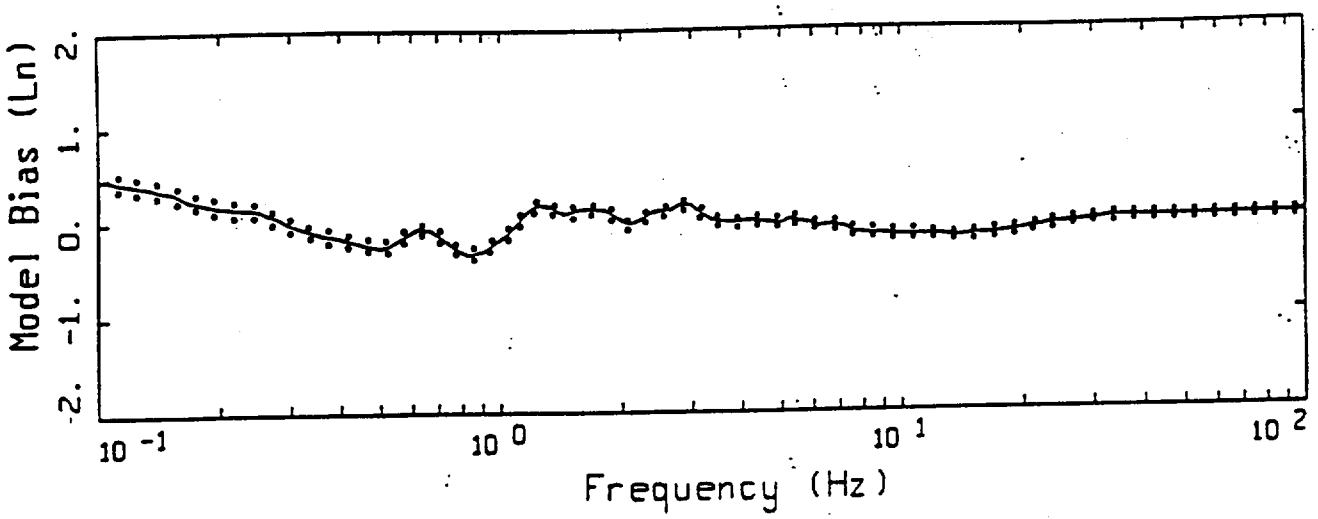

LEGEND

——— MODELING BIAS

..... 90% CONFIDENCE INTERVAL OF MODELING BIAS

..... 90% CONFIDENCE INTERVAL OF MODELING BIAS

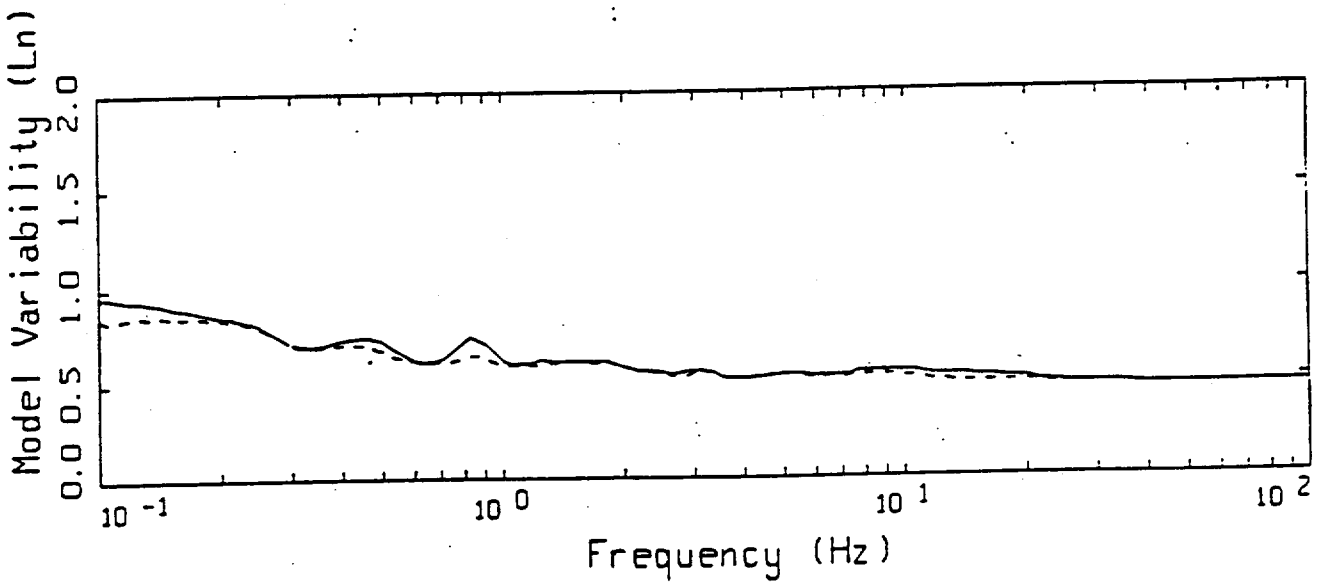

LEGEND

——— MEAN=0.0

------ BIAS CORRECTED

15 EARTHQUAKES FINITE-SOURCE
NONLINEAR, ALL 328 SOIL SITES

Figure 5.156

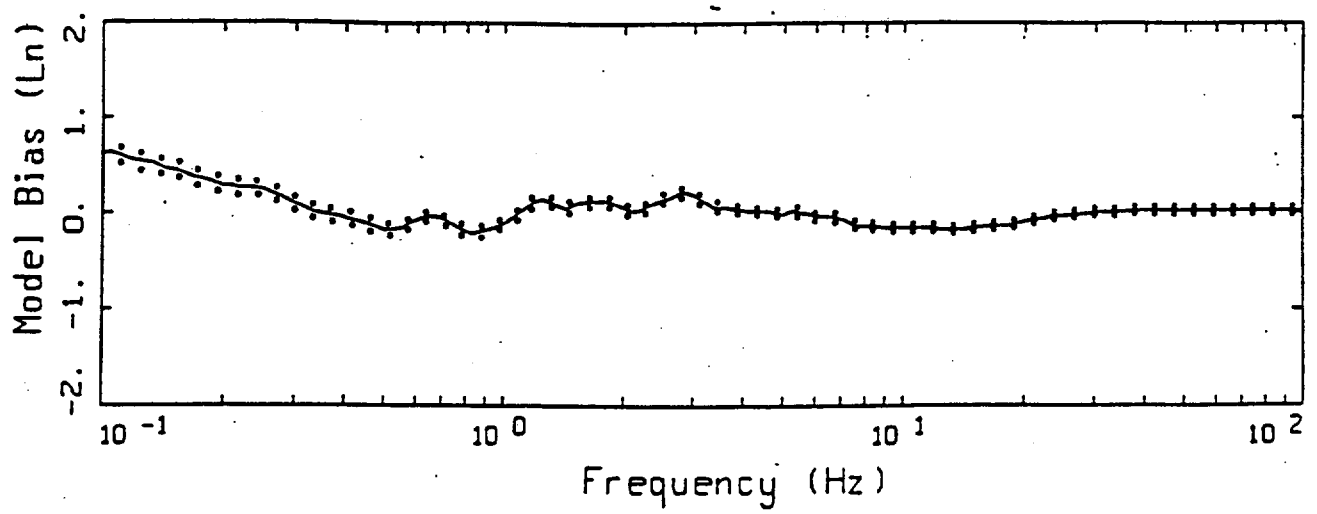

LEGEND
——— MODELING BIAS
..... 90% CONFIDENCE INTERVAL OF MODELING BIAS
..... 90% CONFIDENCE INTERVAL OF MODELING BIAS

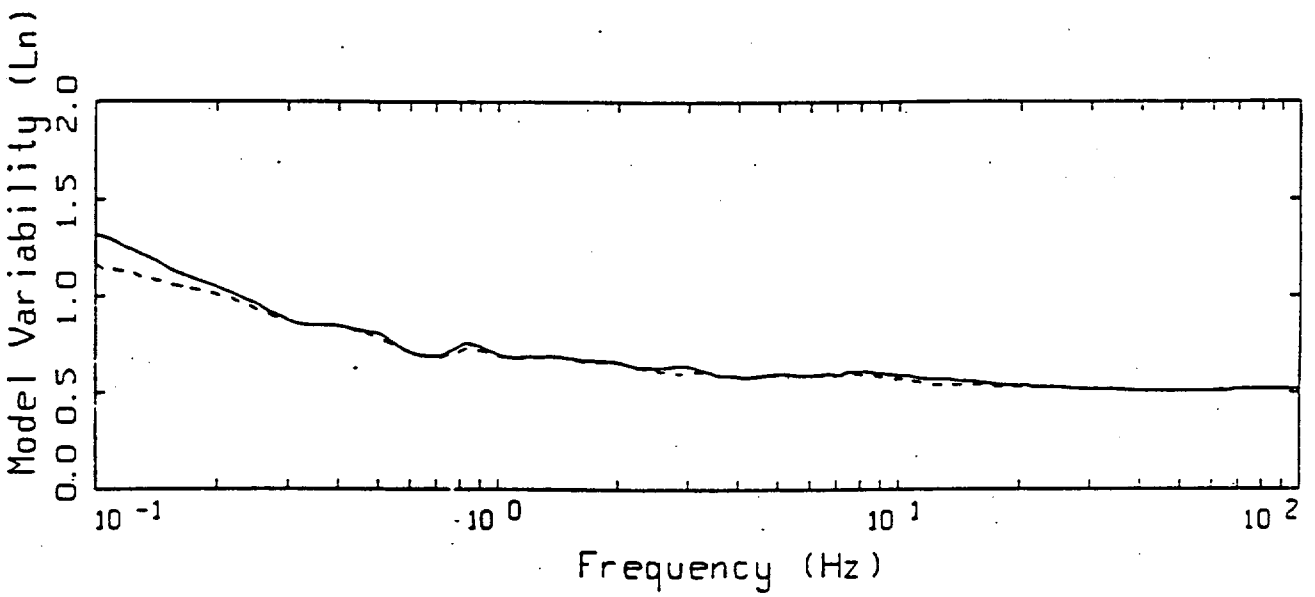

LEGEND
——— MEAN=0.0
------ BIAS CORRECTED

15 EARTHQUAKES FINITE-SOURCE
NONLINEAR, ALL 487 SITES

Figure 5.155

Section 3.4

Anderson and Zeng Simulations

March 10, 1997

Revised Synthetics for Yucca Mountain Earthquake Scenarios

Yuehua Zeng and John G. Anderson

Seismological Laboratory /174, University of Nevada, Reno Nevada 89557.

Contents

1. List of 16 Cases

2. Plots of the Source-receiver Geometry

3. Description of Model Parameters

4. Table of PGA, PGV and Their Standard Errors

5. Table of SA and Their Standard Errors

6. Plots of SA vs. Frequency

7. Plots of PSV vs. Frequency

1. List of 16 Cases

Case	M	Depth	Fault Type	R_h	R_{rup}	R_{JB}
1	5.0	shallow	Strike-Slip	1.0	3.64	1.0
2	5.0	shallow	Normal (HW)	1.0	3.76	0.84
3	5.0	deep	Strike-Slip	5.0	11.63	5.0
4	5.0	deep	Normal (HW)	5.0	10.66	0.34
5	5.8	deep	Strike-Slip	10.0	12.21	10.0
6	5.8	deep	Normal (HW)	20.0	17.89	12.99
7	6.5	shallow	Strike-Slip	1.0	1.0	1.0
8	6.5	shallow	Normal (HW)	1.0	0.89	0.0
9	6.5	shallow	Normal (FW)	1.0	1.0	1.0
10	6.5	shallow	Normal (HW)	5.0	4.47	0.0
11	6.5	shallow	Normal (FW)	5.0	5.0	5.0
12	6.5	shallow	Strike-Slip	50.0	50.0	50.0
13	6.5	shallow	Normal (HW)	50.0	45.97	44.76
14	7.0	shallow	Strike-Slip	10.0	10.0	10.0
15	7.5	shallow	Strike-Slip	50.0	50.0	50.0
16	7.5	shallow	Normal (HW)	50.0	45.21	42.99

R_h: horizontal distance (km) from surface trace of "fault"
R_{rup}: closest distance to the rupture plane
R_{JB}: closest distance to the surface projection of rupture plane

2. Plots of the Source-receiver Geometry

Map View (case 1)

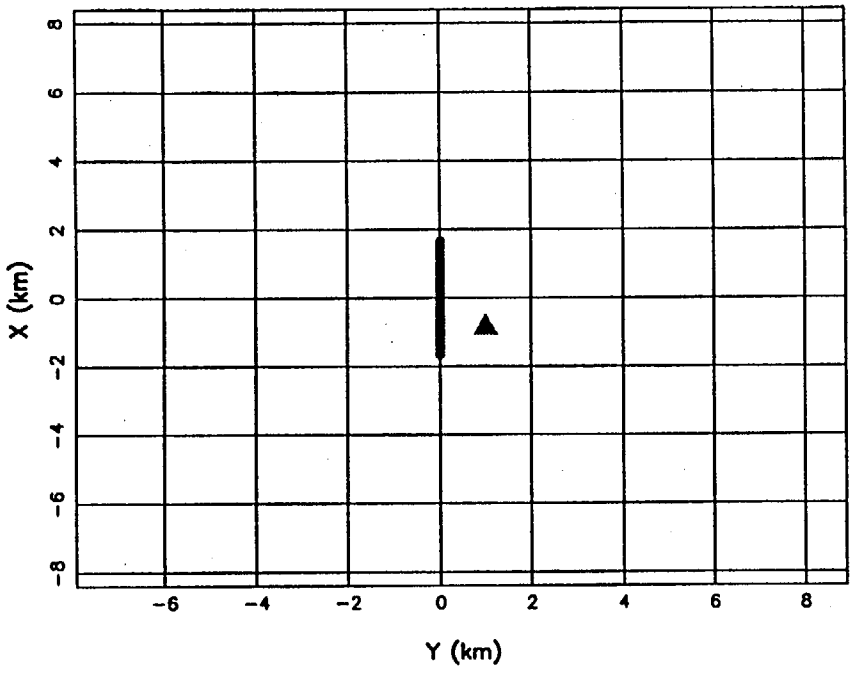

Cross View

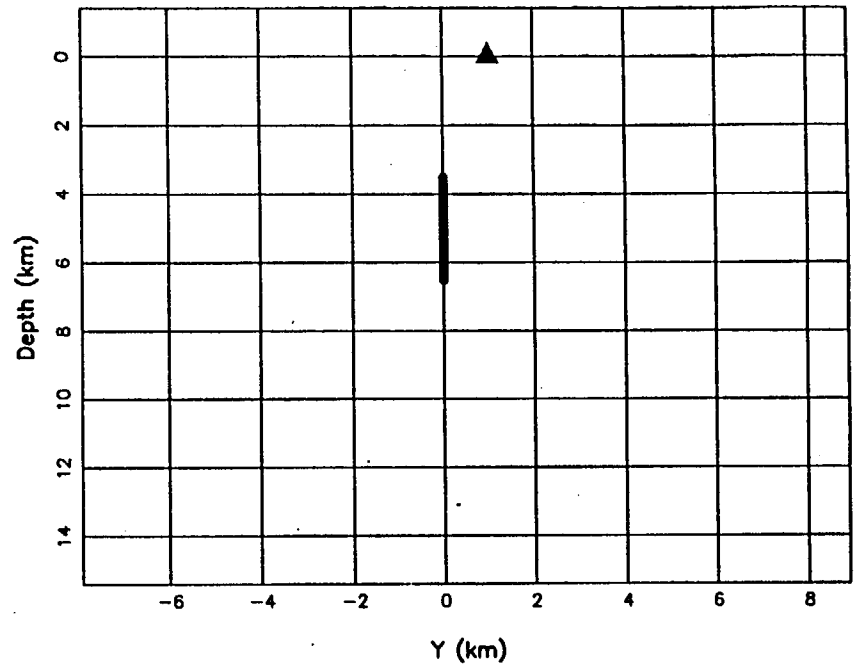

Map View (case 2)

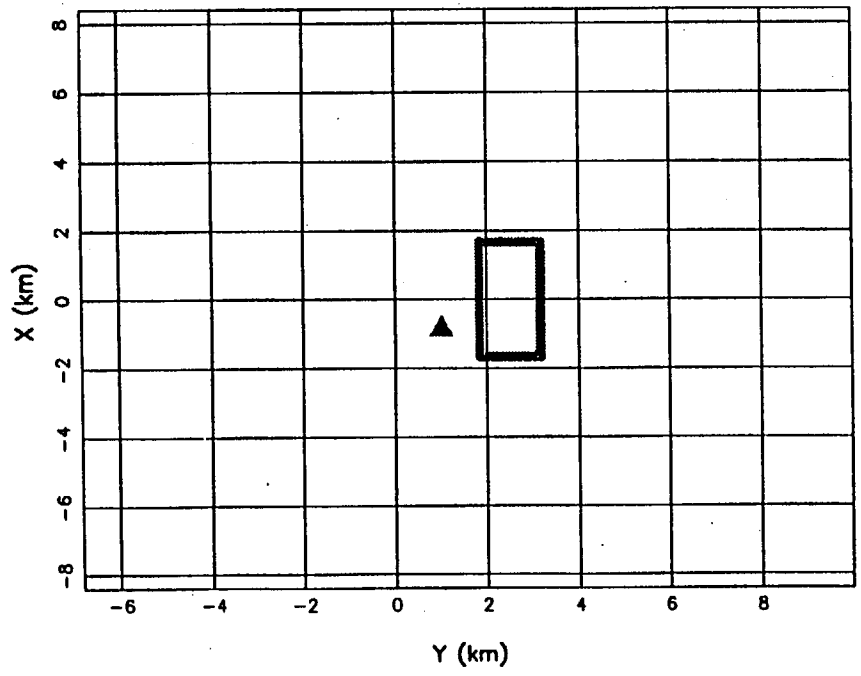

Cross View

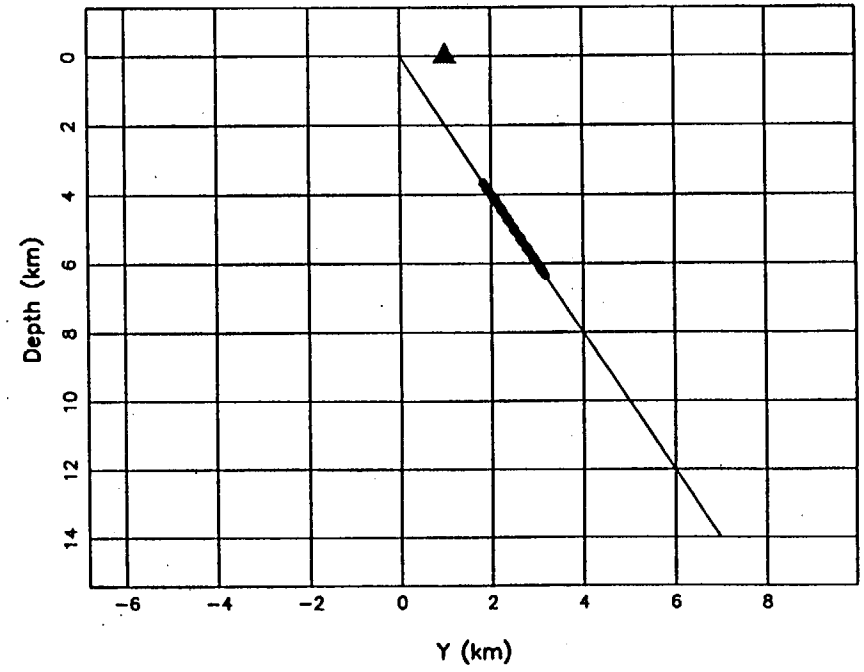

3.4.1-4

Map View (case 3)

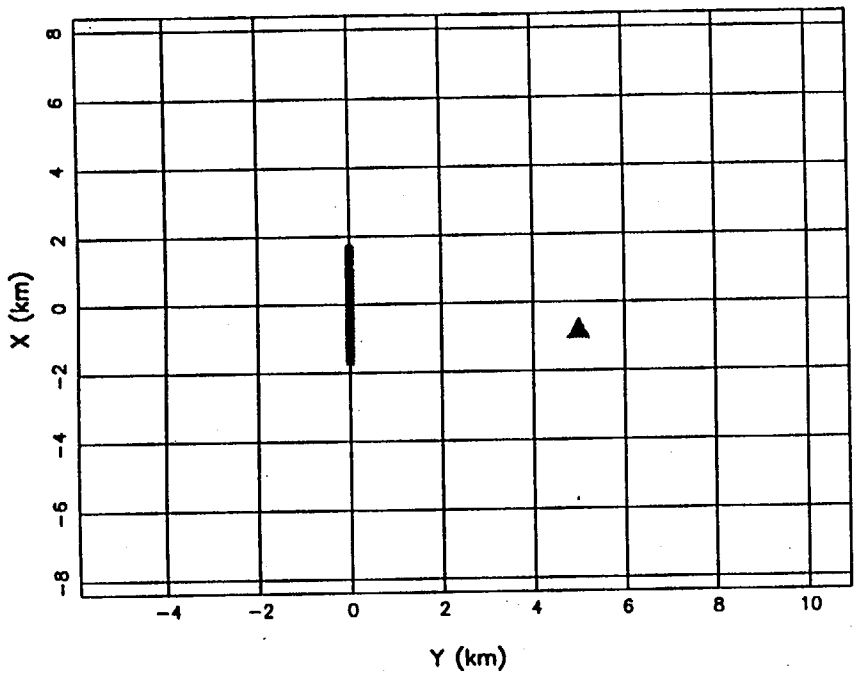

Cross View

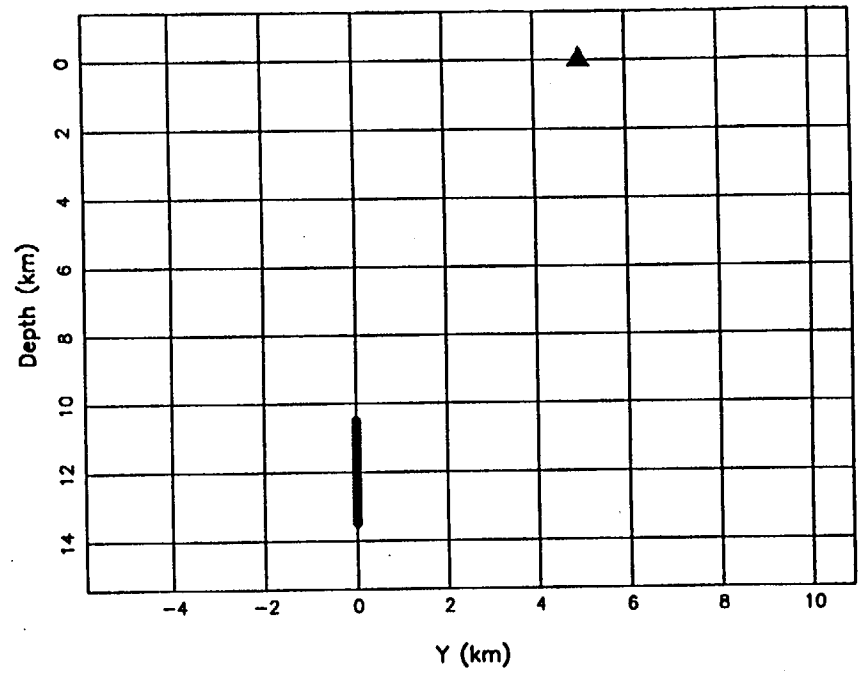

Map View (case 4)

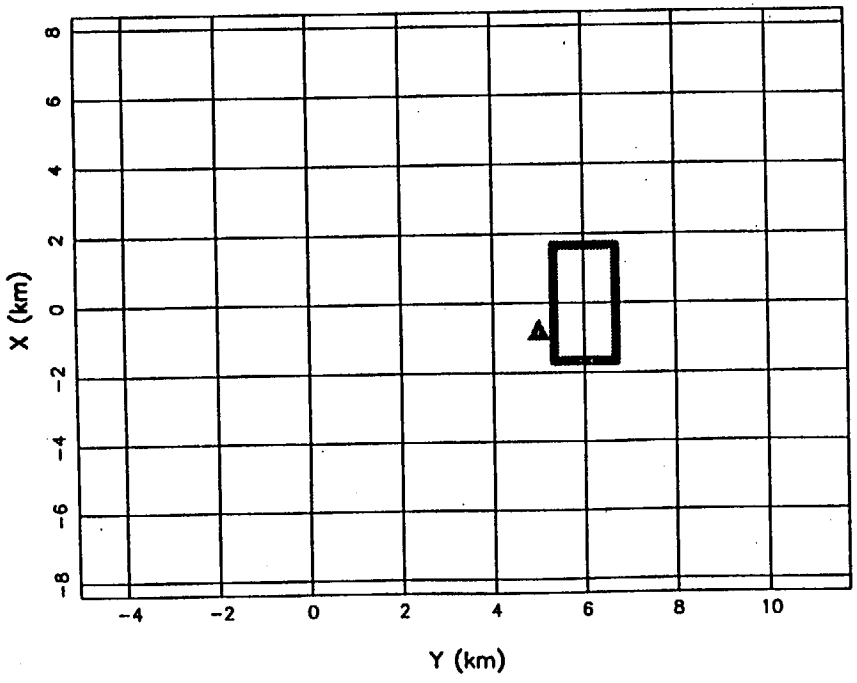

Cross View

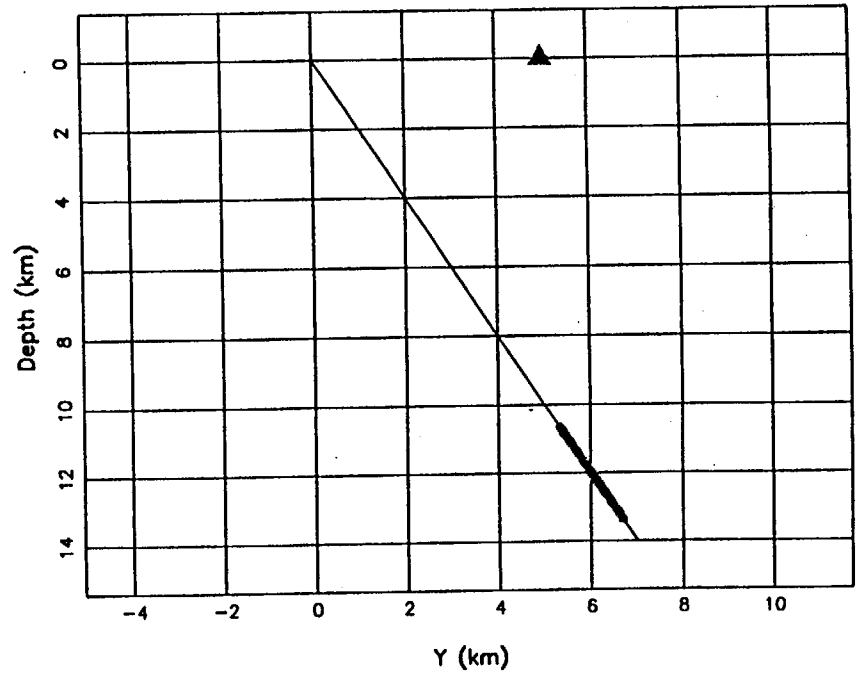

3.4.1-5

Map View (case 5)

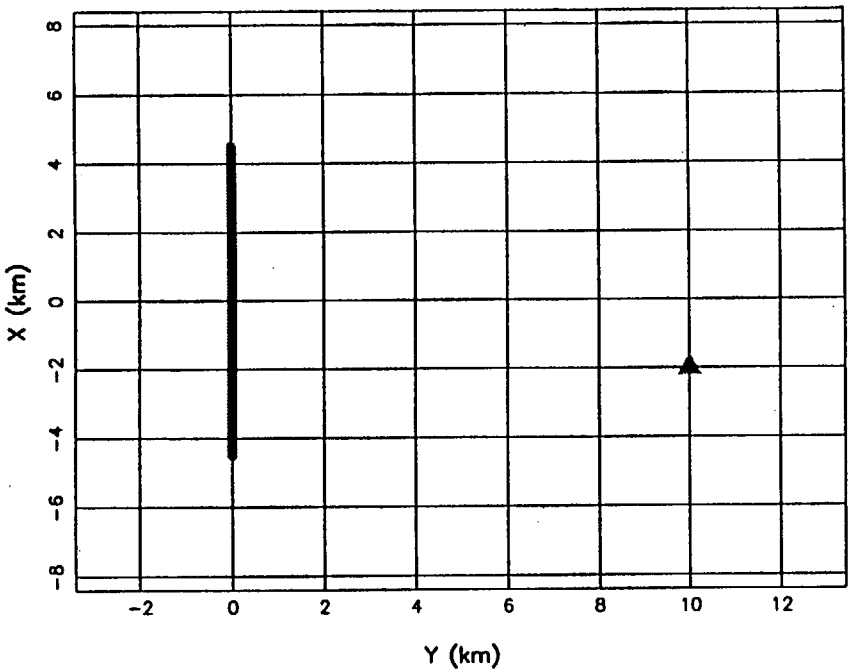

Cross View

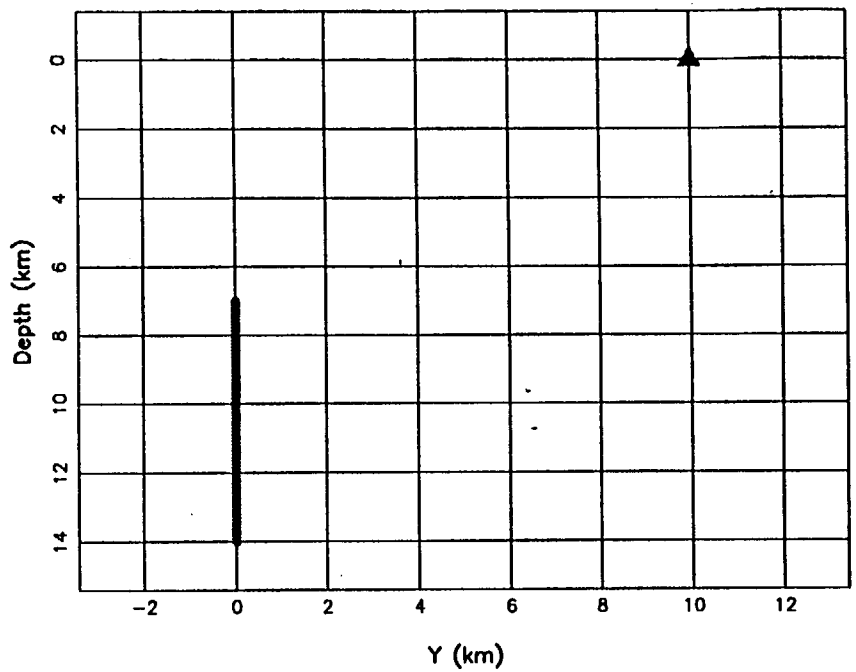

Map View (case 6)

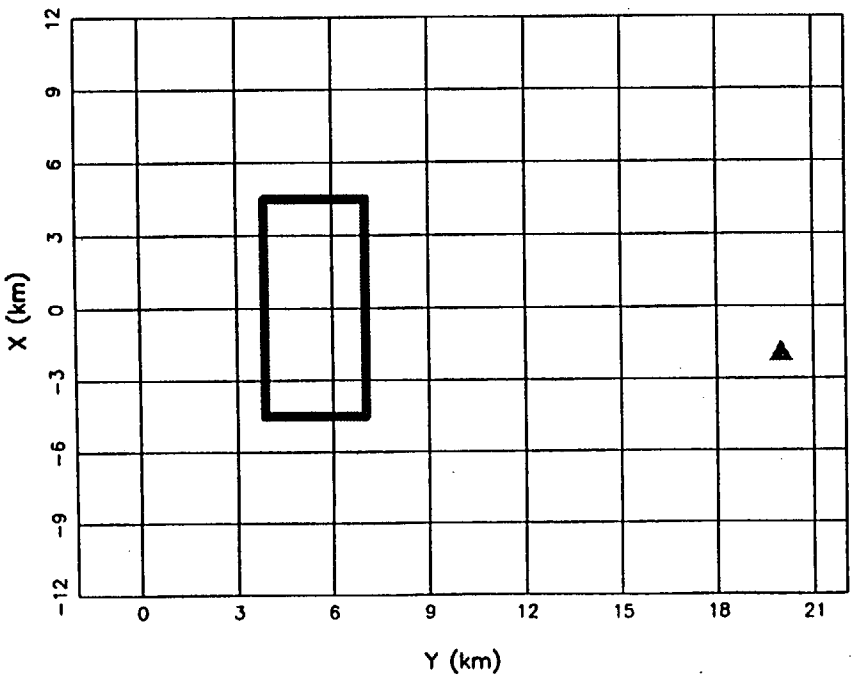

Cross View

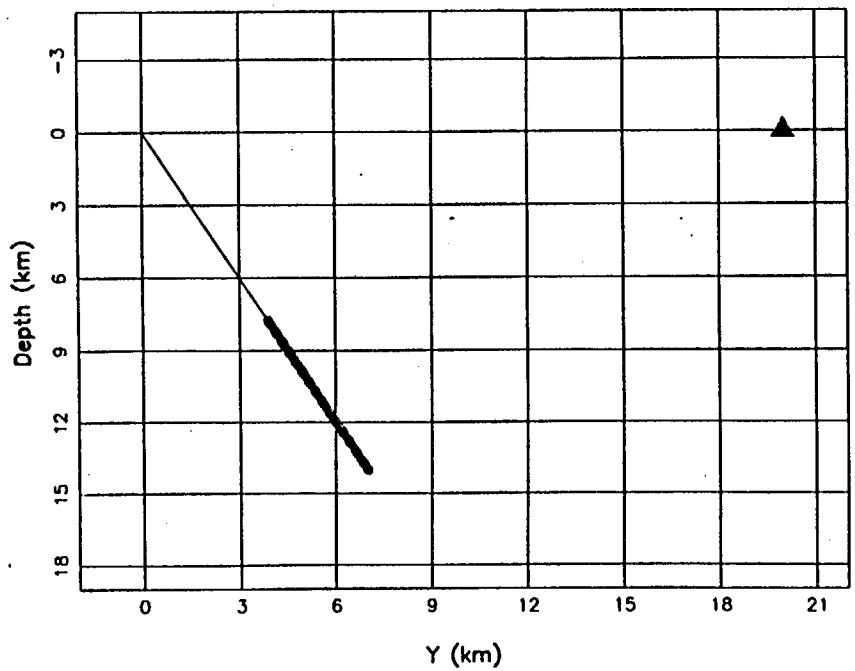

3.4.1-6

Map View (case 7)

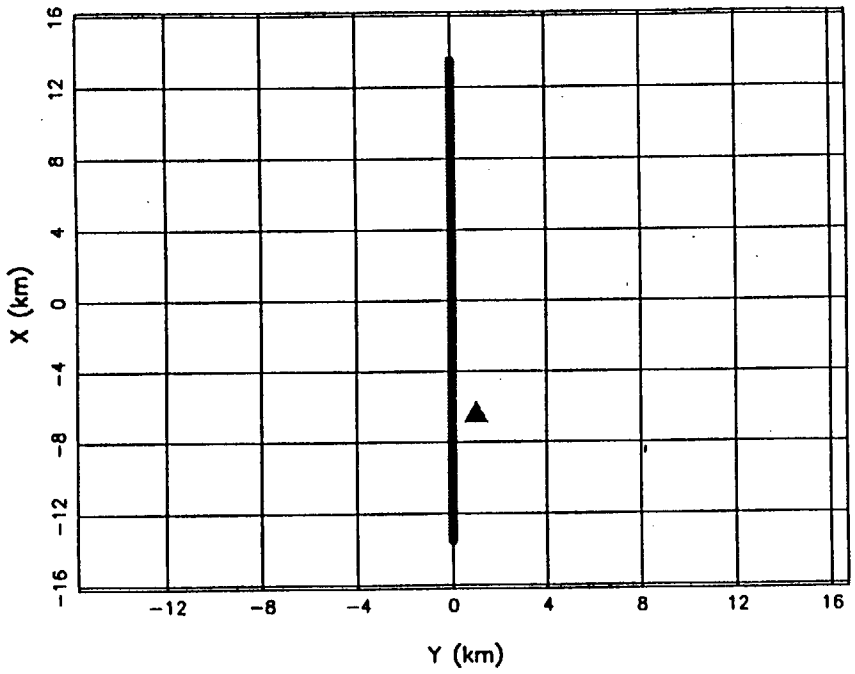

Cross View

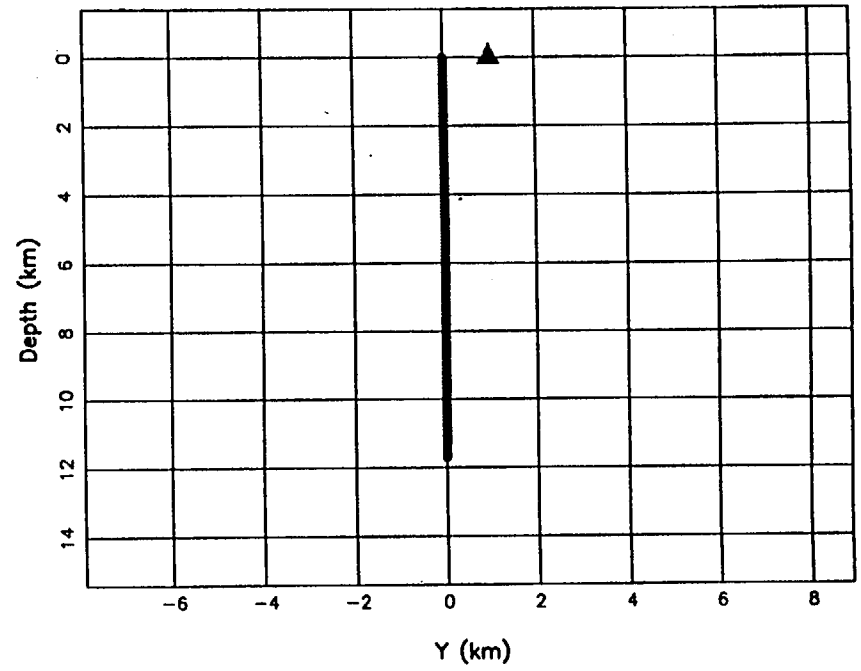

Map View (case 8)

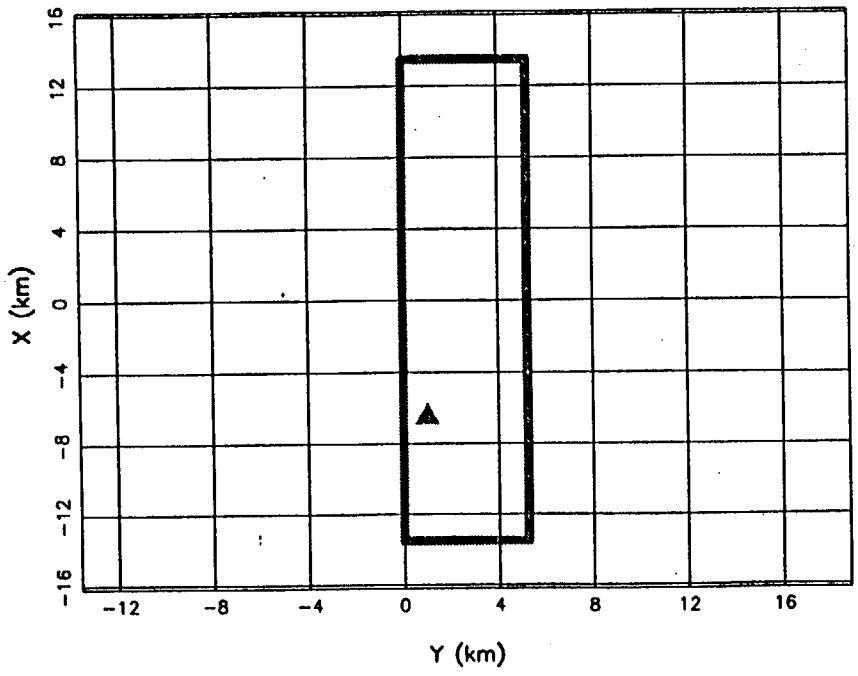

Cross View

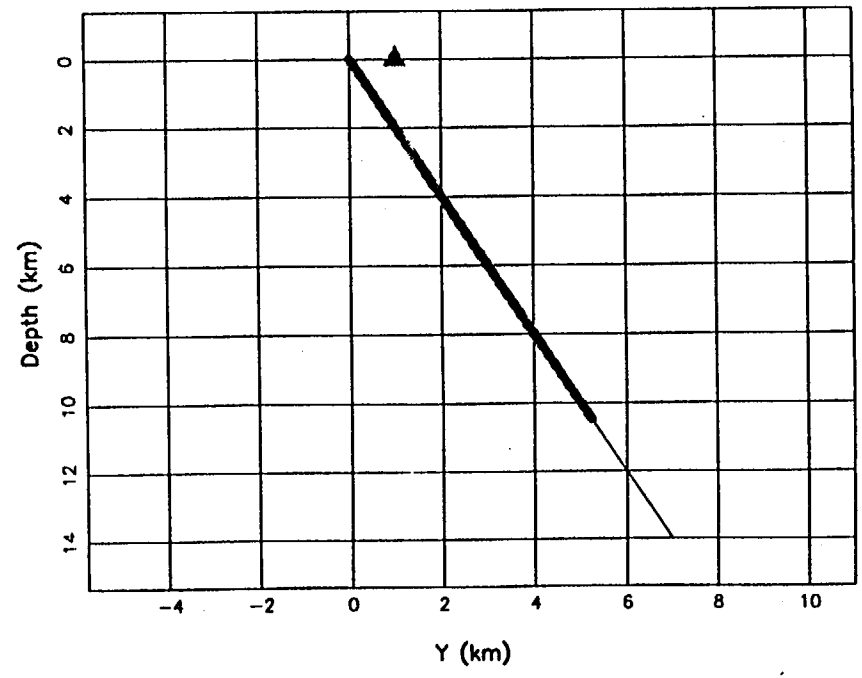

3.4.1-7

Map View (case 1)

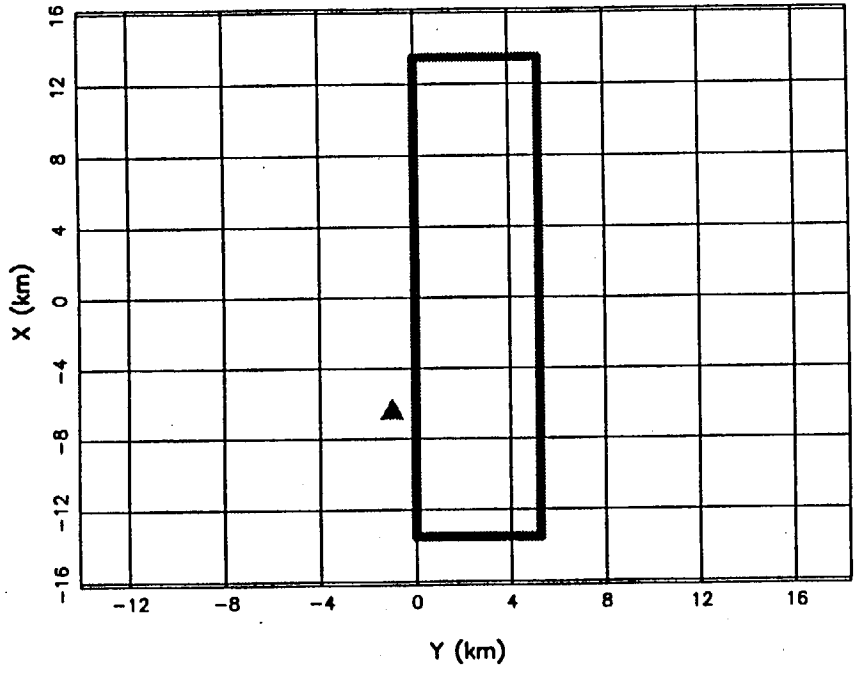

Cross View

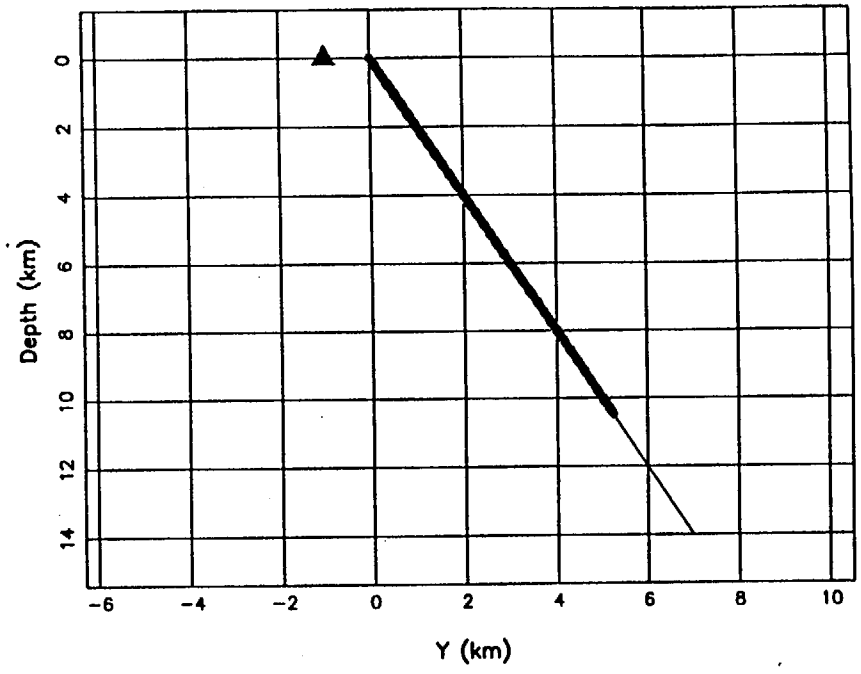

Map View (case 2)

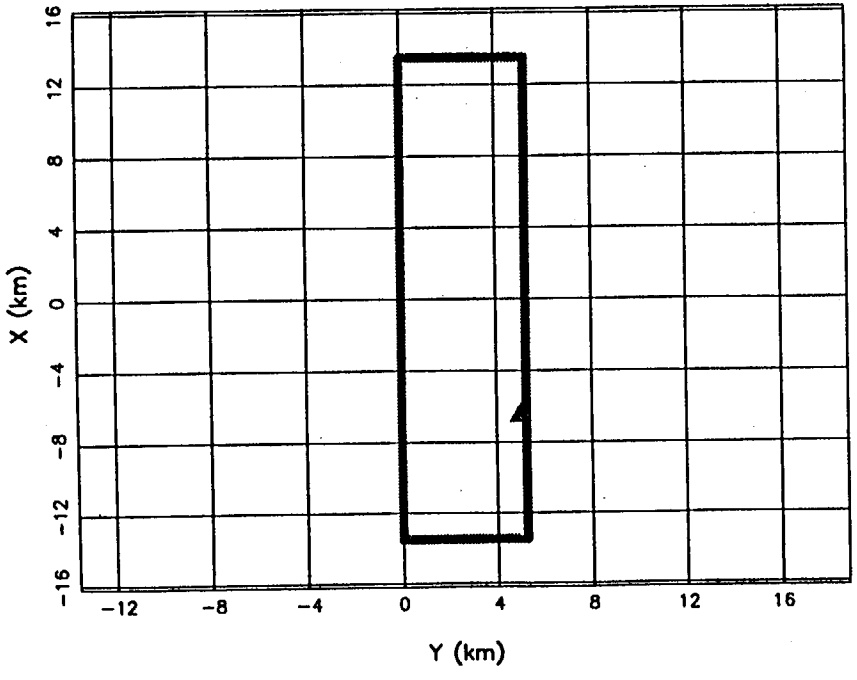

Cross View

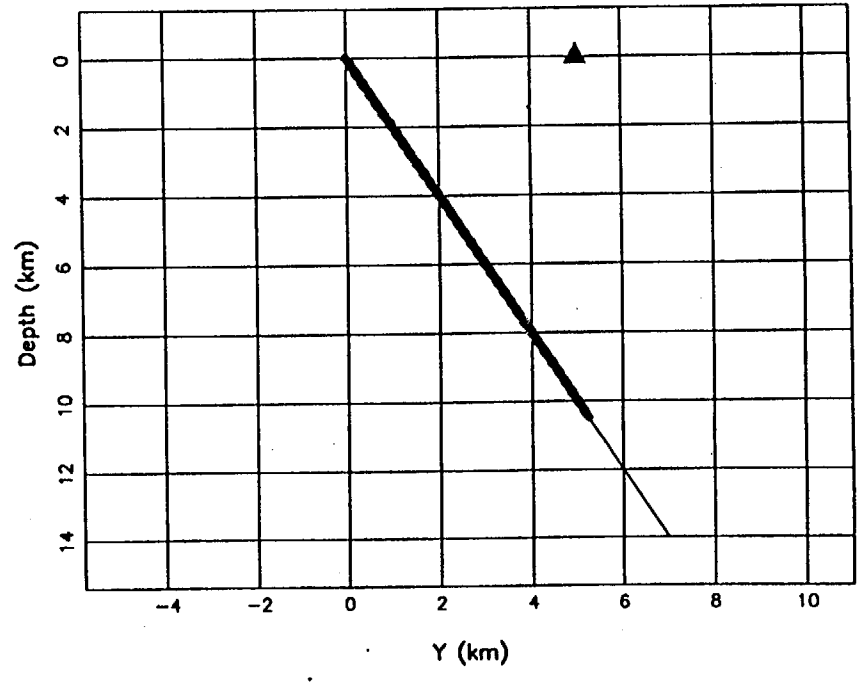

3.4.1-8

Map View (case 3)

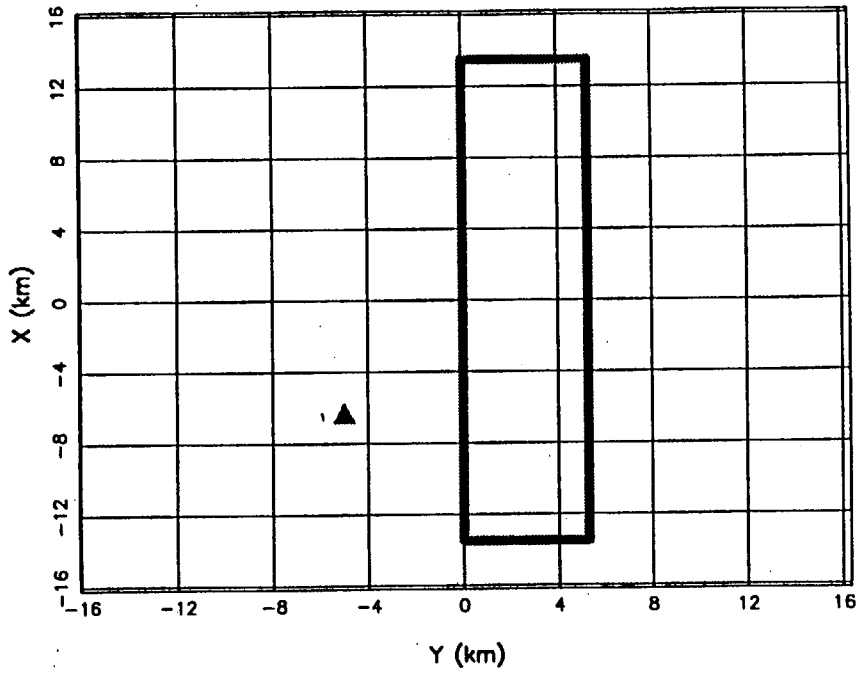

Cross View

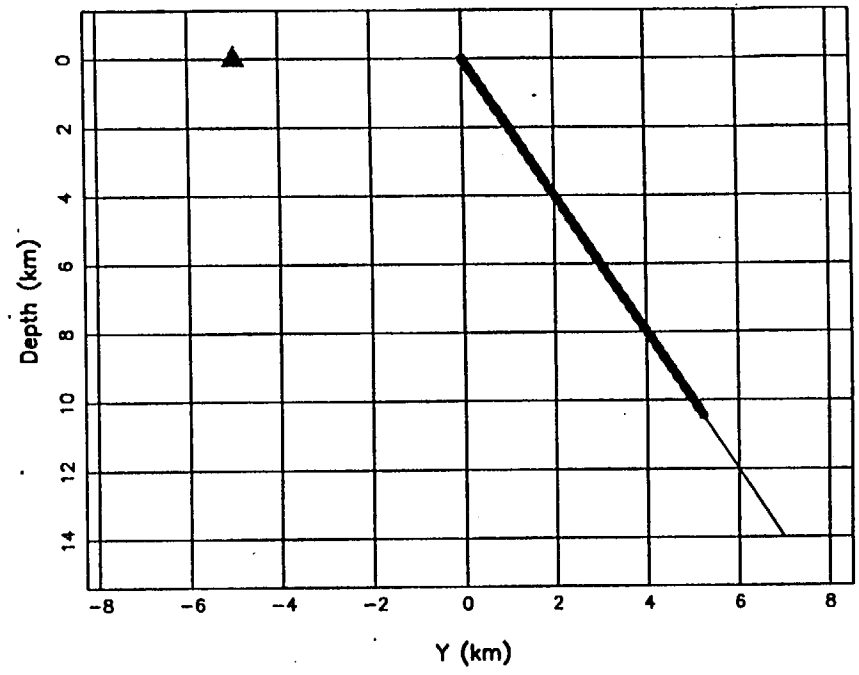

Map View (case 4)

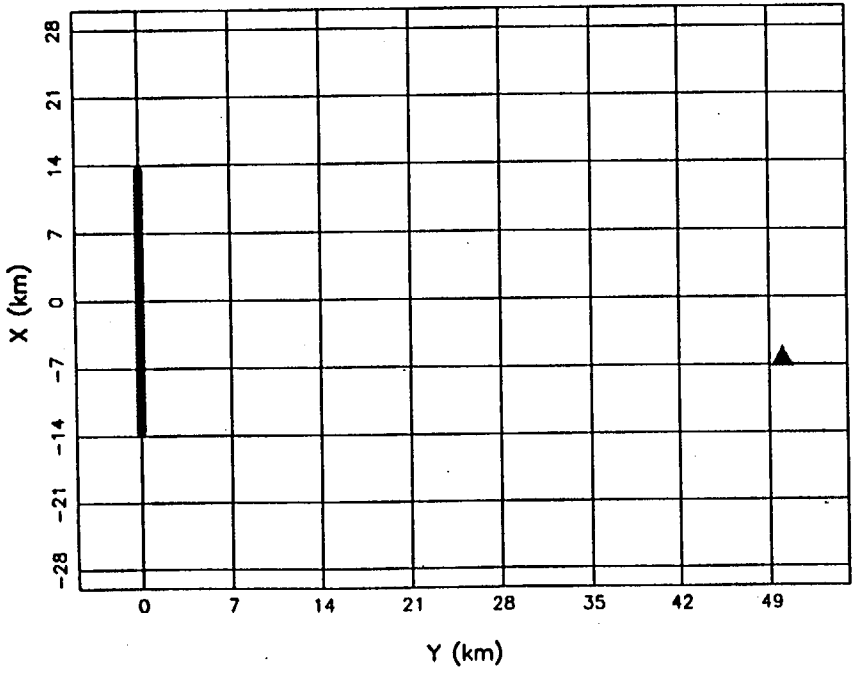

Cross View

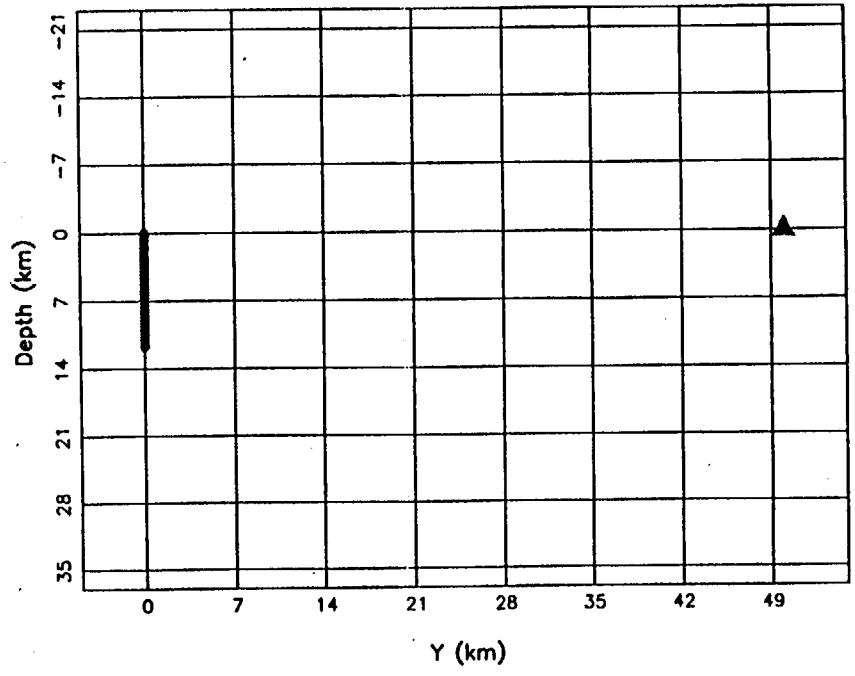

3.4.1-9

Map View (case 13)

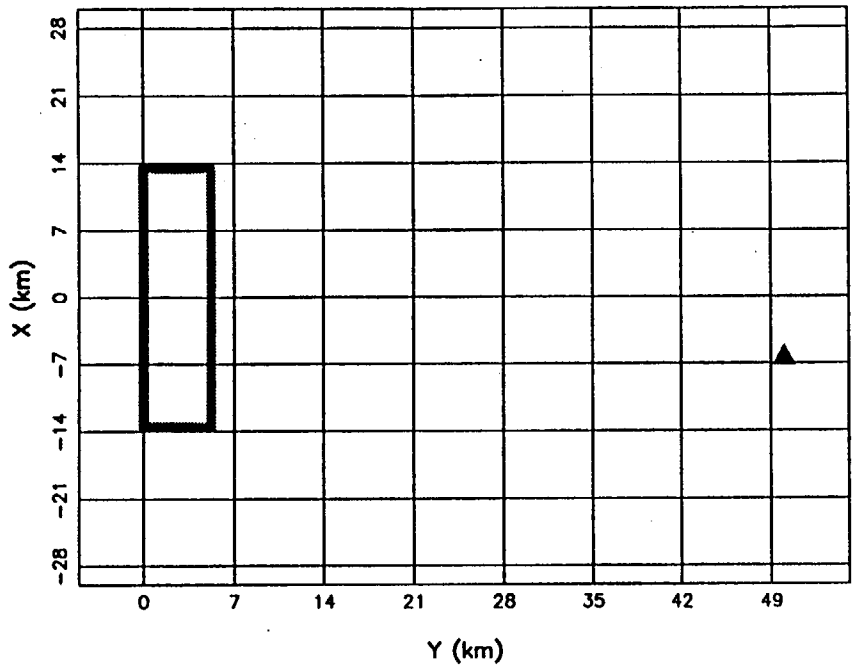

Cross View

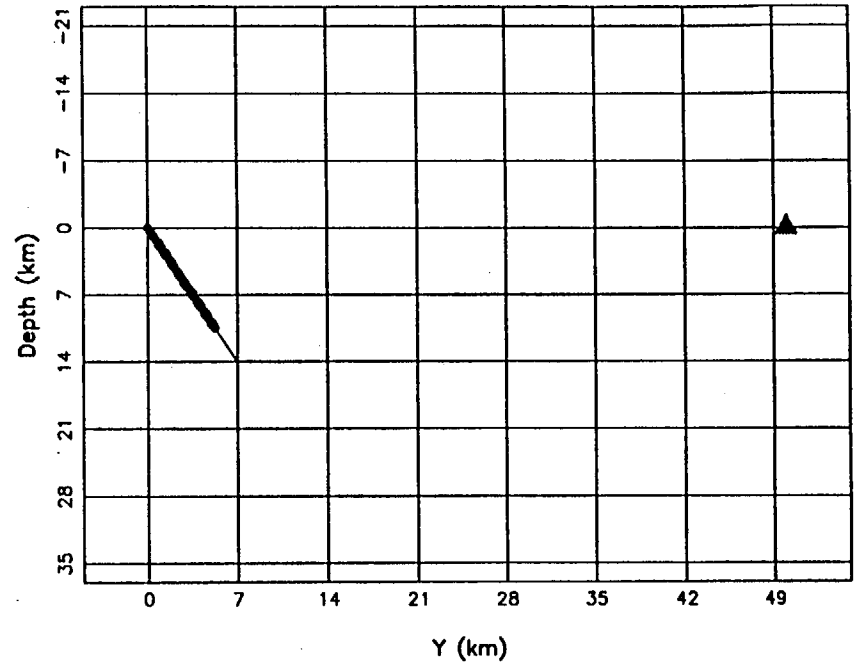

Map View (case 14)

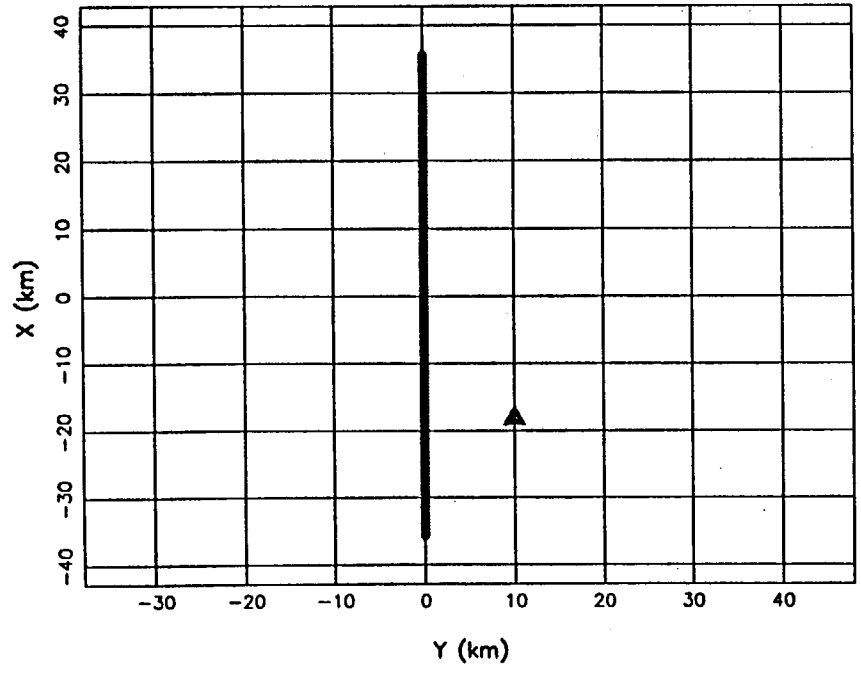

Cross View

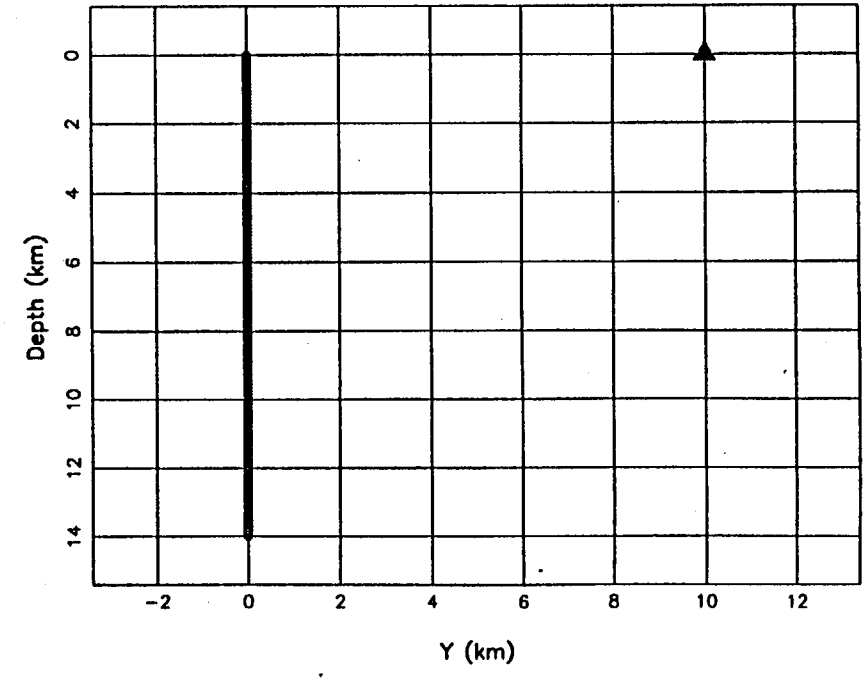

Map View (case 15)

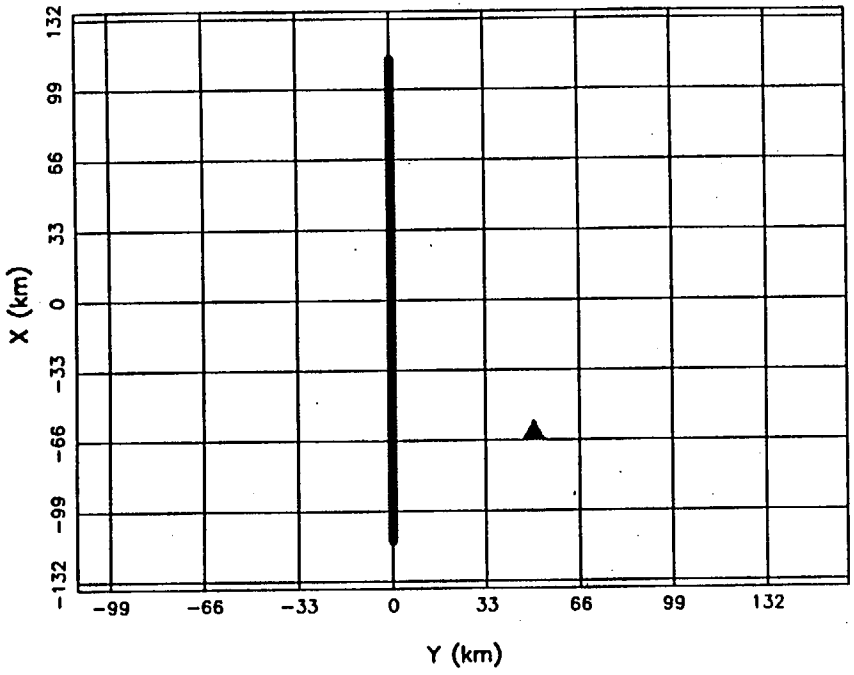

Cross View

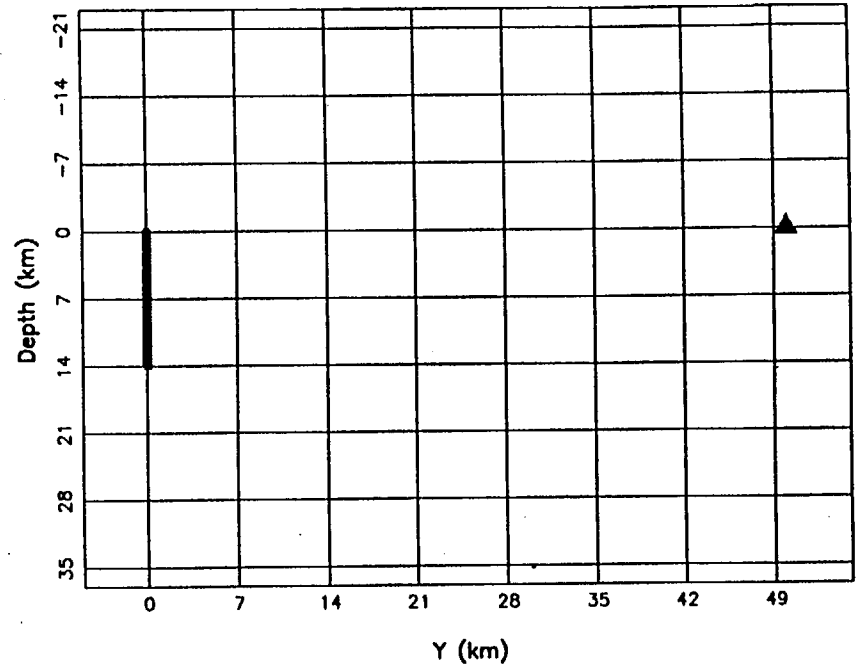

Map View (case 16)

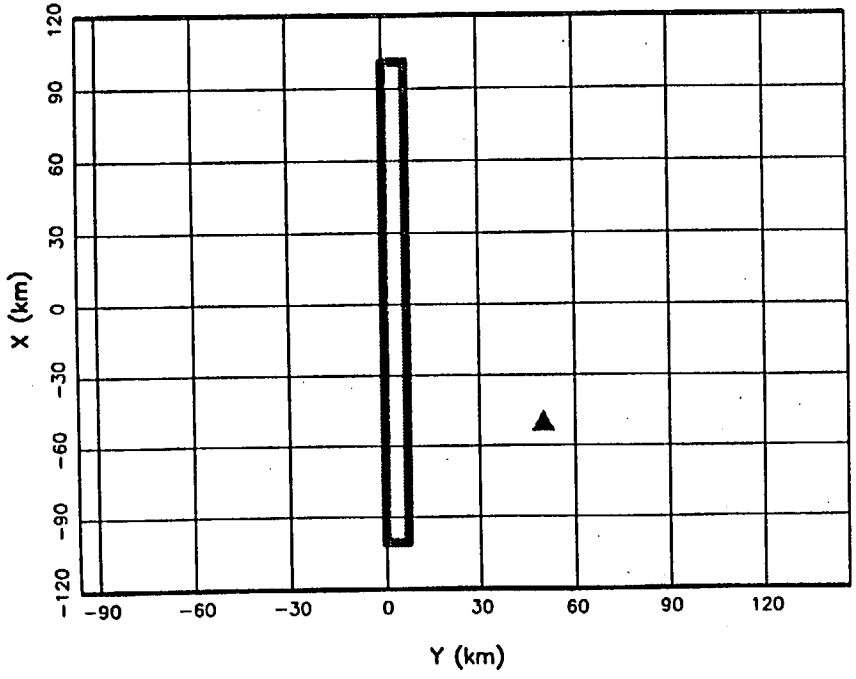

Cross View

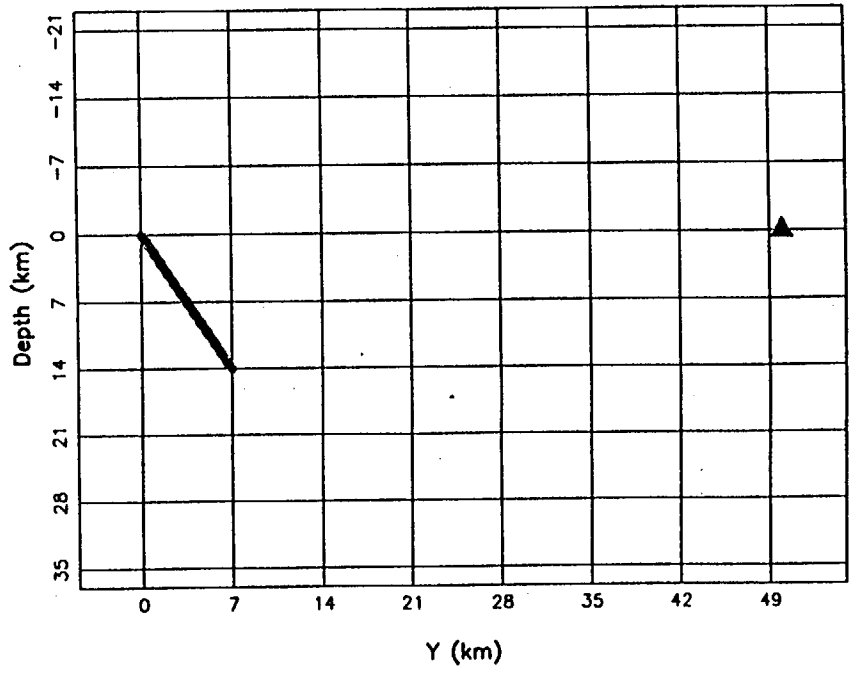

3. Description of Model Parameters

3.1 Layered Velocity Model

Layer thickness	0.70	0.60	1.50	2.20	10.70	16.00	1000.0
P-wave velocity	3.2	3.6	5.0	5.8	6.2	6.5	7.8
P-wave Q	150.0	200.0	300.0	800.0	800.0	800.0	800.0
S-wave velocity	1.9	2.1	2.9	3.4	3.5	3.8	4.6
S-wave Q	70.0	100.0	150.0	400.0	400.0	400.0	400.0
Density	2.4	2.4	2.5	2.7	2.75	2.9	3.3

No additional kappa added to the synthetics except that giving by the above Q model. The velocity randomization in the upper 1 km only affect the phase term of the Green's function. Any effect on seismic energy due to the randomization has been compensated.

3.2 Coda wave scattering mean free path = 100 km
intrinsic attenuation = $240*f^{0.5}$

3.3 Source Parameters

- D (fractal dimension) = 2.0
- Dynamic (subevent) stress drop range from 40 - 60 bars
- Rupture velocity = 2.8 km/sec
- Maximum subevents radius

Magnitude	5.0	5.8	6.5	7.0	7.5
R_{max} (km)	1.0	2.5	4.0	5.0	6.0

- Number of source realization for each case is 30

- Subevent stress drops are linearly tapered to zero from 5 km depth to the free surface to simulate the effect of nonseismogenic zone in the upper 2 km of the crust.

- The rupture area $A = 10^{M-4}$

- The seismic moment $M_0 = 10^{1.5*Mw+16}$

4.1 Table of PGA, PGV and Their Standard Errors for the horizontal component

CASE	PGA (mg)	Error	PGV (cm/s)	Error
1	158.09	0.34	5.12	0.32
2	478.64	0.31	18.45	0.30
3	56.62	0.30	1.55	0.27
4	164.12	0.35	6.18	0.27
5	150.59	0.30	5.80	0.21
6	139.34	0.28	6.21	0.23
7	882.68	0.27	47.52	0.25
8	1689.99	0.26	80.02	0.32
9	1175.74	0.27	57.56	0.31
10	560.59	0.23	31.61	0.24
11	406.84	0.27	20.76	0.23
12	44.77	0.23	3.57	0.16
13	43.37	0.21	3.20	0.20
14	404.84	0.15	30.86	0.19
15	89.03	0.14	10.92	0.18
16	98.35	0.14	12.28	0.15

Note: error is the standard error of ln(PGA or PGV).

4.2 Table of PGA, PGV and Their Standard Errors for the vertical component

CASE	PGA (mg)	Error	PGV (cm/s)	Error
1	69.43	0.33	2.09	0.28
2	181.33	0.32	4.86	0.29
3	28.47	0.27	0.67	0.30
4	50.61	0.34	1.45	0.27
5	70.26	0.32	2.71	0.30
6	170.97	0.27	7.30	0.23
7	325.95	0.27	14.89	0.26
8	600.93	0.28	30.13	0.28
9	679.65	0.26	27.23	0.28
10	495.11	0.23	32.96	0.23
11	342.58	0.25	17.38	0.26
12	33.83	0.22	1.57	0.22
13	41.46	0.22	4.98	0.25
14	217.55	0.16	14.34	0.22
15	63.49	0.17	6.11	0.14
16	97.77	0.13	16.81	0.19

Note: error is the standard error of ln(PGA or PGV).

5. Table of SA and Their Standard Errors

CASE 1

Frequency	0.30	0.50	1.00	2.00	5.00	10.00	20.00
SA (h)	2.57	6.93	31.25	75.55	232.41	360.32	267.76
Error	0.32	0.32	0.35	0.43	0.40	0.42	0.32
SA (v)	1.21	3.87	10.89	24.94	91.57	157.68	162.39
Error	0.24	0.25	0.30	0.36	0.28	0.40	0.37

CASE 2

Frequency	0.30	0.50	1.00	2.00	5.00	10.00	20.00
SA (h)	8.28	25.96	111.69	266.11	686.82	1195.44	699.72
Error	0.24	0.24	0.30	0.30	0.42	0.32	0.29
SA (v)	3.86	9.80	23.39	59.65	160.62	389.07	338.61
Error	0.12	0.16	0.38	0.32	0.38	0.43	0.33

CASE 3

Frequency	0.30	0.50	1.00	2.00	5.00	10.00	20.00
SA (h)	0.81	2.26	8.77	24.58	66.48	110.65	127.60
Error	0.21	0.14	0.25	0.33	0.28	0.34	0.36
SA (v)	0.36	0.97	3.56	9.51	55.10	71.41	54.70
Error	0.16	0.22	0.33	0.38	0.41	0.36	0.31

CASE 4

Frequency	0.30	0.50	1.00	2.00	5.00	10.00	20.00
SA (h)	3.75	9.67	36.24	90.61	243.26	428.73	239.40
Error	0.22	0.16	0.28	0.32	0.29	0.39	0.33
SA (v)	1.46	2.12	7.33	18.80	64.31	124.29	106.56
Error	0.09	0.19	0.24	0.31	0.38	0.40	0.31

CASE 5

Frequency	0.30	0.50	1.00	2.00	5.00	10.00	20.00
SA (h)	7.60	13.92	43.26	90.96	249.71	327.79	311.15
Error	0.20	0.27	0.26	0.27	0.37	0.31	0.35
SA (v)	3.53	5.25	18.07	47.85	119.55	177.13	134.47
Error	0.26	0.33	0.30	0.30	0.34	0.35	0.28

CASE 6

Frequency	0.30	0.50	1.00	2.00	5.00	10.00	20.00
SA (h)	5.75	15.01	60.00	131.11	260.08	315.79	252.82
Error	0.18	0.30	0.25	0.35	0.29	0.28	0.27
SA (v)	8.48	13.57	49.18	195.71	335.92	415.16	299.82
Error	0.21	0.39	0.30	0.34	0.33	0.34	0.27

CASE 7

Frequency	0.30	0.50	1.00	2.00	5.00	10.00	20.00
SA (h)	63.80	130.51	310.81	727.10	1483.31	2141.37	1377.80
Error	0.17	0.25	0.31	0.26	0.28	0.30	0.28
SA (v)	24.29	53.34	101.97	295.34	680.44	713.69	671.99
Error	0.44	0.41	0.37	0.35	0.31	0.27	0.27

CASE 8

Frequency	0.30	0.50	1.00	2.00	5.00	10.00	20.00
SA (h)	78.55	196.70	553.21	1278.57	2904.31	4290.61	2280.01
Error	0.21	0.37	0.31	0.31	0.36	0.32	0.28
SA (v)	61.26	101.07	150.40	416.09	753.22	1287.65	1113.47
Error	0.33	0.34	0.35	0.32	0.31	0.33	0.34

CASE 9

Frequency	0.30	0.50	1.00	2.00	5.00	10.00	20.00
SA (h)	58.11	146.56	407.33	961.44	2129.31	2864.99	1718.32
Error	0.23	0.34	0.29	0.30	0.36	0.28	0.28
SA (v)	48.05	89.10	149.70	411.89	878.86	1414.09	1264.28
Error	0.29	0.30	0.35	0.33	0.29	0.32	0.29

CASE 10

Frequency	0.30	0.50	1.00	2.00	5.00	10.00	20.00
SA (h)	66.49	130.66	263.10	463.25	929.47	1226.92	1073.39
Error	0.30	0.31	0.26	0.20	0.32	0.26	0.27
SA (v)	100.24	146.27	221.30	369.25	791.30	1148.37	954.40
Error	0.34	0.37	0.34	0.26	0.29	0.27	0.31

CASE 11

Frequency	0.30	0.50	1.00	2.00	5.00	10.00	20.00
SA (h)	41.29	84.69	138.98	307.96	726.16	978.74	688.39
Error	0.28	0.33	0.27	0.27	0.28	0.24	0.25
SA (v)	36.66	75.83	121.35	294.63	584.13	814.29	697.18
Error	0.26	0.30	0.28	0.31	0.25	0.23	0.27

CASE 12

Frequency	0.30	0.50	1.00	2.00	5.00	10.00	20.00
SA (h)	11.51	17.82	36.77	62.53	100.11	100.46	66.74
Error	0.37	0.33	0.24	0.25	0.23	0.27	0.26
SA (v)	3.11	5.78	16.14	42.72	67.54	78.45	55.66
Error	0.42	0.34	0.34	0.25	0.23	0.27	0.25

CASE 13

Frequency	0.30	0.50	1.00	2.00	5.00	10.00	20.00
SA (h)	7.05	15.88	41.04	82.04	80.82	83.82	68.35
Error	0.31	0.32	0.27	0.26	0.23	0.24	0.25
SA (v)	20.19	48.12	40.52	58.50	98.09	95.26	79.56
Error	0.44	0.33	0.26	0.25	0.30	0.29	0.30

CASE 14

Frequency	0.30	0.50	1.00	2.00	5.00	10.00	20.00
SA (h)	77.72	112.81	236.89	494.31	718.53	830.70	707.01
Error	0.31	0.31	0.20	0.22	0.19	0.16	0.19
SA (v)	34.65	57.05	122.76	326.56	417.94	451.55	406.93
Error	0.43	0.23	0.32	0.24	0.20	0.19	0.20

CASE 15

Frequency	0.30	0.50	1.00	2.00	5.00	10.00	20.00
SA (h)	47.60	66.24	100.61	191.20	196.97	170.09	123.90
Error	0.23	0.20	0.21	0.20	0.16	0.14	0.13
SA (v)	22.76	40.49	51.58	130.98	133.56	122.21	103.96
Error	0.33	0.31	0.19	0.23	0.15	0.18	0.12

CASE 16

Frequency	0.30	0.50	1.00	2.00	5.00	10.00	20.00
SA (h)	41.35	81.95	131.64	237.08	208.39	175.85	133.63
Error	0.24	0.19	0.20	0.16	0.16	0.17	0.13
SA (v)	71.17	171.95	104.57	137.57	207.85	168.19	159.76
Error	0.23	0.25	0.23	0.16	0.19	0.12	0.15

Note: Error is the error of ln(SA) relative to its mean
Frequency is in Hz
SA is in mg

6. Plots of SA vs. Frequency

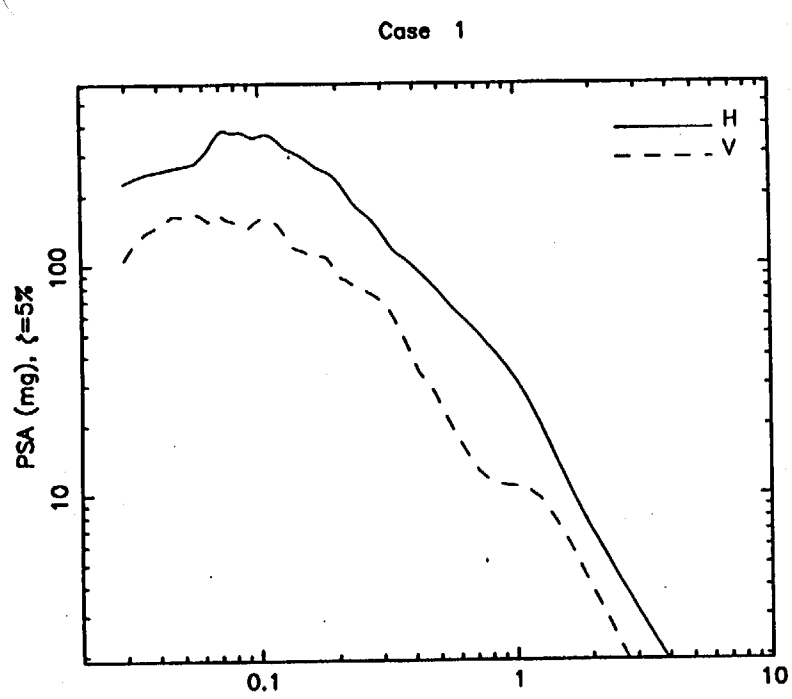
Case 1
H
V
PSA (mg), ζ=5%
100
10
0.1
1
10

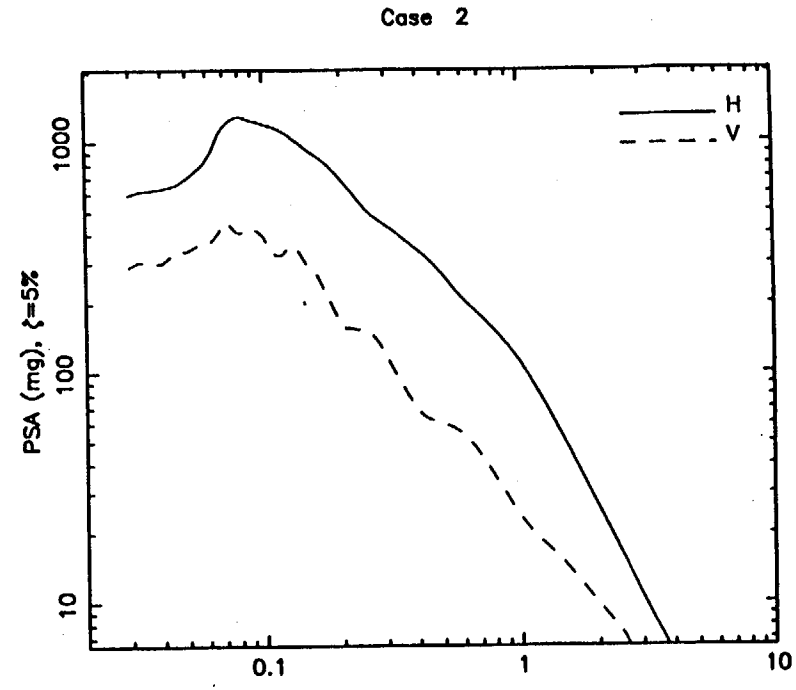
Case 2
H
V
PSA (mg), ζ=5%
1000
100
10
0.1
1
10

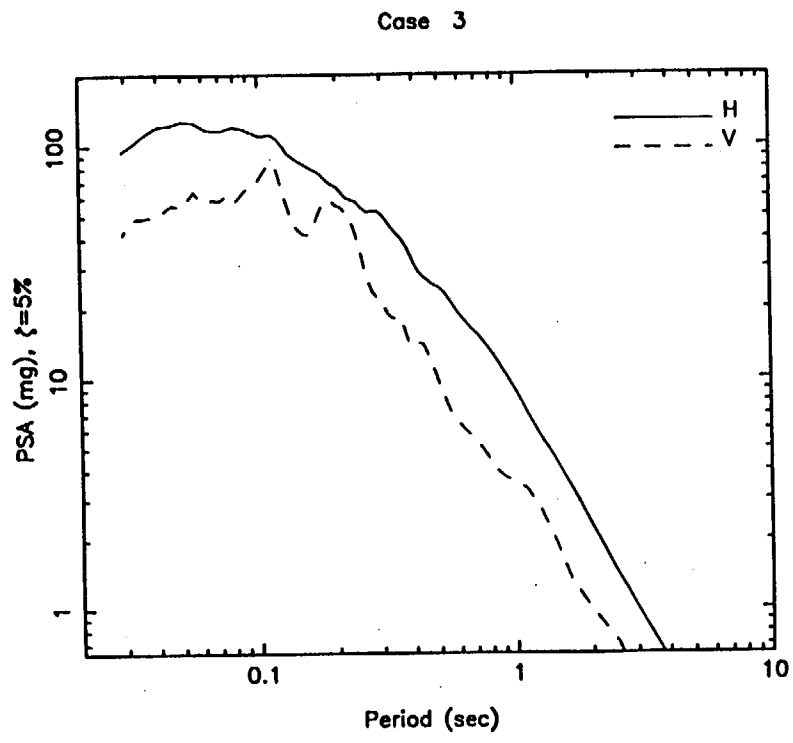
Case 3
H
V
PSA (mg), ζ=5%
100
10
1
0.1
1
10
Period (sec)

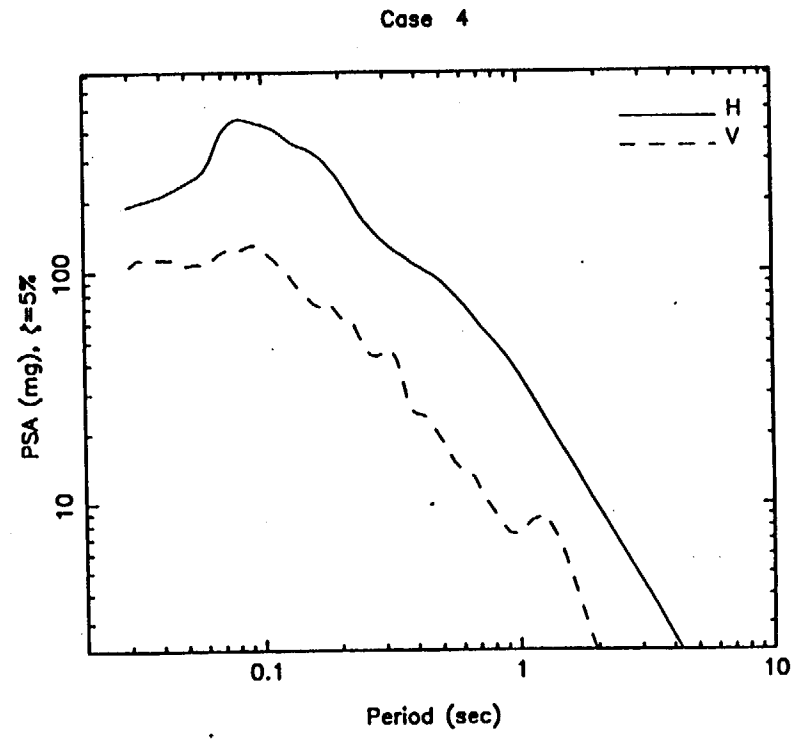
Case 4
H
V
PSA (mg), ζ=5%
100
10
0.1
1
10
Period (sec)

Case 5

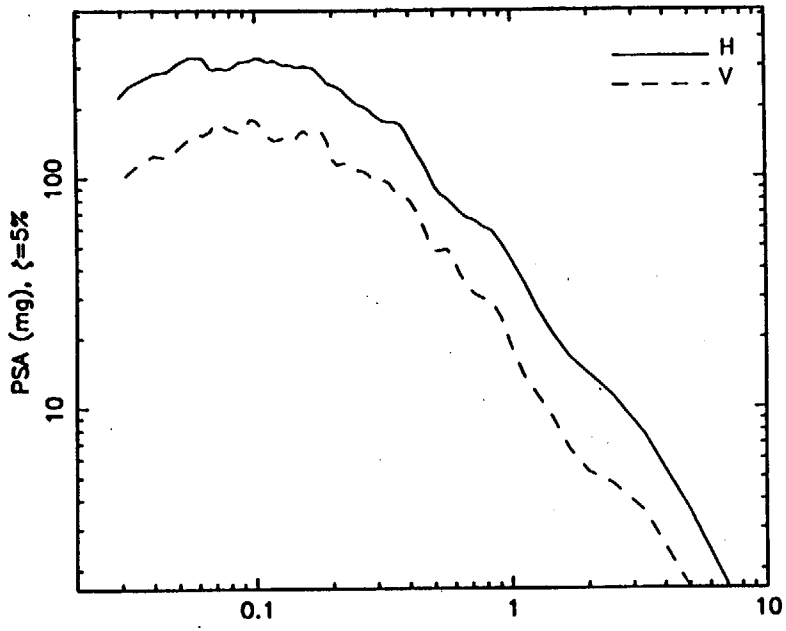

Case 6

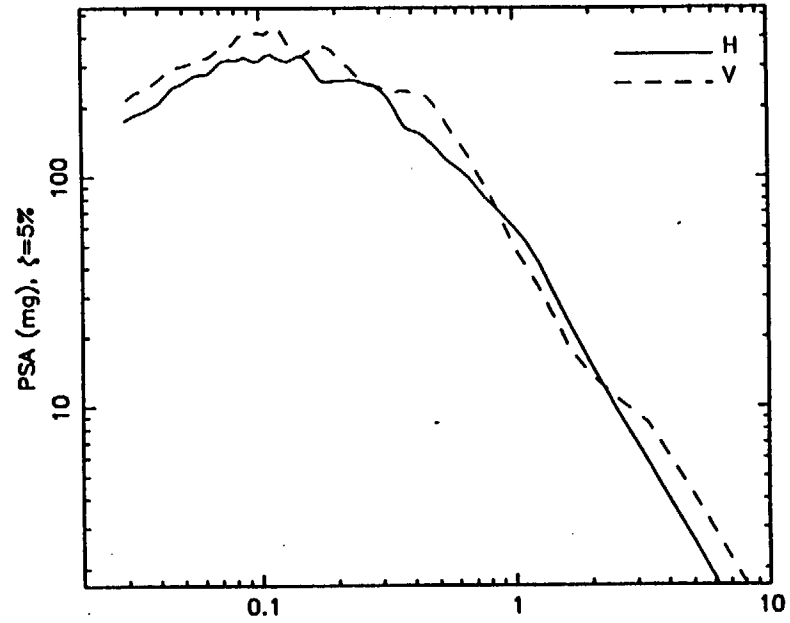

Case 7

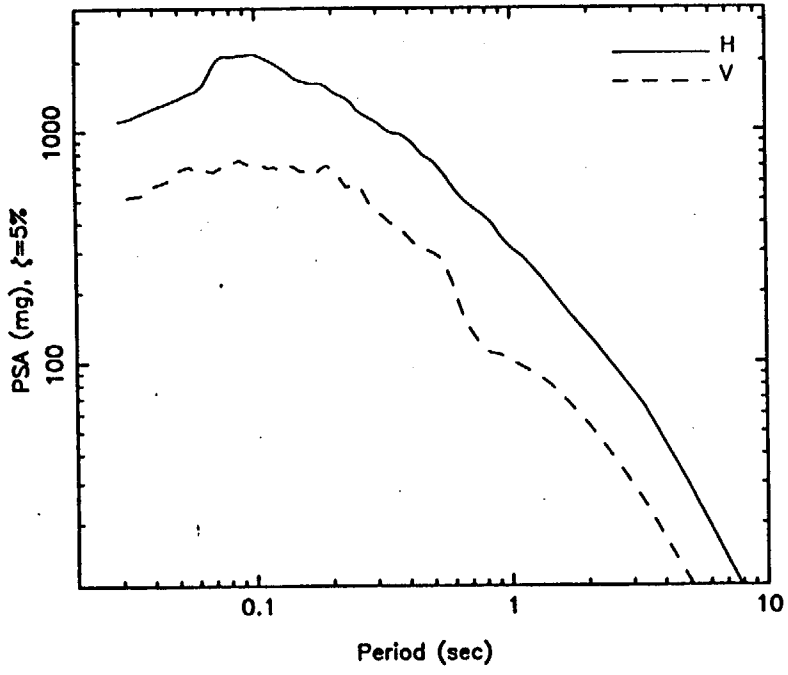

Case 8

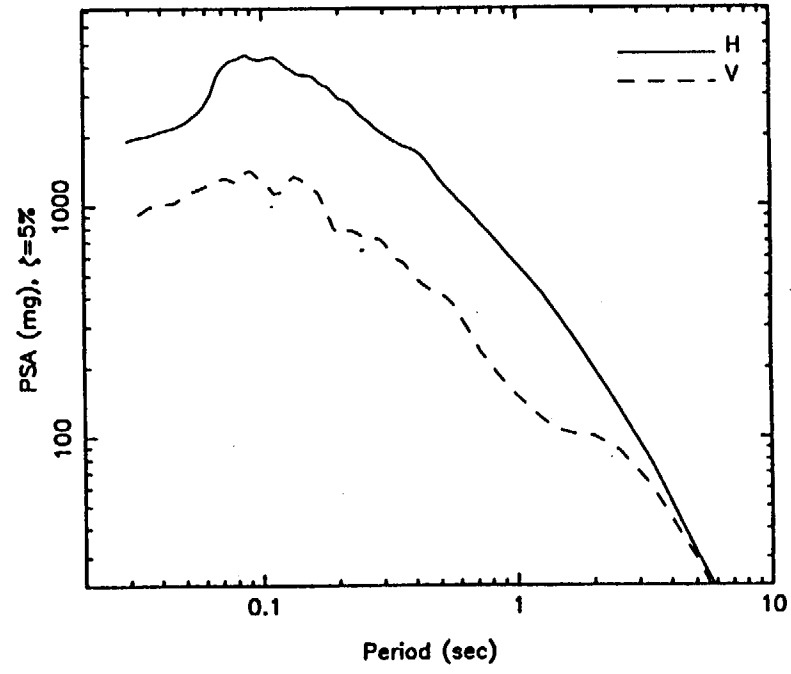

3.4.1-14

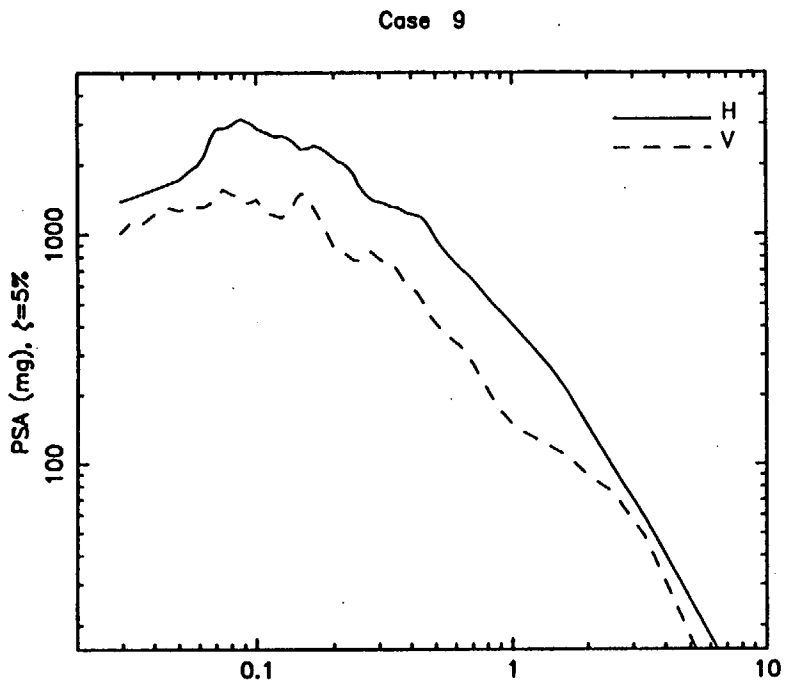
Case 9
H
V
PSA (mg), ζ=5%
1000
100
0.1
1
10

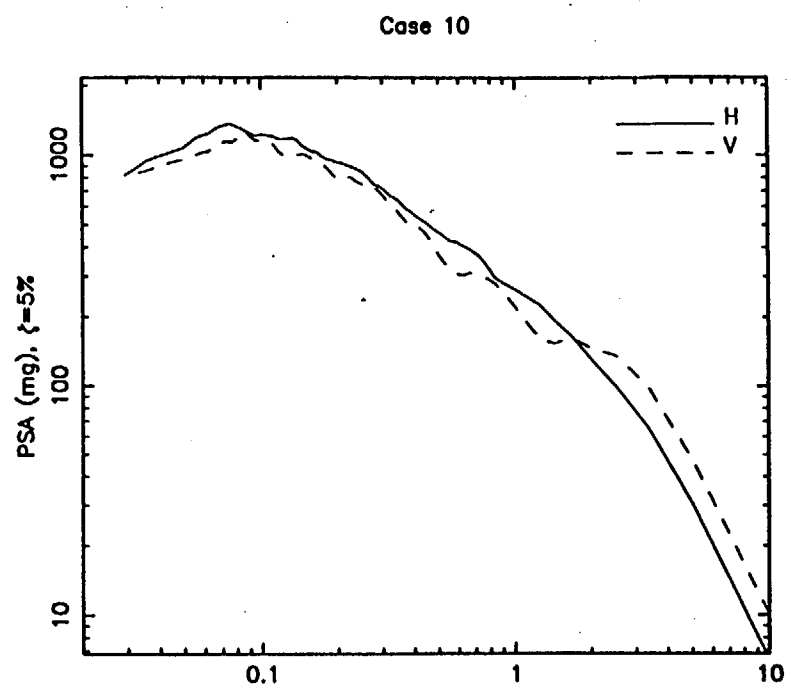
Case 10
H
V
PSA (mg), ζ=5%
1000
100
10
0.1
1
10

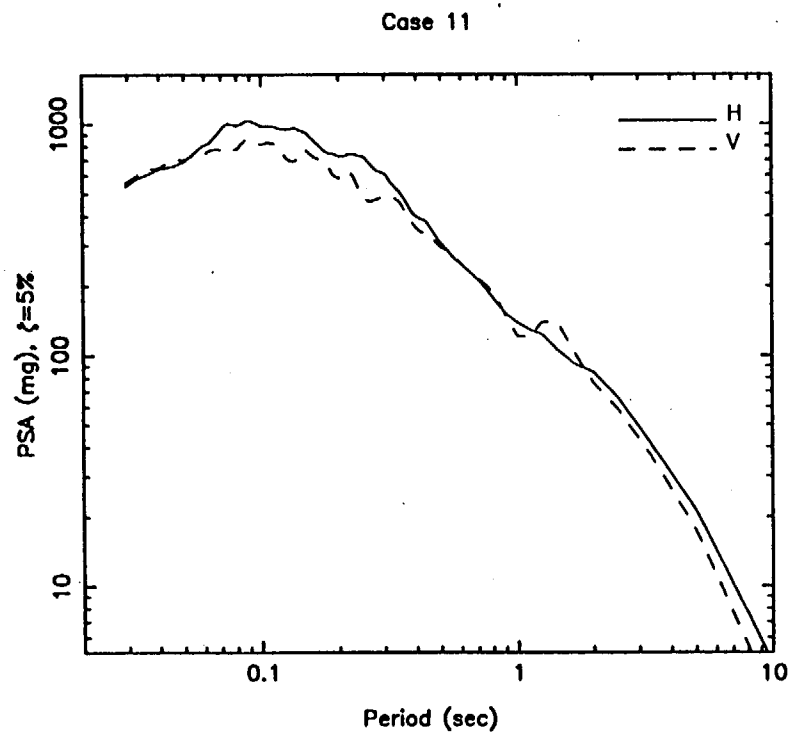
Case 11
H
V
PSA (mg), ζ=5%
1000
100
10
0.1
1
10
Period (sec)

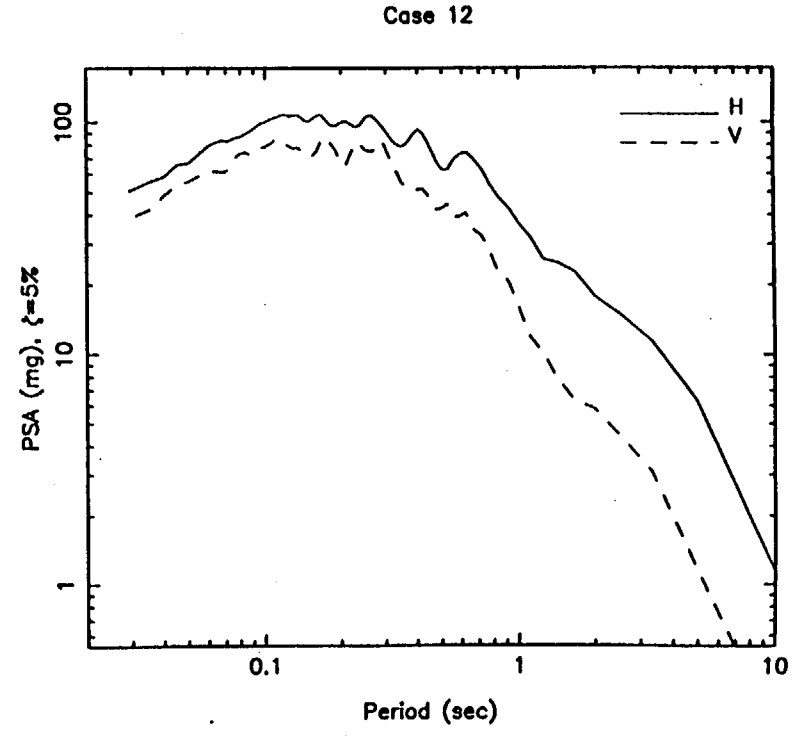
Case 12
H
V
PSA (mg), ζ=5%
100
10
1
0.1
1
10
Period (sec)

Case 13

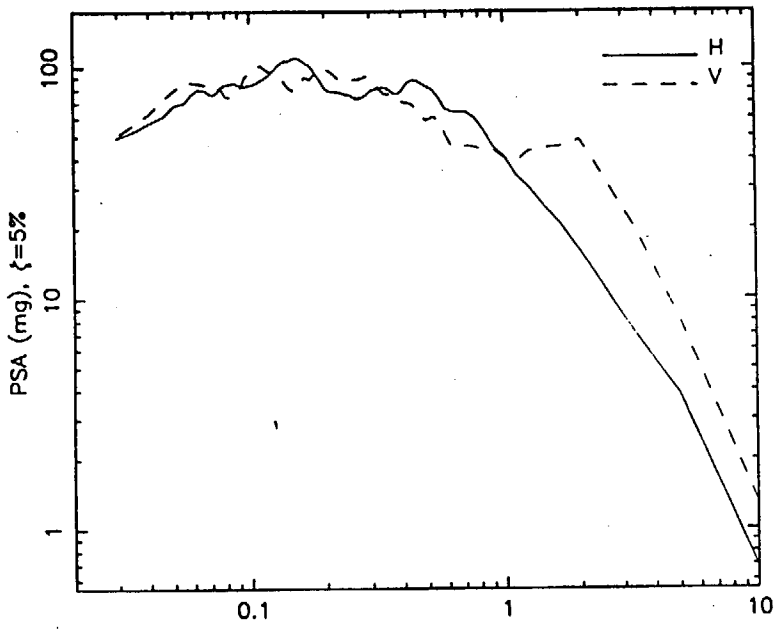

Case 14

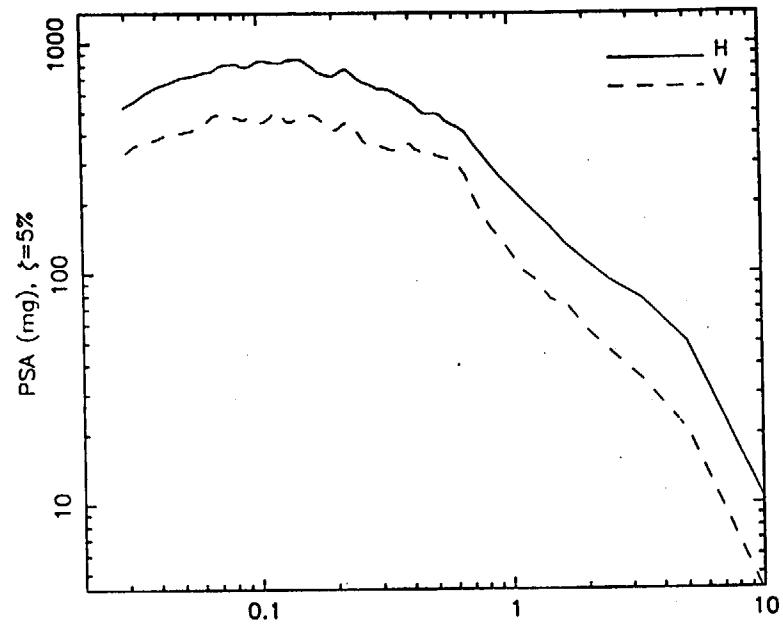

Case 15

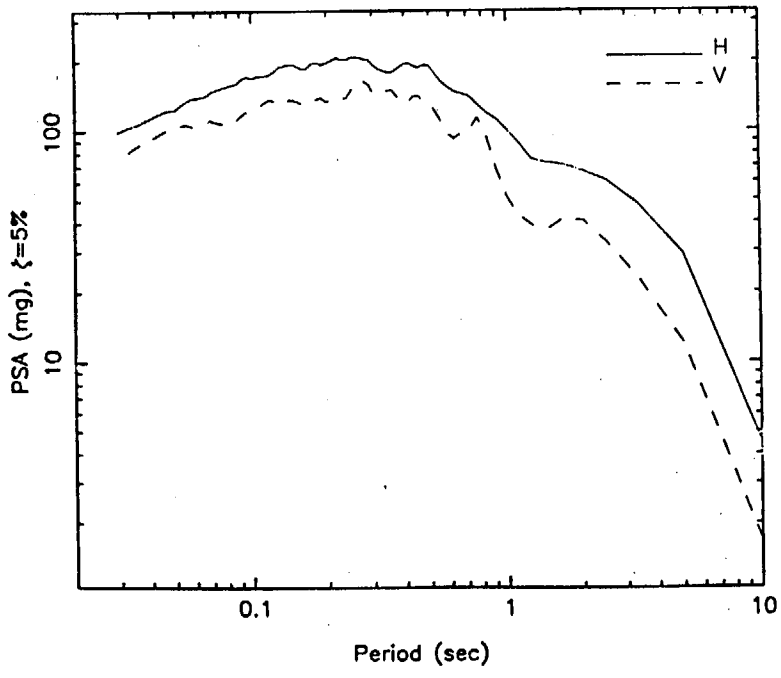

Case 16

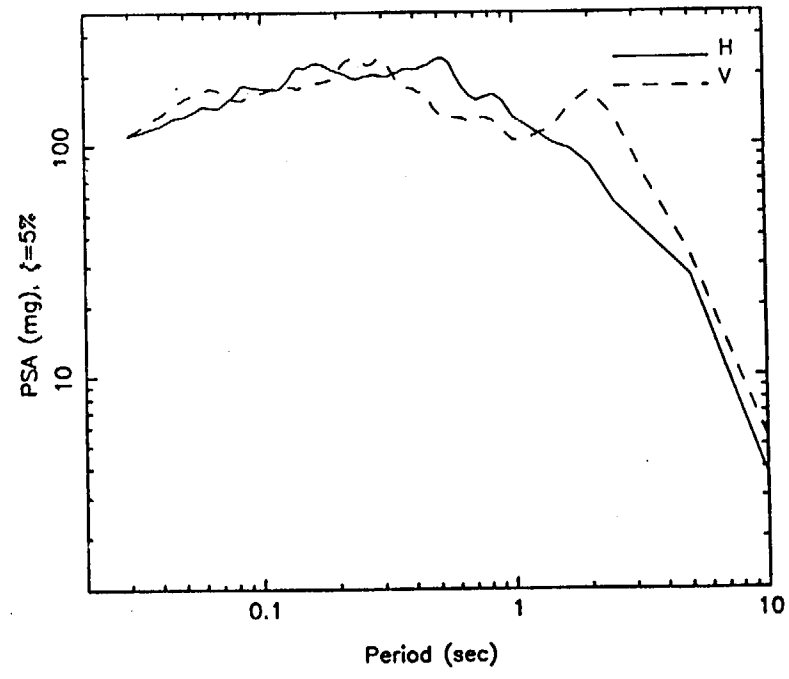

7. Plots of PSV vs. Frequency

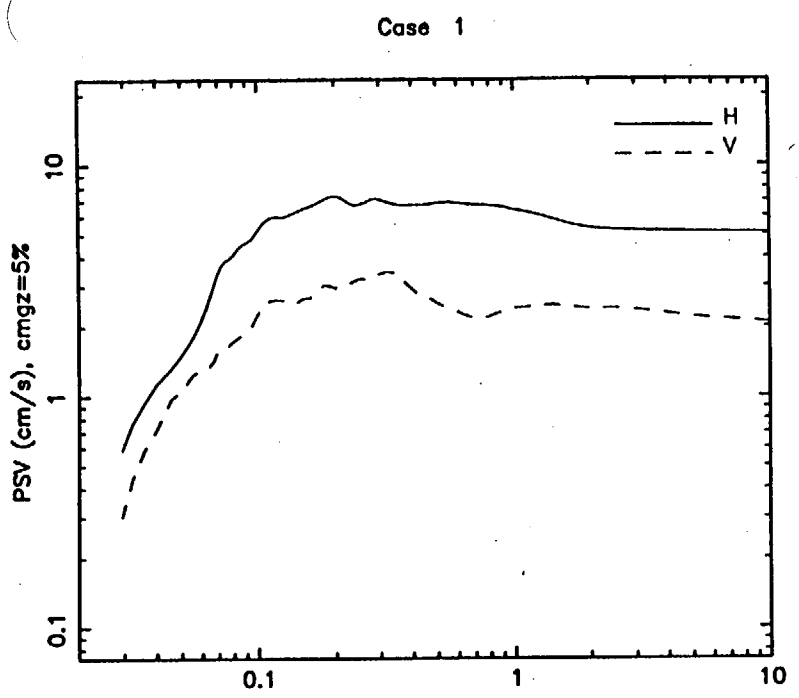
Case 1
H
V
PSV (cm/s), cmgz=5%
0.1
1
10
0.1
1
10

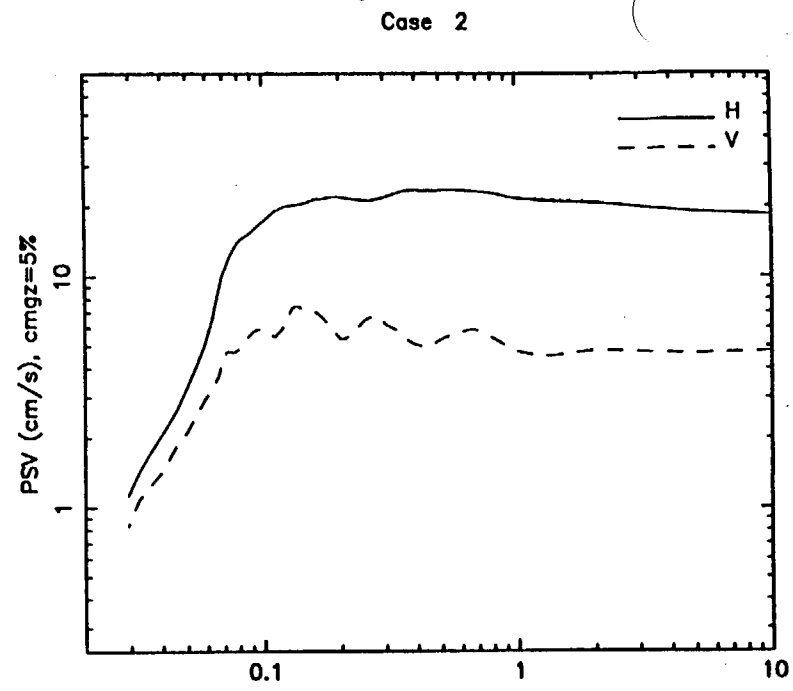
Case 2
H
V
PSV (cm/s), cmgz=5%
1
10
0.1
1
10

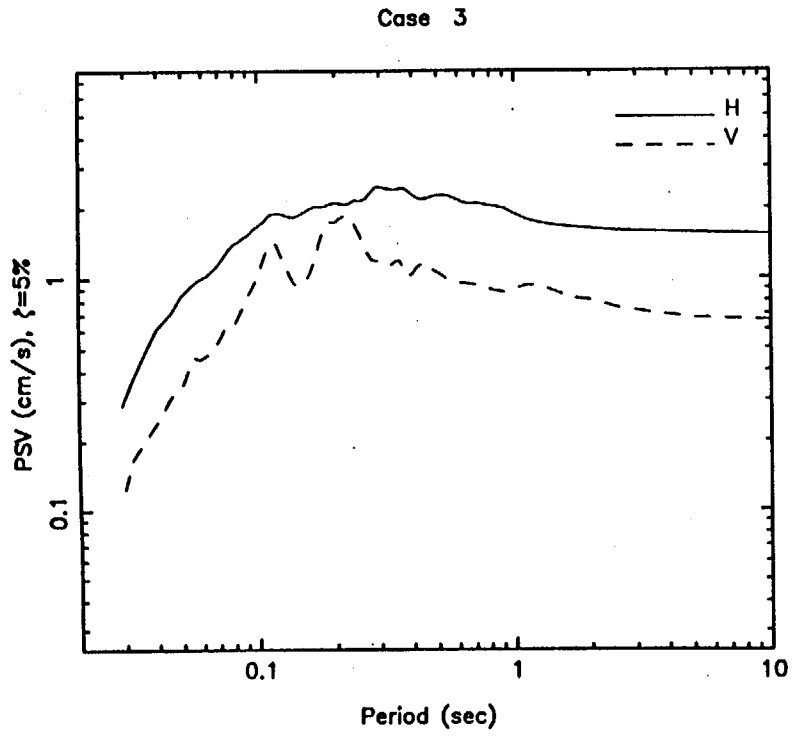
Case 3
H
V
PSV (cm/s), ζ=5%
0.1
1
0.1
1
10
Period (sec)

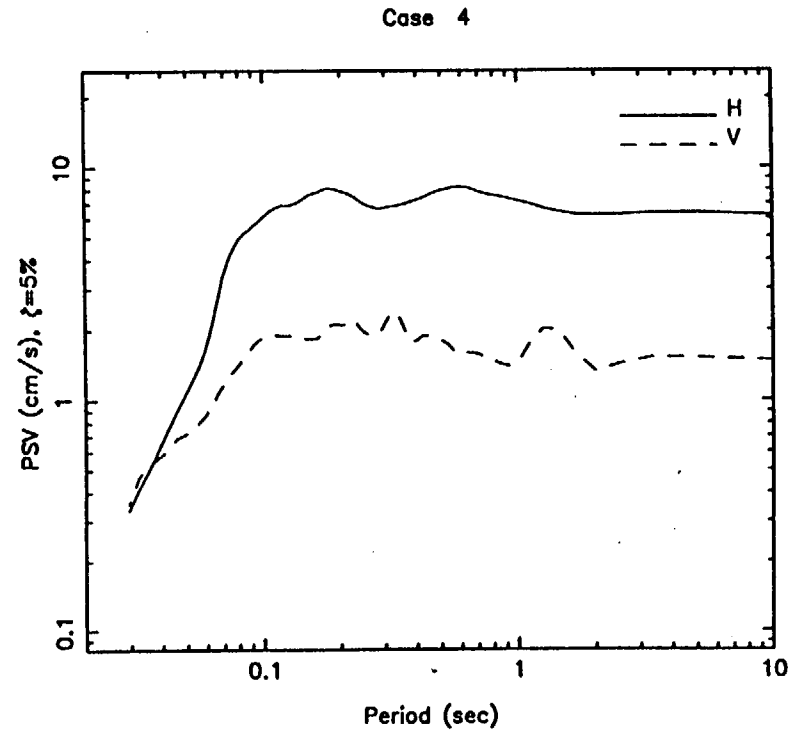
Case 4
H
V
PSV (cm/s), ζ=5%
0.1
1
10
0.1
1
10
Period (sec)

Case 5

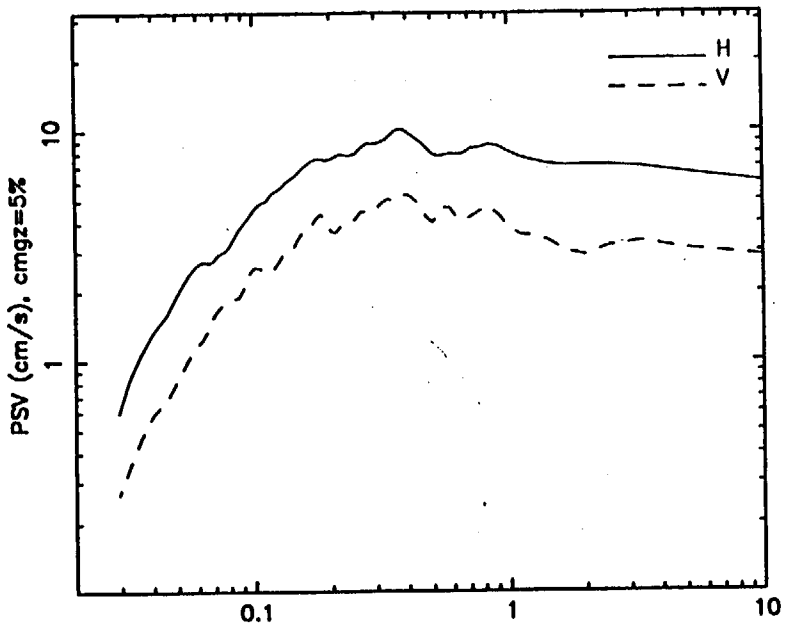

Case 6

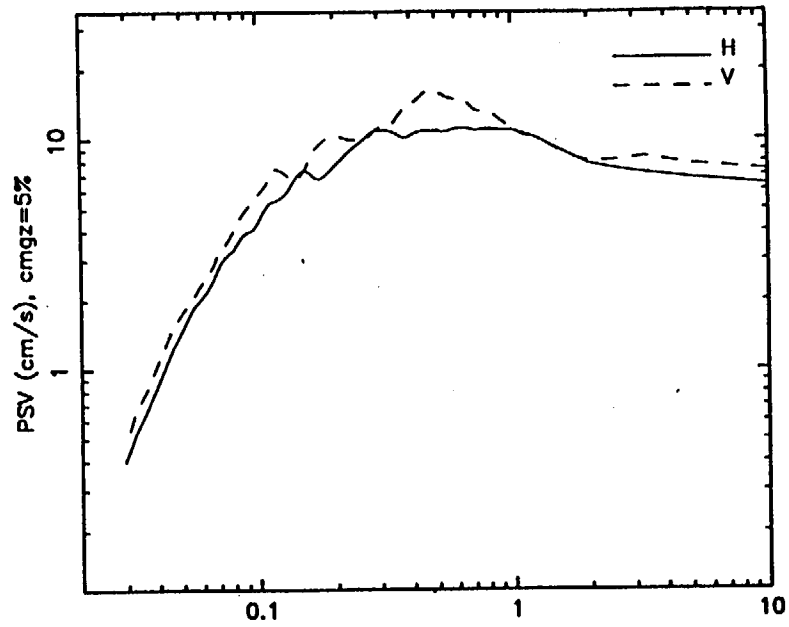

Case 7

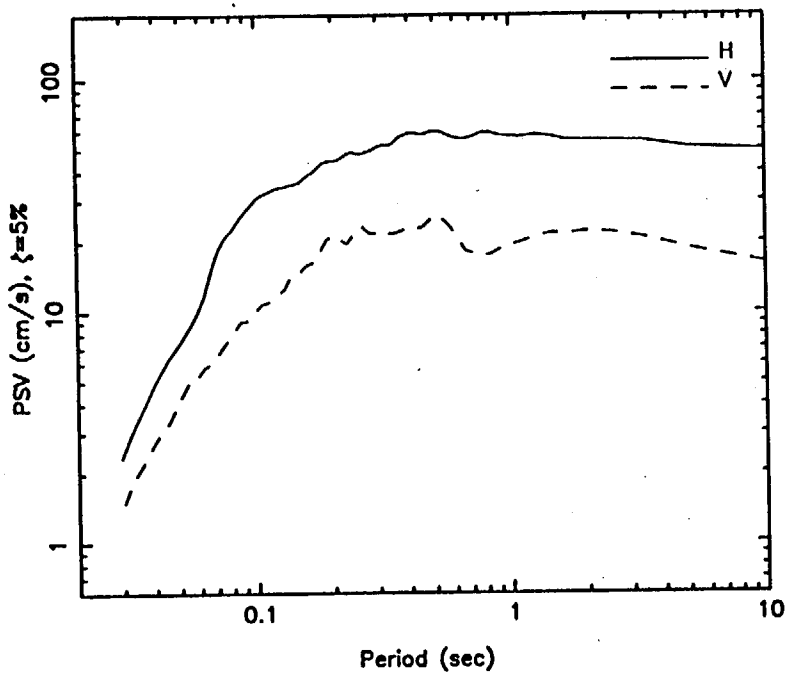

Case 8

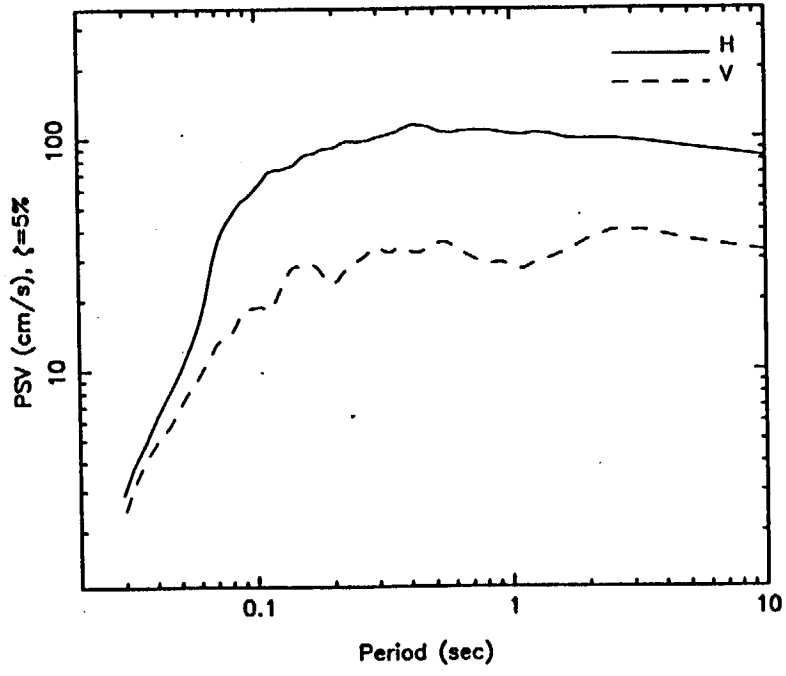

3.4.1-24

Case 9

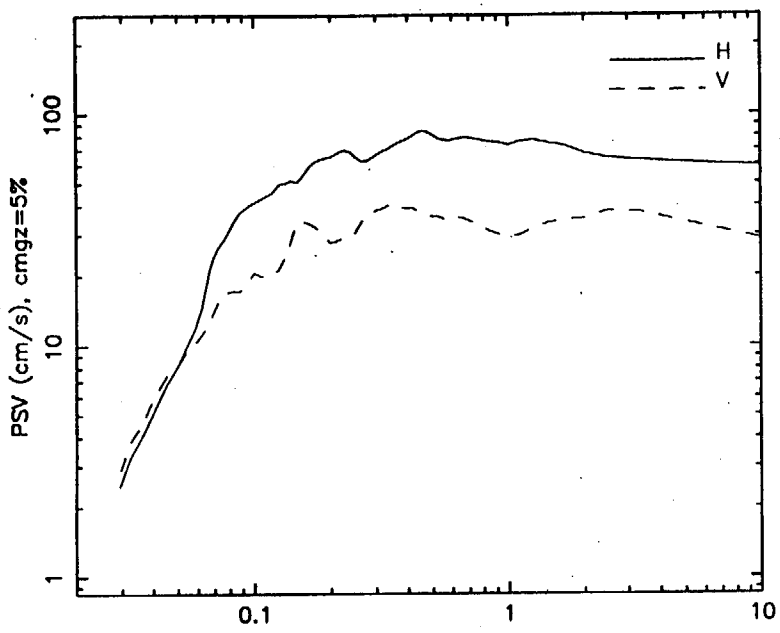

Case 10

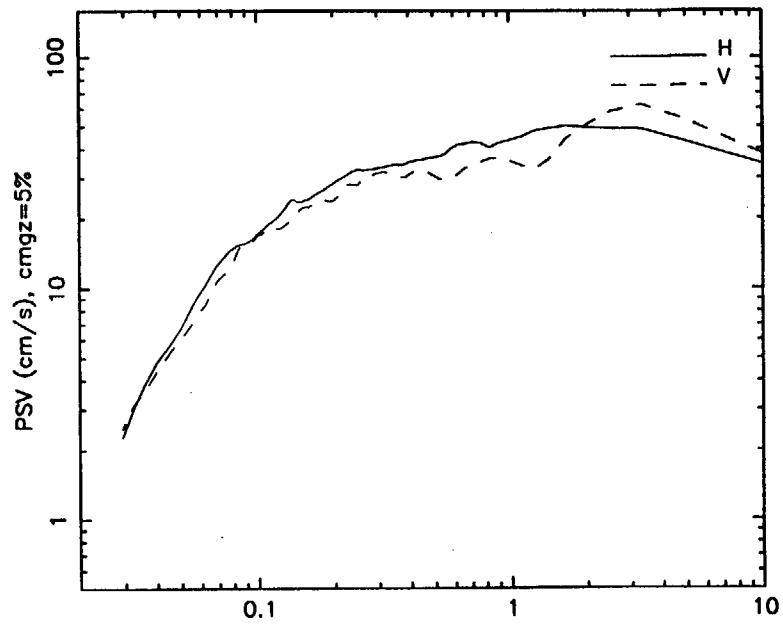

Case 11

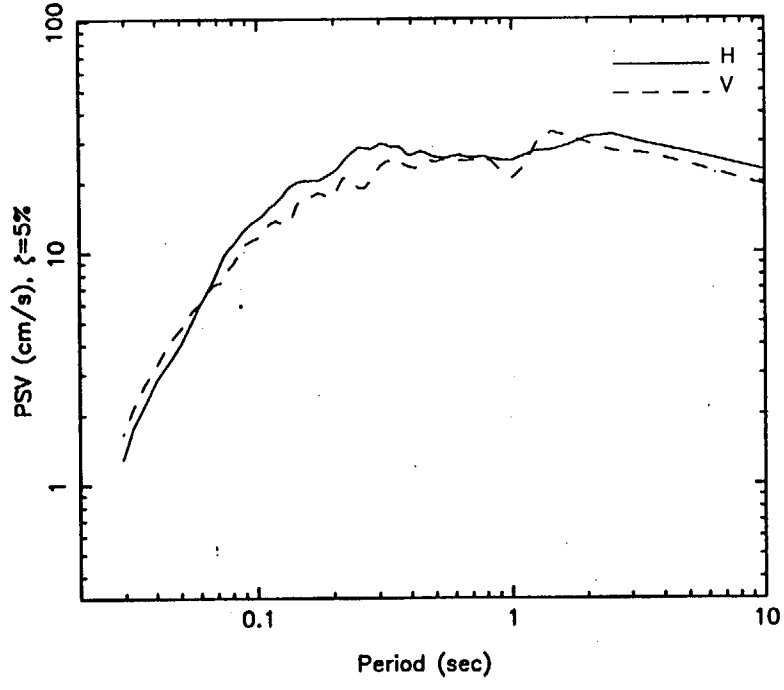

Case 12

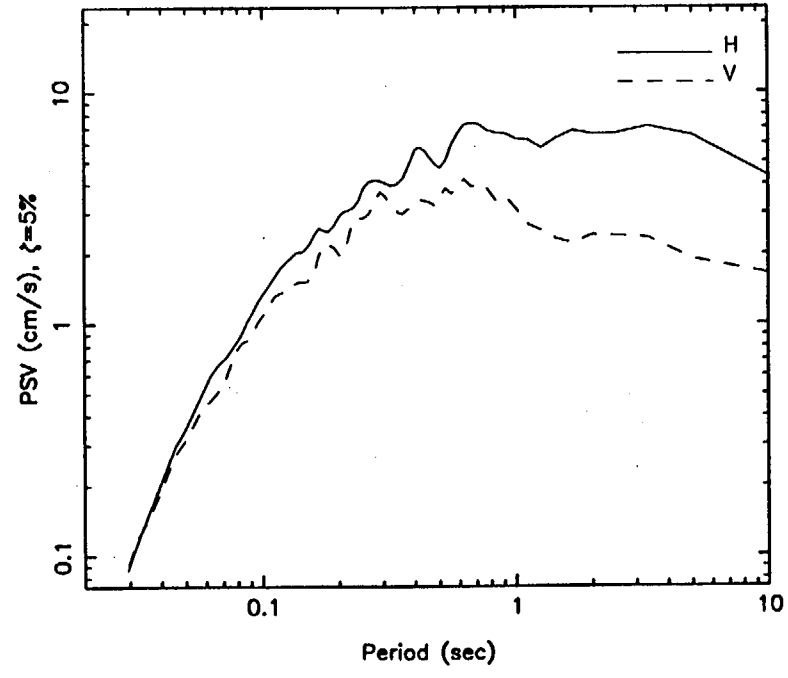

3.4.1-25

Case 13

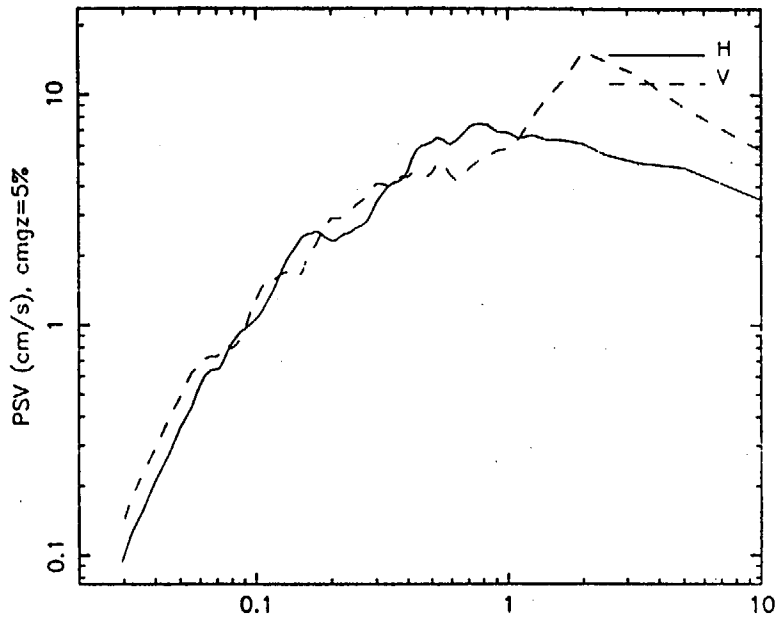

Case 14

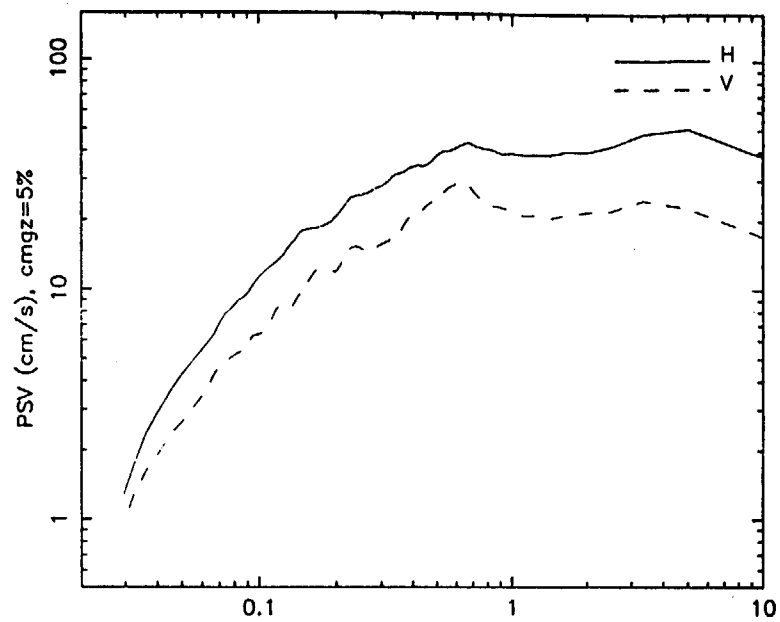

Case 15

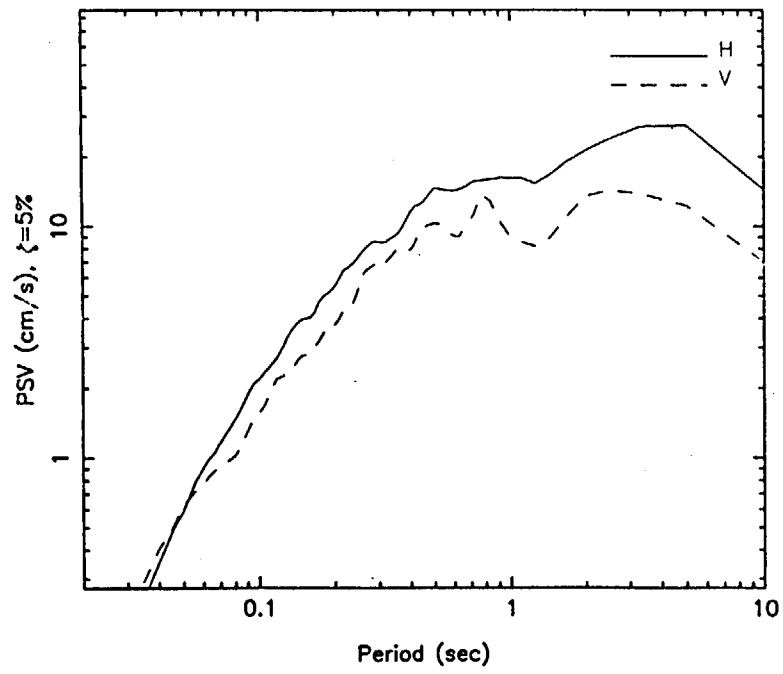

Case 16

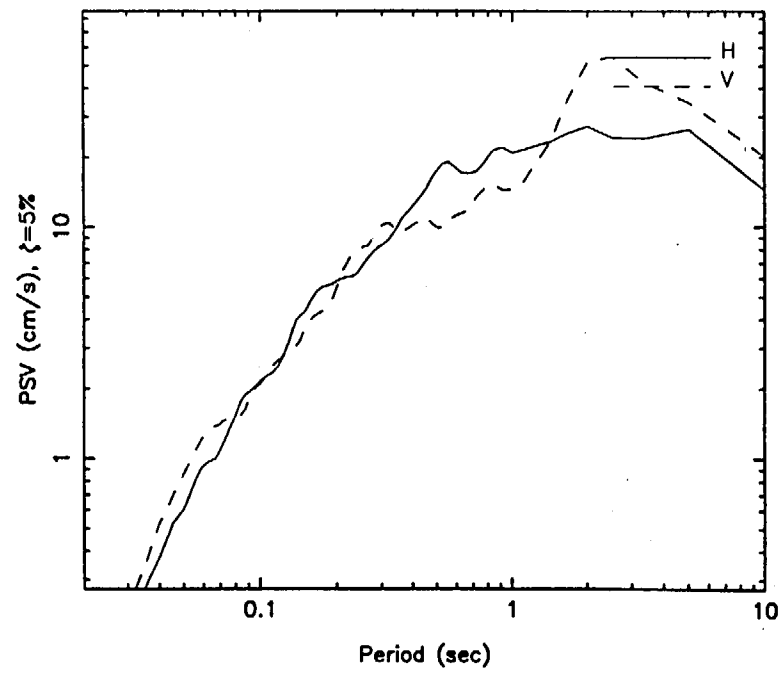

3.4.1-26

UNR: Anderson Finite Fault

Median Sa - Horizontal Component (g):

Frequency (Hz)	M_w 5.0		M_w 5.0 Deep		M_w 5.8 Deep		M_w 6.5							M_w 7.0	M_w 7.5	
	SS	HW	SS	HW	SS	HW	SS	HW	FW	HW	FW	SS	HW	SS	SS	HW
	1 km	1 km	5 km	5 km	10 km	20 km	1 km	1 km	1 km	5 km	5 km	50 km	50 km	10 km	50 km	50 km
0.3	0.00257	0.00828	0.00081	0.00375	0.00760	0.00575	0.06380	0.07855	0.05811	0.06649	0.04129	0.01151	0.00705	0.07772	0.04760	0.04135
0.5	0.00693	0.02596	0.00226	0.00967	0.01392	0.01501	0.13051	0.19670	0.14656	0.13066	0.08469	0.01782	0.01588	0.11281	0.06624	0.08195
1.	0.03125	0.11169	0.00877	0.03624	0.04326	0.06000	0.31081	0.55321	0.40733	0.26310	0.13898	0.03677	0.04104	0.23689	0.10061	0.13164
2.	0.07555	0.26611	0.02458	0.09061	0.09096	0.13111	0.72710	1.27857	0.96144	0.46325	0.30796	0.06253	0.08204	0.49431	0.19120	0.23708
5.	0.23241	0.68682	0.06648	0.24326	0.24971	0.26008	1.48331	2.90431	2.12931	0.92947	0.72616	0.10011	0.08082	0.71853	0.19697	0.20839
10.	0.36032	1.19544	0.11065	0.42873	0.32779	0.31579	2.14137	4.29061	2.86499	1.22692	0.97874	0.10046	0.08382	0.83070	0.17009	0.17585
20.	0.26776	0.69972	0.12760	0.23940	0.31115	0.25282	1.37780	2.28001	1.71832	1.07339	0.68839	0.06674	0.06835	0.70701	0.12390	0.13363
pga	0.15809	0.47864	0.05662	0.16412	0.15059	0.13934	0.88268	1.68999	1.17574	0.56059	0.40684	0.04477	0.04337	0.40484	0.08903	0.09835
pgv cm/sec	5.12	18.45	1.55	6.18	5.80	6.21	47.52	80.02	57.56	31.61	20.76	3.57	3.20	30.86	10.92	12.28

3.4.2-1

Aleatory Variability about Median Sa - Horizontal Component:

Frequency (Hz)	M_w 5.0		M_w 5.0 Deep		M_w 5.8 Deep		M_w 6.5							M_w 7.0	M_w 7.5	
	SS	HW	SS	HW	SS	HW	SS	HW	FW	HW	FW	SS	HW	SS	SS	HW
	1 km	1 km	5 km	5 km	10 km	20 km	1 km	1 km	1 km	5 km	5 km	50 km	50 km	10 km	50 km	50 km
0.3	0.32	0.24	0.21	0.22	0.20	0.18	0.17	0.21	0.23	0.30	0.28	0.37	0.31	0.31	0.23	0.24
0.5	0.32	0.24	0.14	0.16	0.27	0.30	0.25	0.37	0.34	0.31	0.33	0.33	0.32	0.31	0.20	0.19
1.	0.35	0.30	0.25	0.28	0.26	0.25	0.31	0.31	0.29	0.26	0.27	0.24	0.27	0.20	0.21	0.20
2.	0.43	0.30	0.33	0.32	0.27	0.35	0.26	0.31	0.30	0.20	0.27	0.25	0.26	0.22	0.20	0.16
5.	0.40	0.42	0.28	0.29	0.37	0.29	0.28	0.36	0.36	0.32	0.28	0.23	0.23	0.19	0.16	0.16
10.	0.42	0.32	0.34	0.39	0.31	0.28	0.30	0.32	0.28	0.26	0.24	0.27	0.24	0.16	0.14	0.17
20.	0.32	0.29	0.36	0.33	0.35	0.27	0.28	0.28	0.28	0.27	0.25	0.26	0.25	0.19	0.13	0.13
pga	0.34	0.31	0.30	0.35	0.30	0.28	0.27	0.26	0.27	0.23	0.27	0.23	0.21	0.15	0.14	0.14
pgv cm/sec	0.32	0.30	0.27	0.27	0.21	0.23	0.25	0.32	0.31	0.24	0.23	0.16	0.20	0.19	0.18	0.15

Mar 10, 1997

UNR: Anderson Finite Fault

Median Sa - Vertical Component (g):

Frequency	M_w 5.0		M_w 5.0 Deep		M_w 5.8 Deep		M_w 6.5							M_w 7.0	M_w 7.5	
	SS	HW	SS	HW	SS	HW	SS	HW	FW	HW	FW	SS	HW	SS	SS	HW
(Hz)	1 km	1 km	5 km	5 km	10 km	20 km	1 km	1 km	1 km	5 km	5 km	50 km	50 km	10 km	50 km	50 km
0.3	0.0012	0.00386	0.00036	0.00146	0.00353	0.00848	0.02429	0.06126	0.04805	0.10024	0.03666	0.00311	0.02019	0.03465	0.02276	0.07117
0.5	0.0039	0.00980	0.00097	0.00212	0.00525	0.01357	0.05334	0.10107	0.08910	0.14627	0.07583	0.00578	0.04812	0.05705	0.04049	0.17195
1.	0.0109	0.02339	0.00356	0.00733	0.01807	0.04918	0.10197	0.15040	0.14970	0.22130	0.12135	0.01614	0.04052	0.12276	0.05158	0.10457
2.	0.0249	0.05965	0.00951	0.01880	0.04785	0.19571	0.29534	0.41609	0.41189	0.36925	0.29463	0.04272	0.05850	0.32656	0.13098	0.13757
5.	0.0916	0.16062	0.05510	0.06431	0.11955	0.33592	0.68044	0.75322	0.87886	0.79130	0.58413	0.06754	0.09809	0.41794	0.13356	0.20785
10.	0.1577	0.38907	0.07141	0.12429	0.17713	0.41516	0.71369	1.28765	1.41409	1.14837	0.81429	0.07845	0.09526	0.45155	0.12221	0.16819
20.	0.1624	0.33861	0.05470	0.10656	0.13447	0.29982	0.67199	1.11347	1.26428	0.95440	0.69718	0.05566	0.07956	0.40693	0.10396	0.15976
pga	0.06943	0.18133	0.02847	0.05061	0.07026	0.17097	0.32595	0.60093	0.67965	0.49511	0.34258	0.03383	0.04146	0.21755	0.06349	0.09777
pgv cm/sec	2.09	4.86	0.67	1.45	2.71	7.30	14.89	30.13	27.23	32.96	17.38	1.57	4.98	14.34	6.11	16.81

Aleatory Variability about Median Sa - Vertical Component:

Frequency	M_w 5.0		M_w 5.0 Deep		M_w 5.8 Deep		M_w 6.5							M_w 7.0	M_w 7.5	
	SS	HW	SS	HW	SS	HW	SS	HW	FW	HW	FW	SS	HW	SS	SS	HW
(Hz)	1 km	1 km	5 km	5 km	10 km	20 km	1 km	1 km	1 km	5 km	5 km	50 km	50 km	10 km	50 km	50 km
0.3	0.24	0.12	0.16	0.09	0.26	0.21	0.44	0.33	0.29	0.34	0.26	0.42	0.44	0.43	0.33	0.23
0.5	0.25	0.16	0.22	0.19	0.33	0.39	0.41	0.34	0.30	0.37	0.30	0.34	0.33	0.23	0.31	0.25
1.	0.30	0.38	0.33	0.24	0.30	0.30	0.37	0.35	0.35	0.34	0.28	0.34	0.26	0.32	0.19	0.23
2.	0.36	0.32	0.38	0.31	0.30	0.34	0.35	0.32	0.33	0.26	0.31	0.25	0.25	0.24	0.23	0.16
5.	0.28	0.38	0.41	0.38	0.34	0.33	0.31	0.31	0.29	0.29	0.25	0.23	0.30	0.20	0.15	0.19
10.	0.40	0.43	0.36	0.40	0.35	0.34	0.27	0.33	0.32	0.27	0.23	0.27	0.29	0.19	0.18	0.12
20.	0.37	0.33	0.31	0.31	0.28	0.27	0.27	0.34	0.29	0.31	0.27	0.25	0.30	0.20	0.12	0.15
pga	0.33	0.32	0.27	0.34	0.32	0.27	0.27	0.28	0.26	0.23	0.25	0.22	0.22	0.16	0.17	0.13
pgv cm/sec	0.28	0.29	0.30	0.27	0.30	0.23	0.26	0.28	0.28	0.23	0.26	0.22	0.25	0.22	0.14	0.19

3.4.3-1

The modeling uncertainty for the Zeng and Anderson simulation procedure was estimated for the Northridge and Landers earthquakes as part of the SCEC c-cubed study. The resulting modeling uncertainties are plotted here.

Standard Error for Rock Sites

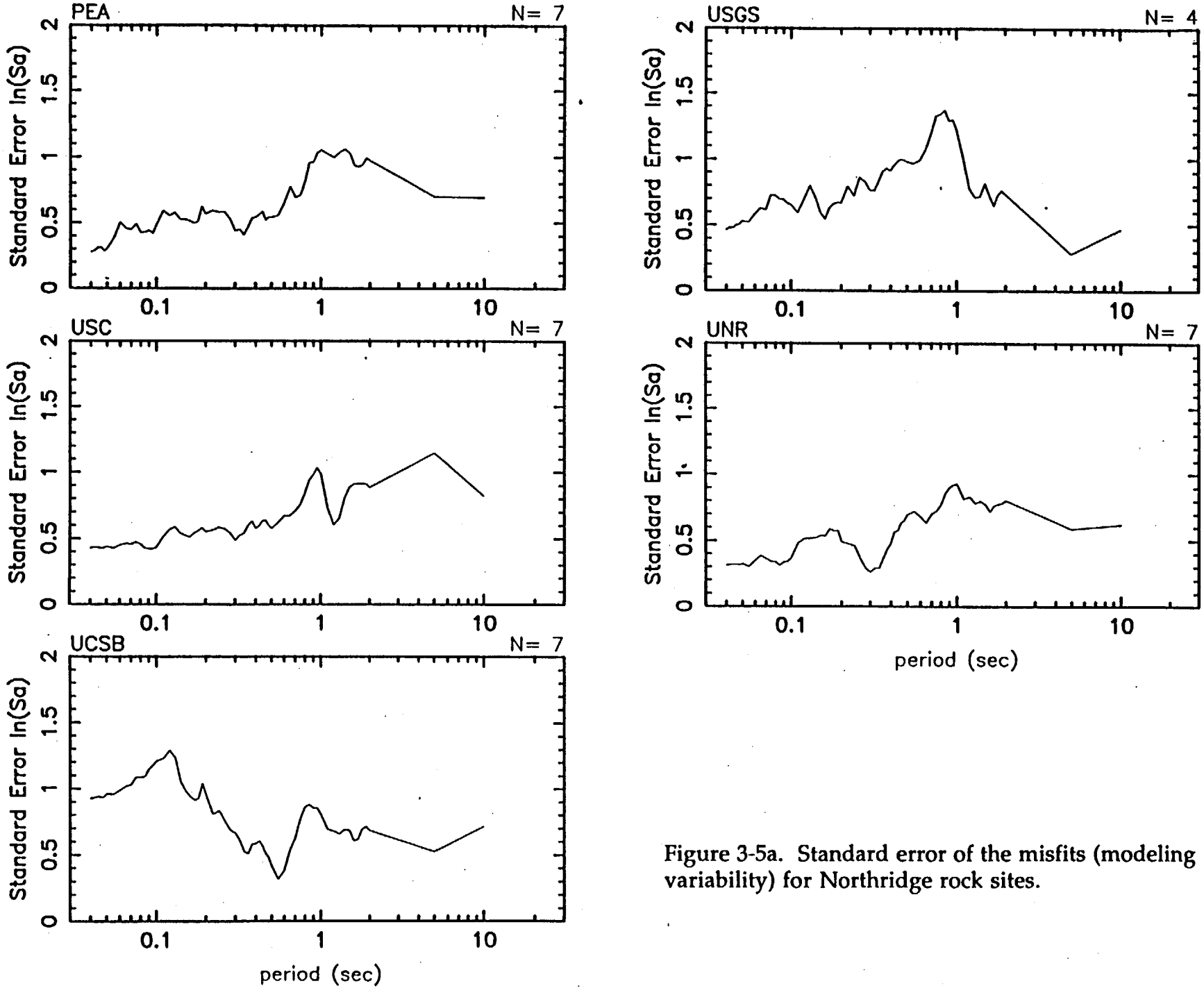

Figure 3-5a. Standard error of the misfits (modeling variability) for Northridge rock sites.

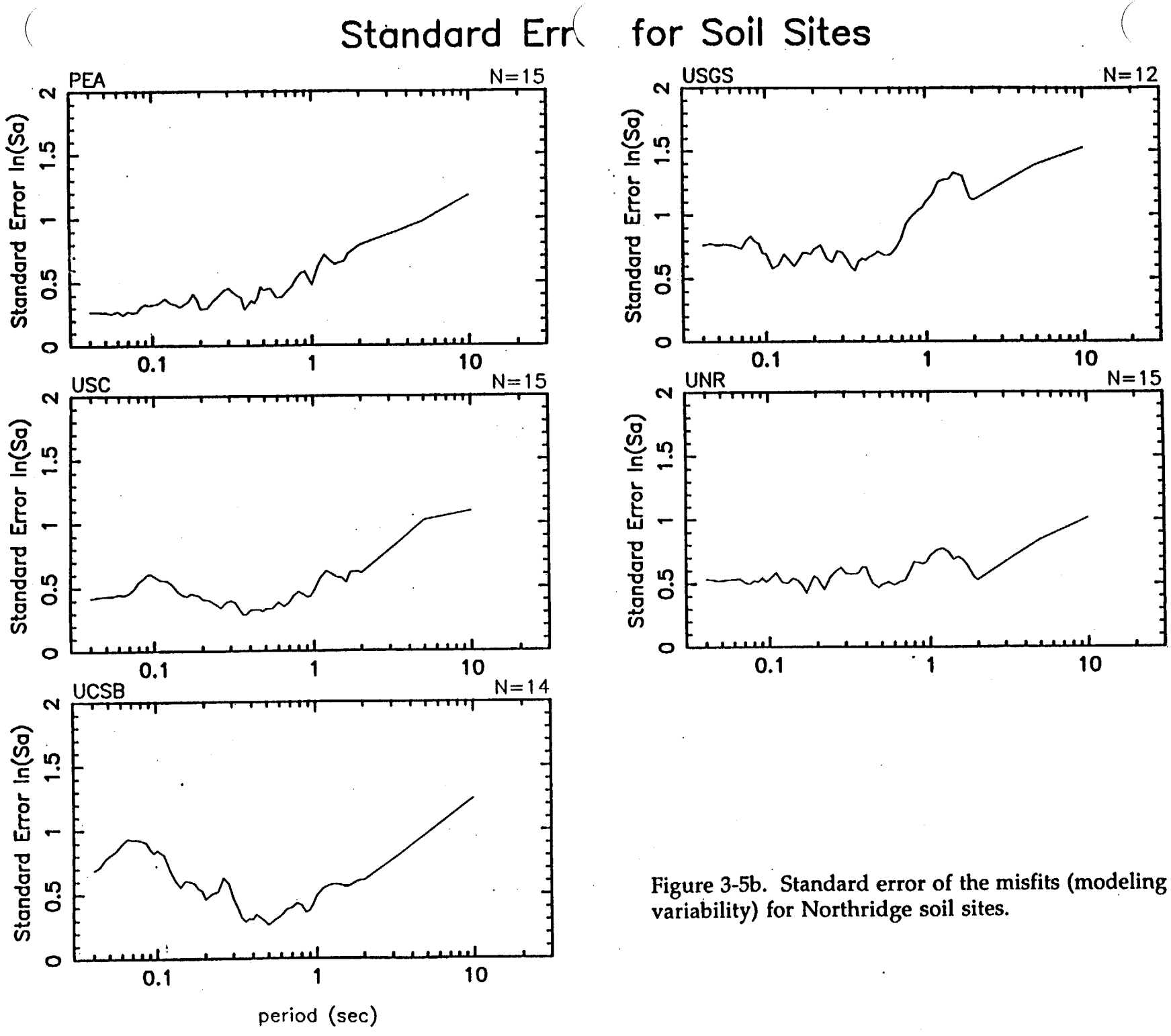

Figure 3-5b. Standard error of the misfits (modeling variability) for Northridge soil sites.

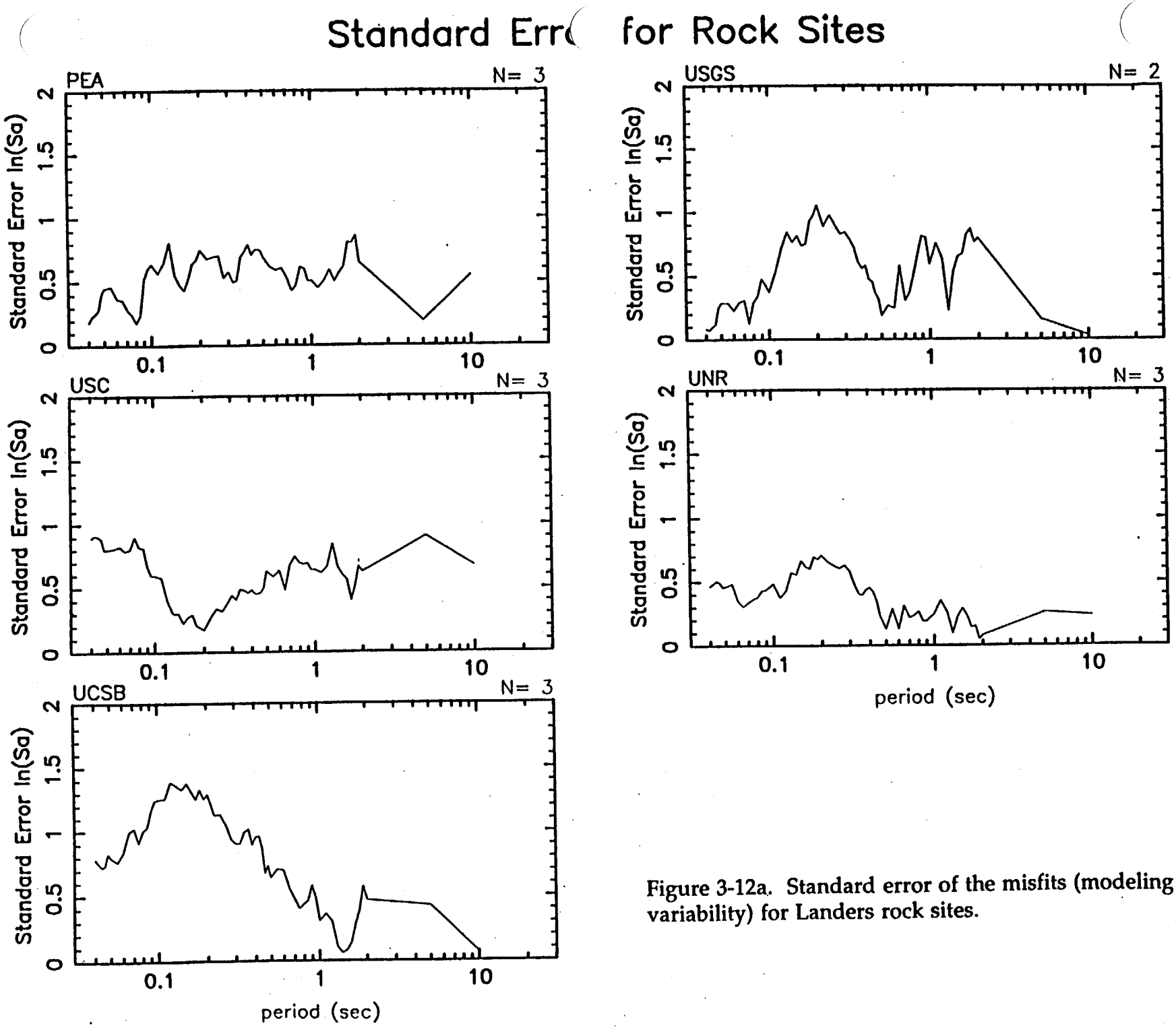

Figure 3-12a. Standard error of the misfits (modeling variability) for Landers rock sites.

Section 4.0

Empirical Models

4.1 Additional Documentation

4.1.1 Abrahamson & Silva update for normal faulting

Abrahamson used the 9 normal faulting events in the Spudich et al (1996) data base to compute style-of-faulting factors for normal faulting events for the Abrahamson & Silva (1997) attenuation model. These new style-of-faulting factors were estimated by holding the magnitude, distance, and site coefficients fixed to the values given in the previous model, and then applying the random effects model.

The resulting coefficients were then smoothed over period to produce the following model:

Abrahamson and Silva (1997) - Modified for Normal faulting

The general functional form is given by:

$$\ln Sa(g) = f_1(m,R_{rup}) + F_1\, f_3(m) + F_3 a_{14} + HW\, f_4(m,R_{rup}) + S\, f_5(\widehat{pga}_{rock}) \tag{28}$$

where S is a dummy variable for the site class (0 for rock or shallow soil, 1 for deep soil) and F =fault type: 0 for strike-slip and normal, 0.5 for reverse/oblique, 1.0 for reverse, and F3=1 for normal and 0 otherwise.

The basic attenuation for strike-slip and normal events at rock sites is given by:

$$f_1(m,r) = \begin{cases} a_1 + a_2(m-m_1) + a_{12}(8.5-m)^n + [a_3+a_{13}(m-m_1)]\ln(R) & \text{for } m \le m_1 \\ a_1 + a_4(m-m_1) + a_{12}(8.5-m)^n + [a_3+a_{13}(m-m_1)]\ln(R) & \text{for } m > m_1 \end{cases} \tag{29}$$

where

$$R = \sqrt{R_{rup}^2 + c_4^2} \tag{30}$$

The style-of-faulting factor is allowed to be magnitude and period dependent:

$$f_3(m) = \begin{cases} a_5 & \text{for } m \le 5.8 \\ a_5 + \dfrac{(a_6-a_5)}{m_1-5.8}(m-5.8) & \text{for } 5.8 < m < m_1 \\ a_6 & \text{for } m \ge m_1 \end{cases} \tag{31}$$

The hanging wall effect for dipping faults is magnitude and distance dependence and is modeled as separable in magnitude and distance so that

$$f_4(m,r) = f_{HW}(m)\, f_{HW}(R_{rup}) \tag{32}$$

where

$$f_{hw}(m) = \begin{cases} 0 & \text{for } m \leq 5.5 \\ m-5.5 & \text{for } 5.5 < m < 6.5 \\ 1 & \text{for } m \geq 6.5 \end{cases} \tag{33}$$

and

$$f_{hw}(R_{rup}) = \begin{cases} 0 & R_{rup}<4 \\ a_9(R_{rup}-4)/4 & 4 < R_{rup} < 8 \\ a_9 & 8 < R_{rup} < 18 \\ a_9(1-(R_{rup}-18)/7) & 18 < R_{rup} < 25 \\ 0 & 25 < R_{rup} \end{cases} \tag{34}$$

The non-linear soil response is modeled by

$$f_5(\widehat{PGA}_{rock}) = a_{10} + a_{11} \ln(\widehat{PGA}_{rock} + c_5) \tag{35}$$

where $\widehat{PGA}_{rock}$ is the expected peak acceleration on rock in g (as predicted by the attenuation relation with S=0).

The standard error is allowed to be magnitude dependent and is modeled as follows:

$$\sigma(m) = \begin{cases} b_1 & \text{for } m \leq 5.0 \\ b_1 - b_2(m-5) & \text{for } 5.0 < m < 7.0 \\ b_1 - 2b_2 & \text{for } m \geq 7.0 \end{cases} \tag{36}$$

*** Changes from previous version.

The change from the previous version is the addition of the a_{14} term for normal faulting events.

Smoothed Model Coefficients

a_{14}

Freq	Horiz	Vert
PGA	-0.16	-0.25
20	-0.16	-0.25
10	-0.16	-0.13
5	-0.12	0.00
2	-0.07	0.07
1	-0.20	-0.08
2	-0.40	-0.30

	L	A	B	C	D	E	F	G	H	I	J	K
Label		Period (Sec)	Mean (h	Stdev (h	Mean (v	Stdev (v		smoothed h	sigma mu Hor		smoothed z	sigma mu ver
1		0.01	-0.087	0.065	-0.203	0.065		-0.16	0.10		-0.25	0.08
2		0.03	-0.132	0.070	-0.300	0.068						
3		0.04	-0.218	0.076	-0.315	0.072						
4		0.05	-0.236	0.081	-0.392	0.076		-0.16	0.11		-0.25	0.16
5		0.06	-0.248	0.085	-0.377	0.079						
6		0.075	-0.274	0.078	-0.364	0.076						
7		0.09	-0.241	0.076	-0.170	0.067						
8		0.1	-0.231	0.078	-0.018	0.070		-0.16	0.11		-0.13	0.13
9		0.12	-0.159	0.070	0.004	0.081						
10		0.15	-0.111	0.075	-0.063	0.072						
11		0.17	-0.106	0.080	-0.010	0.076						
12		0.2	-0.104	0.078	0.045	0.077		-0.12	0.08		0	0.09
13		0.24	-0.112	0.071	0.042	0.070						
14		0.3	-0.090	0.076	0.107	0.082						
15		0.36	-0.073	0.072	0.106	0.088						
16		0.4	-0.055	0.070	0.084	0.085						
17		0.46	0.008	0.073	0.181	0.084						
18		0.5	0.074	0.077	0.171	0.078		-0.07	0.16		0.07	0.13
19		0.6	-0.017	0.083	0.101	0.077						
20		0.75	-0.163	0.089	-0.022	0.083						
21		0.85	-0.179	0.096	-0.062	0.097						
22		1	-0.207	0.103	0.022	0.110		-0.2	0.10		-0.08	0.15
23		1.5	-0.525	0.123	-0.302	0.147						
24		2	-0.726	0.136	-0.632	0.164		-0.4	0.35		-0.3	0.37
25		3	-0.802	0.152	-0.756	0.186		-0.4	0.43		-0.3	0.49
26		4	-0.749	0.164	-0.755	0.204						
27		5	-0.970	0.169	-0.970	0.180						

4.1.2 Boore et al. 1993 Horizontal Component Variability

Most of the ground motion models are for the average horizontal component. For this project, we are interested in the random horizontal component. The variability between the two horizontal components has been estimated by Boore et al (1993) and by Spudich et al (1996).

The following table lists the variability between the two horizontal components (in natural log units) :

Period	Spudich et al (1996)	Boore et al (1993)
0.00	0.22	.23
0.10	0.26	.19
0.20	0.28	.25
0.50	0.30	.30
1.0	0.32	.32
2.0	0.32	.36

This additional source of aleatory uncertainty should be included in the total aleatory uncertainty.

The following attenuation relationship for peak horizontal acceleration at rock sites was developed:

$$Ln(a) = \alpha_o + exp(\alpha_1 + \alpha_2 M) - exp(\beta_1 + \beta_2 M) Ln(R + 10) + F\phi - f(M,R)$$

in which M is moment magnitude; R is the closest distance to the rupture surface in km for $M > 6$ and the hypo-central distance for smaller magnitudes; $F = 0$ for strike slip, $F = 1$ for reverse and $F = ½$ for oblique sources. The parameters α_o, α_1, α_2, β_1, β_2 and ϕ are given below:

for $M < 6$	$\alpha_o = 0.010$	$\alpha_1 = 1.175$	$\alpha_2 = 0.0105$;
	$\beta_1 = 1.117$	$\beta_2 = -0.102$;	$f(M,R) = 0$, and
for $M \geq 6$	$\alpha_o = 0$	$\alpha_1 = 3.132$	$\alpha_2 = -0.309$;
	$\beta_1 = 2.354$	$\beta_2 = -0.306$;	

$$f(M,R) = (0.48 - 0.06M)(1 - 0.1R)(1 - tanh(R/20))$$

and $\phi = 0.28$ for all magnitudes and distances. The standard error term for peak horizontal accelerations is given by: $SE = 1.29 - 0.12M$, with $SE \geq 0.42$ (natural logarithm basis).

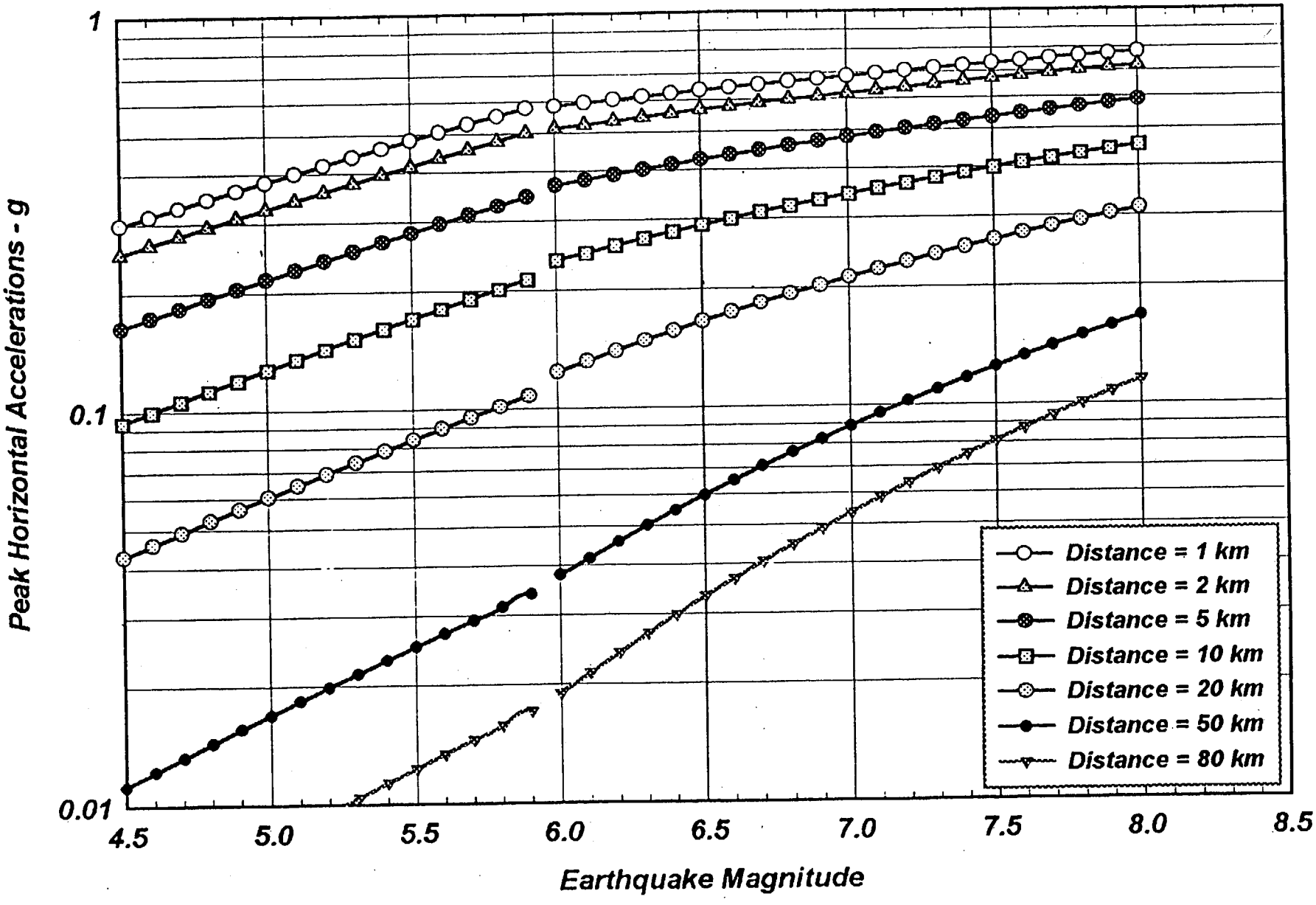

lml - 1996 – November 4, 1996

Section 4.1.4: McGarr (1984) Estimates

Magnitude	Depth	x	Mech	PGV, cm/s
5.0	shallow	1	SS	7.3
5.0	shallow	1	HW	7.1
5.0	deep	5	SS	5.6
5.0	deep	5	HW	5.9
5.8	deep	10	SS	12.1
5.8	deep	20	HW	10.9
6.5	shallow	1	SS	34.9
6.5	shallow	1	HW	33.3
6.5	shallow	1	FW	31.0
6.5	shallow	5	HW	36.0
6.5	shallow	5	FW	25.8
7.0	shallow	10	SS	48.4

4.3 Plots for Empirical Models Without Adjustments

M=5.0, Strike-slip, Shallow, Horizontal, Case 1

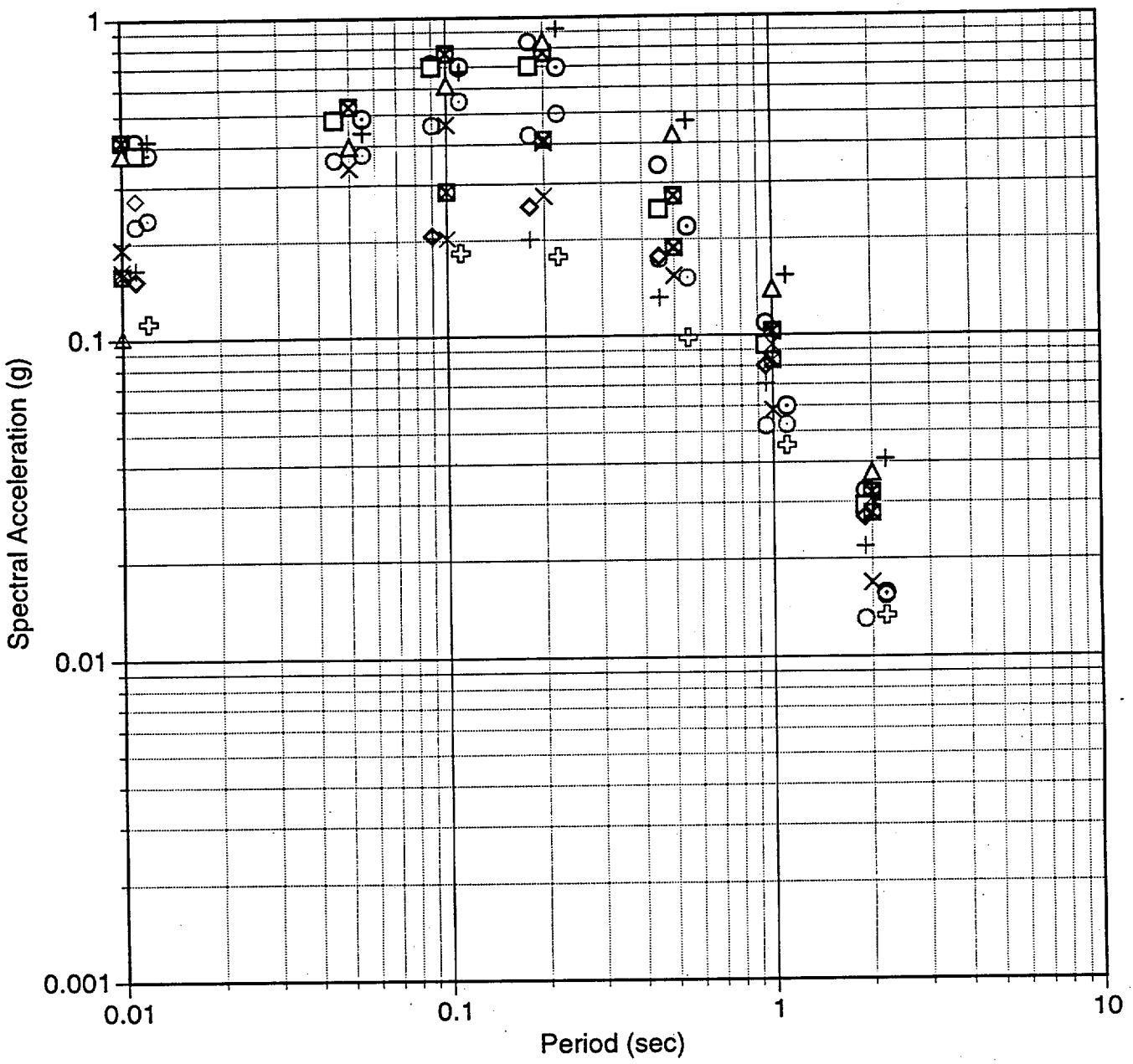

× AS97	□ Camp93/94(HR)	✠ BJF94(ClassA)	⊠ SP97
○ Camp97(SR)	+ Camp90/94(SR)	× BJF94(ClassB)	+ Spudichetal.97
⊙ Camp97(HR)	△ Camp90/94(HR)	○ Idriss91	△ McGarr84(Ext.)
⊠ Camp93/94(SR)	◇ BJF97(Vs=620m/s)	⊙ Sadighetal.93	◇ McGarr84(Comp)

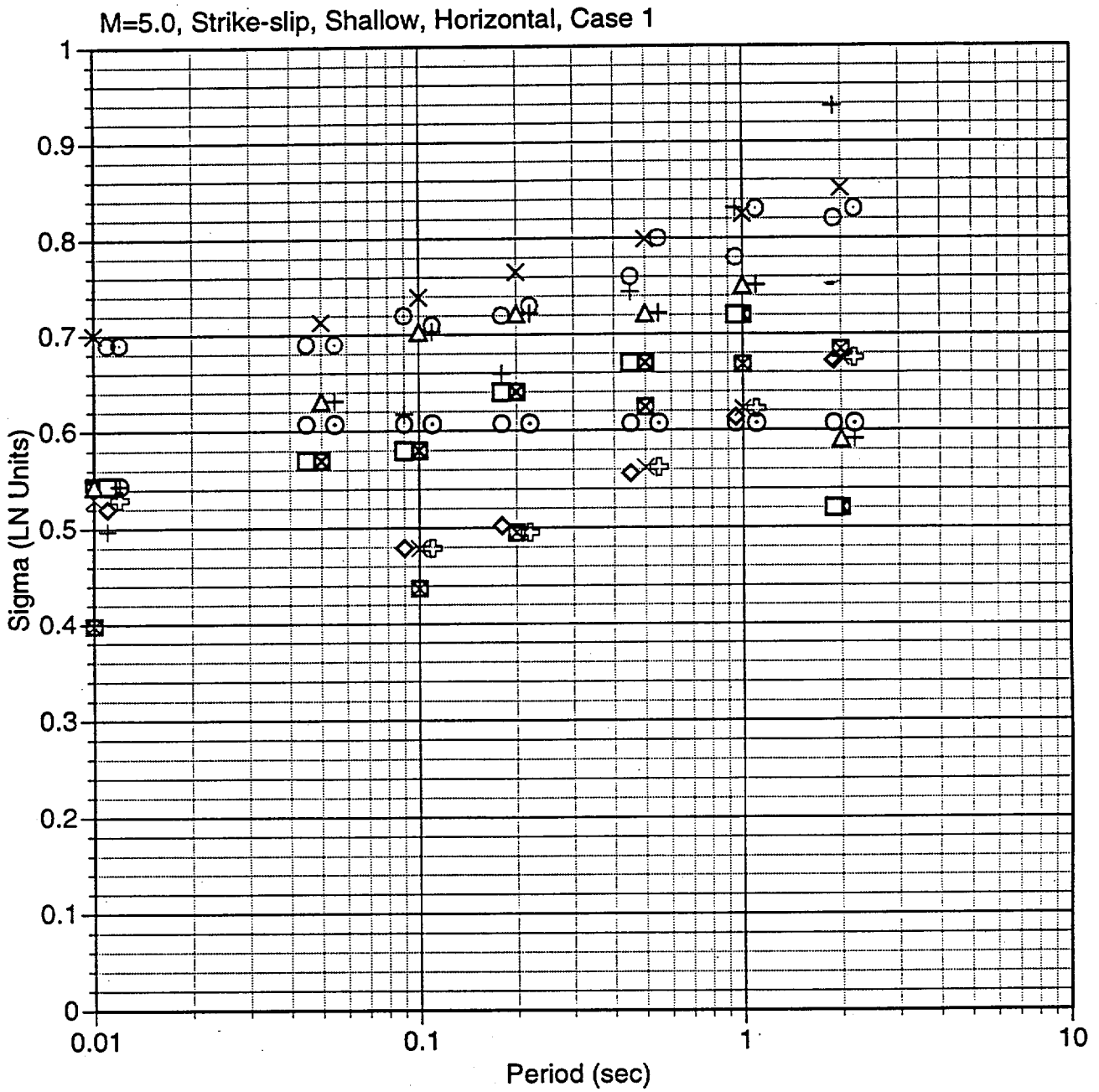

× AS97	□ Camp93/94(HR)	⊕ BJF94(ClassA)	⊠ SP97
○ Camp97(SR)	+ Camp90/94(SR)	× BJF94(ClassB)	+ Spudichetal.97
⊙ Camp97(HR)	△ Camp90/94(HR)	○ Idriss91	△ McGarr84(Ext.)
⊠ Camp93/94(SR)	◇ BJF97(Vs=620m/s)	⊙ Sadighetal.93	◇ McGarr84(Comp)

M=5.0, Strike-slip, Shallow, Vertical, Case 1

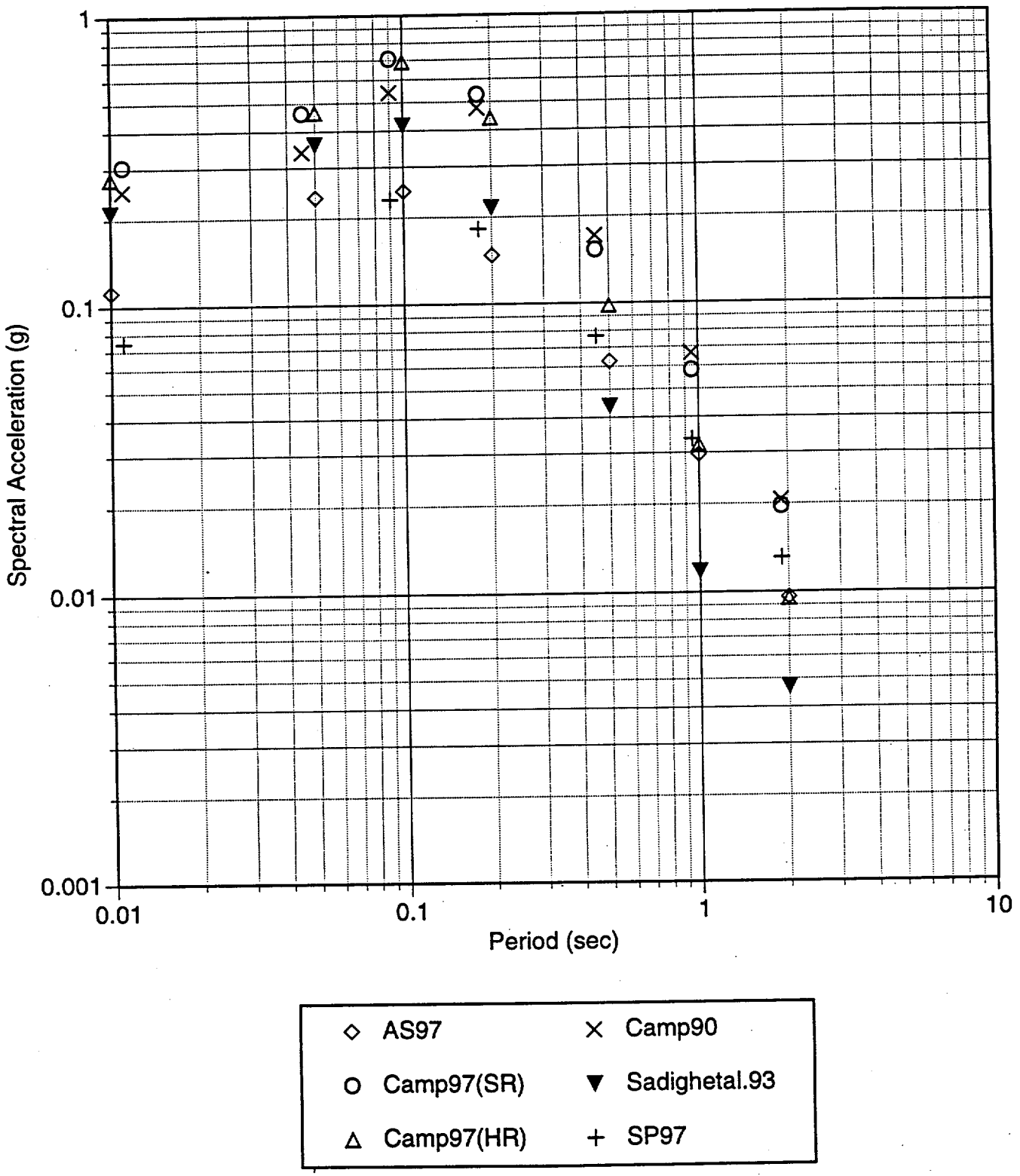

M=5.0, Strike-slip, Shallow, Vertical, Case 1

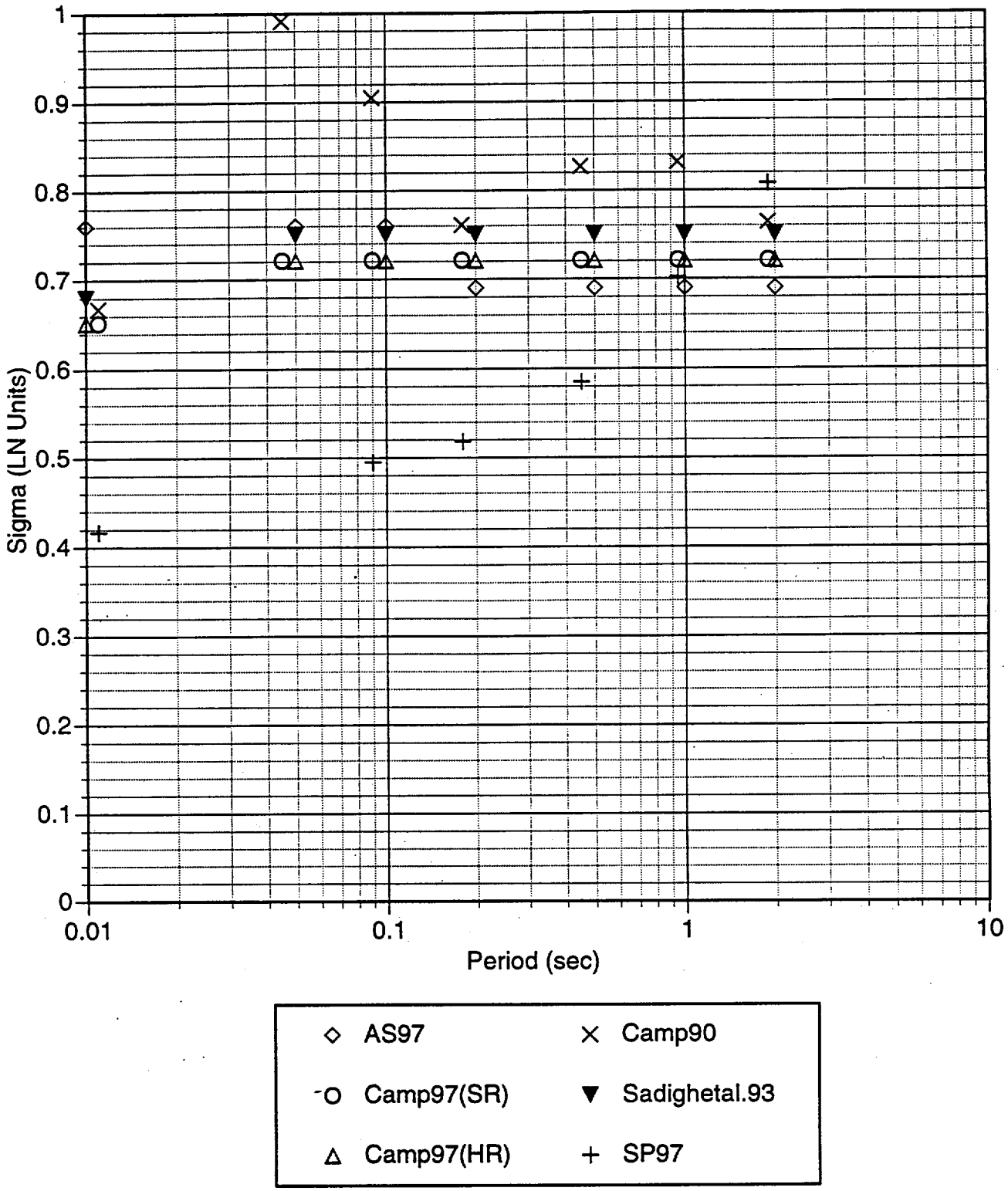

M=5.0, Hanging Wall, Shallow, Horizontal, Case 2

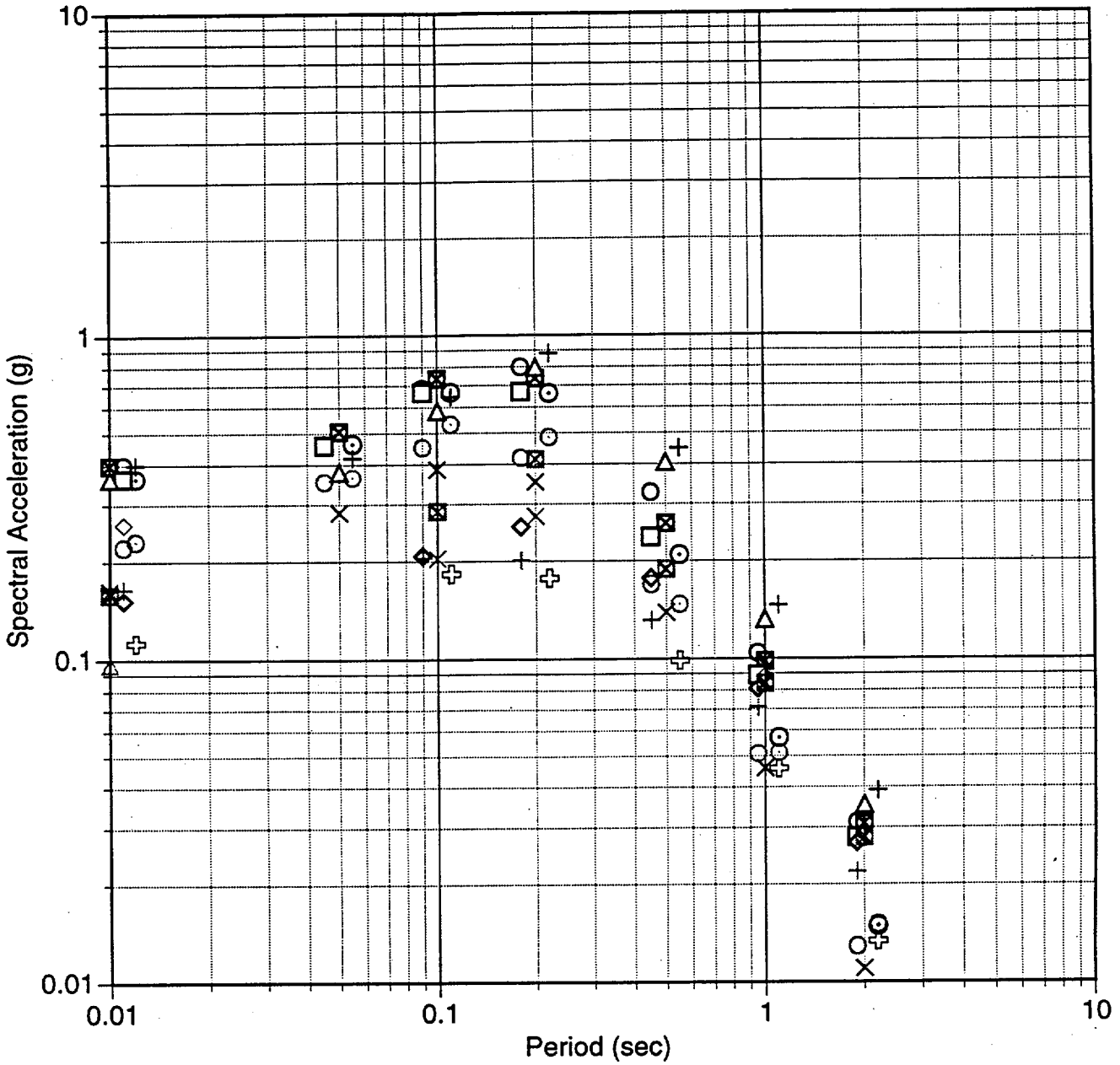

× AS97	□ Camp93/94(HR)	✚ BJF94(ClassA)	⊠ SP97
○ Camp97(SR)	+ Camp90/94(SR)	× BJF94(ClassB)	+ Spudichetal.97
⊙ Camp97(HR)	△ Camp90/94(HR)	○ Idriss91	△ McGarr84(Ext.)
⊠ Camp93/94(SR)	◇ BJF97(Vs=620m/s)	⊙ Sadighetal.93	◇ McGarr84(Comp)

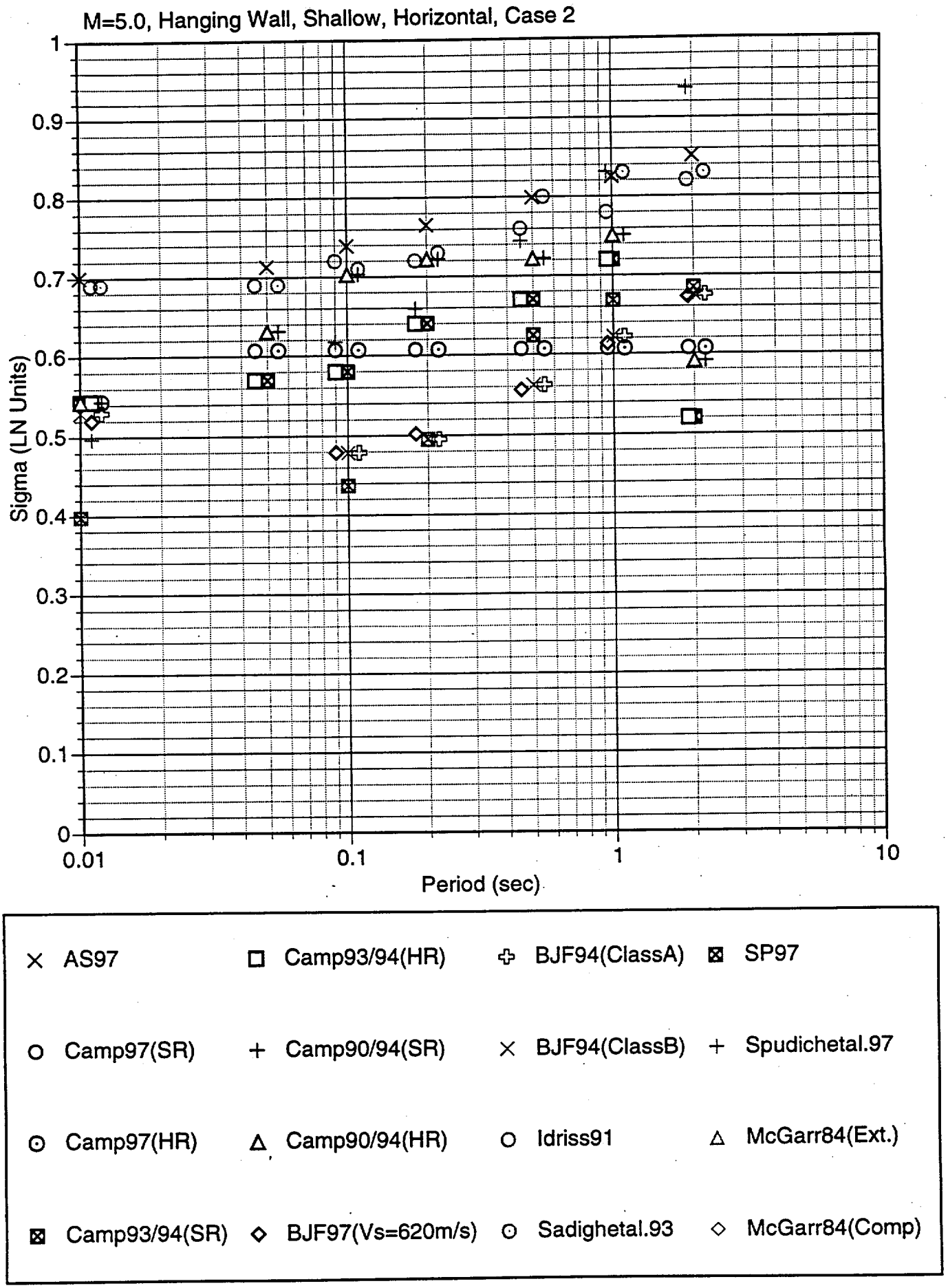
M=5.0, Hanging Wall, Shallow, Horizontal, Case 2
Sigma (LN Units)
Period (sec)
0
0.1
0.2
0.3
0.4
0.5
0.6
0.7
0.8
0.9
1
0.01
0.1
1
10
AS97
Camp93/94(HR)
BJF94(ClassA)
SP97
Camp97(SR)
Camp90/94(SR)
BJF94(ClassB)
Spudichetal.97
Camp97(HR)
Camp90/94(HR)
Idriss91
McGarr84(Ext.)
Camp93/94(SR)
BJF97(Vs=620m/s)
Sadighetal.93
McGarr84(Comp)

M=5.0, Hanging Wall, Shallow, Vertical, Case 2

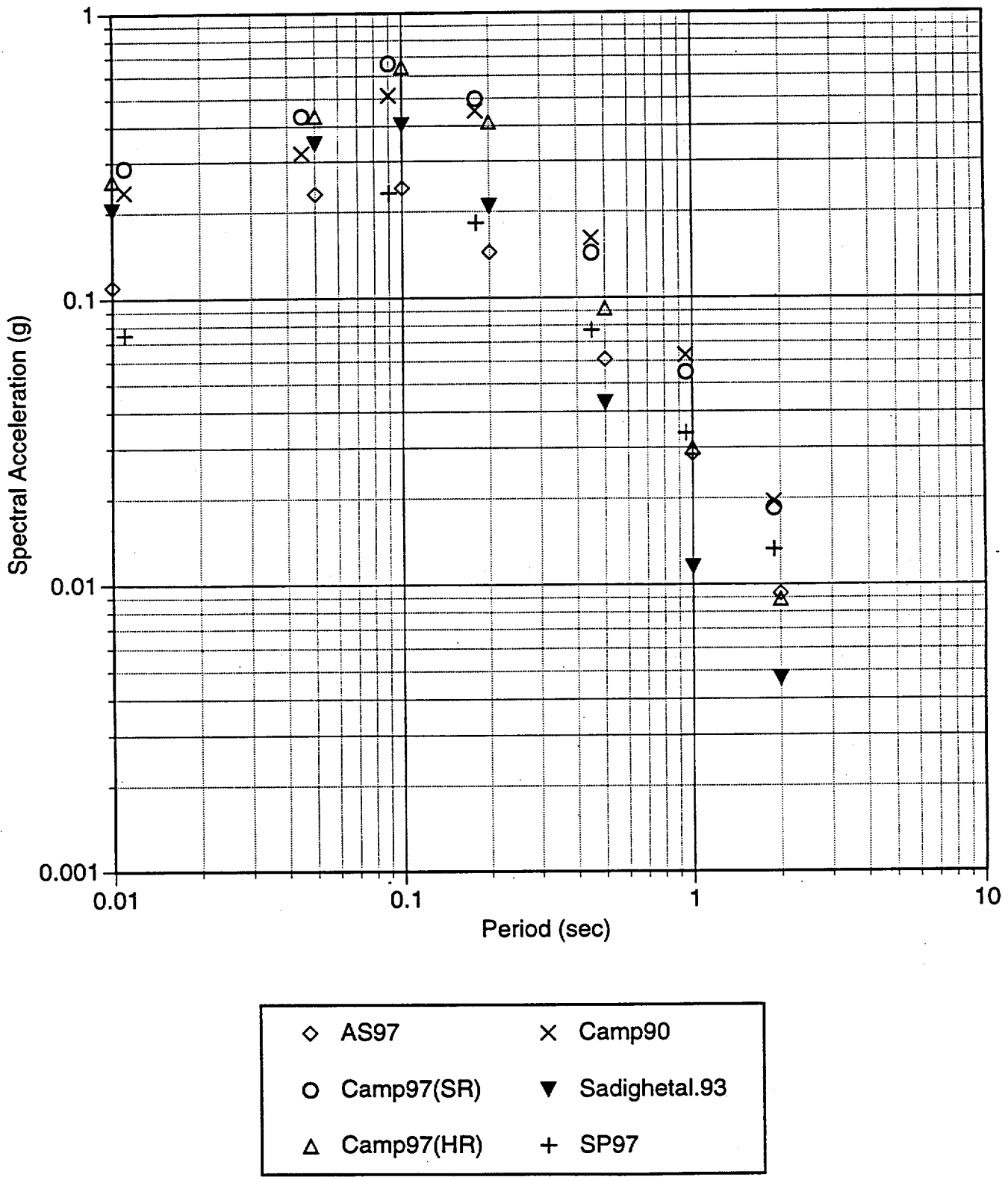

M=5.0, Hanging Wall, Shallow, Vertical, Case 2

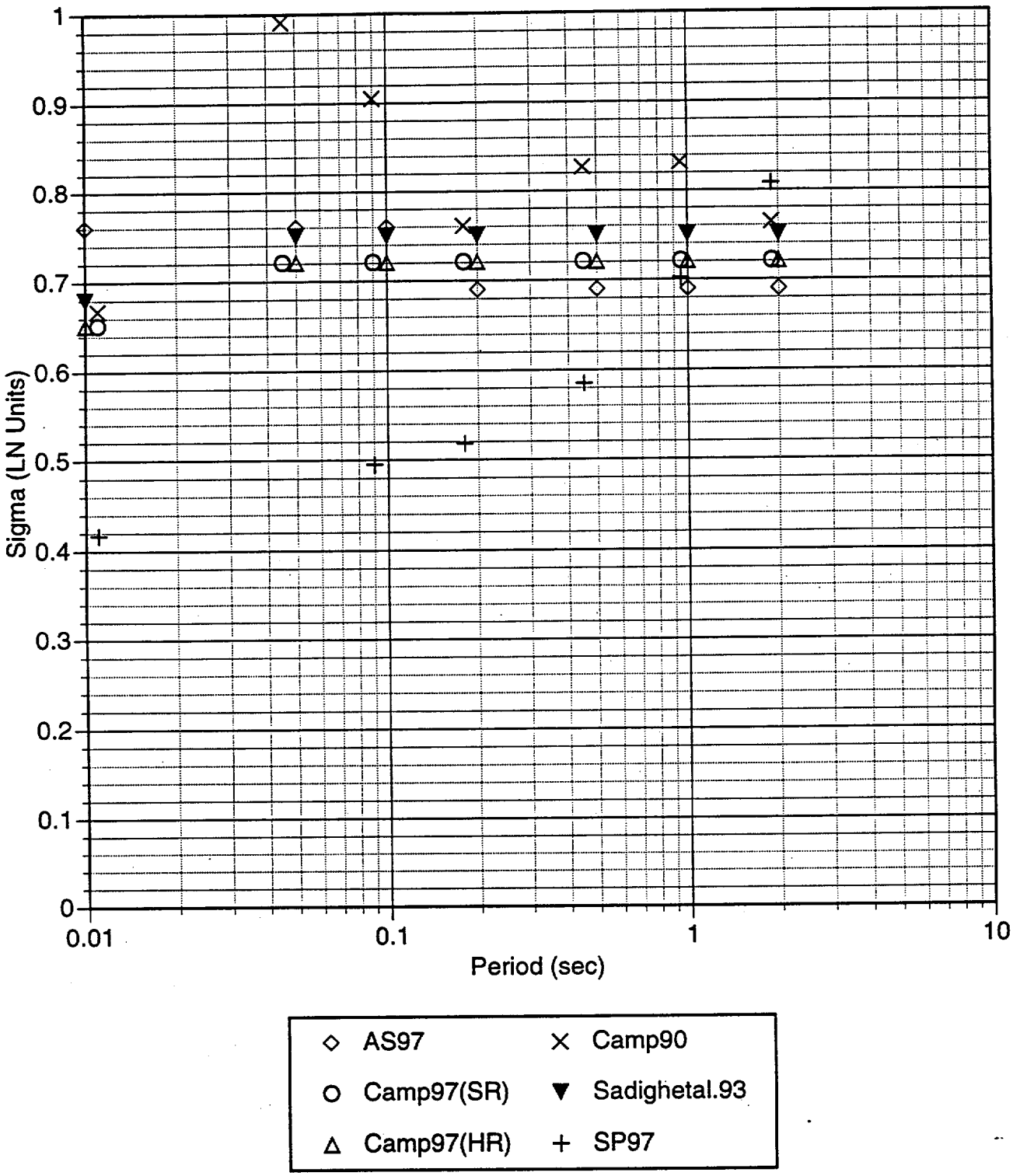

M=5.0, Strike-slip, Deep, Horizontal, Case 3

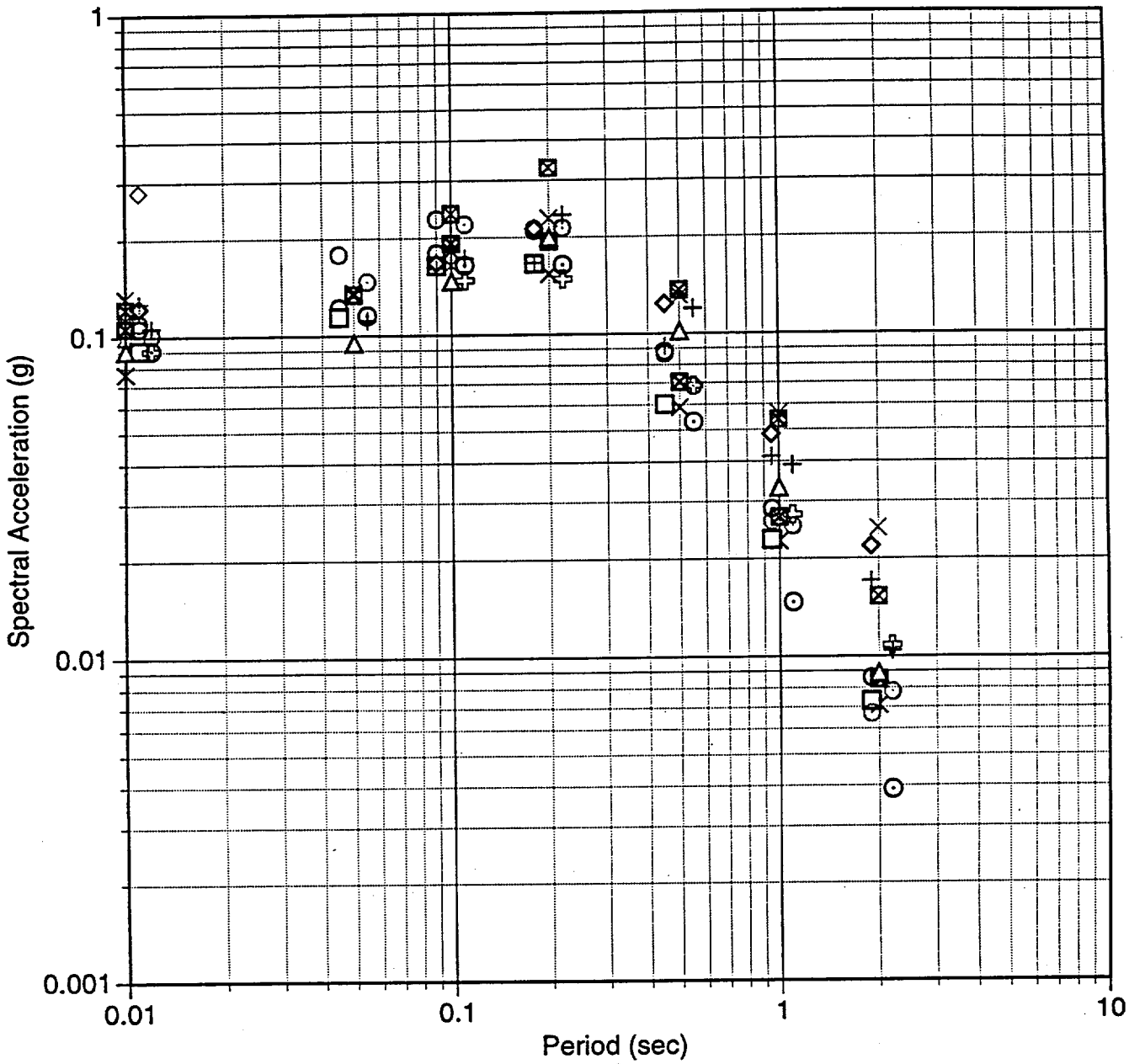

× AS97	□ Camp93/94(HR)	✚ BJF94(ClassA)	⊠ SP97
○ Camp97(SR)	+ Camp90/94(SR)	× BJF94(ClassB)	+ Spudichetal.97
⊙ Camp97(HR)	△ Camp90/94(HR)	○ Idriss91	△ McGarr84(Ext.)
⊠ Camp93/94(SR)	◇ BJF97(Vs=620m/s)	⊙ Sadighetal.93	◇ McGarr84(Comp)

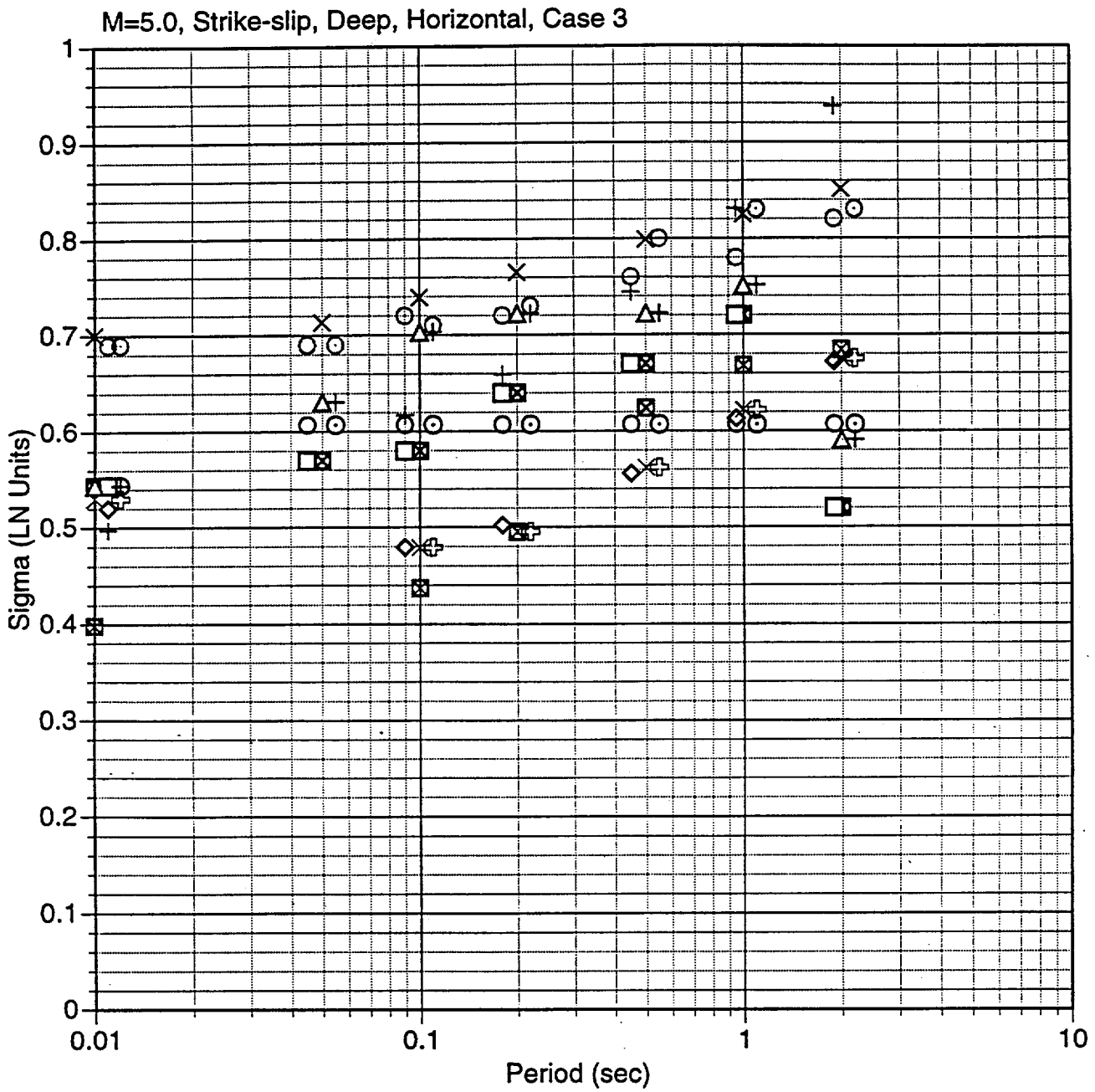

× AS97	□ Camp93/94(HR)	✚ BJF94(ClassA)	⊠ SP97
○ Camp97(SR)	+ Camp90/94(SR)	× BJF94(ClassB)	+ Spudichetal.97
⊙ Camp97(HR)	△ Camp90/94(HR)	○ Idriss91	△ McGarr84(Ext.)
⊠ Camp93/94(SR)	◇ BJF97(Vs=620m/s)	⊙ Sadighetal.93	◇ McGarr84(Comp)

M=5.0, Strike-slip, Deep, Vertical, Case 3

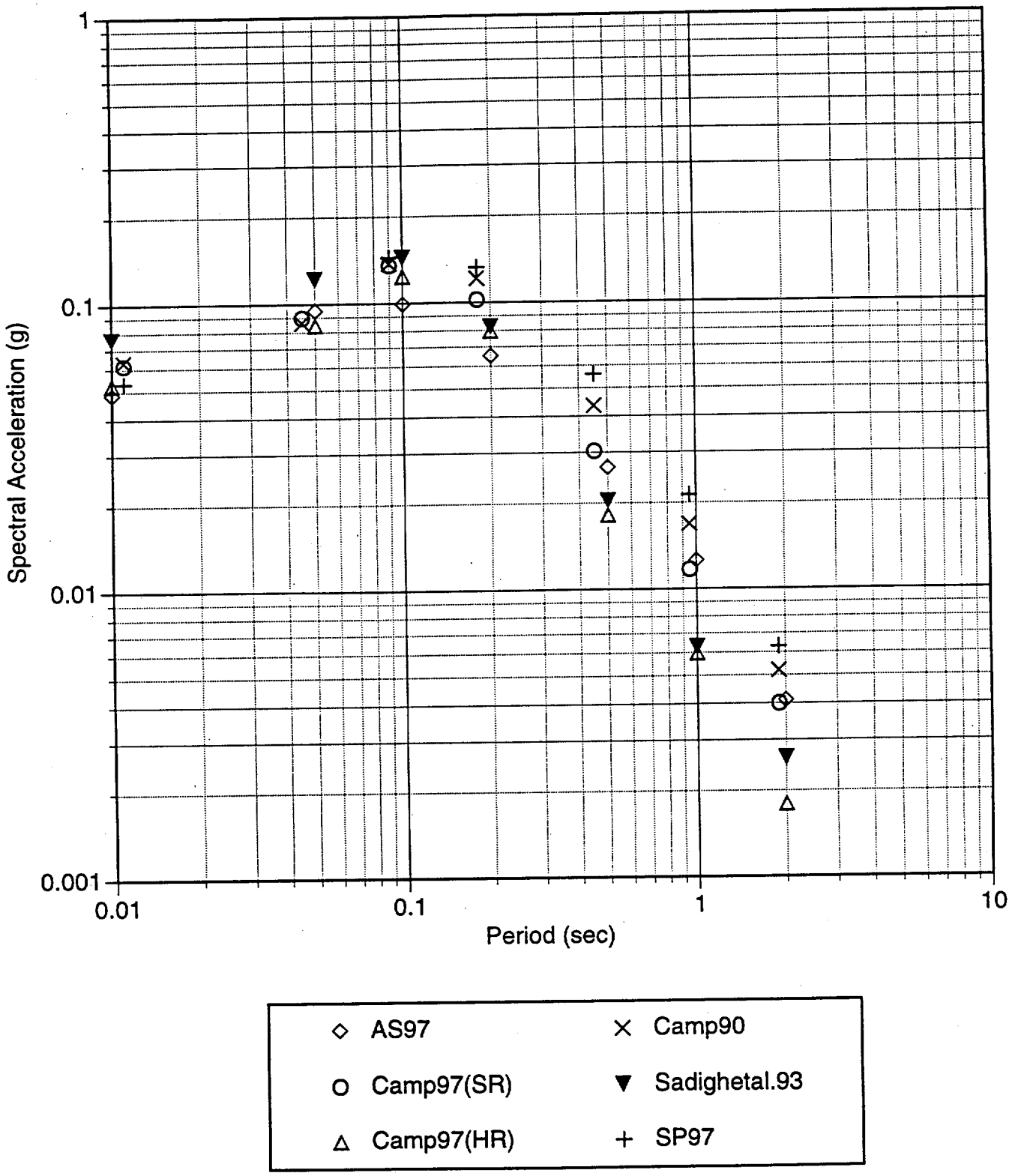

M=5.0, Strike-slip, Deep, Vertical, Case 3

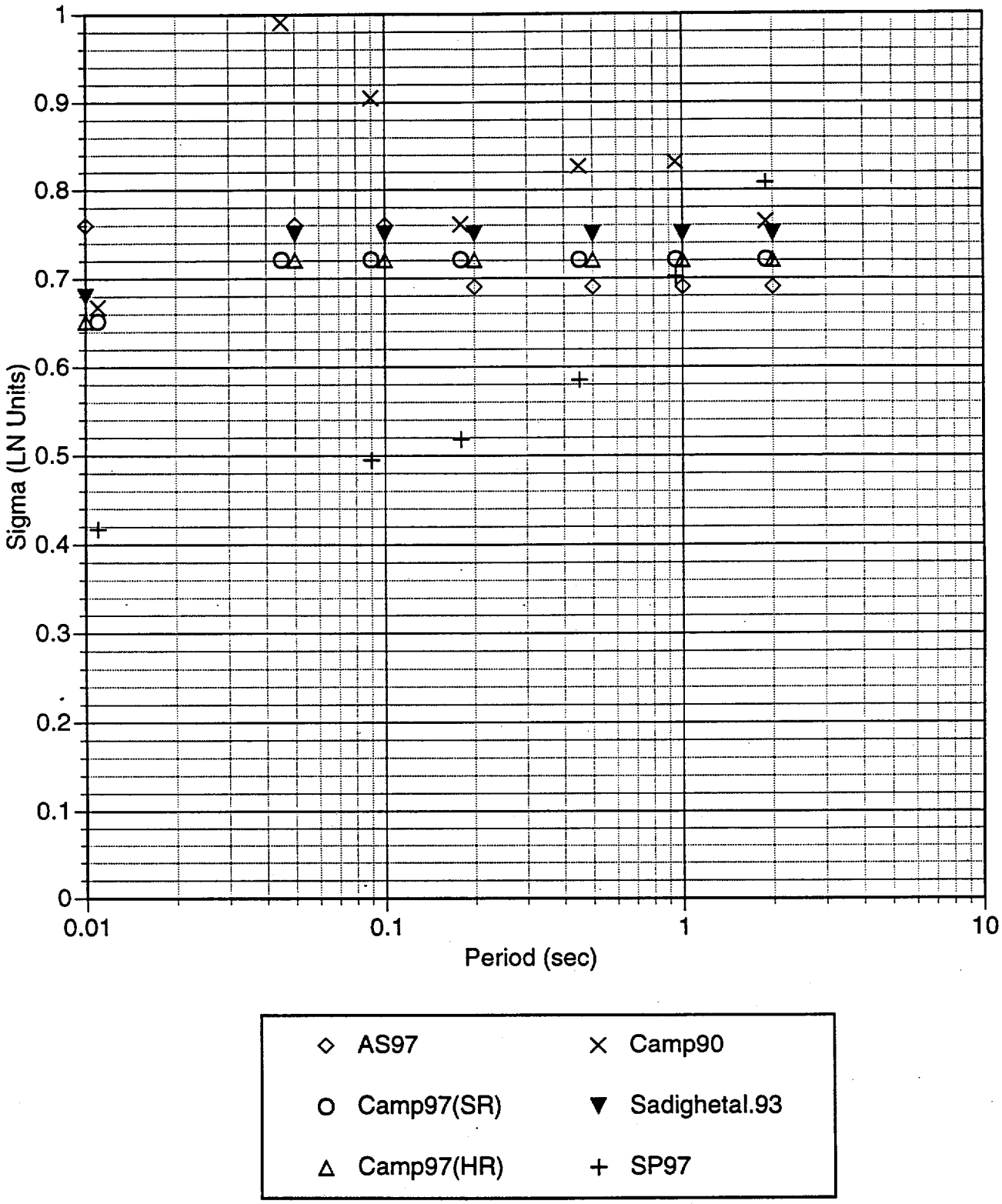

M=5.0, Hanging Wall, Deep, Horizontal, Case 4

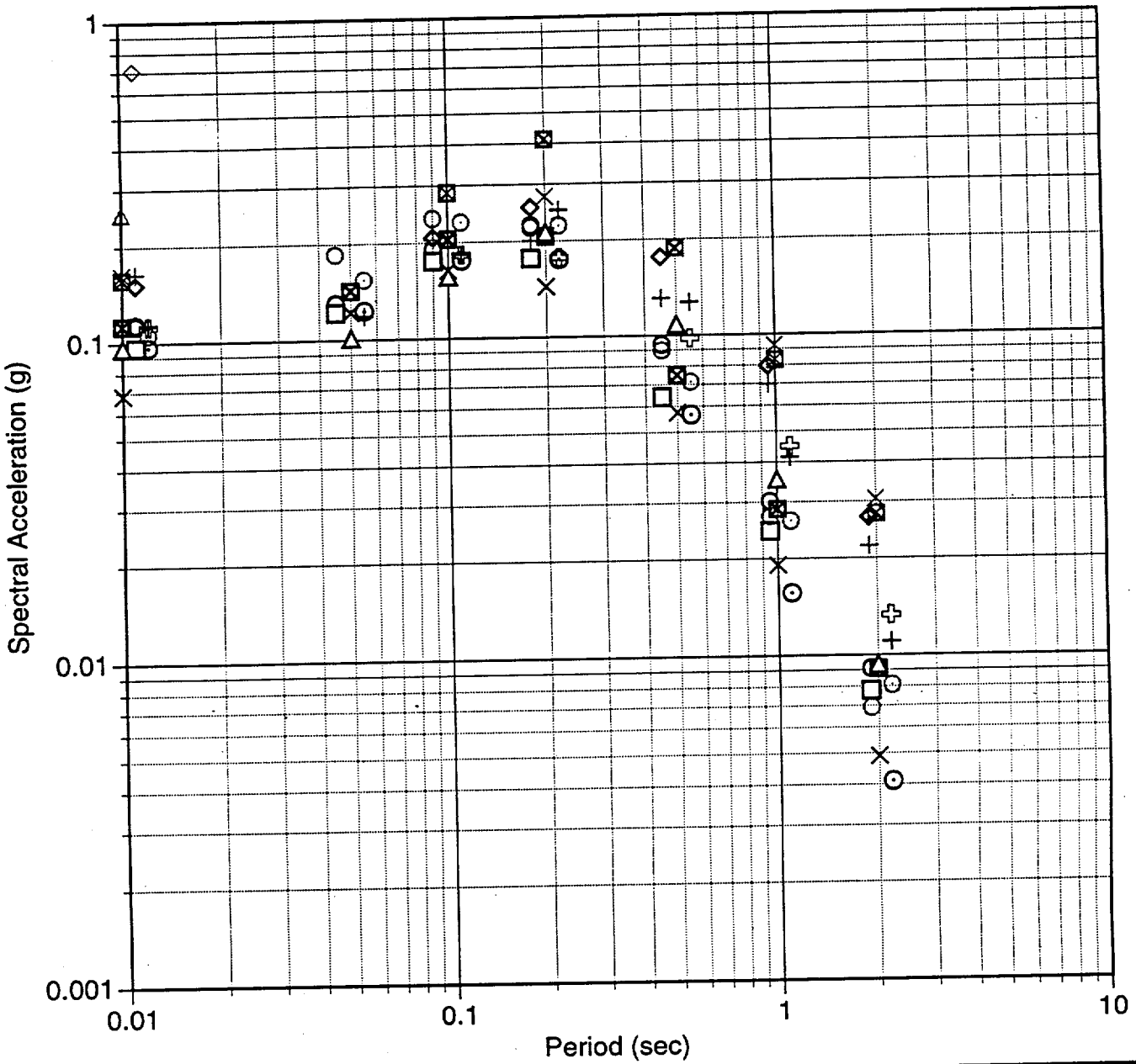

× AS97	□ Camp93/94(HR)	✚ BJF94(ClassA)	⊠ SP97
○ Camp97(SR)	+ Camp90/94(SR)	× BJF94(ClassB)	+ Spudichetal.97
⊙ Camp97(HR)	△ Camp90/94(HR)	○ Idriss91	△ McGarr84(Ext.)
⊠ Camp93/94(SR)	◇ BJF97(Vs=620m/s)	⊙ Sadighetal.93	◇ McGarr84(Comp)

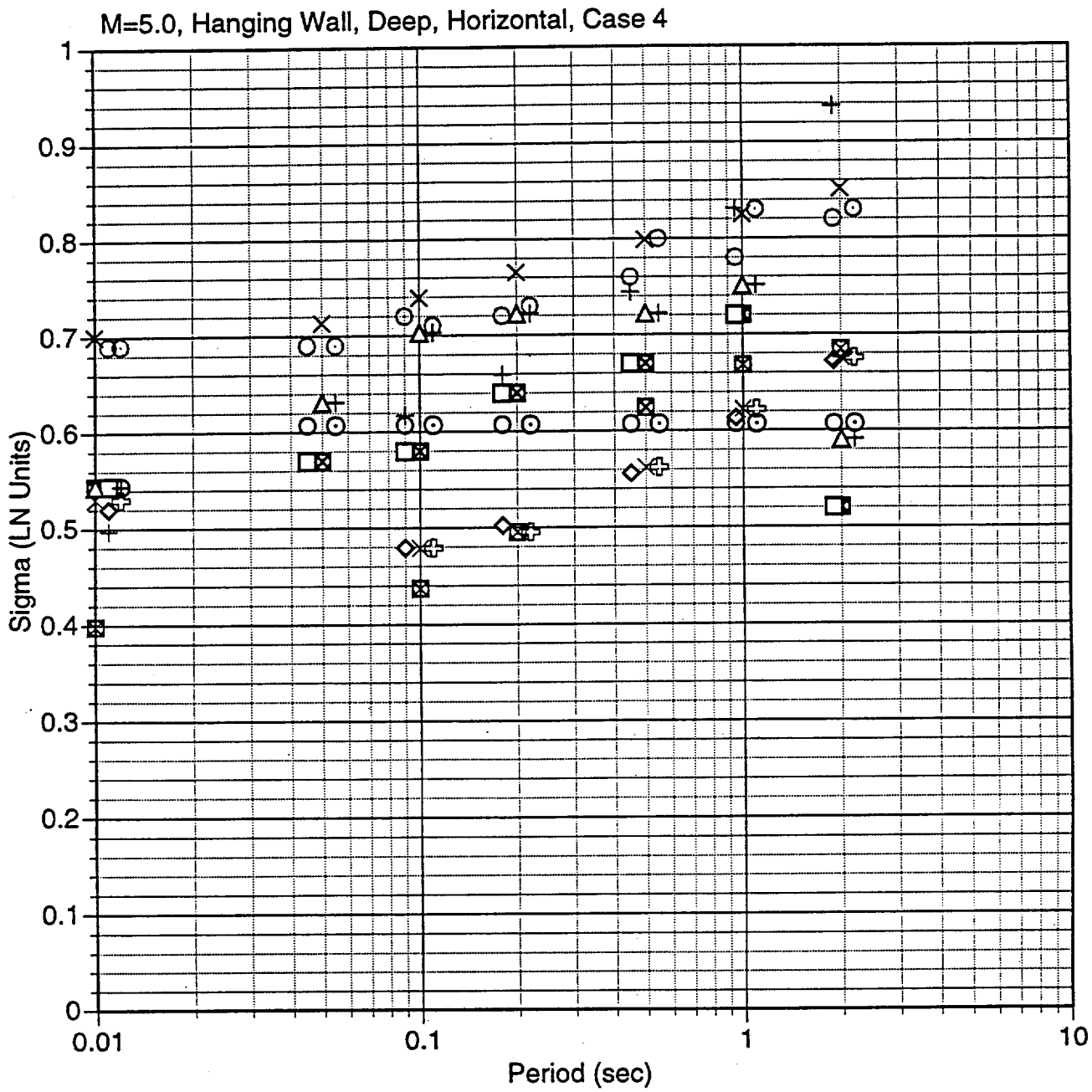

× AS97	□ Camp93/94(HR)	✚ BJF94(ClassA)	⊠ SP97
○ Camp97(SR)	+ Camp90/94(SR)	× BJF94(ClassB)	+ Spudichetal.97
⊙ Camp97(HR)	△ Camp90/94(HR)	○ Idriss91	△ McGarr84(Ext.)
⊠ Camp93/94(SR)	◇ BJF97(Vs=620m/s)	⊙ Sadighetal.93	◇ McGarr84(Comp)

M=5.0, Hanging Wall, Deep, Vertical, Case 4

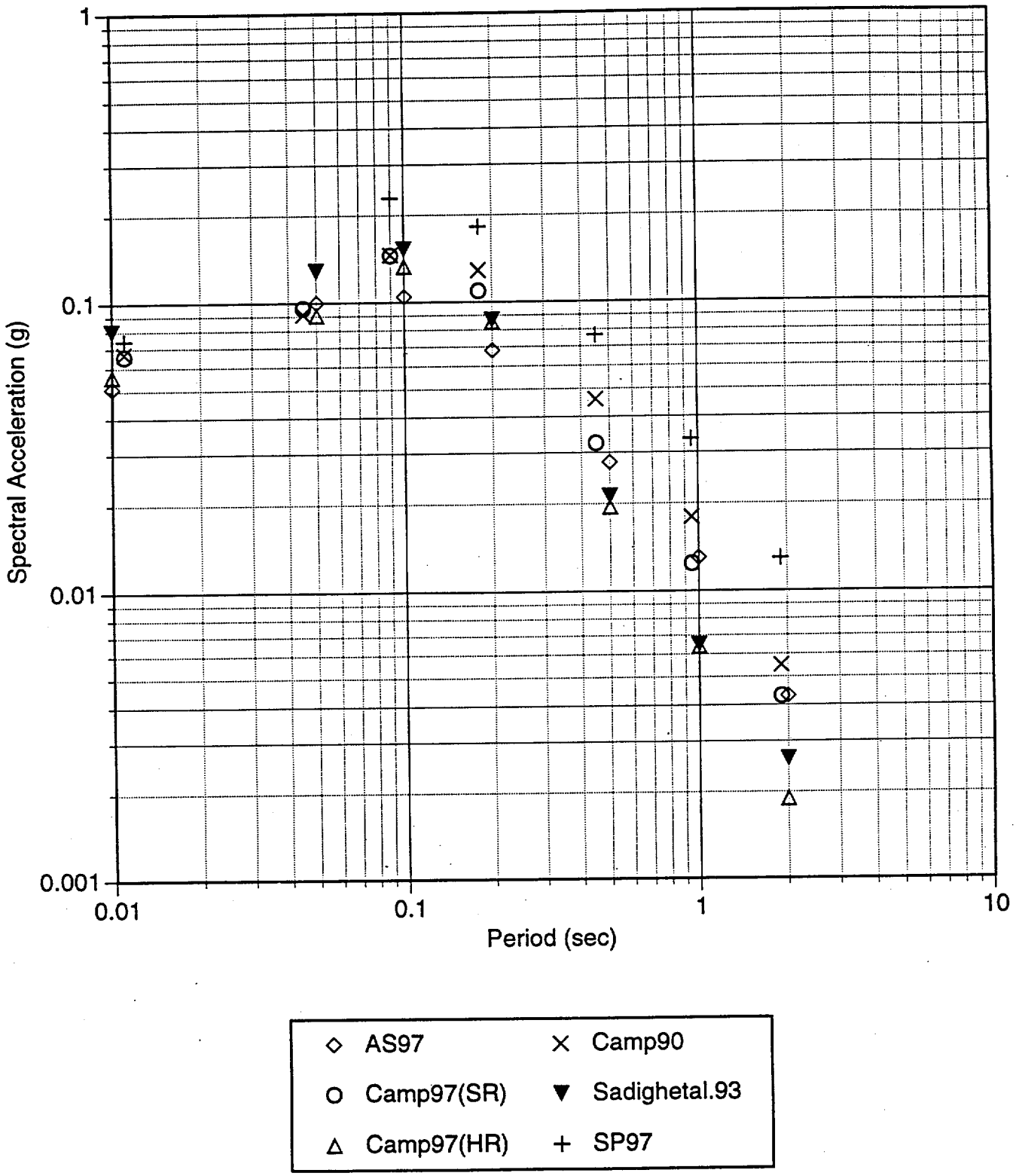

M=5.0, Hanging Wall, Deep, Vertical, Case 4

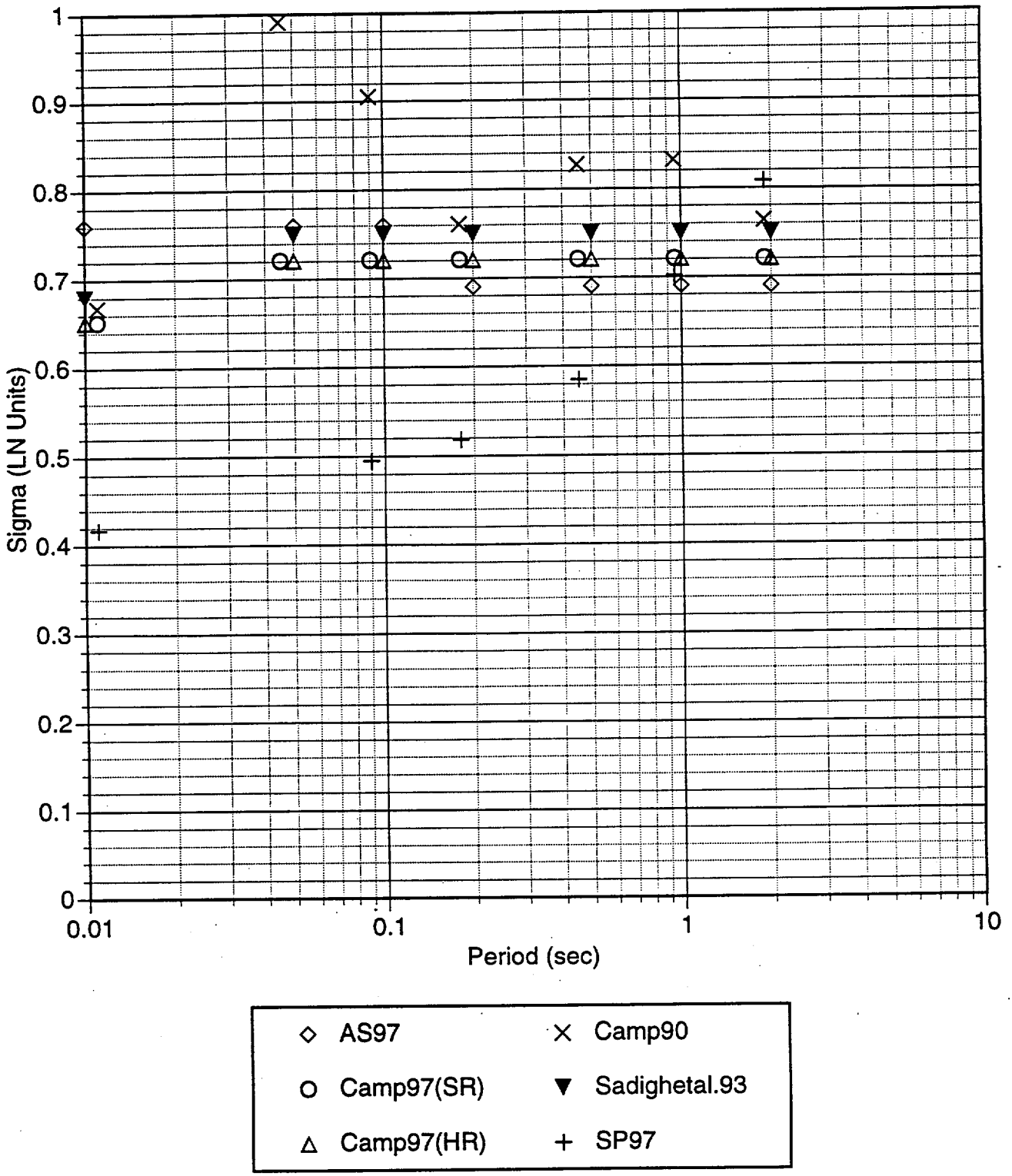

M=5.8, Strike-slip, Deep, Horizontal, Case 5

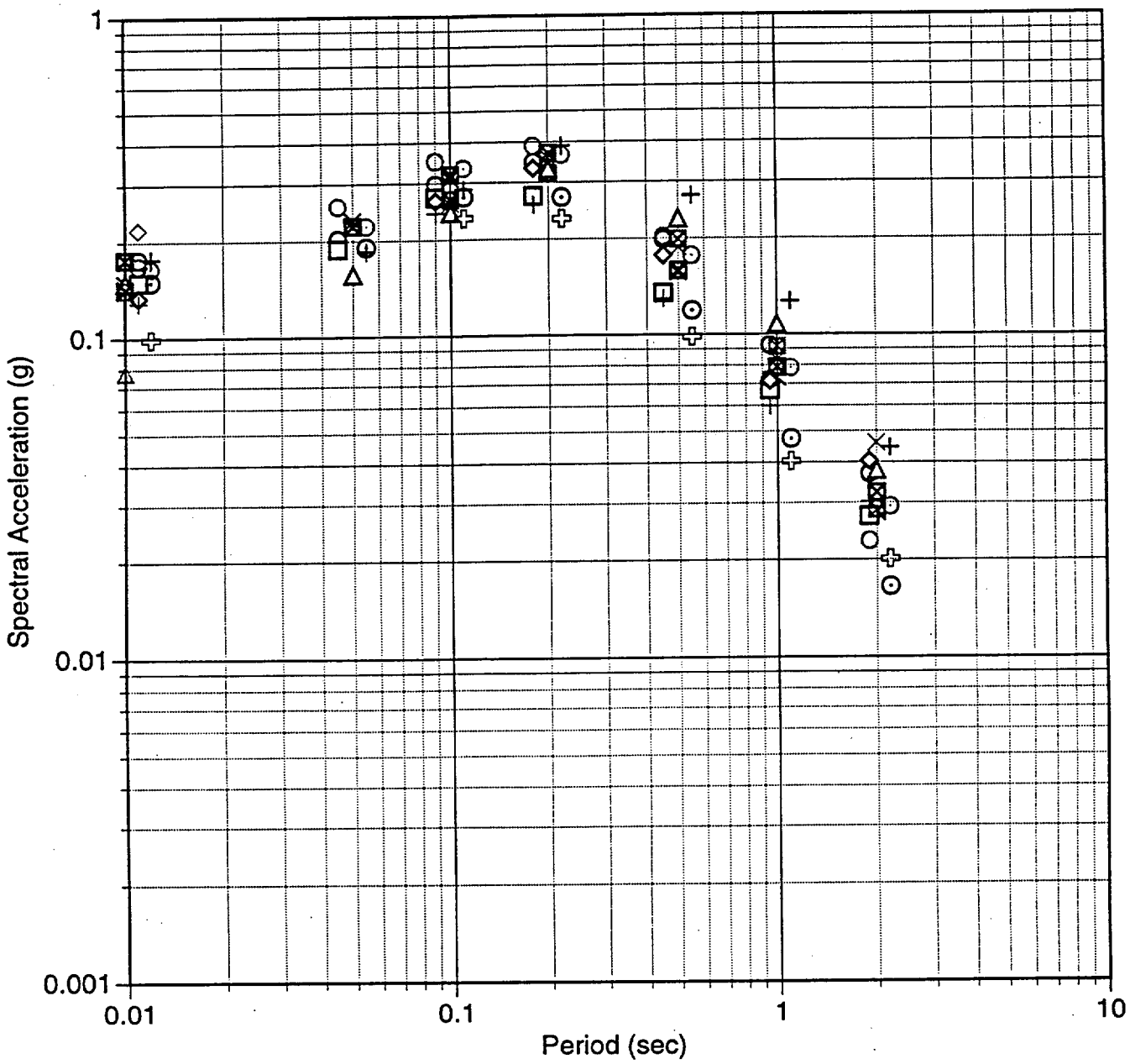

× AS97	□ Camp93/94(HR)	✣ BJF94(ClassA)	⊠ SP97
○ Camp97(SR)	+ Camp90/94(SR)	× BJF94(ClassB)	+ Spudichetal.97
⊙ Camp97(HR)	△ Camp90/94(HR)	○ Idriss91	△ McGarr84(Ext.)
⊠ Camp93/94(SR)	◇ BJF97(Vs=620m/s)	⊙ Sadighetal.93	◇ McGarr84(Comp)

M=5.8, Strike-slip, Deep, Horizontal, Case 5

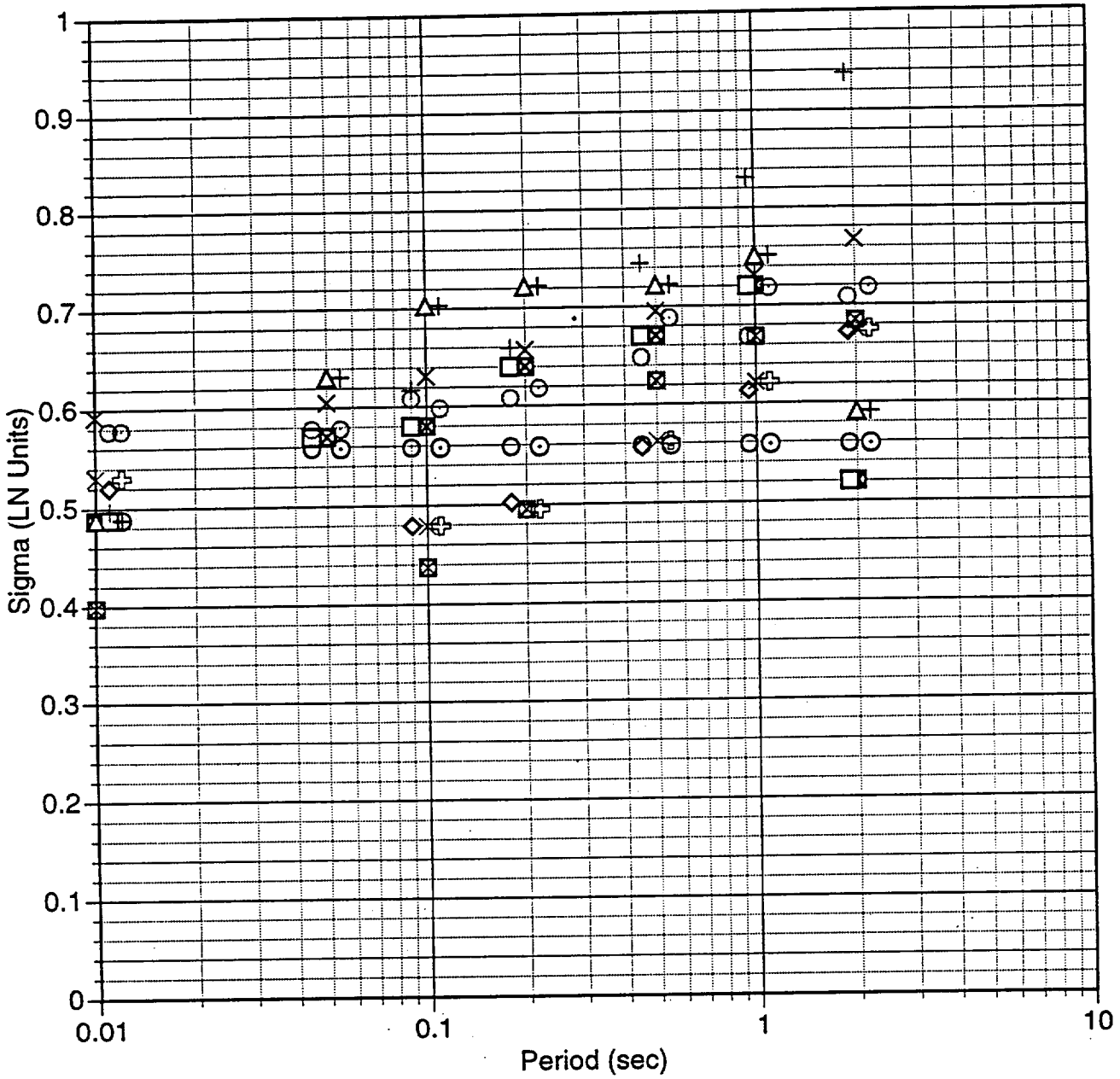

× AS97	□ Camp93/94(HR)	✚ BJF94(ClassA)	⊠ SP97
○ Camp97(SR)	+ Camp90/94(SR)	× BJF94(ClassB)	+ Spudichetal.97
⊙ Camp97(HR)	△ Camp90/94(HR)	○ Idriss91	△ McGarr84(Ext.)
⊠ Camp93/94(SR)	◇ BJF97(Vs=620m/s)	⊙ Sadighetal.93	◇ McGarr84(Comp)

M=5.8, Strike-slip, Deep, Vertical, Case 5

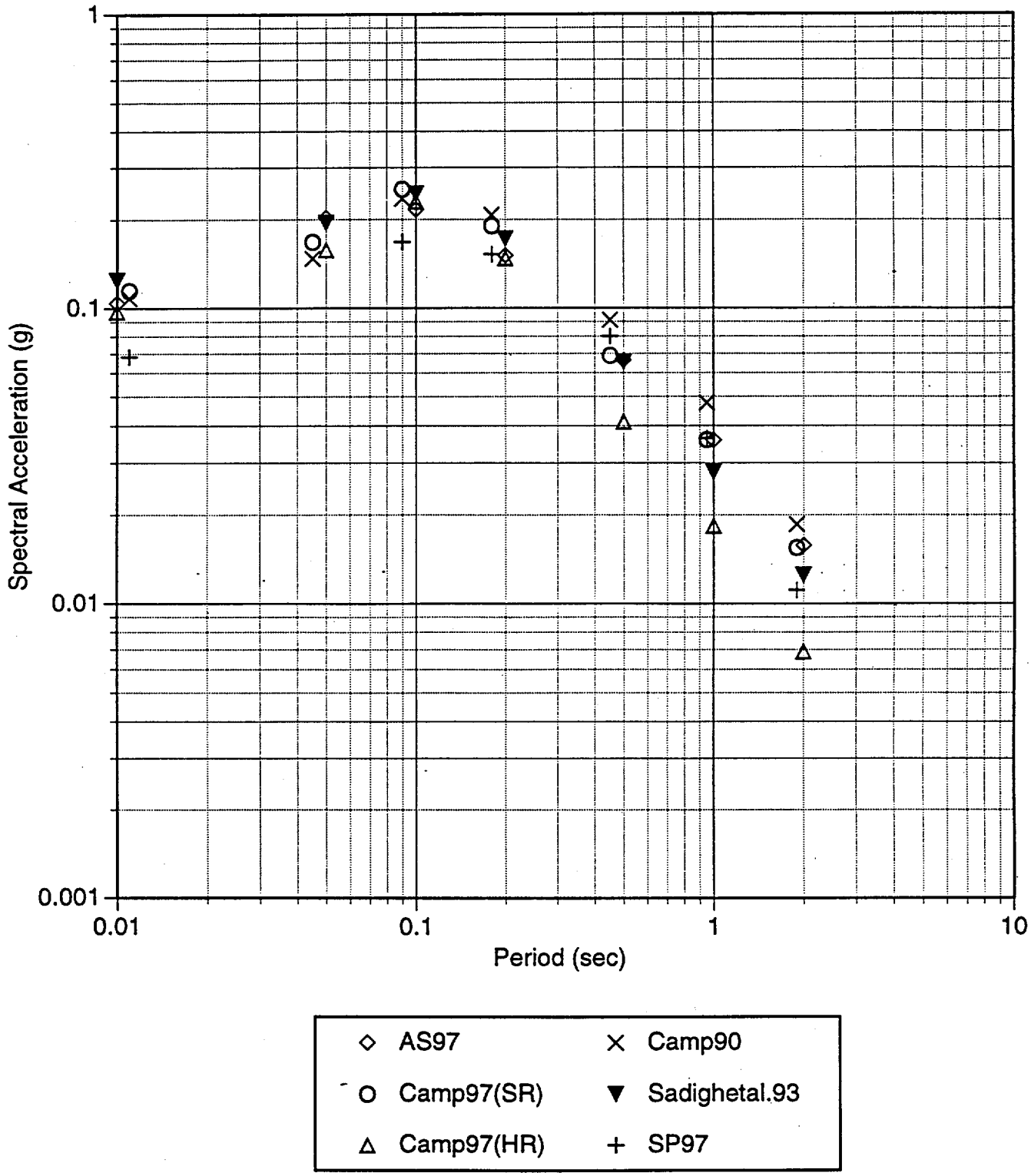

M=5.8, Strike-slip, Deep, Vertical, Case 5

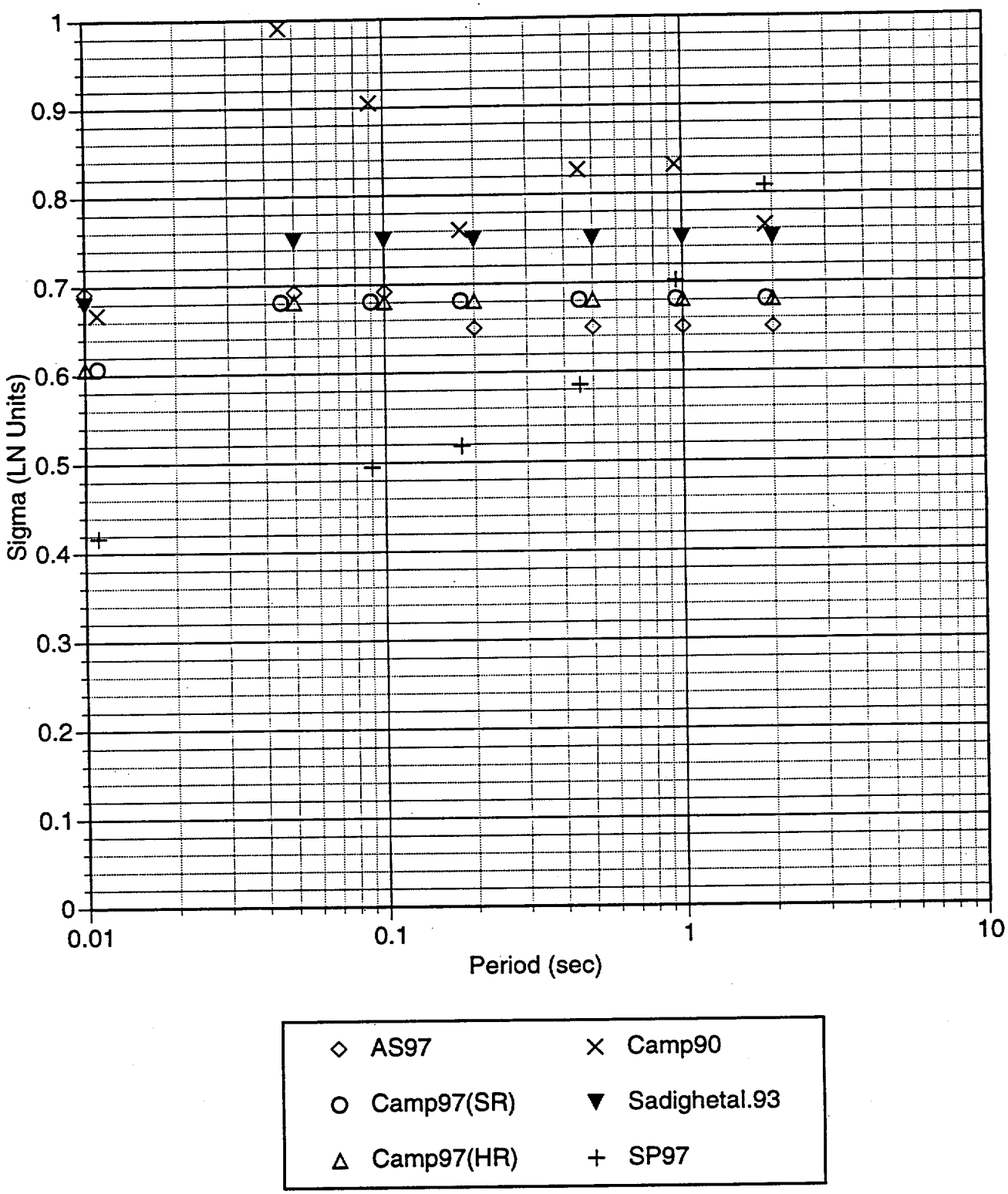

M=5.8, Hanging Wall, Deep, Horizontal, Case 6

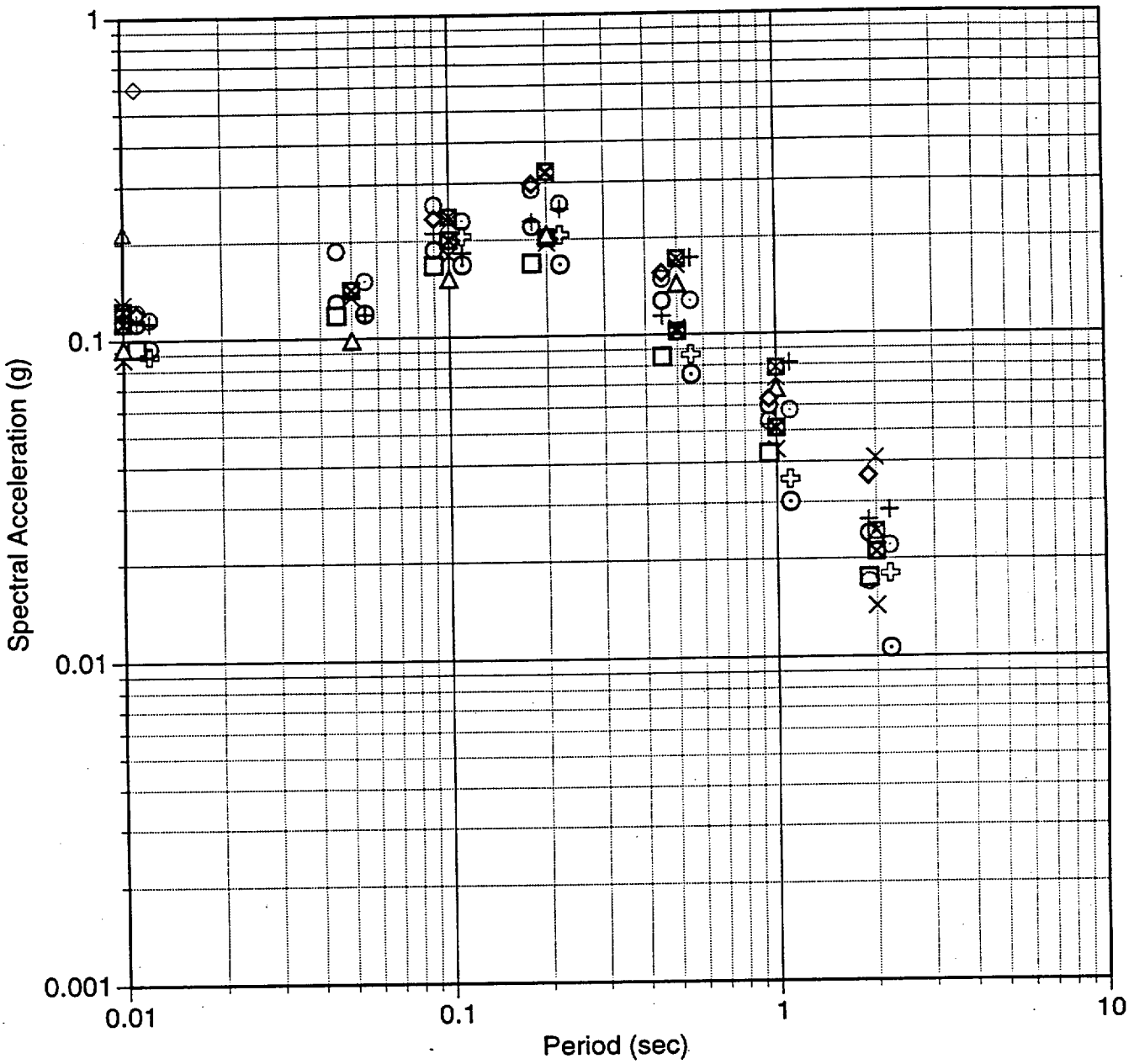

× AS97	□ Camp93/94(HR)	✚ BJF94(ClassA)	⊠ SP97
○ Camp97(SR)	+ Camp90/94(SR)	× BJF94(ClassB)	+ Spudichetal.97
⊙ Camp97(HR)	△ Camp90/94(HR)	○ Idriss91	△ McGarr84(Ext.)
⊠ Camp93/94(SR)	◇ BJF97(Vs=620m/s)	⊙ Sadighetal.93	◇ McGarr84(Comp)

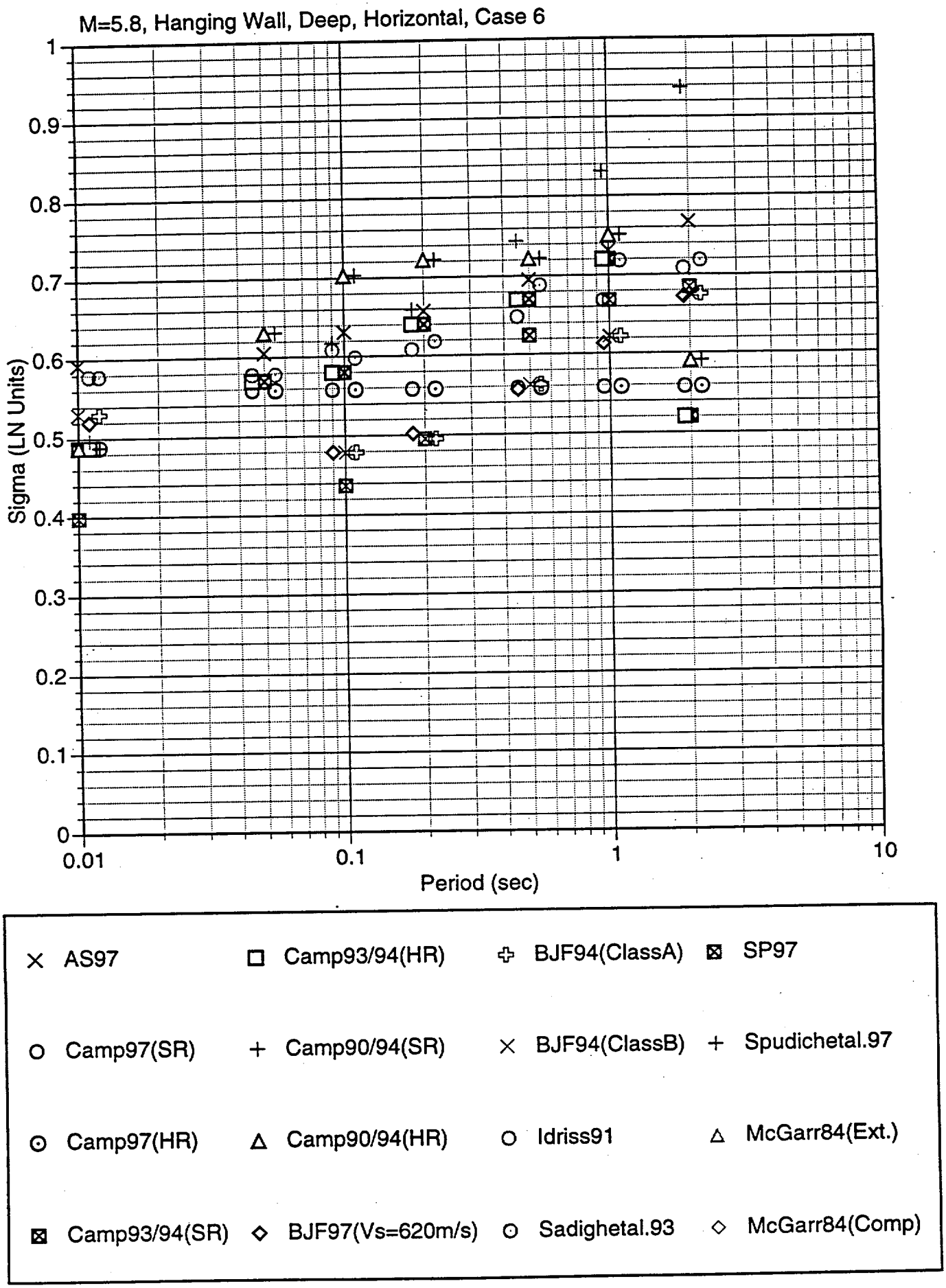
M=5.8, Hanging Wall, Deep, Horizontal, Case 6
Sigma (LN Units)
Period (sec)
0
0.1
0.2
0.3
0.4
0.5
0.6
0.7
0.8
0.9
1
0.01
0.1
1
10
AS97
Camp93/94(HR)
BJF94(ClassA)
SP97
Camp97(SR)
Camp90/94(SR)
BJF94(ClassB)
Spudichetal.97
Camp97(HR)
Camp90/94(HR)
Idriss91
McGarr84(Ext.)
Camp93/94(SR)
BJF97(Vs=620m/s)
Sadighetal.93
McGarr84(Comp)

M=5.8, Hanging Wall, Deep, Vertical, Case 6

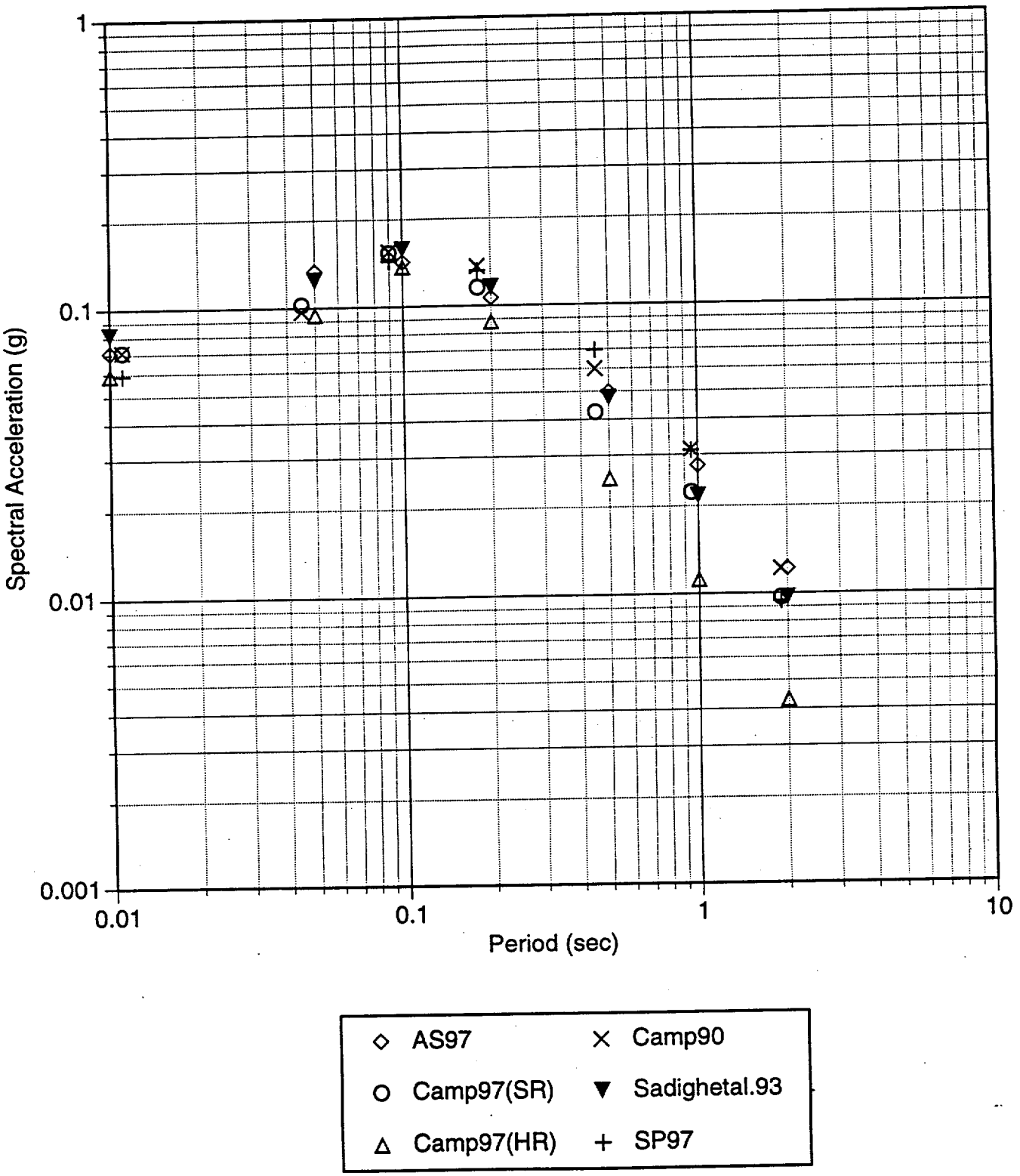

M=5.8, Hanging Wall, Deep, Vertical, Case 6

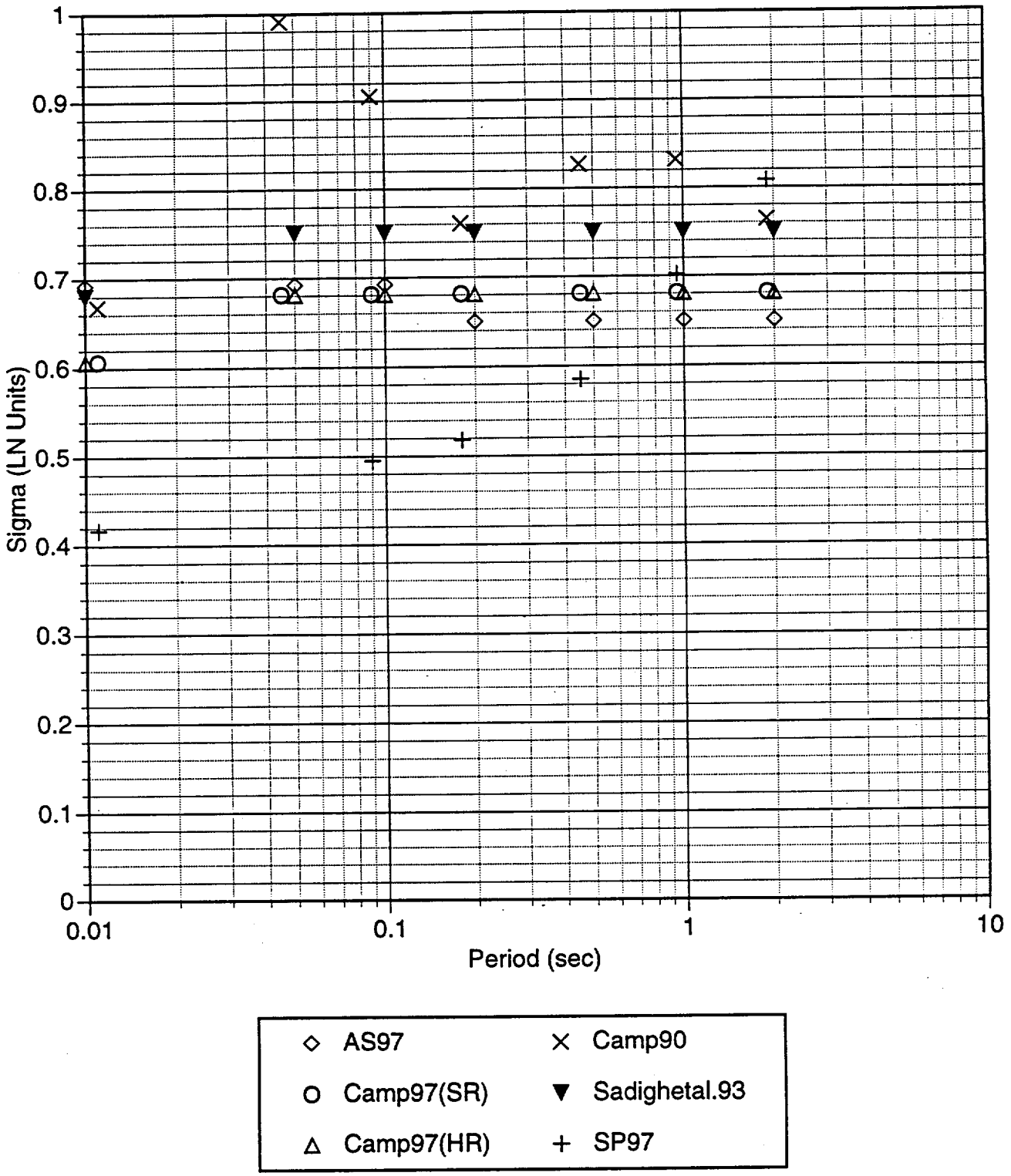

M=6.5, Strike-slip, Shallow, Horizontal, Case 7

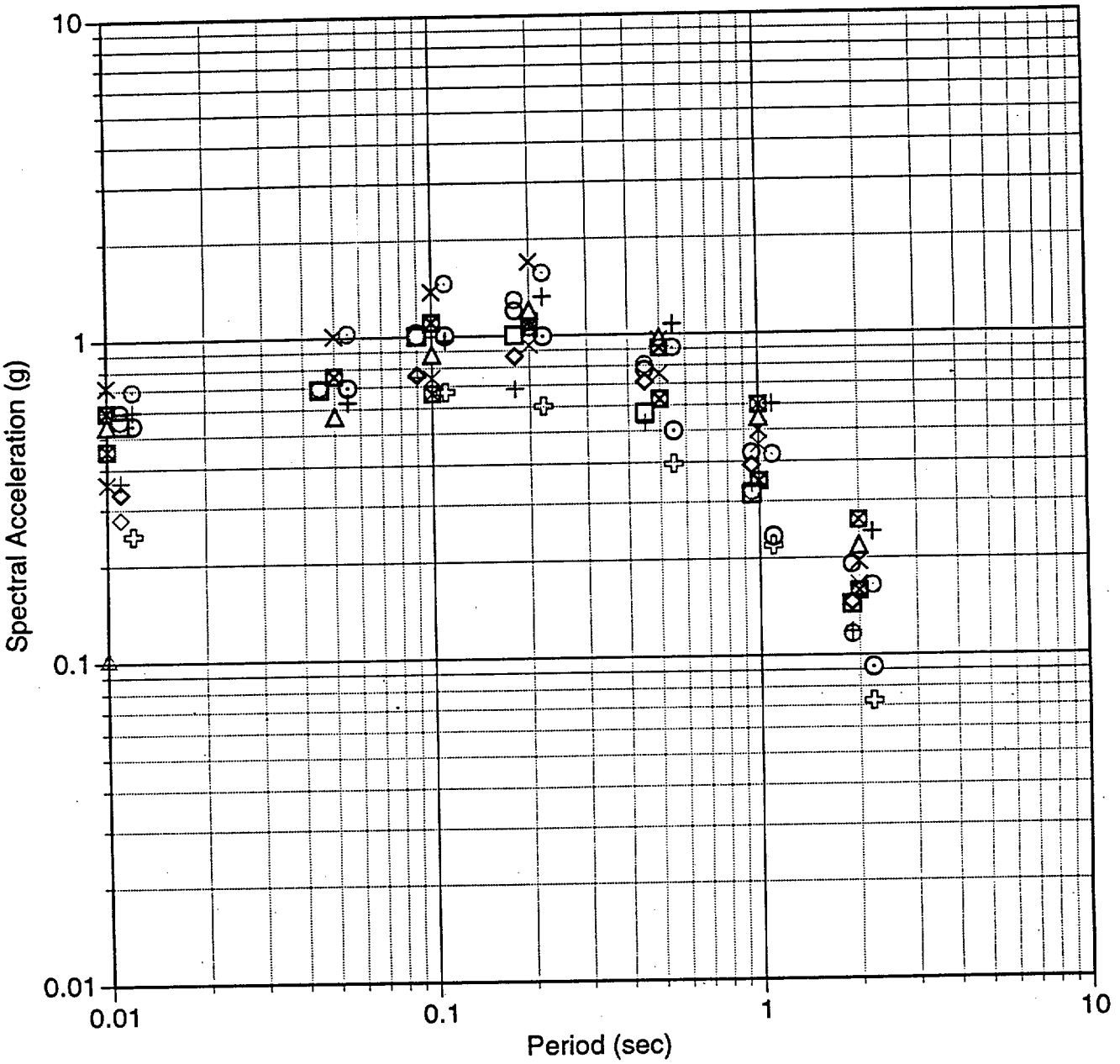

× AS97	□ Camp93/94(HR)	✚ BJF94(ClassA)	⊠ SP97
○ Camp97(SR)	+ Camp90/94(SR)	× BJF94(ClassB)	+ Spudichetal.97
⊙ Camp97(HR)	△ Camp90/94(HR)	○ Idriss91	△ McGarr84(Ext.)
⊠ Camp93/94(SR)	◇ BJF97(Vs=620m/s)	⊙ Sadighetal.93	◇ McGarr84(Comp)

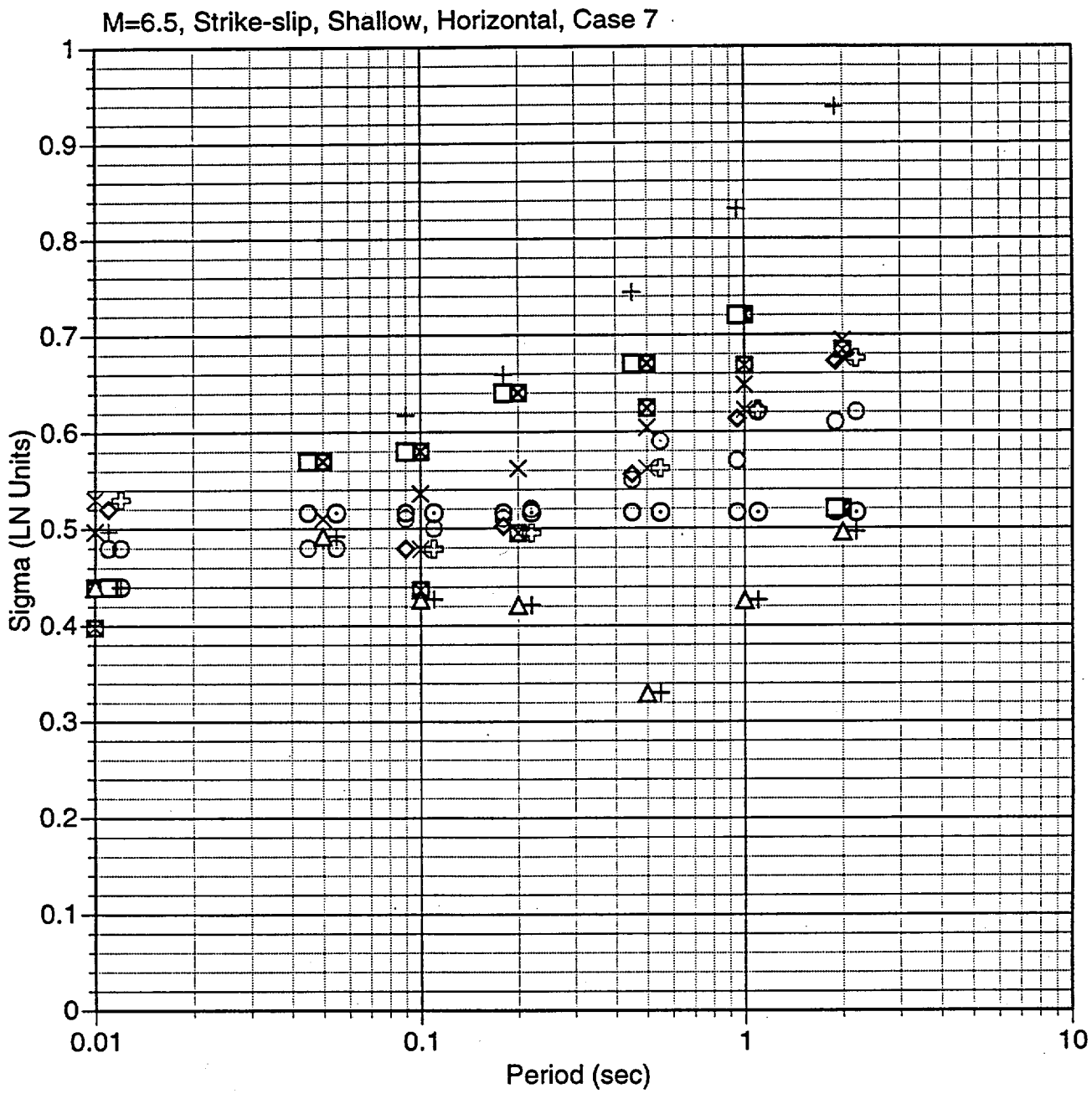

× AS97	□ Camp93/94(HR)	✚ BJF94(ClassA)	⊠ SP97
○ Camp97(SR)	+ Camp90/94(SR)	× BJF94(ClassB)	+ Spudichetal.97
⊙ Camp97(HR)	△ Camp90/94(HR)	○ Idriss91	△ McGarr84(Ext.)
⊠ Camp93/94(SR)	◇ BJF97(Vs=620m/s)	⊙ Sadighetal.93	◇ McGarr84(Comp)

M=6.5, Strike-slip, Shallow, Vertical, Case 7

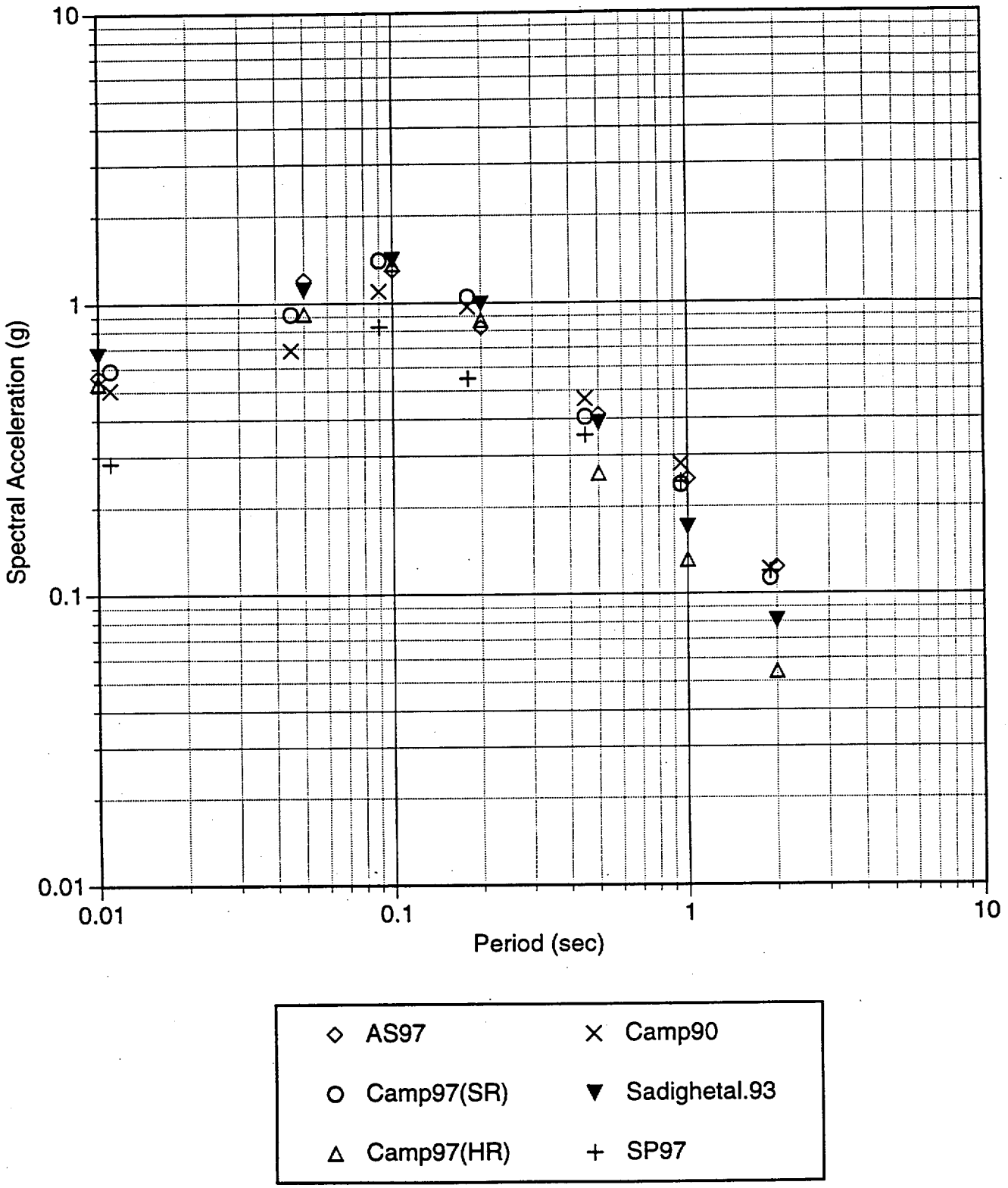

M=6.5, Strike-slip, Shallow, Vertical, Case 7

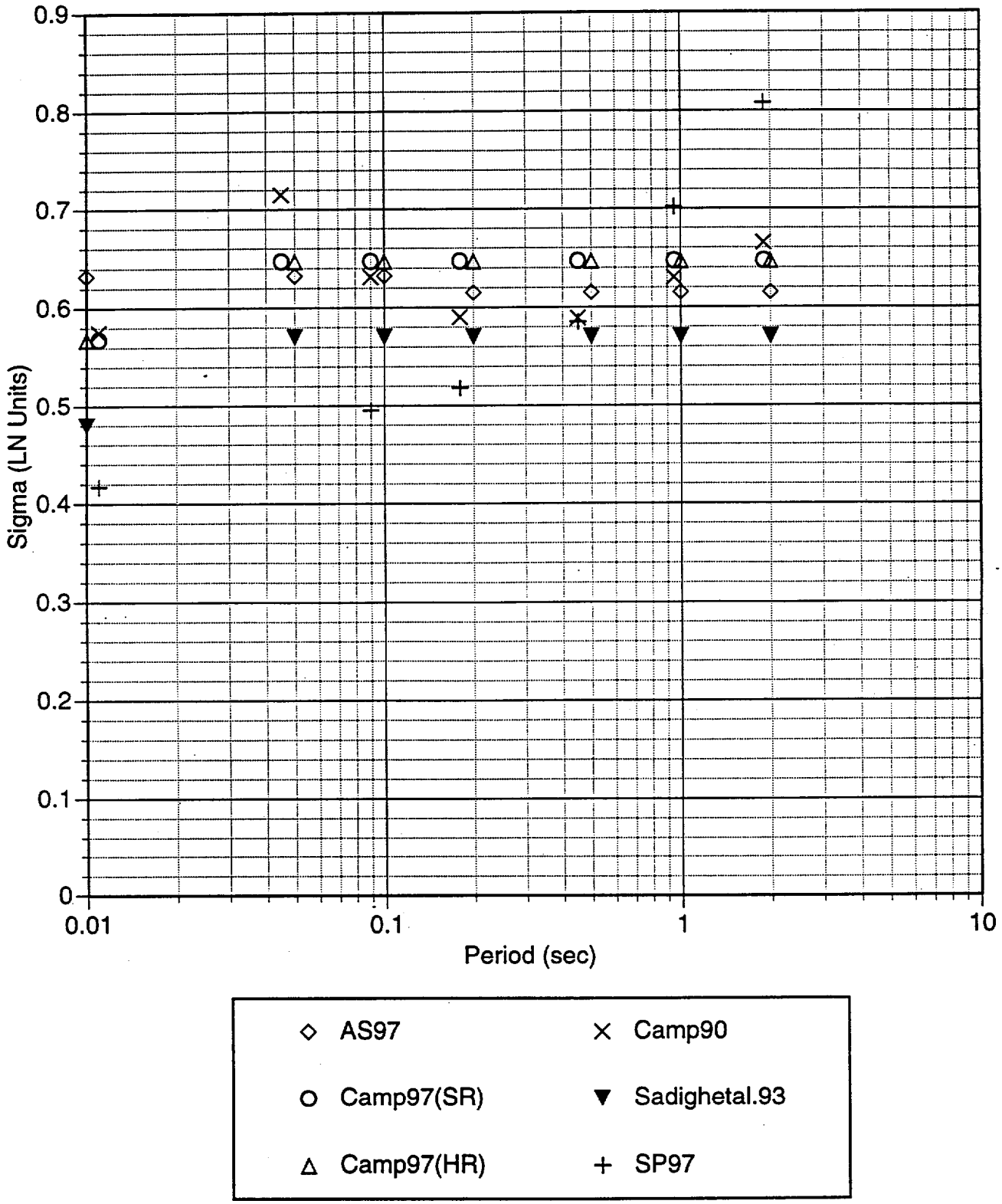

M=6.5, Hanging Wall, Shallow, Horizontal, Case 8

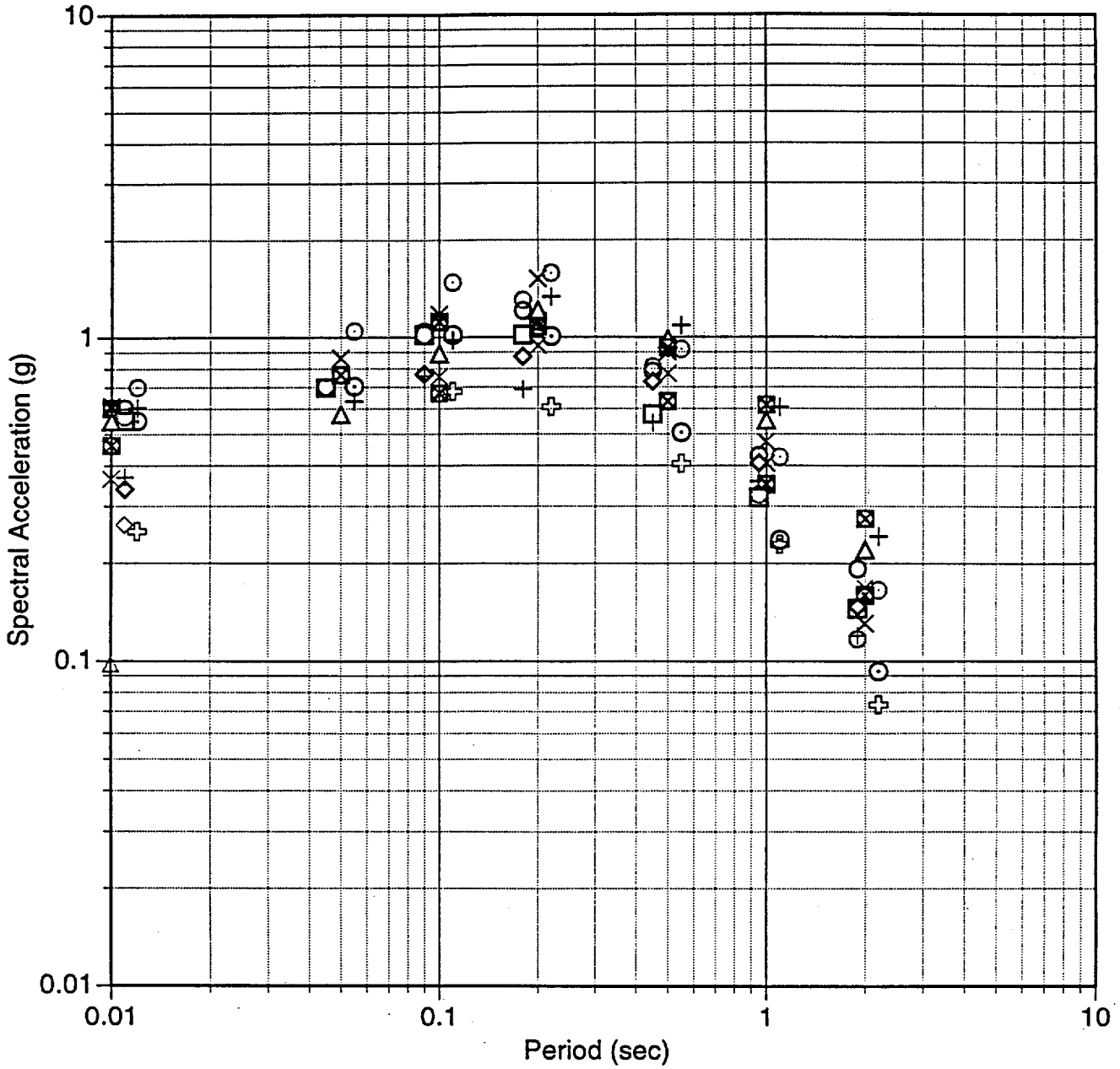

× AS97	□ Camp93/94(HR)	✚ BJF94(ClassA)	⊠ SP97
○ Camp97(SR)	+ Camp90/94(SR)	× BJF94(ClassB)	+ Spudichetal.97
⊙ Camp97(HR)	△ Camp90/94(HR)	○ Idriss91	△ McGarr84(Ext.)
⊠ Camp93/94(SR)	◇ BJF97(Vs=620m/s)	⊙ Sadighetal.93	◇ McGarr84(Comp)

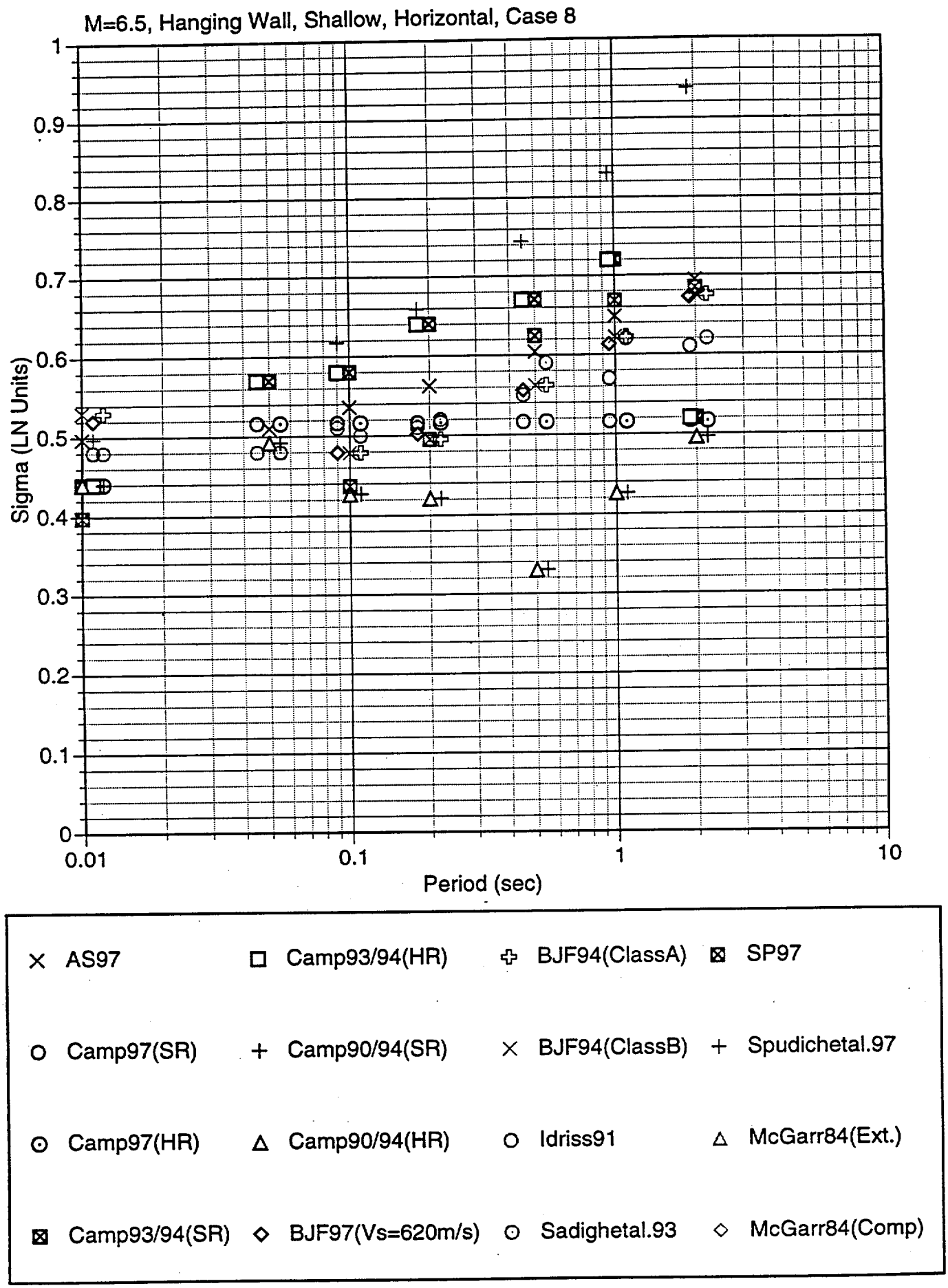
M=6.5, Hanging Wall, Shallow, Horizontal, Case 8
Sigma (LN Units)
Period (sec)
0
0.1
0.2
0.3
0.4
0.5
0.6
0.7
0.8
0.9
1
0.01
0.1
1
10
AS97
Camp93/94(HR)
BJF94(ClassA)
SP97
Camp97(SR)
Camp90/94(SR)
BJF94(ClassB)
Spudichetal.97
Camp97(HR)
Camp90/94(HR)
Idriss91
McGarr84(Ext.)
Camp93/94(SR)
BJF97(Vs=620m/s)
Sadighetal.93
McGarr84(Comp)

M=6.5, Hanging Wall, Shallow, Vertical, Case 8

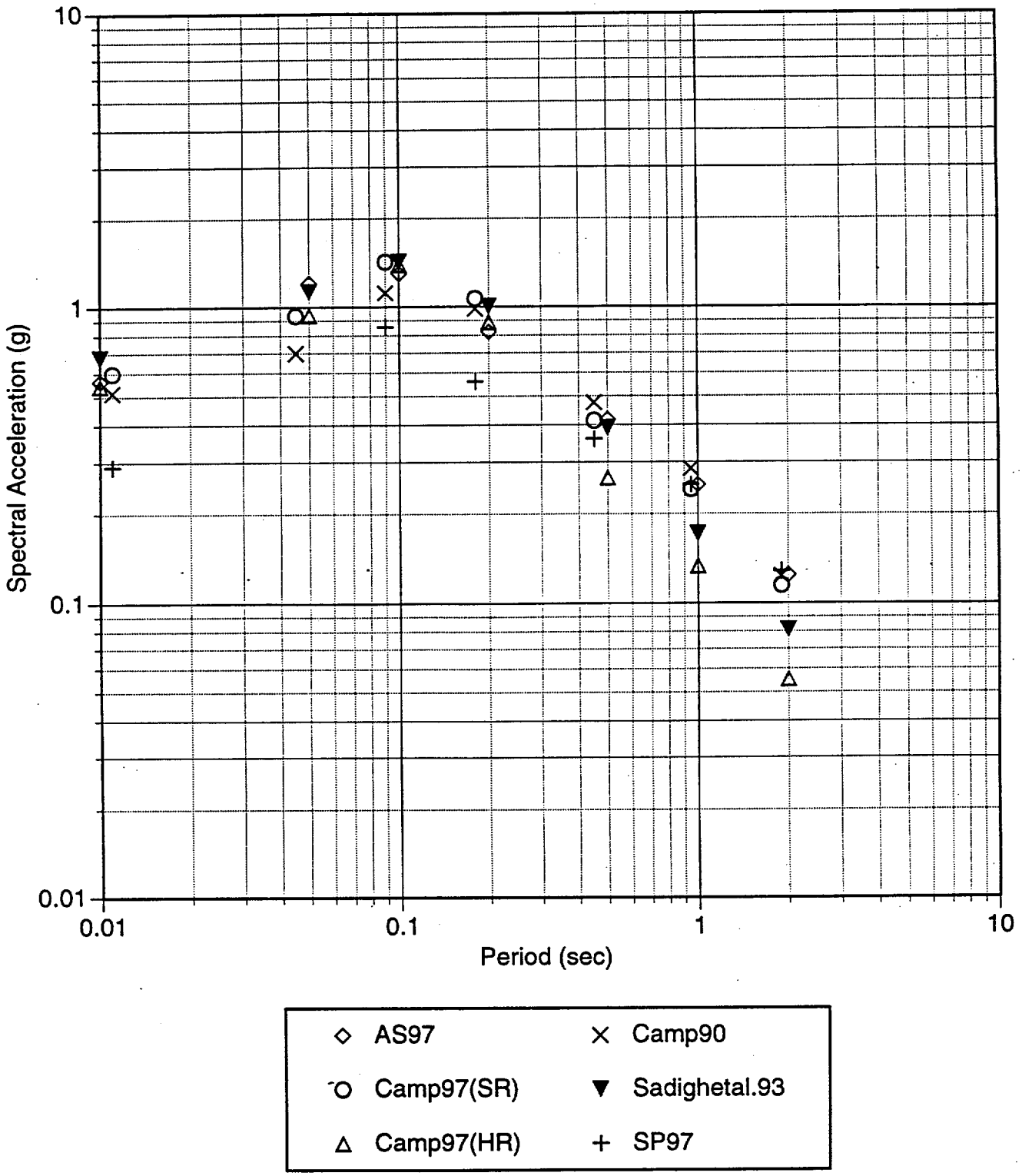

M=6.5, Hanging Wall, Shallow, Vertical, Case 8

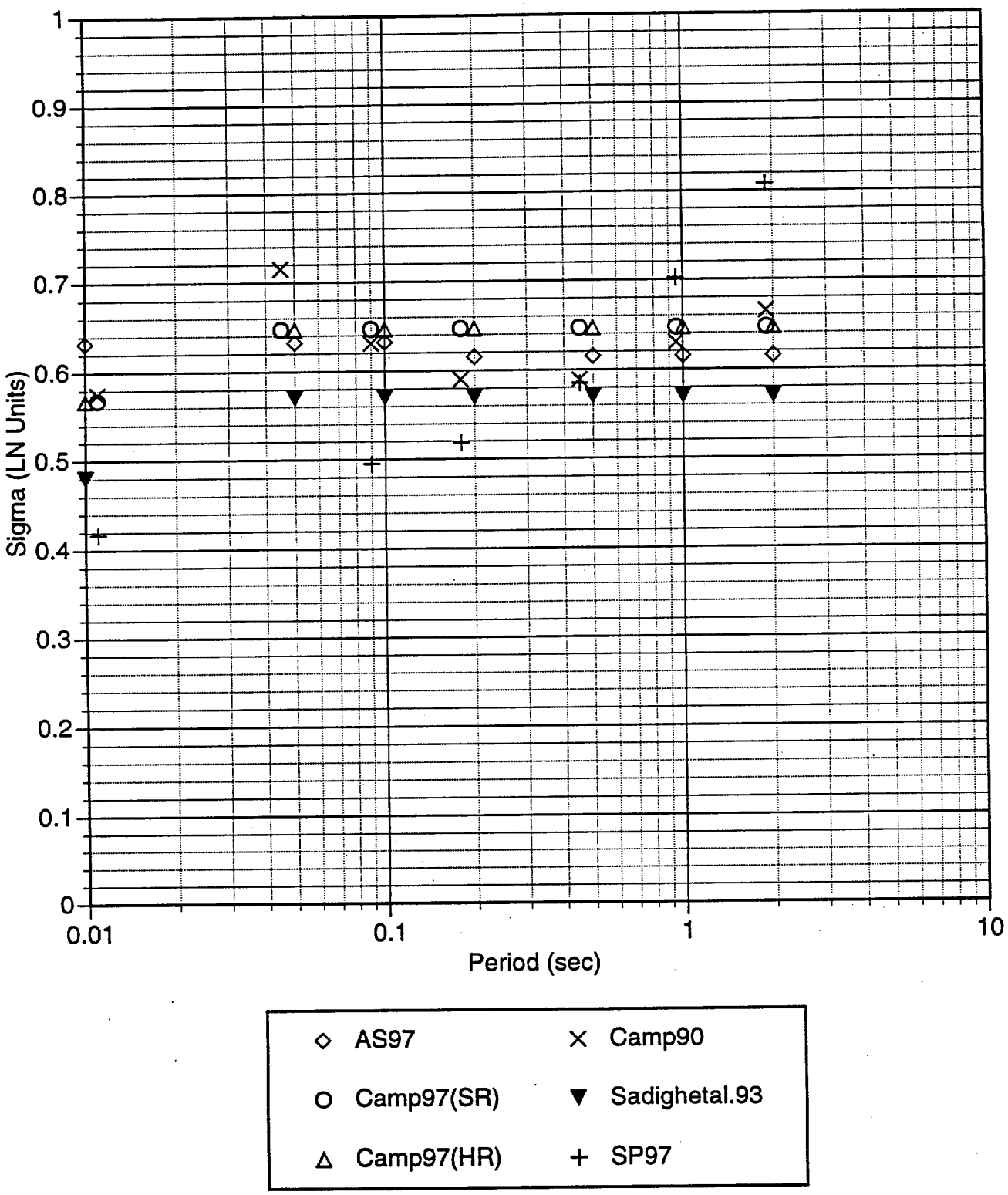

M=6.5, Footwall, Shallow, Horizontal, Case 9

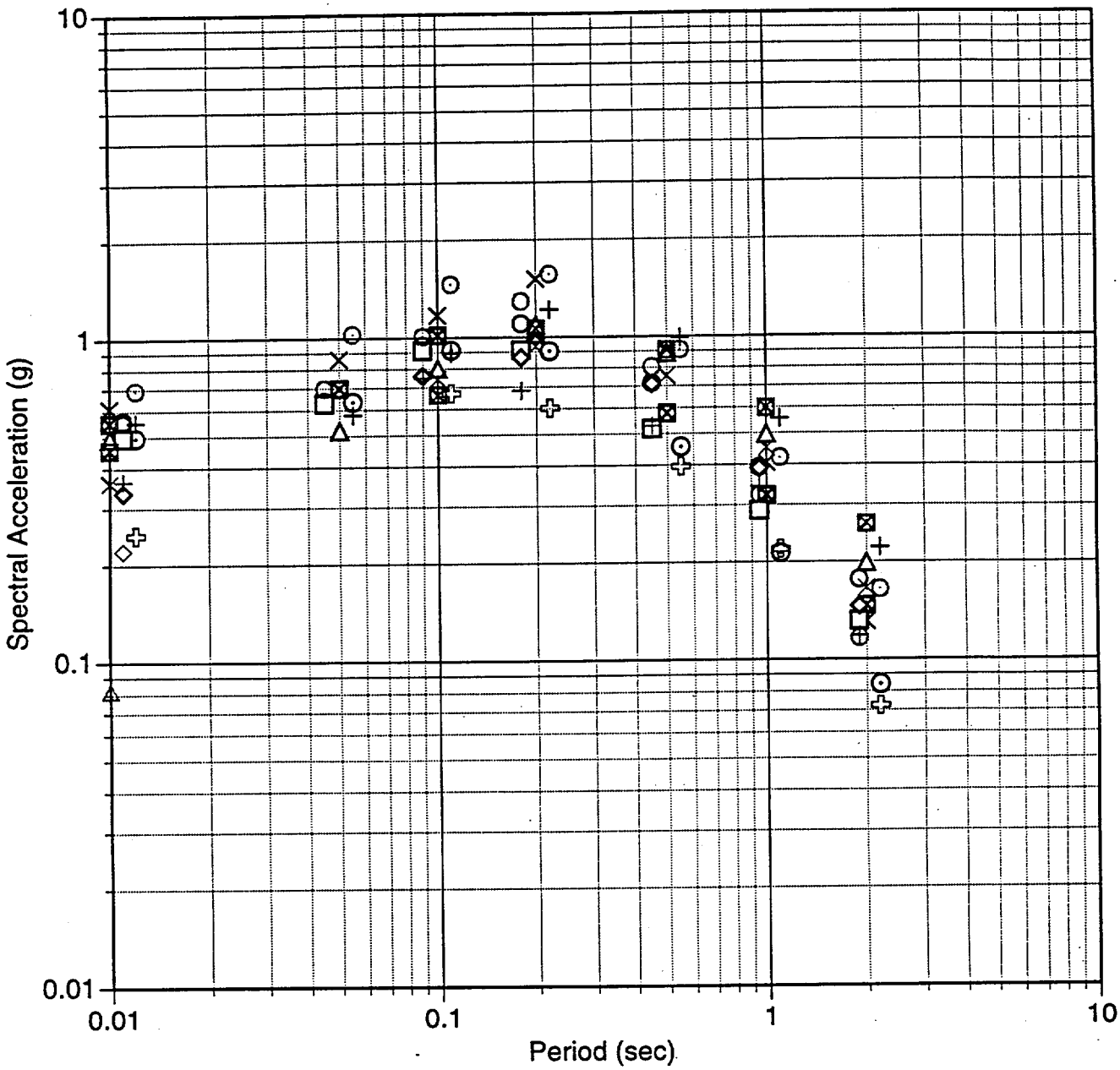

× AS97	□ Camp93/94(HR)	✚ BJF94(ClassA)	⊠ SP97
○ Camp97(SR)	+ Camp90/94(SR)	× BJF94(ClassB)	+ Spudichetal.97
⊙ Camp97(HR)	△ Camp90/94(HR)	○ Idriss91	△ McGarr84(Ext.)
⊠ Camp93/94(SR)	◇ BJF97(Vs=620m/s)	⊙ Sadighetal.93	◇ McGarr84(Comp)

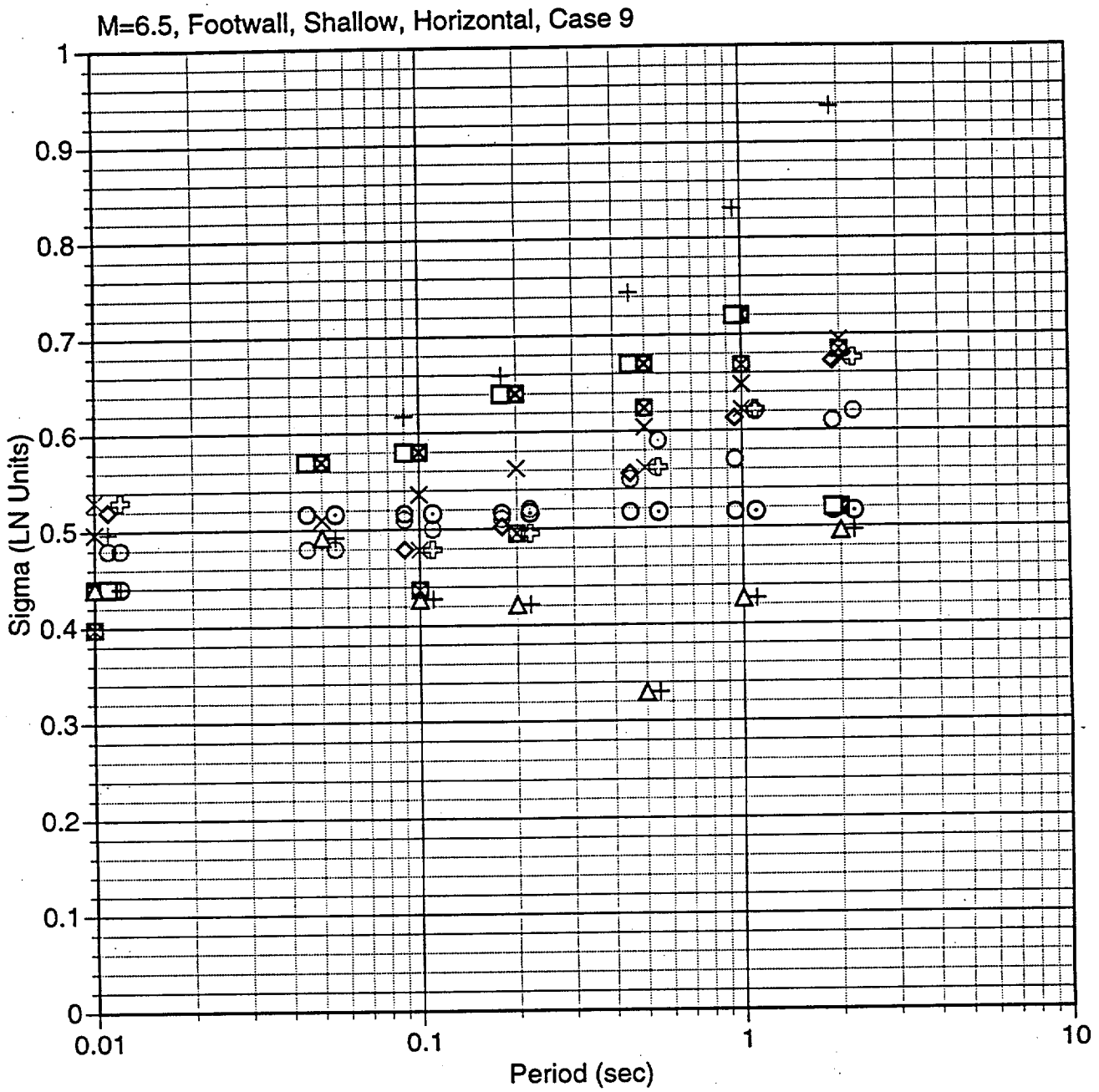

× AS97	□ Camp93/94(HR)	✚ BJF94(ClassA)	⊠ SP97
○ Camp97(SR)	+ Camp90/94(SR)	× BJF94(ClassB)	+ Spudichetal.97
⊙ Camp97(HR)	△ Camp90/94(HR)	○ Idriss91	△ McGarr84(Ext.)
⊠ Camp93/94(SR)	◇ BJF97(Vs=620m/s)	⊙ Sadighetal.93	◇ McGarr84(Comp)

M=6.5, Footwall, Shallow, Vertical, Case 9

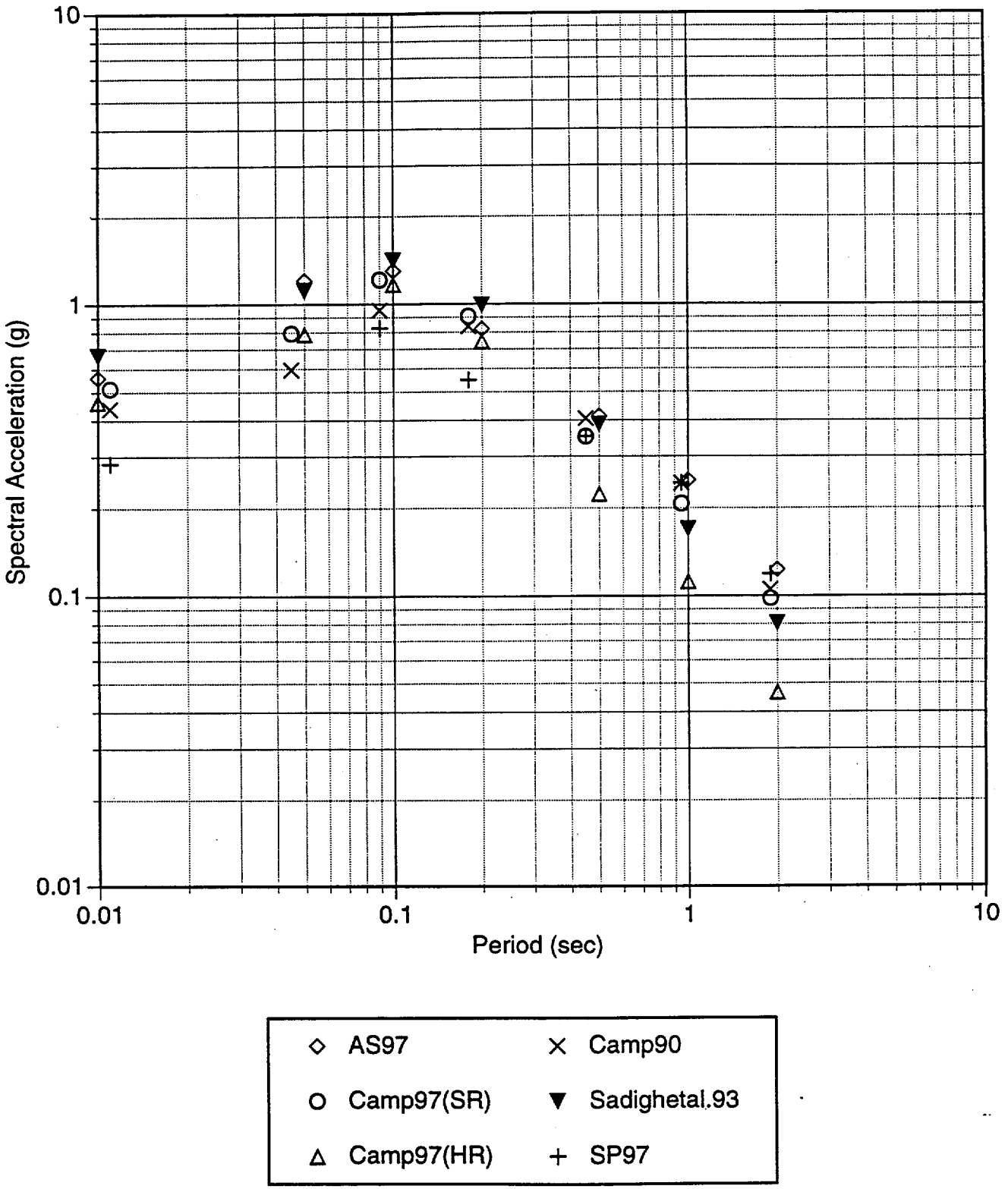

M=6.5, Footwall, Shallow, Vertical, Case 9

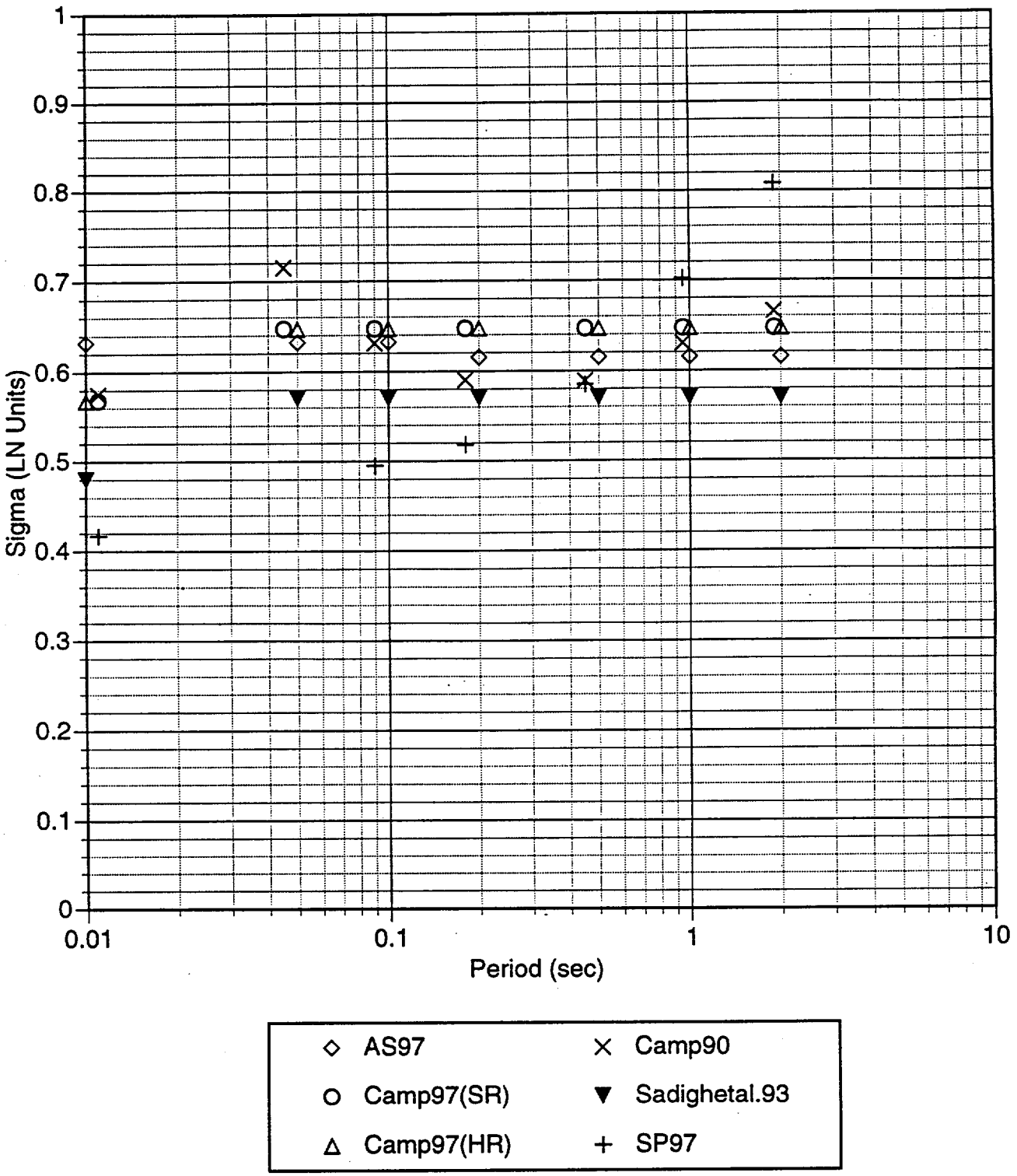

M=6.5, Hanging Wall, Shallow, Horizontal, Case 10

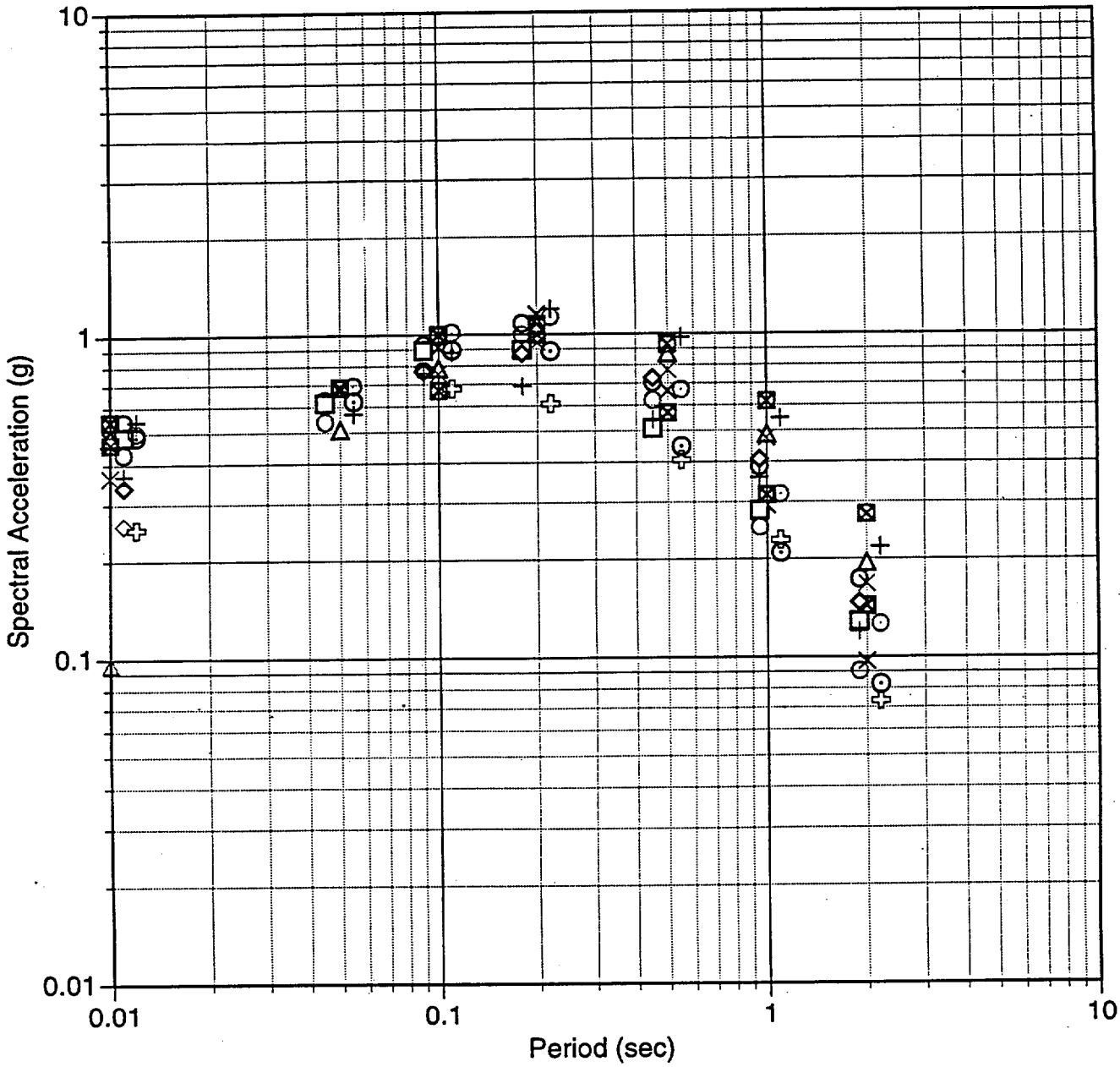

× AS97	□ Camp93/94(HR)	✚ BJF94(ClassA)	⊠ SP97
○ Camp97(SR)	+ Camp90/94(SR)	× BJF94(ClassB)	+ Spudichetal.97
⊙ Camp97(HR)	△ Camp90/94(HR)	○ Idriss91	△ McGarr84(Ext.)
⊠ Camp93/94(SR)	◇ BJF97(Vs=620m/s)	⊙ Sadighetal.93	◇ McGarr84(Comp)

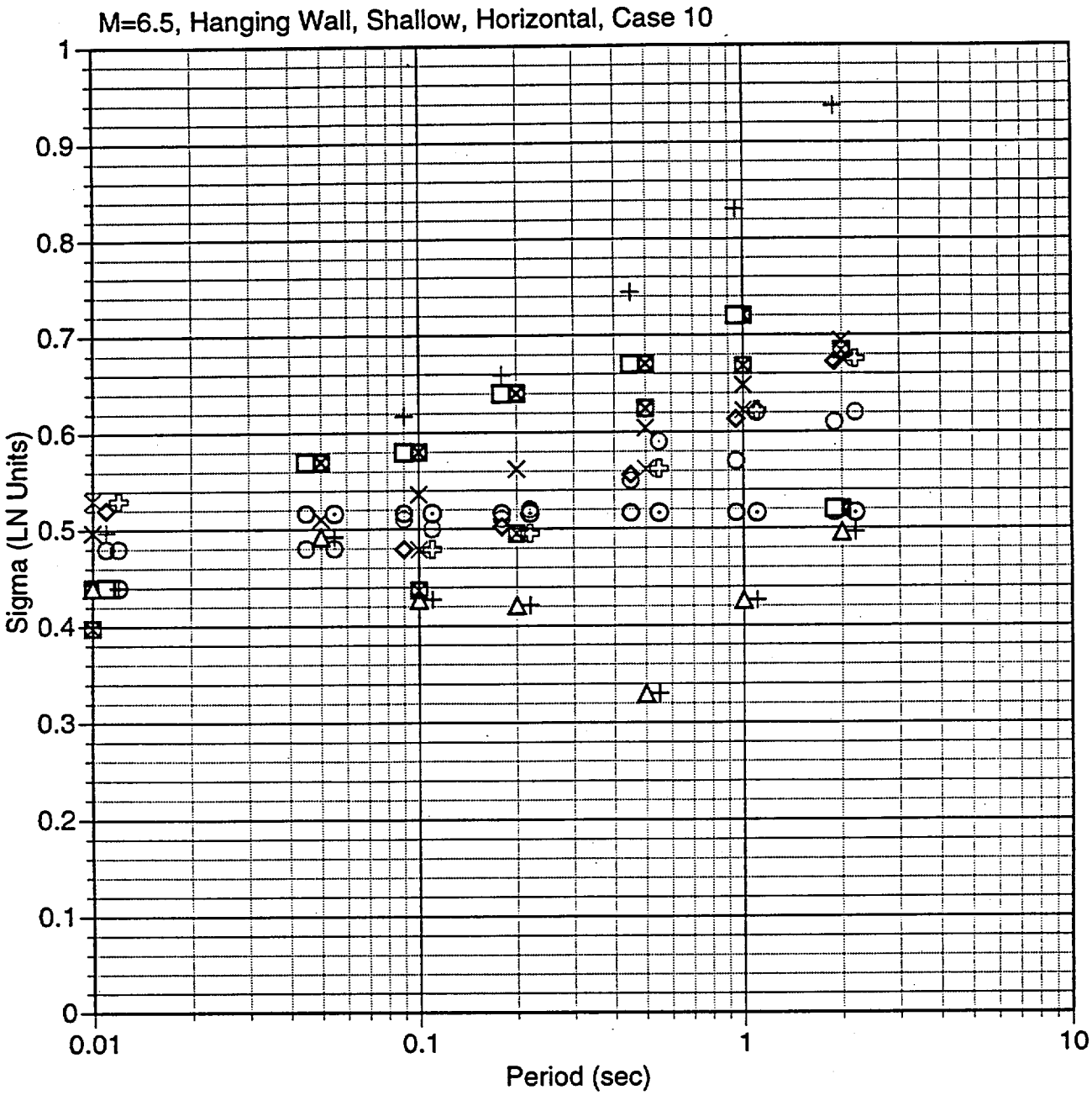

× AS97	□ Camp93/94(HR)	✚ BJF94(ClassA)	⊠ SP97
○ Camp97(SR)	+ Camp90/94(SR)	× BJF94(ClassB)	+ Spudichetal.97
⊙ Camp97(HR)	△ Camp90/94(HR)	○ Idriss91	△ McGarr84(Ext.)
⊠ Camp93/94(SR)	◇ BJF97(Vs=620m/s)	⊙ Sadighetal.93	◇ McGarr84(Comp)

M=6.5, Hanging Wall, Shallow, Vertical, Case 10

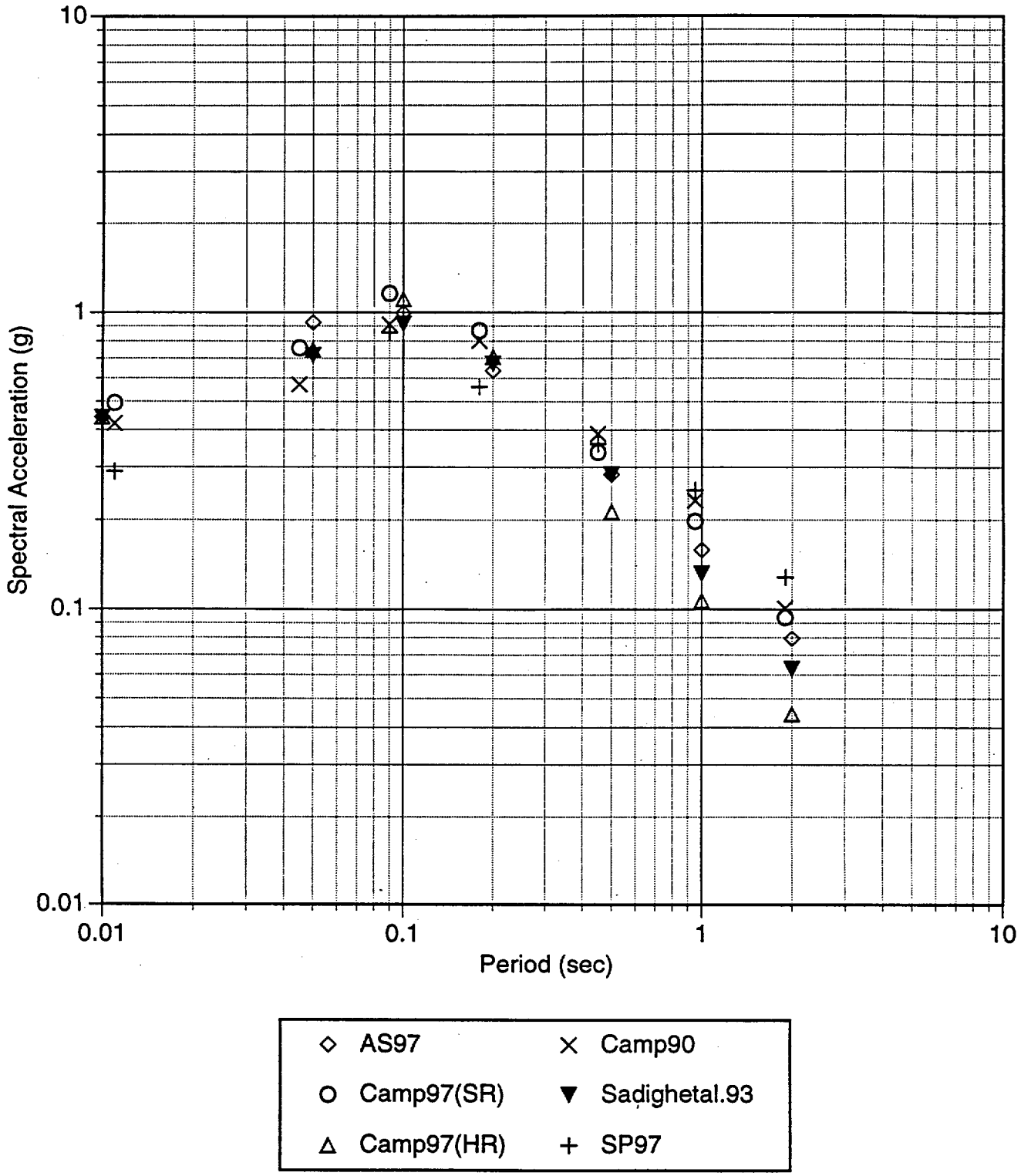

M=6.5, Hanging Wall, Shallow, Vertical, Case 10

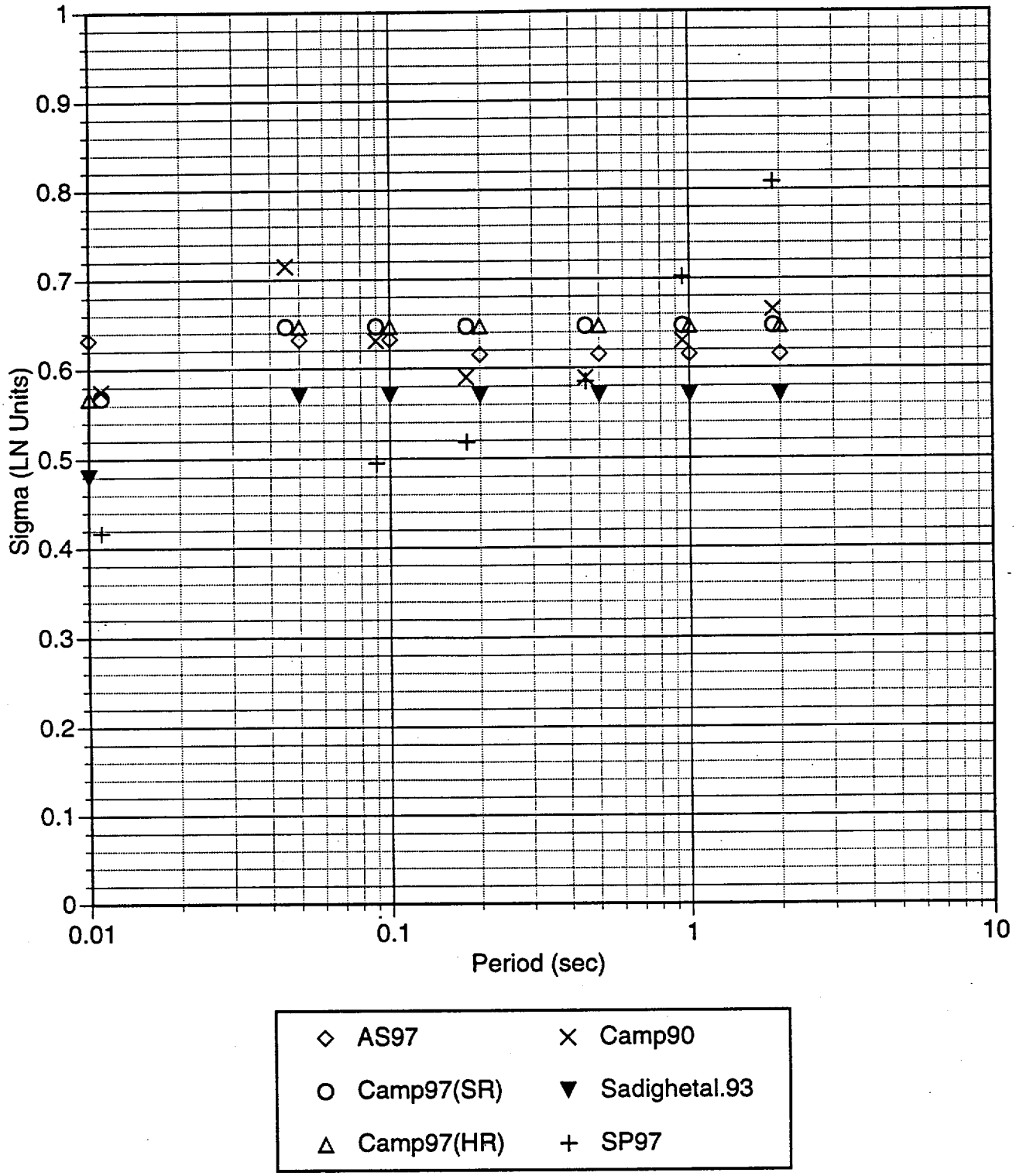

M=6.5, Footwall, Shallow, Horizontal, Case 11

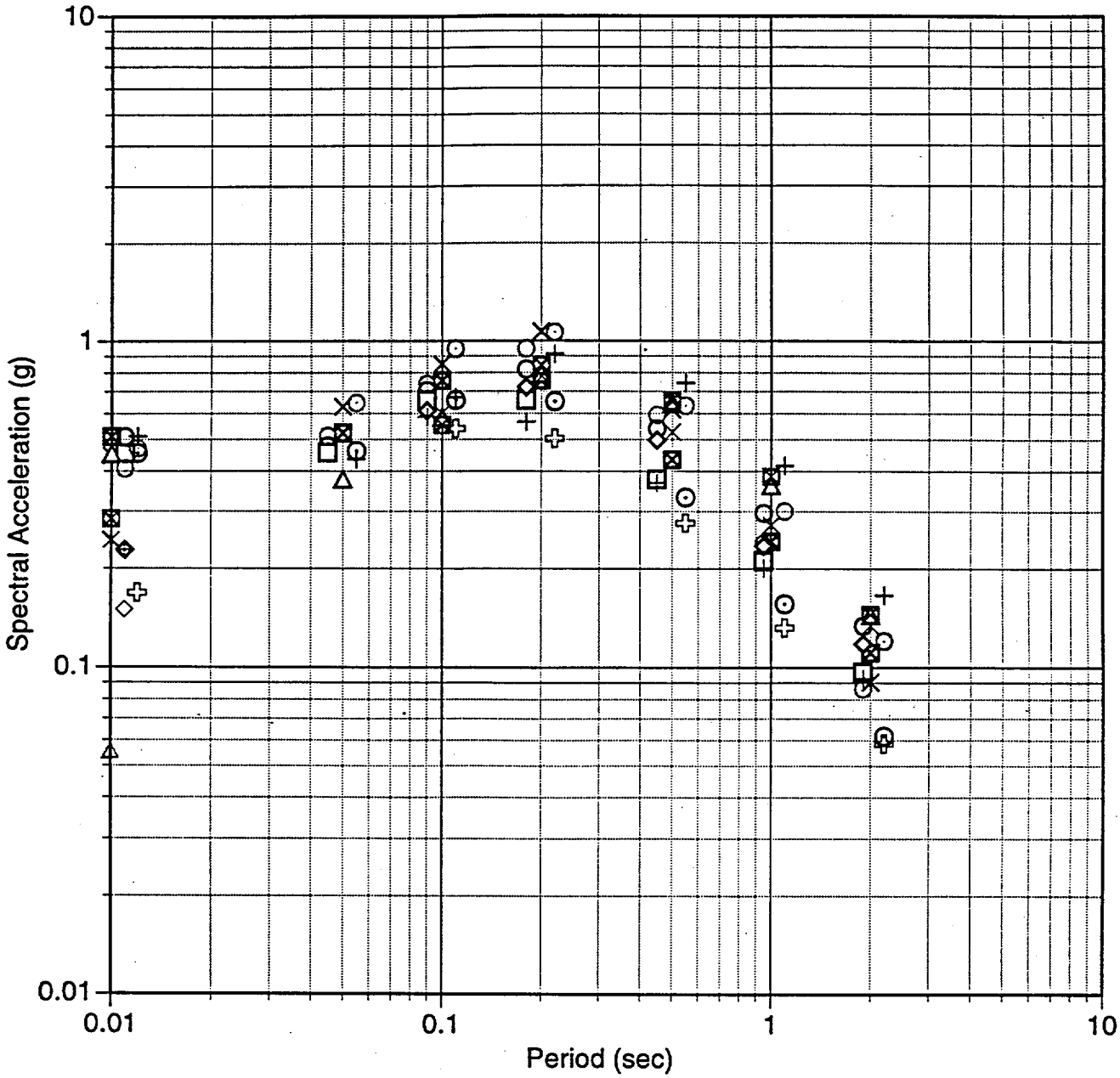

× AS97	□ Camp93/94(HR)	✣ BJF94(ClassA)	⊠ SP97
○ Camp97(SR)	+ Camp90/94(SR)	× BJF94(ClassB)	+ Spudichetal.97
⊙ Camp97(HR)	△ Camp90/94(HR)	○ Idriss91	△ McGarr84(Ext.)
⊠ Camp93/94(SR)	◇ BJF97(Vs=620m/s)	⊙ Sadighetal.93	◇ McGarr84(Comp)

M=6.5, Footwall, Shallow, Horizontal, Case 11

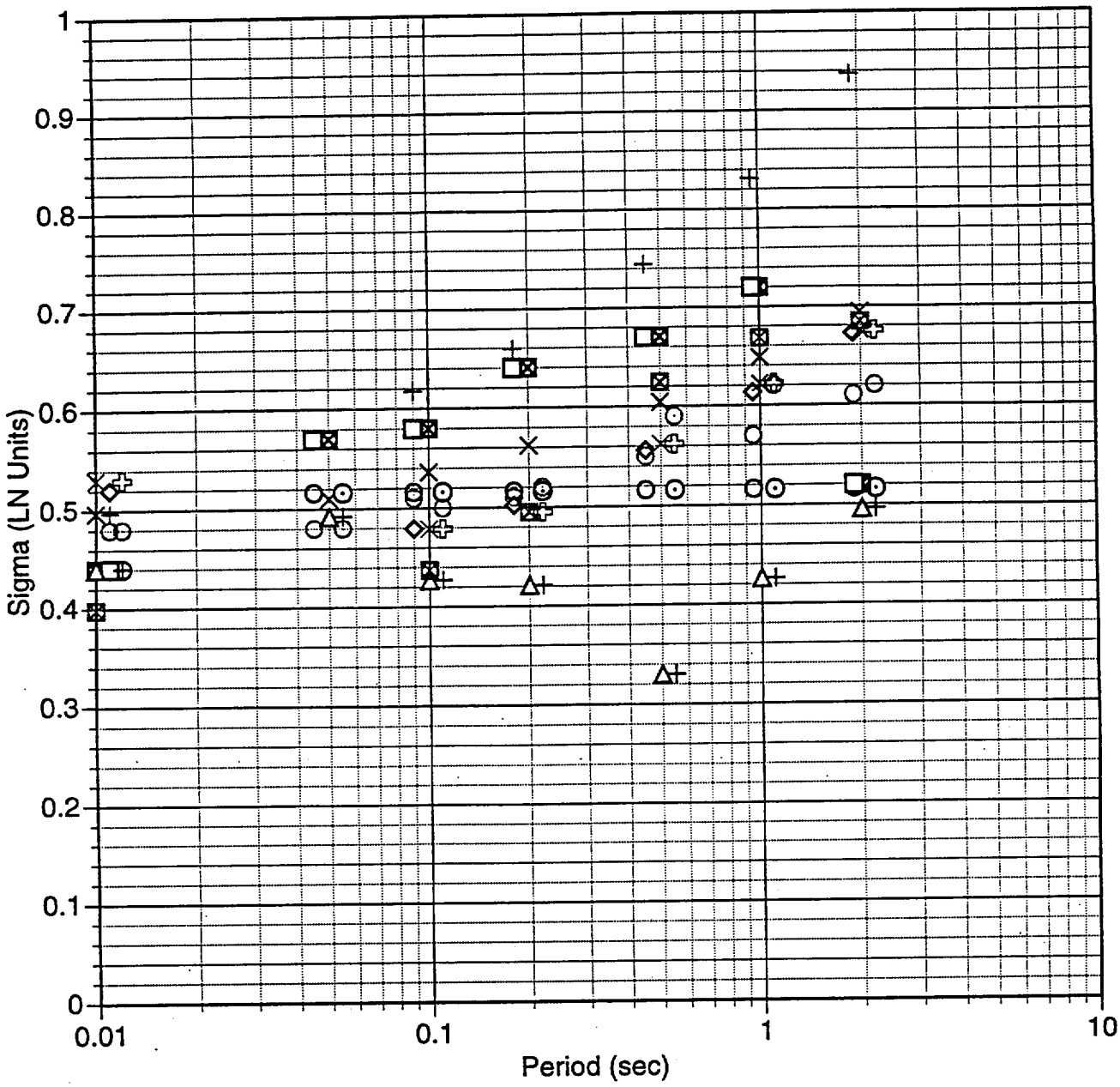

× AS97	□ Camp93/94(HR)	✚ BJF94(ClassA)	⊠ SP97
○ Camp97(SR)	+ Camp90/94(SR)	× BJF94(ClassB)	+ Spudichetal.97
⊙ Camp97(HR)	△ Camp90/94(HR)	○ Idriss91	△ McGarr84(Ext.)
⊠ Camp93/94(SR)	◇ BJF97(Vs=620m/s)	⊙ Sadighetal.93	◇ McGarr84(Comp)

M=6.5, Footwall, Shallow, Vertical, Case 11

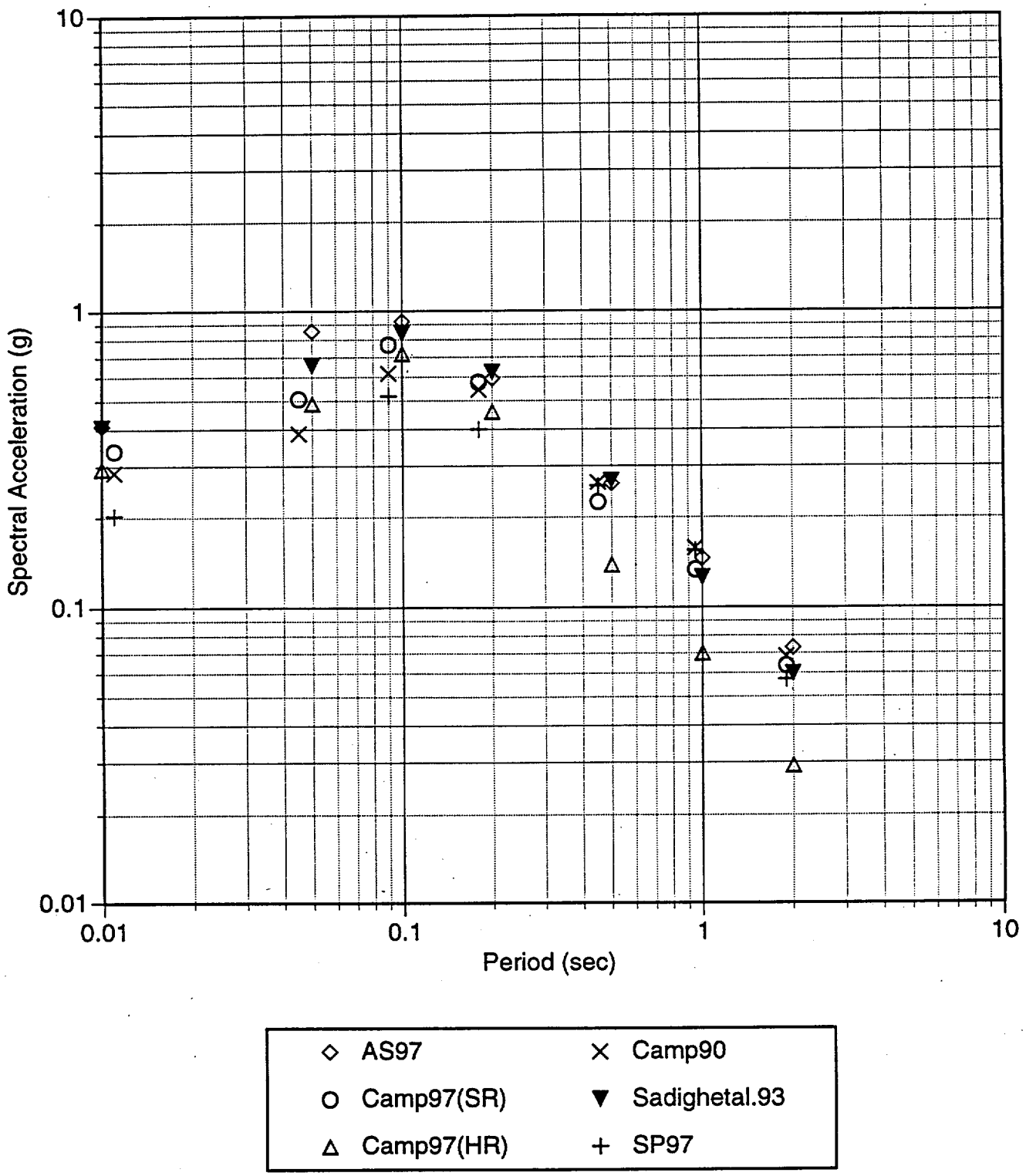

M=6.5, Footwall, Shallow, Vertical, Case 11

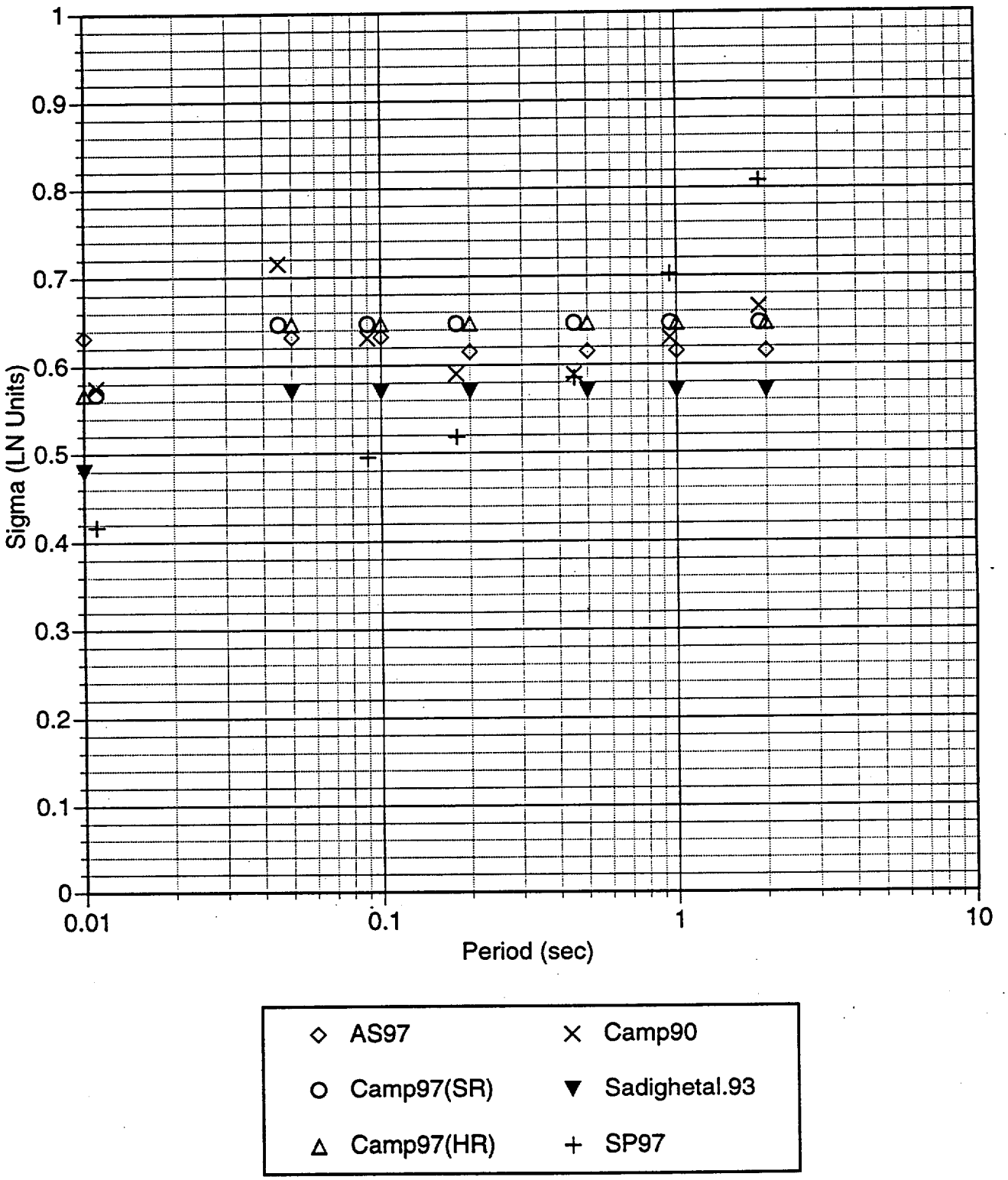

M=6.5, Strike-slip, Shallow, Horizontal, Case 12

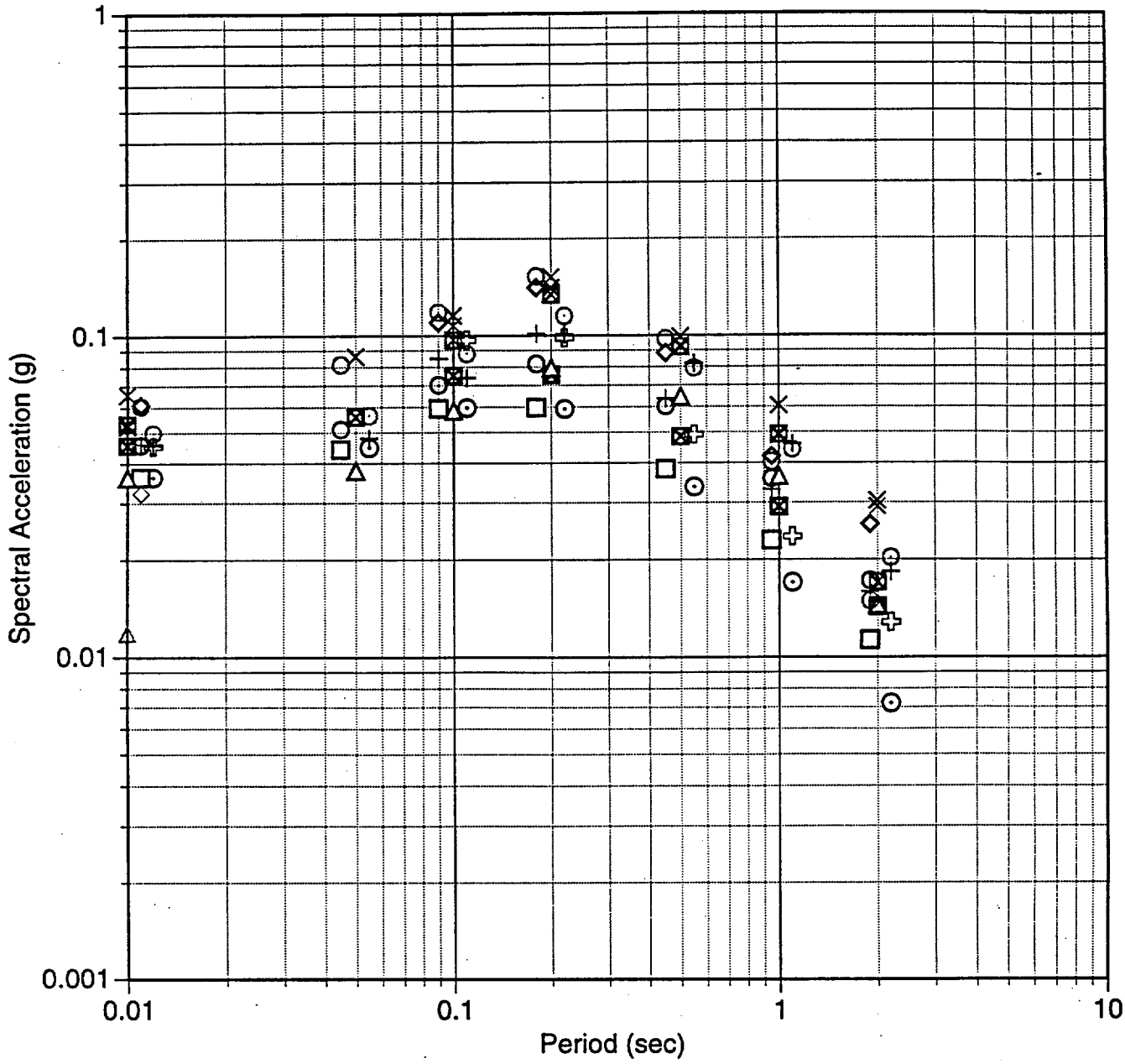

× AS97	□ Camp93/94(HR)	✚ BJF94(ClassA)	⊠ SP97
○ Camp97(SR)	+ Camp90/94(SR)	× BJF94(ClassB)	+ Spudichetal.97
⊙ Camp97(HR)	△ Camp90/94(HR)	○ Idriss91	△ McGarr84(Ext.)
⊠ Camp93/94(SR)	◇ BJF97(Vs=620m/s)	⊙ Sadighetal.93	◇ McGarr84(Comp)

M=6.5, Strike-slip, Shallow, Horizontal, Case 12

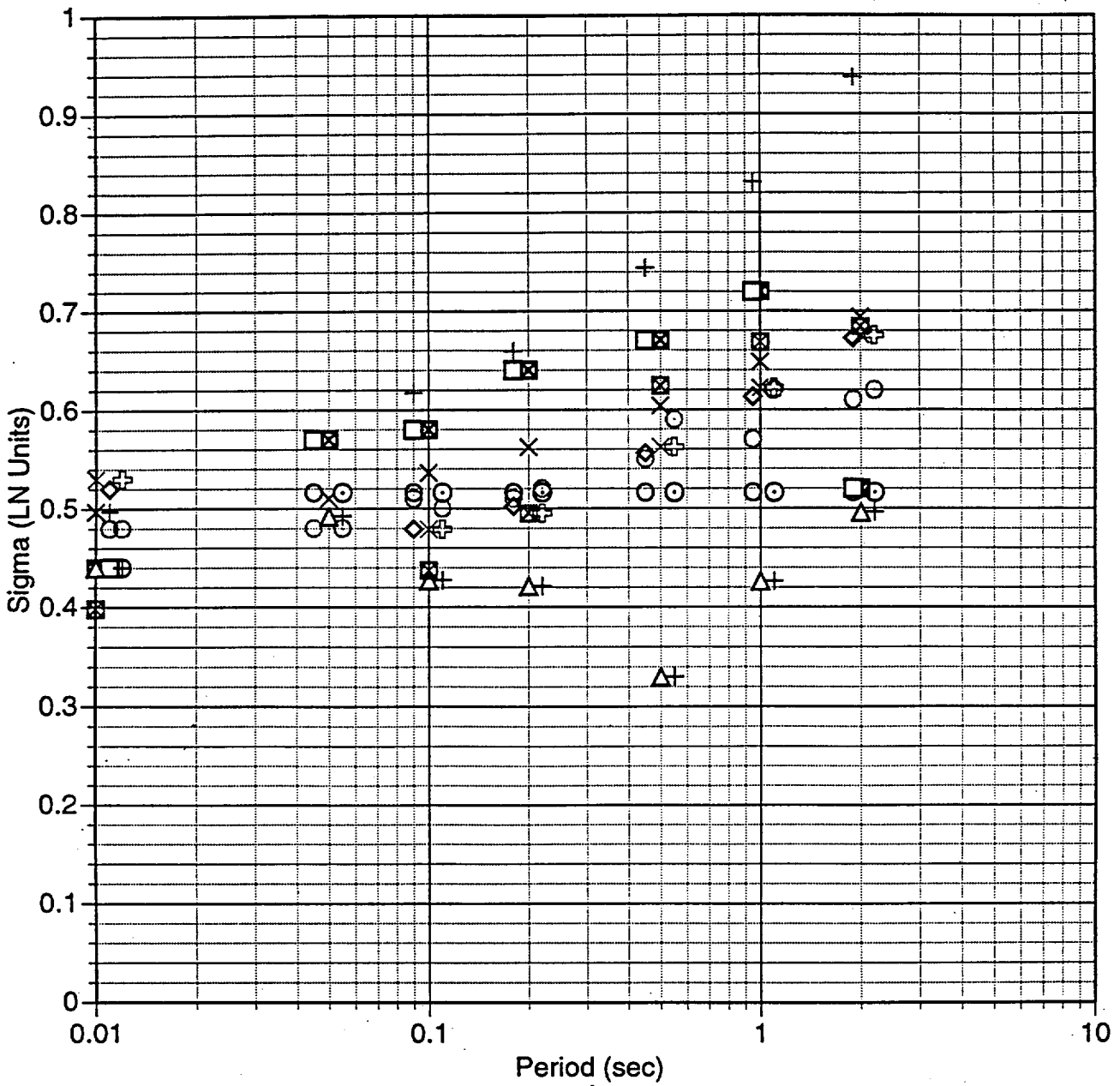

× AS97	□ Camp93/94(HR)	✚ BJF94(ClassA)	⊠ SP97
○ Camp97(SR)	+ Camp90/94(SR)	× BJF94(ClassB)	+ Spudichetal.97
⊙ Camp97(HR)	△ Camp90/94(HR)	○ Idriss91	△ McGarr84(Ext.)
⊠ Camp93/94(SR)	◇ BJF97(Vs=620m/s)	⊙ Sadighetal.93	◇ McGarr84(Comp)

M=6.5, Strike Slip, Shallow, Vertical, Case 12

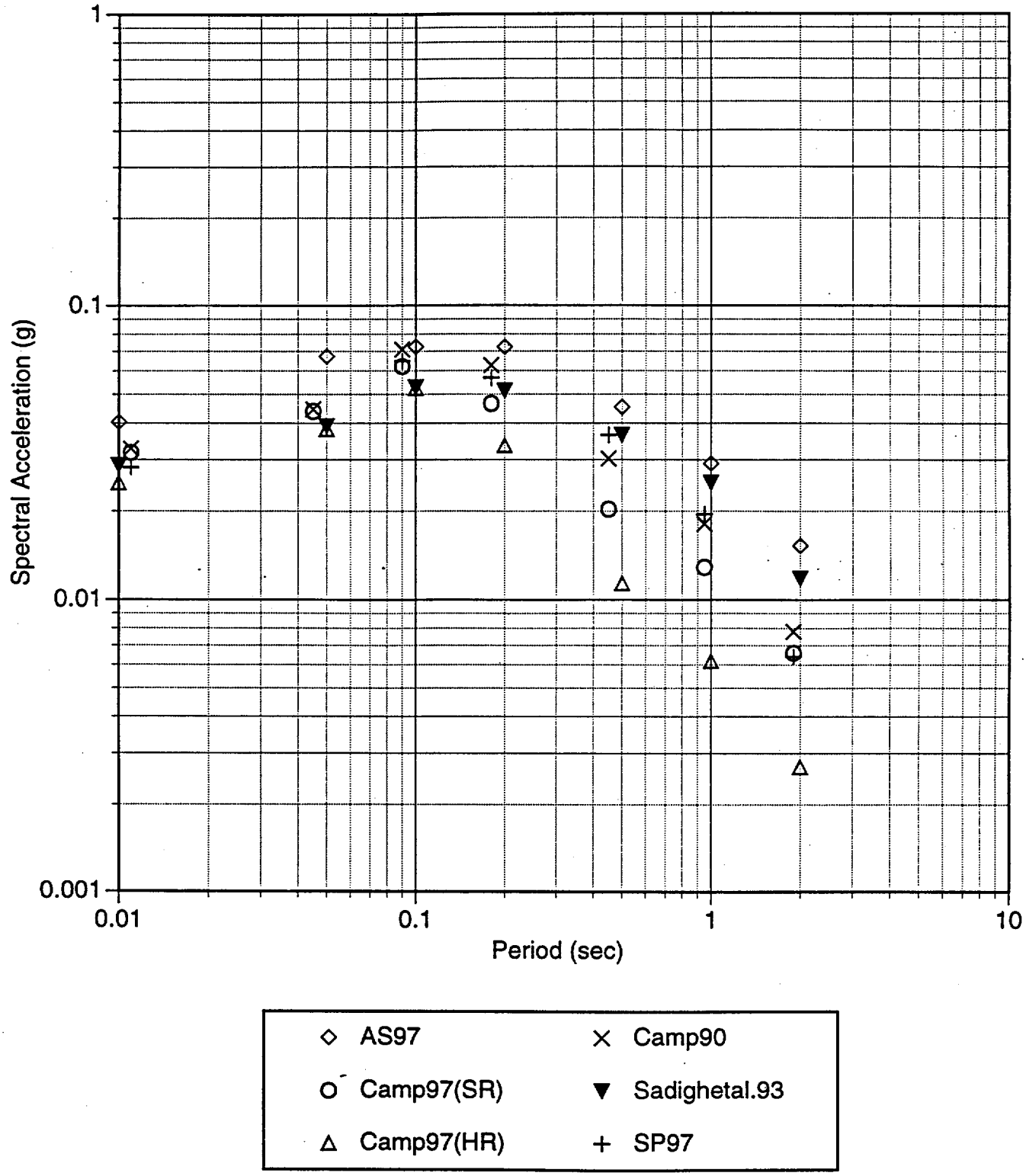

M=6.5, Strike-slip, Shallow, Vertical, Case 12

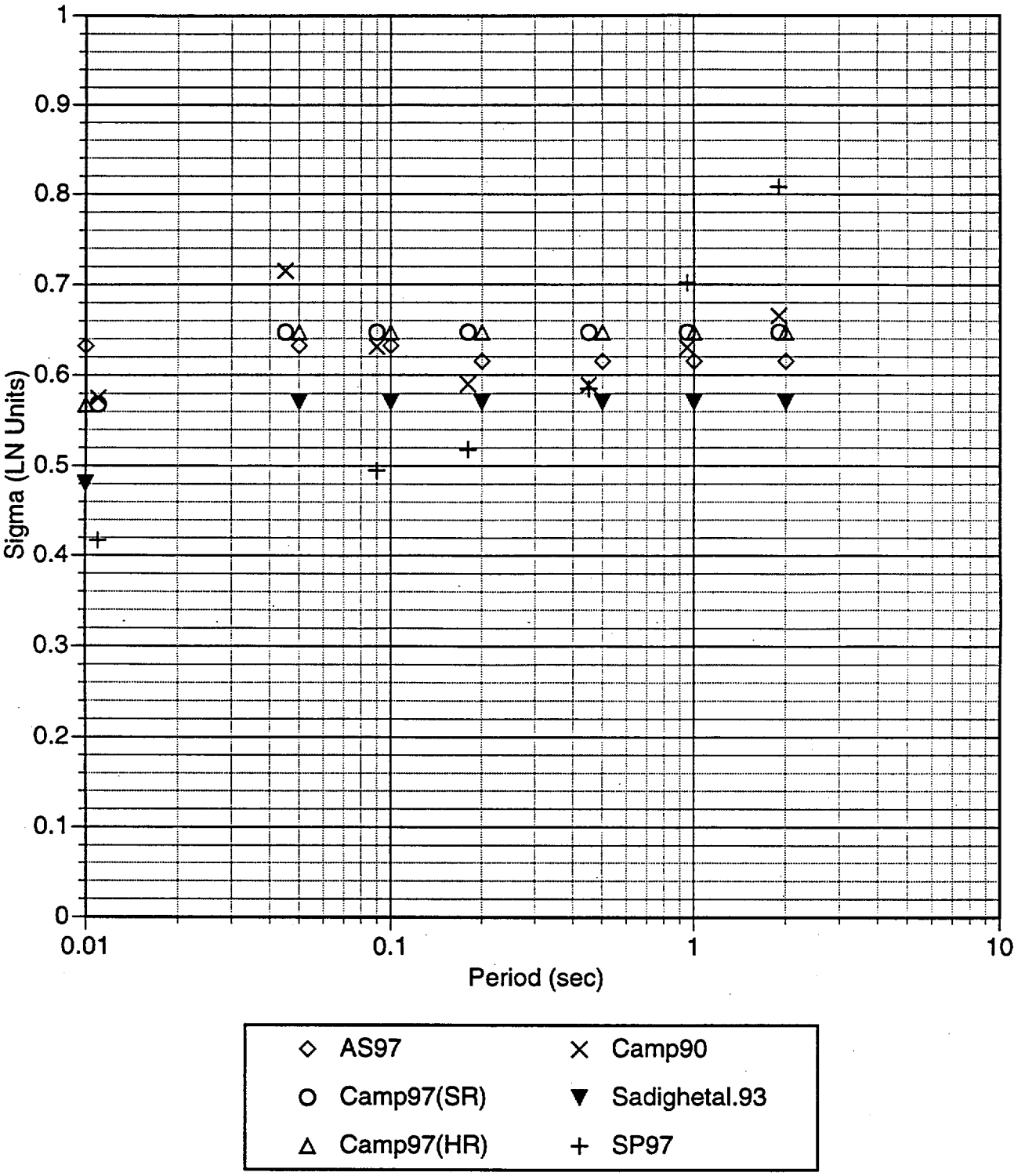

M=6.5,Hanging Wall, Shallow, Horizontal, Case 13

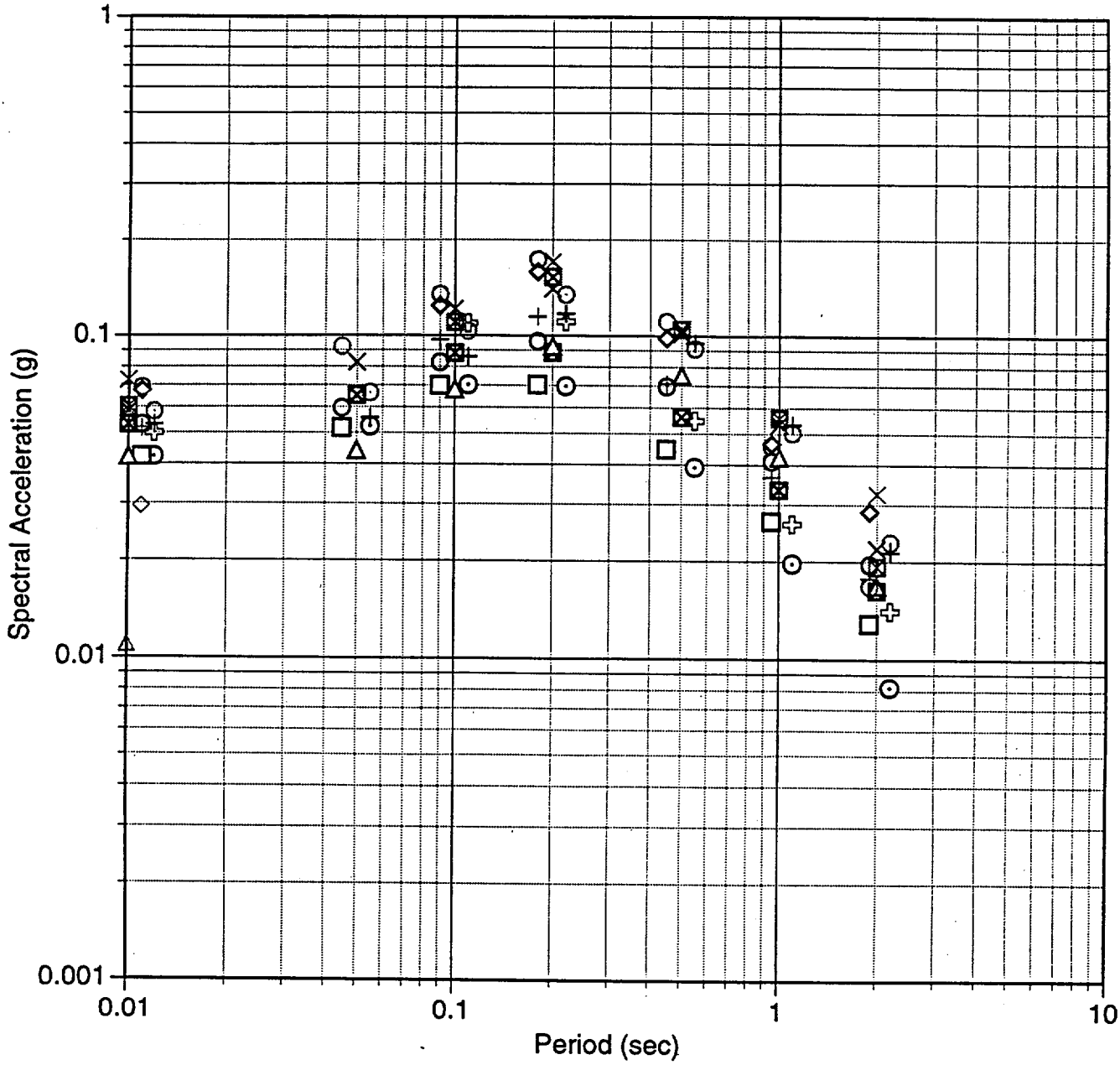

× AS97	□ Camp93/94(HR)	✣ BJF94(ClassA)	⊠ SP97
○ Camp97(SR)	+ Camp90/94(SR)	× BJF94(ClassB)	+ Spudichetal.97
⊙ Camp97(HR)	△ Camp90/94(HR)	○ Idriss91	△ McGarr84(Ext.)
⊠ Camp93/94(SR)	◇ BJF97(Vs=620m/s)	⊙ Sadighetal.93	◇ McGarr84(Comp)

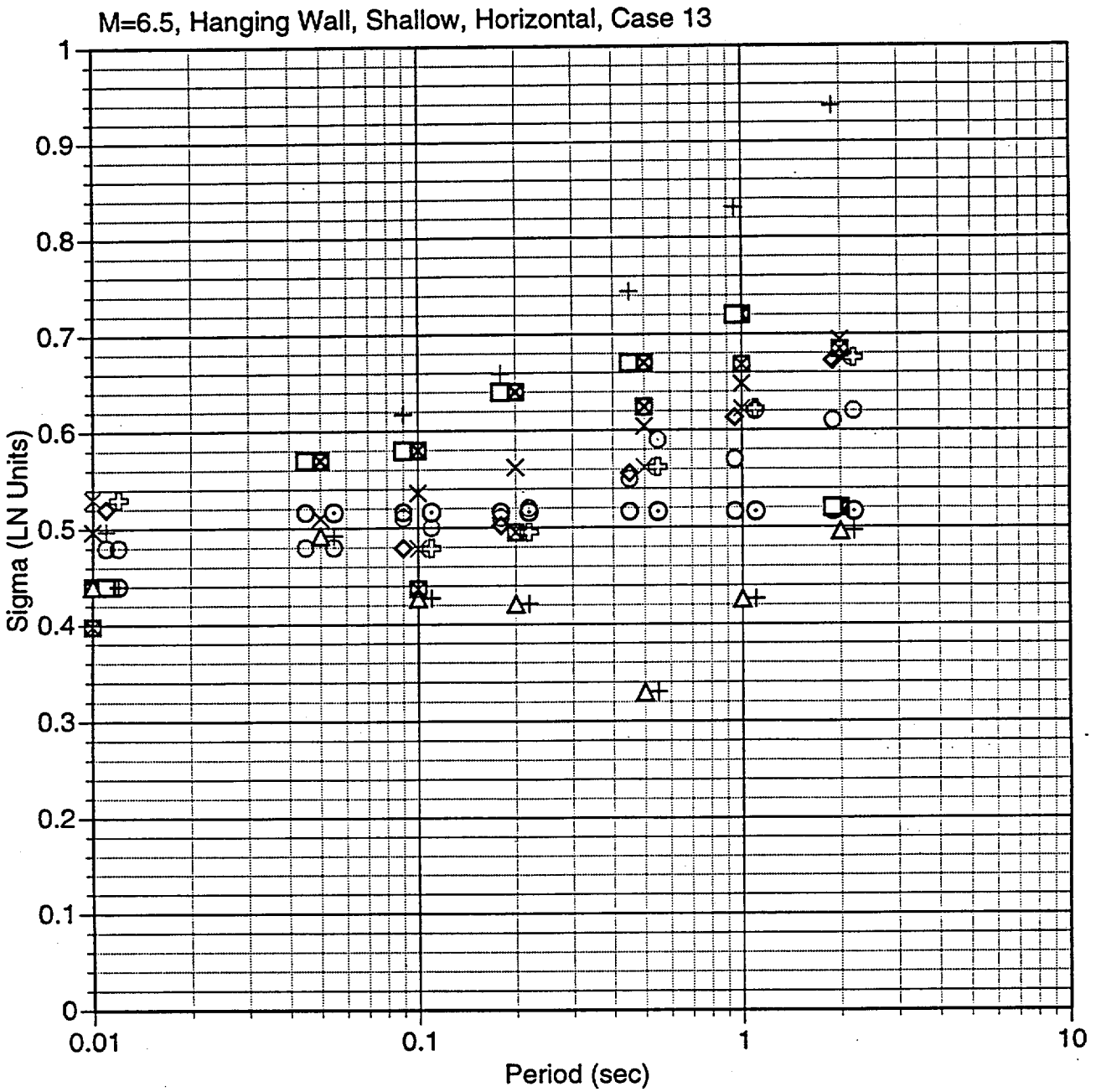

× AS97	□ Camp93/94(HR)	✚ BJF94(ClassA)	⊠ SP97
○ Camp97(SR)	+ Camp90/94(SR)	× BJF94(ClassB)	+ Spudichetal.97
⊙ Camp97(HR)	△ Camp90/94(HR)	○ Idriss91	△ McGarr84(Ext.)
⊠ Camp93/94(SR)	◇ BJF97(Vs=620m/s)	⊙ Sadighetal.93	◇ McGarr84(Comp)

M=6.5, Hanging Wall, Shallow, Vertical, Case 13

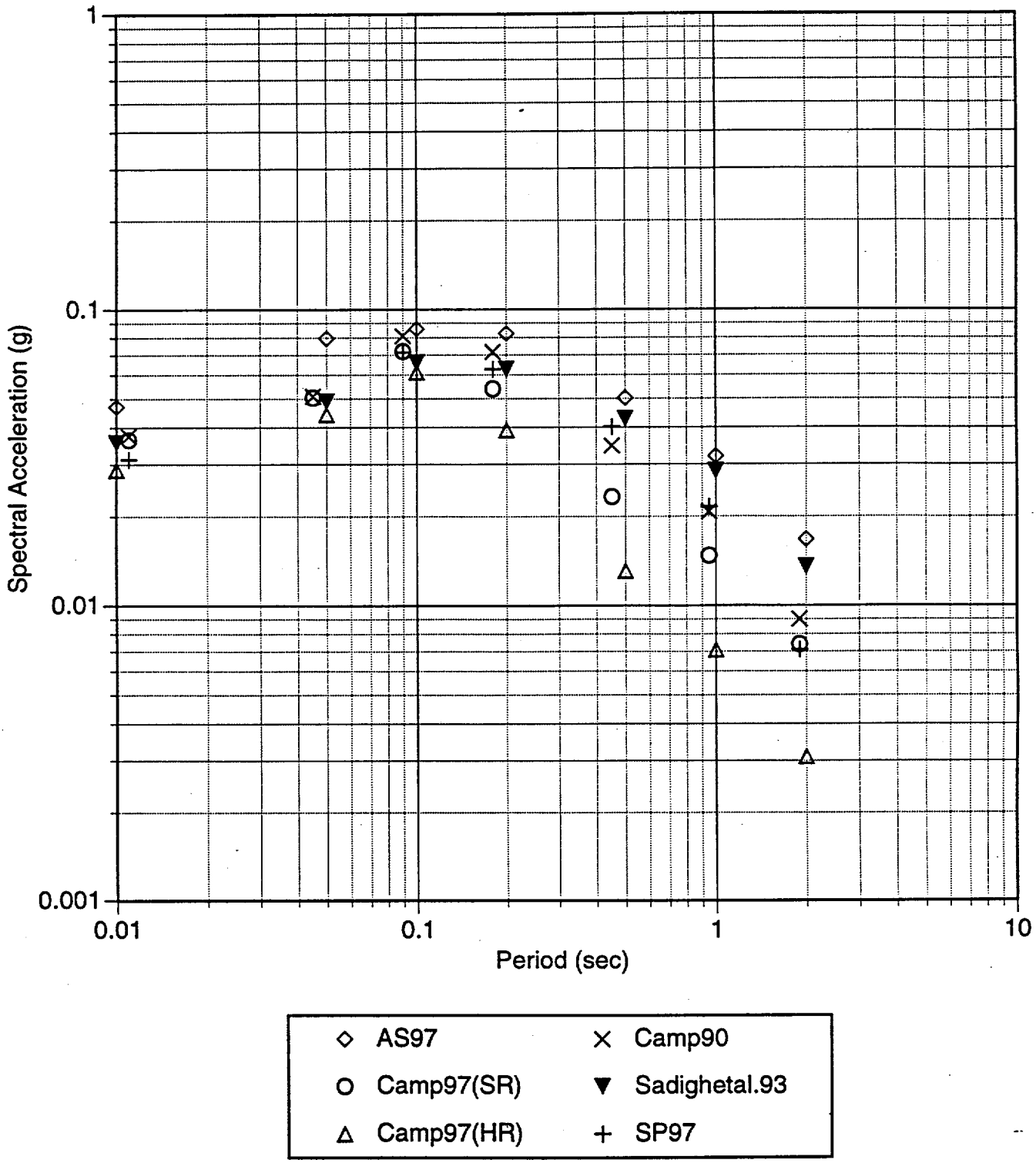

M=6.5, Hanging Wall, Shallow, Vertical, Case 13

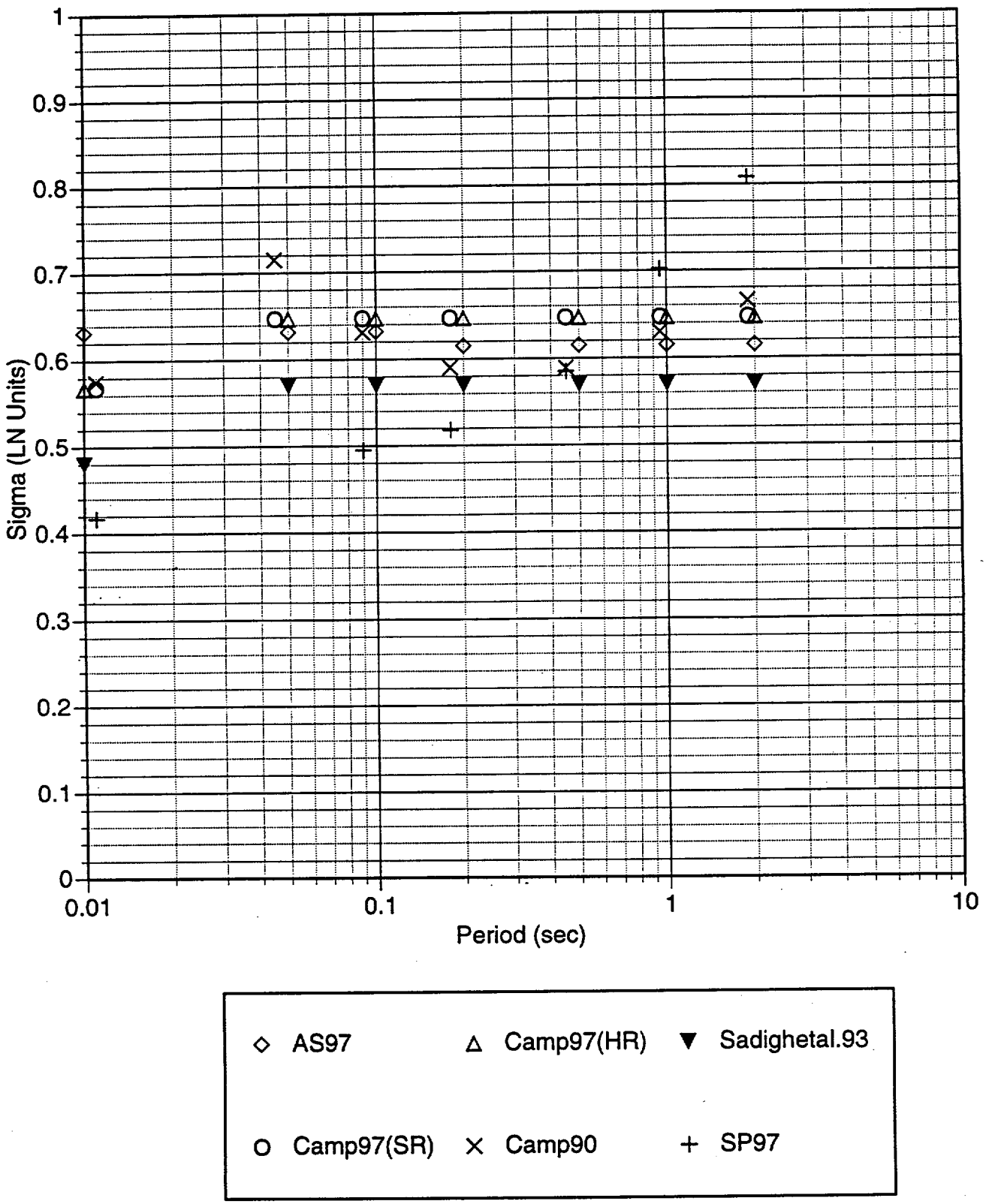

M=7.0,Strike-slip, Shallow, Horizontal, Case 14

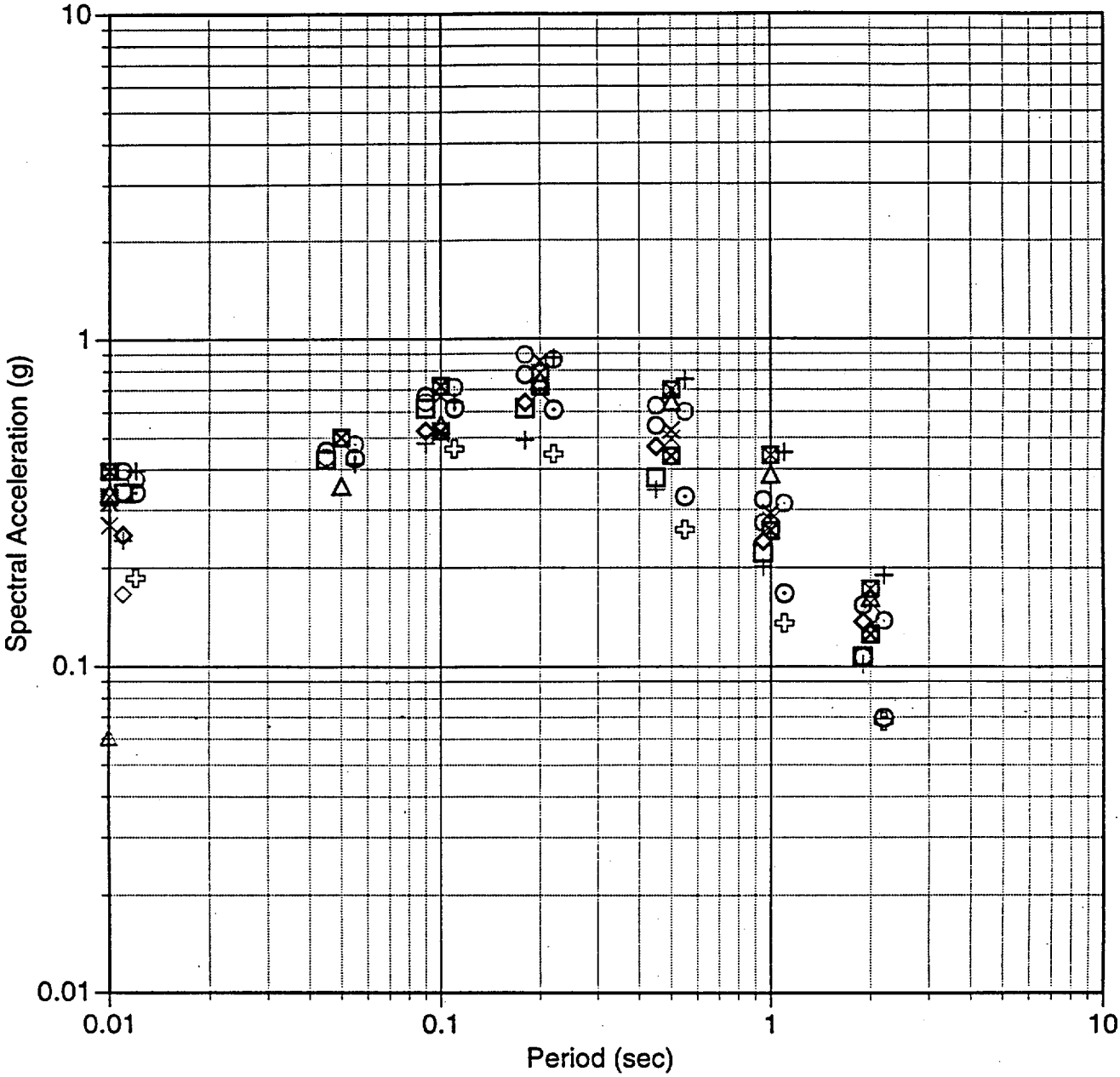

× AS97	□ Camp93/94(HR)	✣ BJF94(ClassA)	⊠ SP97
○ Camp97(SR)	+ Camp90/94(SR)	× BJF94(ClassB)	+ Spudichetal.97
⊙ Camp97(HR)	△ Camp90/94(HR)	○ Idriss91	△ McGarr84(Ext.)
⊠ Camp93/94(SR)	◇ BJF97(Vs=620m/s)	⊙ Sadighetal.93	◇ McGarr84(Comp)

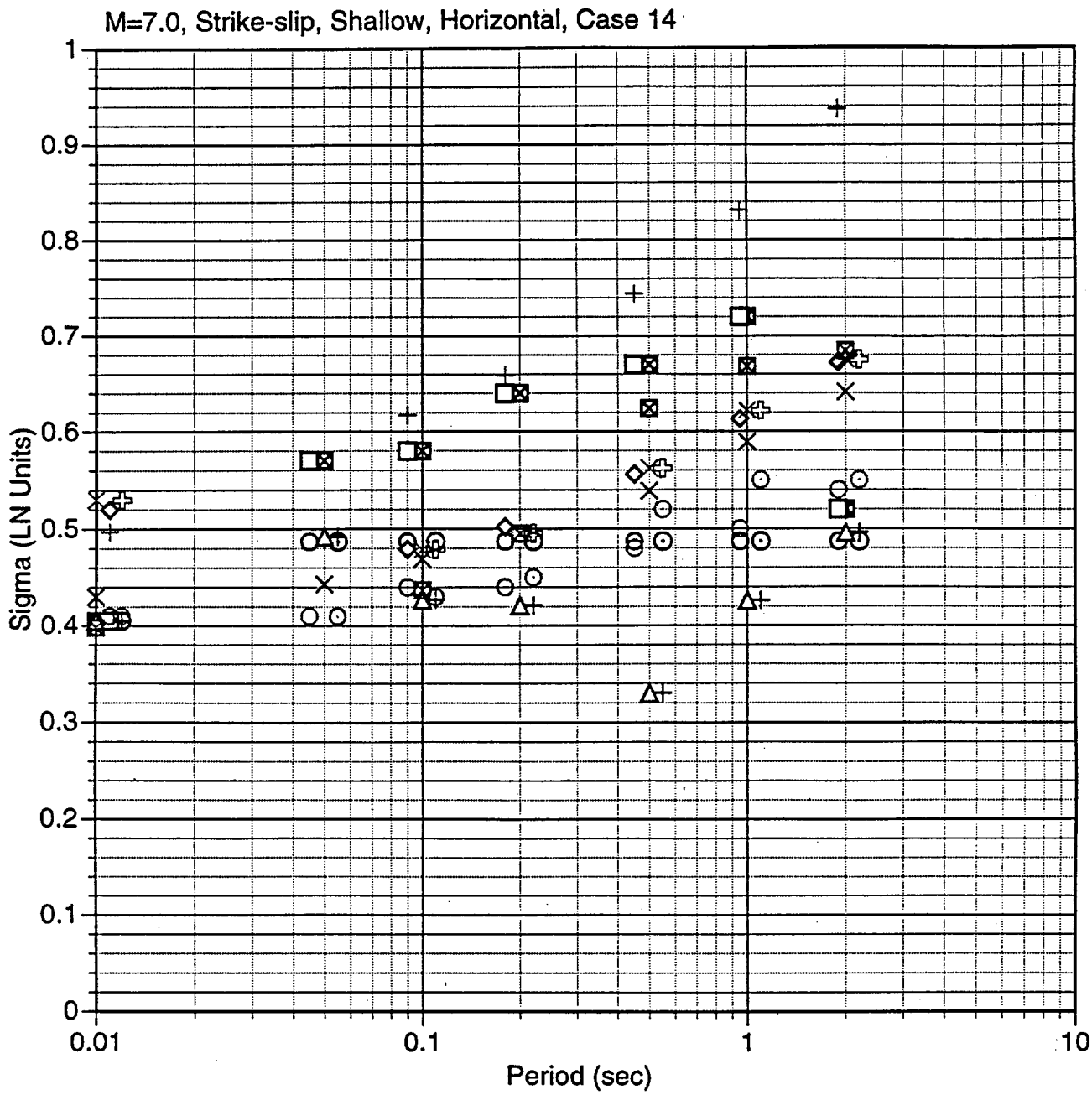

× AS97	□ Camp93/94(HR)	✠ BJF94(ClassA)	⊠ SP97
○ Camp97(SR)	+ Camp90/94(SR)	× BJF94(ClassB)	+ Spudichetal.97
⊙ Camp97(HR)	△ Camp90/94(HR)	○ Idriss91	△ McGarr84(Ext.)
⊠ Camp93/94(SR)	◇ BJF97(Vs=620m/s)	⊙ Sadighetal.93	◇ McGarr84(Comp)

M=7.0, Strike-slip, Shallow, Vertical, Case 14

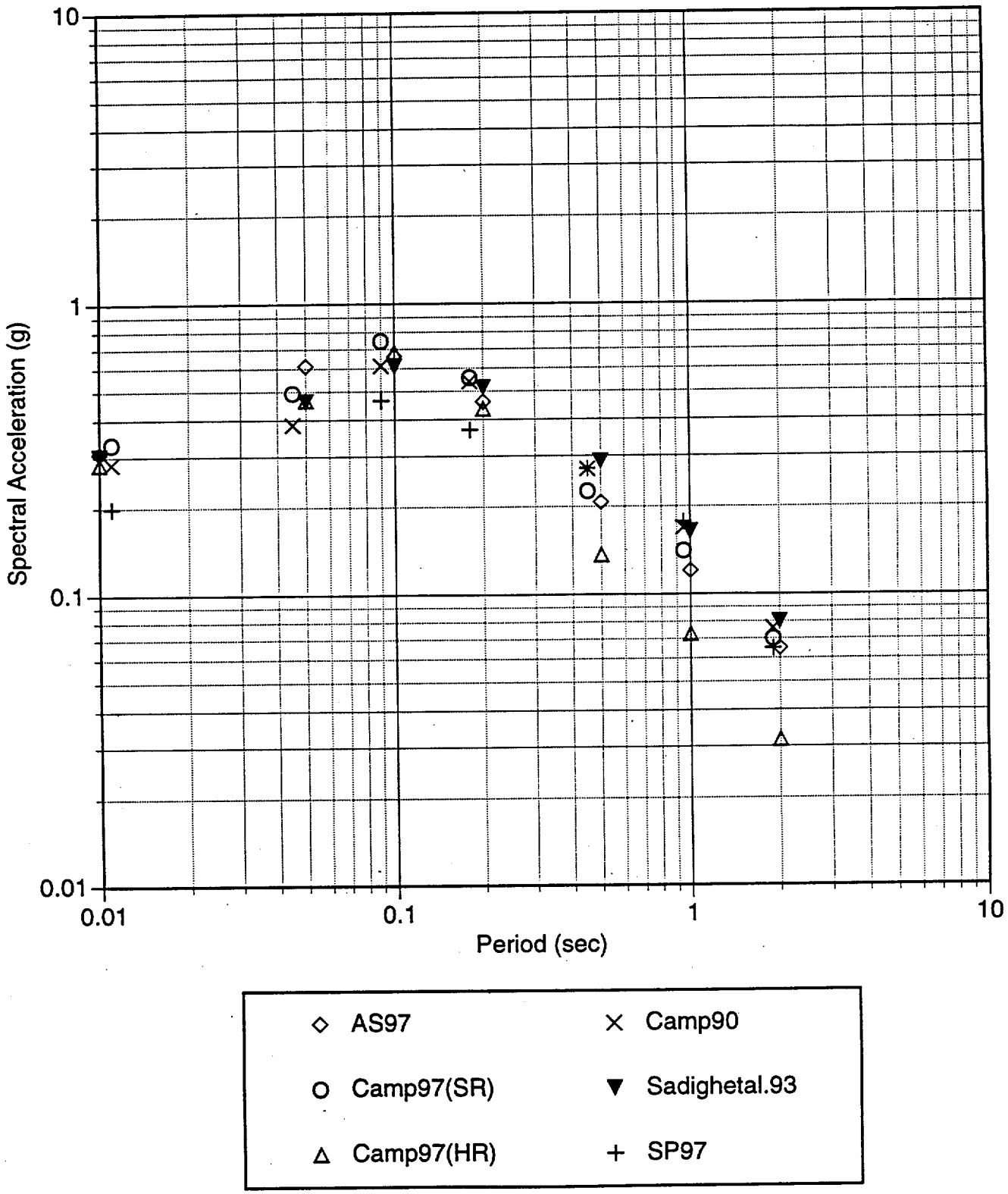

M=7.0, Strike-slip, Shallow, Vertical, Case 14

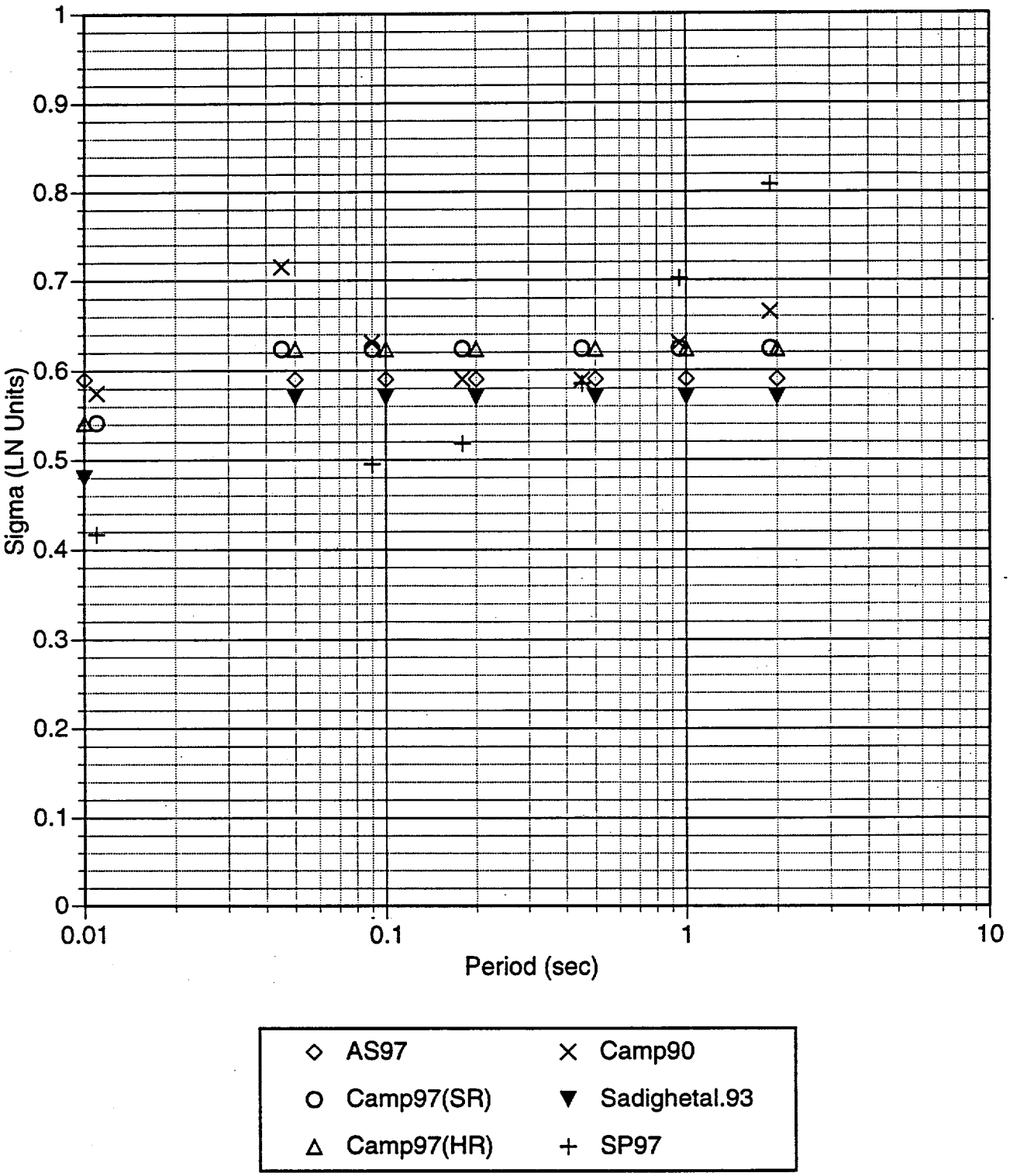

M=7.5,Strike-slip, Shallow, Horizontal, Case 15

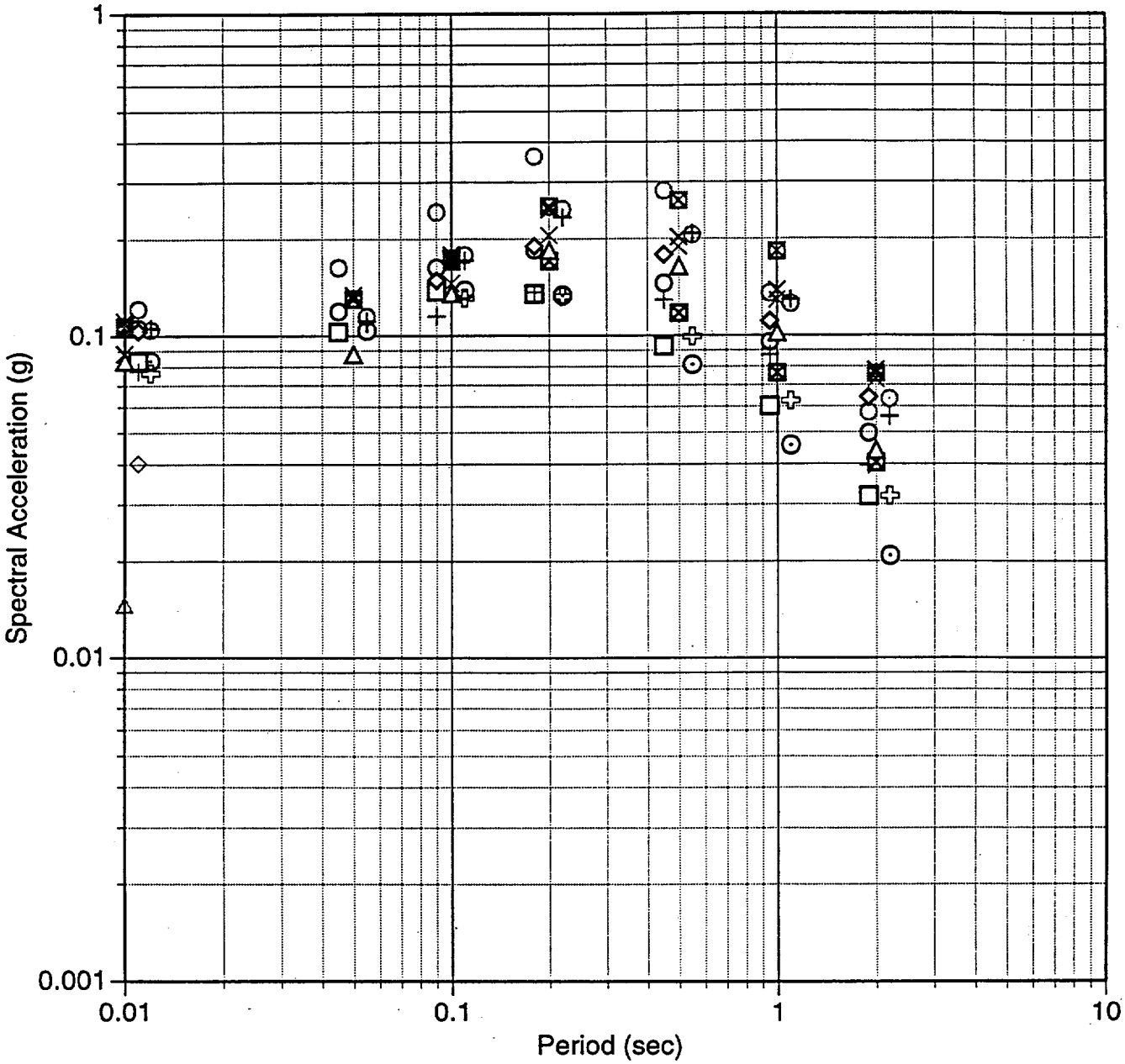

× AS97	□ Camp93/94(HR)	✚ BJF94(ClassA)	⊠ SP97
○ Camp97(SR)	+ Camp90/94(SR)	× BJF94(ClassB)	+ Spudichetal.97
⊙ Camp97(HR)	△ Camp90/94(HR)	○ Idriss91	△ McGarr84(Ext.)
⊠ Camp93/94(SR)	◇ BJF97(Vs=620m/s)	⊙ Sadighetal.93	◇ McGarr84(Comp)

M=7.5, Strike-slip, Shallow, Horizontal, Case 15

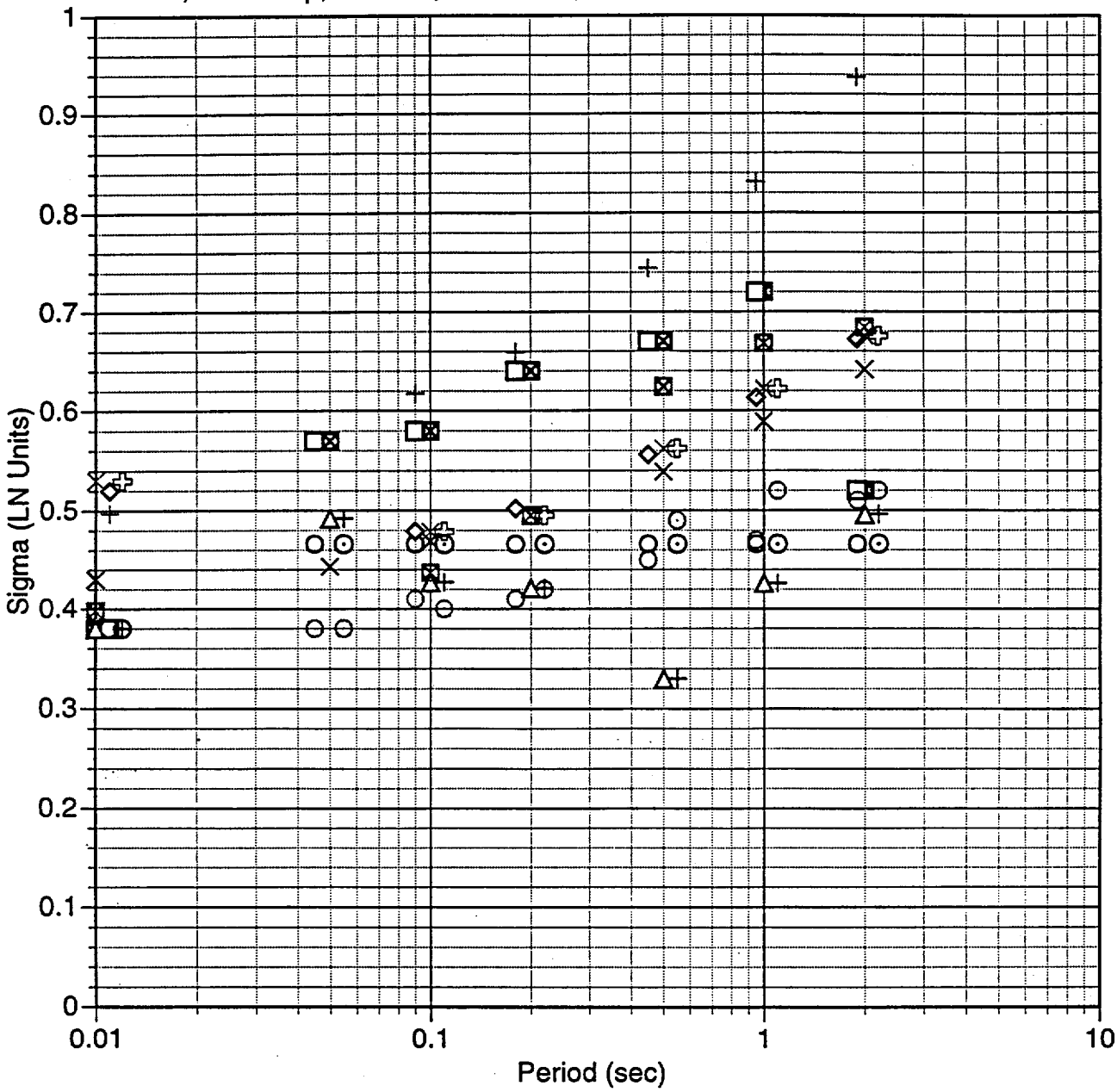

× AS97	□ Camp93/94(HR)	✚ BJF94(ClassA)	⊠ SP97
○ Camp97(SR)	+ Camp90/94(SR)	× BJF94(ClassB)	+ Spudichetal.97
⊙ Camp97(HR)	△ Camp90/94(HR)	○ Idriss91	△ McGarr84(Ext.)
⊠ Camp93/94(SR)	◇ BJF97(Vs=620m/s)	⊙ Sadighetal.93	◇ McGarr84(Comp)

M=7.5, Strike-slip, Shallow, Vertical, Case 15

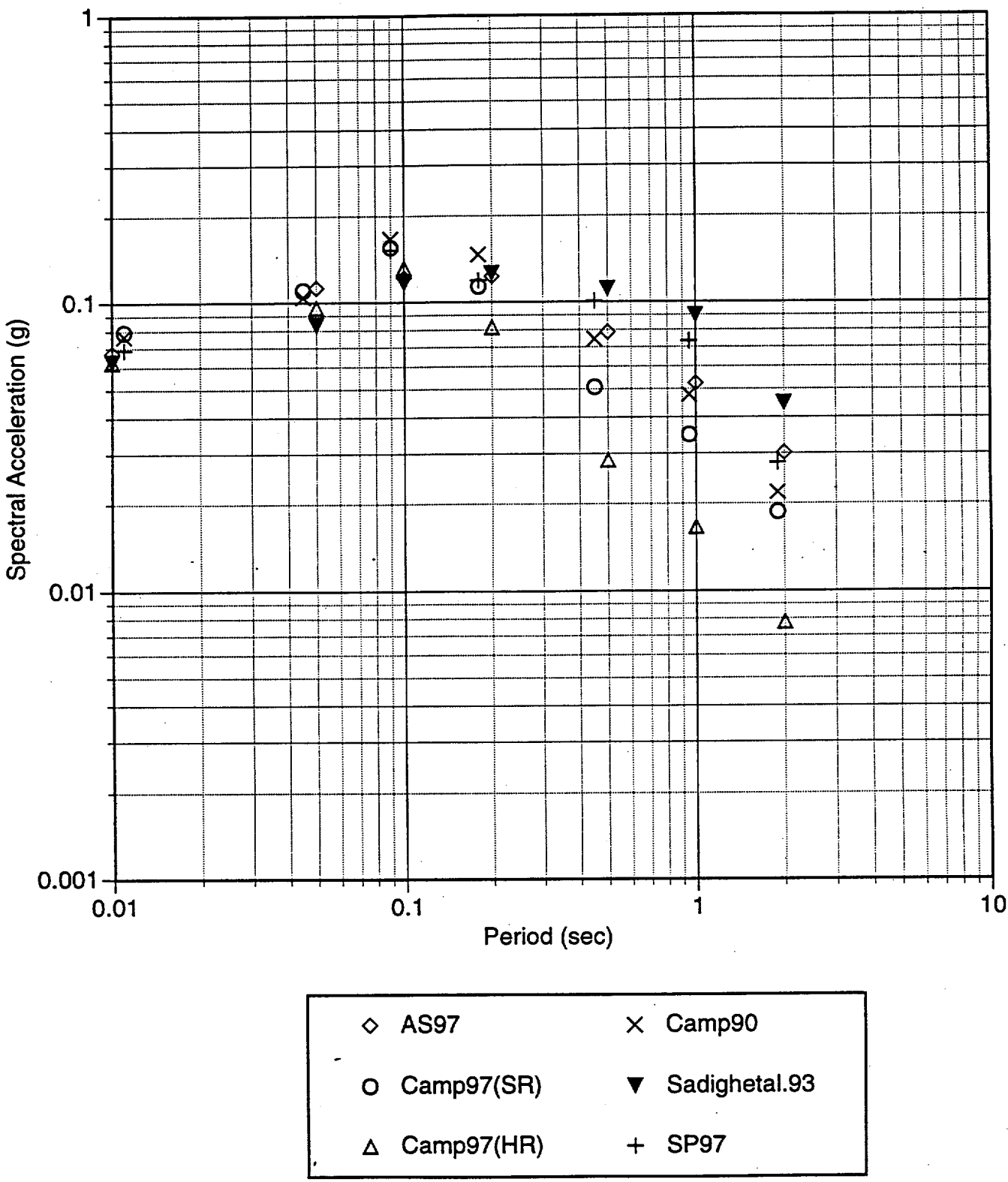

M=7.5, Strike-slip, Shallow, Vertical, Case 15

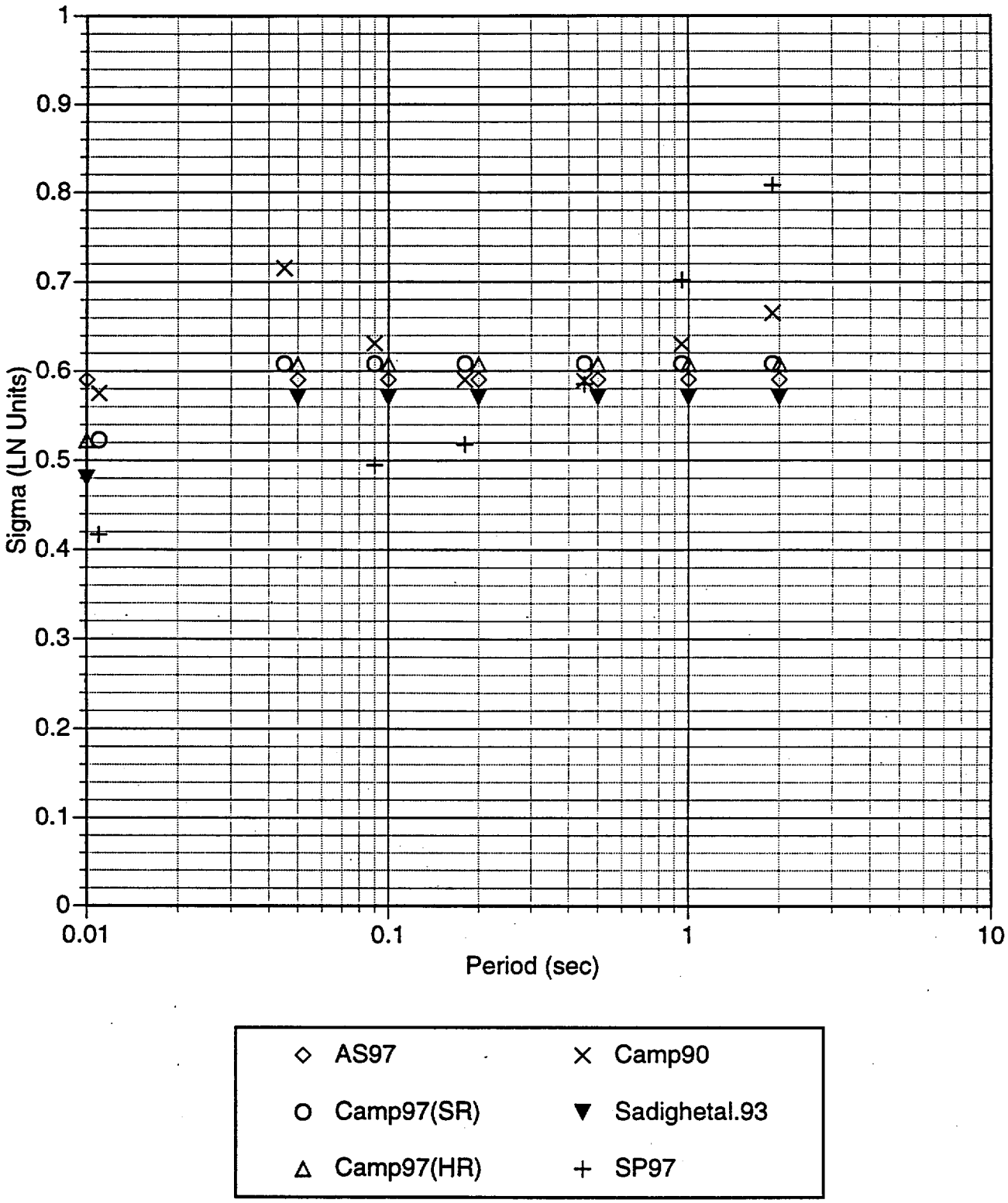

M=7.5,Hanging Wall, Shallow, Horizontal, Case 16

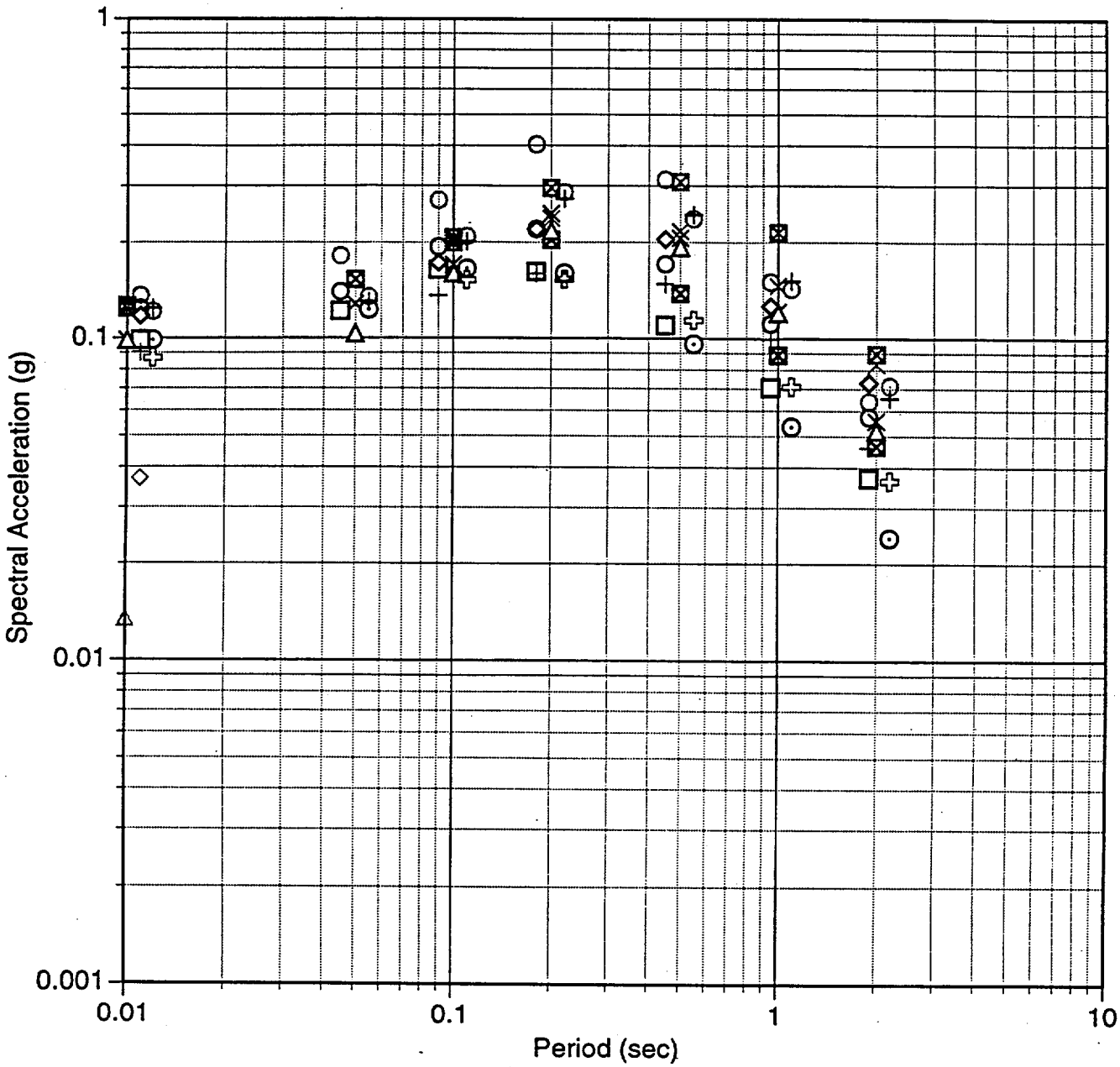

× AS97	□ Camp93/94(HR)	✚ BJF94(ClassA)	⊠ SP97
○ Camp97(SR)	+ Camp90/94(SR)	× BJF94(ClassB)	+ Spudichetal.97
⊙ Camp97(HR)	△ Camp90/94(HR)	○ Idriss91	△ McGarr84(Ext.)
⊠ Camp93/94(SR)	◇ BJF97(Vs=620m/s)	⊙ Sadighetal.93	◇ McGarr84(Comp)

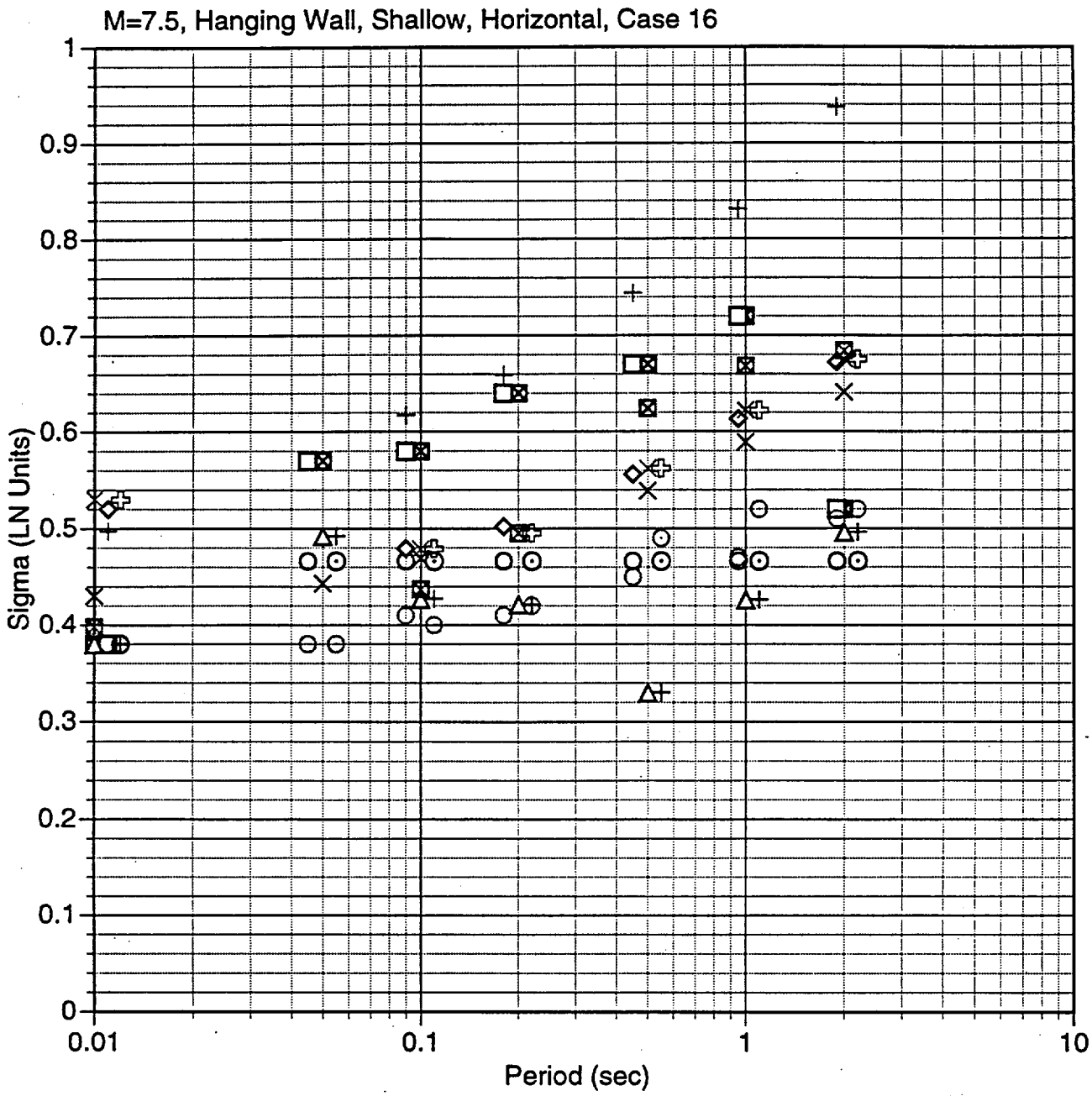

× AS97	□ Camp93/94(HR)	✠ BJF94(ClassA)	⊠ SP97
○ Camp97(SR)	+ Camp90/94(SR)	× BJF94(ClassB)	+ Spudichetal.97
⊙ Camp97(HR)	△ Camp90/94(HR)	○ Idriss91	△ McGarr84(Ext.)
⊠ Camp93/94(SR)	◇ BJF97(Vs=620m/s)	⊙ Sadighetal.93	◇ McGarr84(Comp)

M=7.5, Hanging Wall, Shallow, Vertical, Case 16

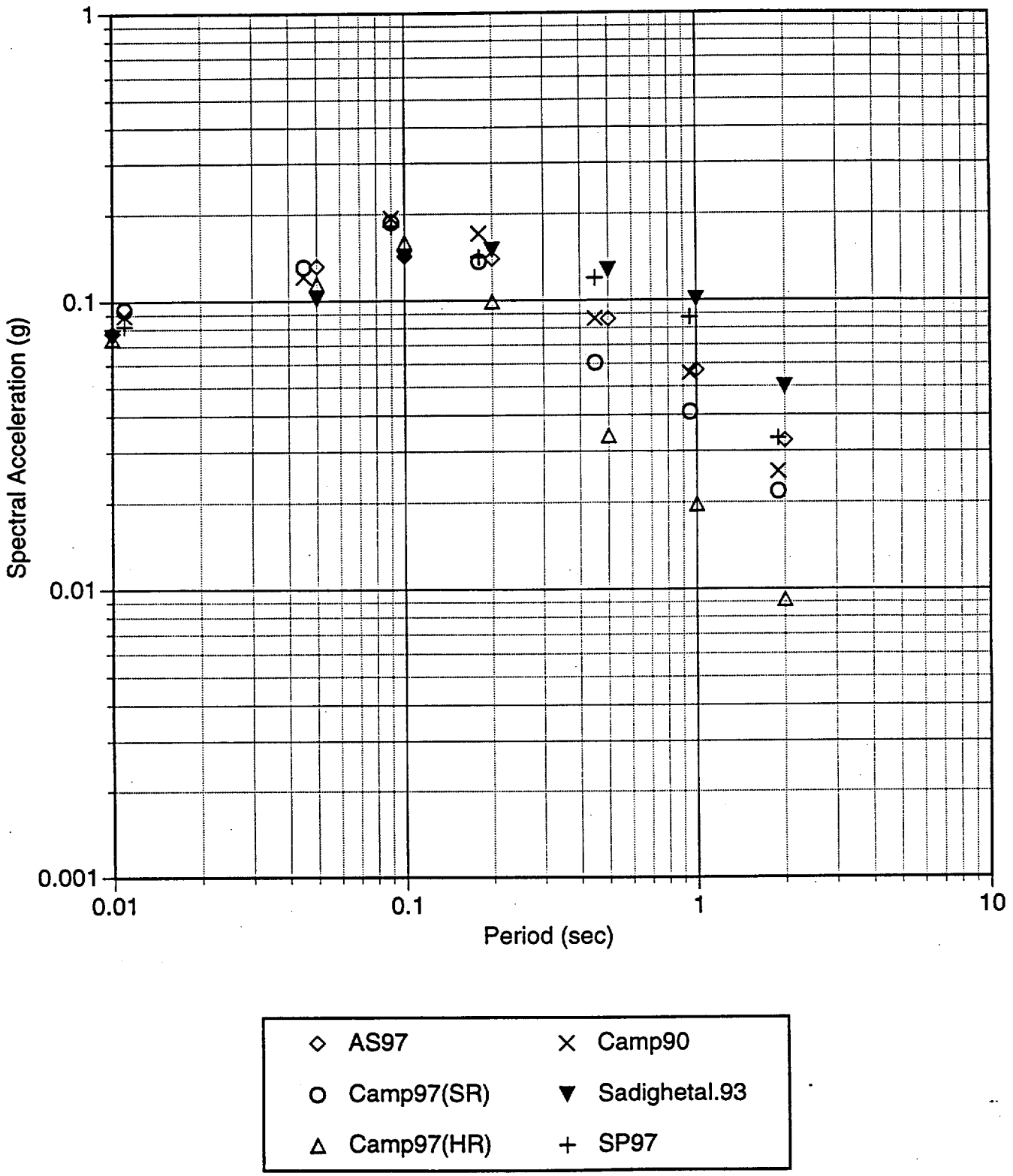

M=7.5, Hanging Wall, Shallow, Vertical, Case 16

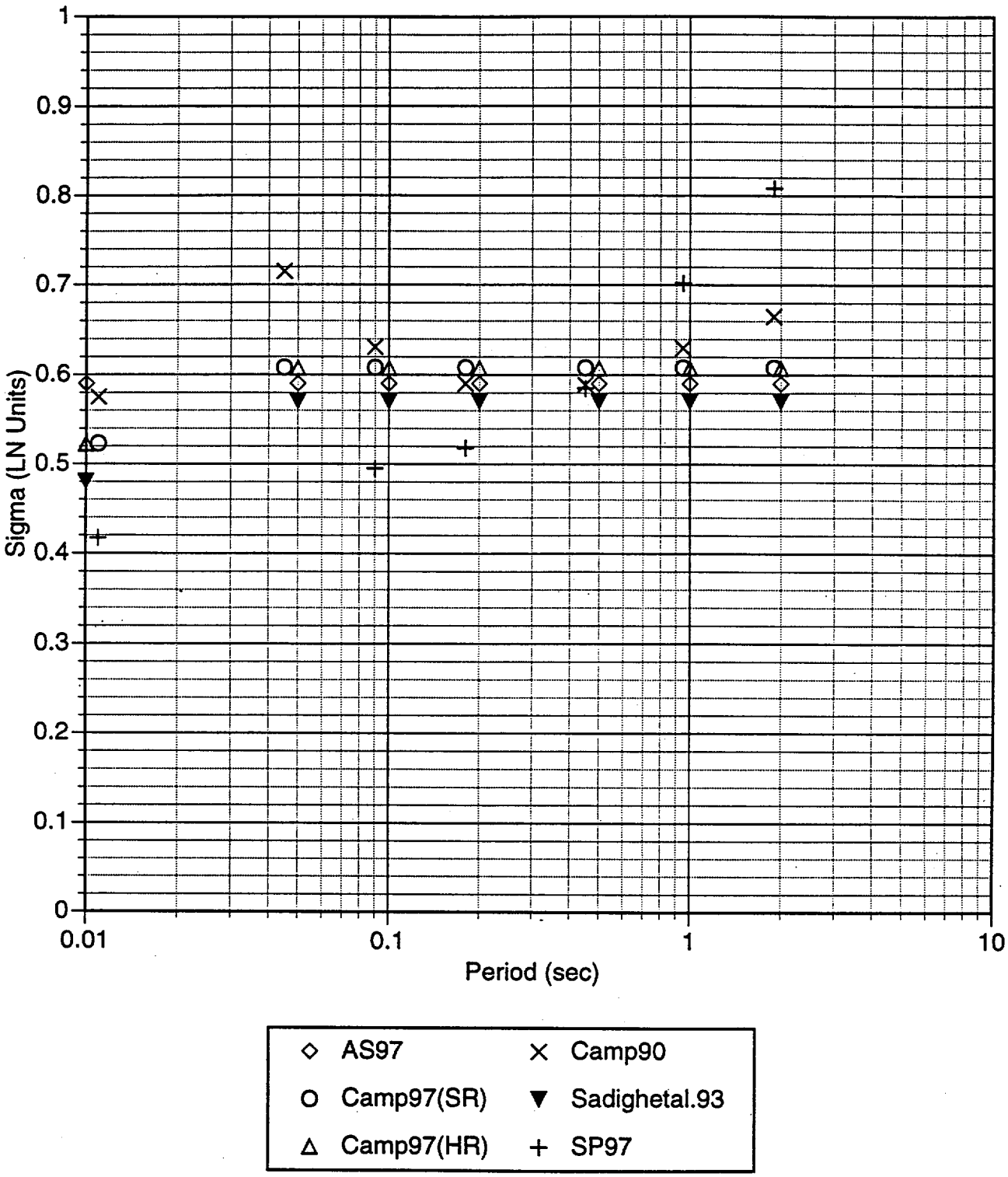

Section 5

Blast Experience Models

5.1 Blast Experience Model Names

Short Name	Description
Blast 1	NTS source and NTS attenuation
Blast 2	NTS attenuation with Sadigh 1993 spectral shape
Blast 3	Little Skull Mtn spectral shape and Sadigh magnitude scaling

5.2 Description of the Blast Experience Models

8.0 Explosion-Based Empirical Modeling Results

8.1 Background and Method Development

As noted above, the explosion-based empirical modeling approach described in this section is fundamentally different from the physical modeling methods used by the other investigators to predict ground motion for the scenario earthquakes at the Yucca Mountain site. In developing an empirical basis for predicting strong ground motion from earthquakes at a site like Yucca Mountain, the ideal would be to have recorded ground motion in the site vicinity covering a range of earthquake magnitudes which might be expected and covering distances at which such events might affect the site. However, as is the case with most engineering projects, such information is generally not available for the Yucca Mountain site. What we do have for Yucca Mountain are the records of strong ground motion made in the same general region as the site for a fairly large earthquake (viz. the 1992 Little Skull Mountain event) and for a large number of seismic events (viz. underground nuclear explosion tests) covering a range of strong motion levels and distances similar to those which are of interest for earthquake-resistant design at the Yucca Mountain site. These data provide information on region-specific attenuation, site response, and the uncertainties associated with these elements of the ground motion prediction problem. One objective of this project has been to identify procedures which permit us to utilize this region-specific knowledge of strong-ground motion to make reasonable inferences about seismic motions from large scenario earthquakes which might be postulated for the Yucca Mountain site. Our investigations under this element of the program have focused on utilization of the nuclear explosion experience base and the strong motion records from the Little Skull Mountain earthquake.

From the late 1950's until just recently, hundreds of underground nuclear explosions have been conducted at NTS. The yields of these explosions have ranged from less than 1 kiloton (kt) to 1200 kt, and the ground motions produced by these events were recorded at ranges from less than 1 km out to more than 100 km (cf. ERC, 1974; Bennett and Murphy, 1993). More than 1300 strong motion observations from this large explosion database were analyzed by ERC (1974) and used to develop prediction relations for the region surrounding NTS. These ERC prediction relations took the form of a power law model

$$A = A_0 W^B R^C \tag{8.1.1}$$

where A is either a peak time-domain ground motion measure or the spectral response at some frequency, W is explosion yield in kilotons, and R is range. The coefficient term, A_0, and the exponential terms, B and C, were derived from standard regression and covariance analyses of the explosion data. Similar power law models and regression analyses have subsequently been used by other authors to further analyze NTS explosion observations and to predict ground motions for the Yucca Mountain site (cf. Vortman, 1986; Phillips, 1991; Bennett and Murphy, 1993) from potential future NTS nuclear explosion tests. For the spectral response, which is the main focus of the studies presented in this section, A is a function of frequency and the coefficient and exponential terms are frequency dependent and determined by the regression analysis for each frequency. The response spectra predicted by these empirical relations have been found to be quite reliable for analyzing ground motion and building response from explosions at sites throughout the region.

The procedures used to extend this model to predict earthquake ground motions have been developed over the relatively short term of this project. Three distinct schemes based on the NTS explosion knowledge base have been identified and implemented to predict earthquake ground motions for the vicinity of the Yucca Mountain site. These three models are characterized as follows:

- Equivalent explosion with NTS attenuation relationship
- Geomatrix/ATC spectral shape with NTS attenuation relationship

- Little Skull Mountain earthquake spectral shape with NTS attenuation relationship and Geomatrix/ATC magnitude scaling

For the first of these models, we have attempted to use empirical relationships between magnitude and yield to identify an explosion source which is approximately equivalent to the postulated earthquake scenario. The scenario earthquakes are specified in terms of moment magnitude, M_W, while the most reliable relationship between magnitude and yield for underground nuclear explosions uses the body-wave magnitude, m_b. Lacking reliable empirical relationships between moment magnitude and yield for explosions, we resorted to an indirect approach. It is well known from seismic discrimination studies (e.g. Bolt, 1976; OTA, 1988) that nuclear explosions and earthquakes are generally different with respect to their relative excitation of long-period versus short-period seismic waves and this produces differences in surface-wave magnitude, M_S, with respect to m_b between the two source types. Similar differences are also implied for M_W versus m_b for the two source types. If we assume that seismic events with the same M_W have approximately equal M_S, then, based on experience with worldwide earthquakes (cf. Richter, 1957) and with NTS explosions (cf. Marshall et al., 1971; Murphy, 1977; Bache, 1982; OTA, 1988), for the same M_W we can infer

$$m_b \text{ (Explosion)} \approx m_b \text{ (Earthquake)} + 0.60 \qquad (8.1.2)$$

at magnitude levels of interest here. Finally, using empirical relations based on NTS experience between m_b and yield for explosions and the results of Houston and Kanamori (1986) for the empirical relationship between m_b and M_W for worldwide earthquakes, we have after some simplification

$$\log W \text{ (Equivalent Explosion)} \approx 0.654\, M_W \text{ (Earthquake)} - 0.780 \qquad (8.1.3)$$

where W is the yield in kilotons for the explosion equivalent to the earthquake with moment magnitude of M_W. To arrive at the ground motion predictions for this model, we used this approximate relationship to estimate yields for the equivalent explosions corresponding to the M_W's for the scenario earthquakes and simply applied the NTS explosion prediction relationship to obtain the 5-% damped PSRV response spectra. Figure 8.1 shows a comparison of 5-% damped PSRV spectra based on this equivalent explosion model for a fixed reference distance (viz. 10 km) and corresponding to a set of moment magnitudes, M_W, in the general range of interest. It should be noted for this and subsequent predictions derived from the NTS explosion experience that the period band for the spectra are somwhat more limited, mainly due to response of the recording systems

The second explosion-based empirical model involves a modification of the Geomatrix/ATC response spectra empirical model, as defined by Geomatrix (1992) and Sadigh et al. (1995), to include the region-specific attenuation information from the explosion experience appropriate to the vicinity of NTS and the Yucca Mountain site. The original Geomatrix model was based on analyses of the large empirical database of earthquake strong motion records principally from the California region. In our modified model we use the Geomatrix model to develop 5-% damped PSRV response spectra for the horizontal rock motions at a reference distance of 10 km for each of the postulated scenario earthquakes. Thus, the Geomatrix model establishes the level and the shape of the response spectrum at this reference distance. We then use the attenuation relationship from the power law model, derived from the experience with NTS explosions, to scale the spectrum at the reference distance to nearer or farther ranges. It is clear from this procedure that the calculated response spectra will generally match the standard Geomatrix model at distances near the reference distance and that departures away from that distance should be indicative of attenuation differences between the NTS region and the average for the Geomatrix data sample. Figure 8.2 shows that the somewhat stronger attenuation in the NTS

model causes the modified Geomatrix/ATC spectrum to lie above the standard spectrum at ranges less than 10 km and fall below the standard spectrum at farther ranges.

The third empirical model which we developed uses a reference response spectrum derived from the 1992 Little Skull Mountain earthquake which has been modified using the attenuation information from NTS explosion experience and scaled for magnitude based on the Geomatrix/ATC model, described above. In developing this model we used the 5-% damped PSRV spectra computed at eight strong motion sites for the 5.68 M_W Little Skull Mountain earthquake to determine a power law spectral model based on those observed data alone. We next derived a spectrum at a reference distance of 36 km, the average distance of the eight stations. This reference spectral shape was then scaled to nearer and farther distances corresponding to postulated scenario earthquakes using the NTS explosion-based attenuation exponents. After determining the spectrum for the appropriate distance, we scaled the ground motion up to the appropriate magnitude using the same magnitude dependence which is built into the Geomatrix/ATC empirical model. As will be shown in the following section, this model does a very good job in predicting the observed response spectra for the Little Skull Mountain earthquake, as would be expected since the ground motion attenuation observed from the Little Skull Mountain earthquake is not greatly different from that based on NTS explosion experience and no magnitude scaling is required.

8.2 Comparison of Predictions to 1992 Little Skull Mountain Earthquake Observations

The 1992 Little Skull Mountain earthquake is clearly important in seismic design consideration for the Yucca Mountain site because it represents a fairly large earthquake in a similar tectonic and propagation environment like that for several of the postulated scenario earthquakes. The main shock with magnitude 5.68 M_W was recorded at several surrounding strong motion stations at ranges between 12.9 km and 99.1 km from the fault. These strong motion records provide an excellent data sample to analyze characteristics of the ground motion from earthquakes in the vicinity of Yucca Mountain and to test modeling and prediction capability for such motions. As part of this project, we performed analyses of the attenuation characteristics of the PSRV spectra observed at the eight strong motion sites which recorded the Little Skull Mountain earthquake and attempted to test the explosion-based empirical prediction techniques described in the preceding section using the observed response spectra.

To analyze the attenuation of the strong motion observations from the main shock, we applied a power law model similar to that described above in equation 8.1.1. Because we were concerned with attenuation from a single event, there was no dependence on magnitude and the model reduced to

$$L(f) = L_0(f)\ R^{n(f)} \qquad (8.2.1)$$

for the PSRV spectra. Comparison of the N-S and E-W components of the PSRV spectra revealed insignificant (less than a factor of two) differences between the two observations at most stations and frequencies. We, therefore, performed the regression analyses on the combined data set with both horizontal components included as separate observations at each frequency. The attenuation exponent, n(f) in equation 8.2.1, was determined for each frequency as the slope of the least-squares linear fit to the response spectra measurements in log-log space. The attenuation exponents determined from the analysis of the Little Skull Mountain earthquake observations are compared to the attenuation exponents from the NTS explosion experience in Figure 8.3. The attenuation exponents from the NTS experience are seen to lie within the 95-% confidence limits bounding the mean values determined for the Little Skull Mountain earthquake at all periods in the left-hand figure. However, on the right the attenuation exponents for the Little Skull Mountain earthquake are seen to lie slightly above the rather narrow confidence bounds about the average NTS experience in a period band from about 0.2 to 2.0 seconds. Thus, over this band the Little Skull Mountain earthquake appears to show somewhat greater attenuation than that based on

average NTS explosion experience; but the differences are well within the statistical uncertainty in both estimates. The insignificance of the attenuation differences was further demonstrated by comparing the observed Little Skull Mountain response spectra at the eight strong motion sites with spectral predictions (1) based on the power law model derived directly from the Little Skull Mountain earthquake data and (2) based on the Little Skull Mountain earthquake spectral shape from a fixed reference distance scaled to other distance ranges using the NTS explosion attenuation exponents. There was little discernible difference found in the fits to the observations using these two approaches; the predictions for both approaches were generally within a factor of two of the observations at all stations and periods, and residuals for the two approaches were seen to have similar trends.

Figure 8.4 shows the 5-% damped PSRV spectrum derived from the power law model applied to the Little Skull Mountain earthquake observations. The figure compares the spectrum from the model at the average distance of the strong motion sites (viz. 35.7 km) with response spectra predicted for three other models: (1) the standard Geomatrix/ATC empirical model, (2) the modified Geomatrix/ATC model including NTS attenuation, and (3) the equivalent explosion model. At short periods (up to nearly 1 second) the three models show reasonable agreement among themselves and with the spectrum derived from the Little Skull Mountain earthquake observations. The standard Geomatrix/ATC empirical model actually appears to provide a somewhat better fit to the observed Little Skull Mountain earthquake spectrum over the period band from about 0.05 to 0.3 seconds. This is a little surprising considering that within this period range the attenuation derived from the Little Skull Mountain earthquake observations agreed quite well with NTS explosion experience, and this region-specific attenuation would be expected then to provide a better fit. Nevertheless, we find the agreement (within a factor of two) between the models within the short period band, up to almost 1-second period, is quite remarkable, particularly considering the simplicity of the assumptions used to develop some of the models, like the equivalent explosion model. It is only at long periods that we see divergence, with the three predictions all overestimating the observed response. One explanation for the differences seen here might be relatively poor excitation of longer-period surface waves or higher modes by the Little Skull Mountain earthquake because of a somewhat deeper than normal focal depth. We would certainly expect this to be the case for the equivalent explosion model because of the shallow explosion sources that contribute to the spectral shape there, but predictions based on the Geomatrix/ATC spectral shape are also significantly enhanced relative to the observations at periods from about 1 to 3 seconds. As described above, we have used the spectral estimate at the reference distance shown here for the Little Skull Mountain earthquake observations as the basis for our third ground motion prediction scheme. Thus, the PSRV spectrum labeled "LSM Observed" in Figure 8.4 serves as the reference spectral shape which we adjust for distance using NTS attenuation and scale with magnitude where necessary to provide our predictions.

We used the three explosion-based empirical models to compute 5-% damped PSRV spectral predictions for each of the eight strong motion sites from the Little Skull Mountain earthquake. For these calculations we used the magnitude of 5.68 M_W and the ranges to the stations measured from the surface projection of the fault - i.e. ranges between 12.9 km and 99.1 km. Figure 8.5 shows the spectra determined for the three modeling schemes at 12.9 km, the distance to the nearest station. The figure presents comparisons between the model predictions and the horizontal-component PSRV response spectra observed for the Little Skull Mountain earthquake at the Lathrop Wells site. The predictions all match the observations fairly well at periods up to about 1 second. At periods less than 0.1 seconds the predictions are tightly grouped and agree with the observations within a factor of about 1.4. Between periods of 0.1 and 1 second, there is somewhat more variability in the observations, but the predictions are generally within about a factor of 2. The best fit appears to be that provided by the Little Skull Mountain earthquake spectral shape scaled using the NTS attenuation, which provides a good fit to the two horizontal-component observations over nearly the entire period band shown, including longer periods. The other prediction schemes again tend to overestimate the observations at longer periods; the largest divergence from the observations is seen in the equivalent explosion prediction

which overestimates by about a factor of 4 at periods near 2 seconds. Similar results were found for comparisons between the explosion-based empirical model predictions and observations for the Little Skull Mountain earthquake spectra at other strong motion sites. These test cases for the Little Skull Mountain earthquake appear to provide some confirmation that the explosion-based empirical modeling schemes defined here, or some variant of those schemes, can provide a useful supplement to the alternative ground motion prediction methods based on physical models.

8.3 Ground Motion Predictions for Earthquake Scenarios at the Yucca Mountain Site

The earthquake hazard to the Yucca Mountain site can be defined in terms of a number of scenario earthquakes associated with faults in the general vicinity of the site. For this project six faults were considered: Bow Ridge, Paintbrush Canyon, Solitario Canyon, Bare Mountain, Rock Valley, and Furnace Creek. For the first four faults the scenario earthquakes have normal-slip mechanisms, based on the dominant sense of displacement observed for the fault, and are assumed to be represented by a moment magnitude of 6.4 M_W. For the Rock Valley and Furnace Creek faults the scenario earthquakes have strike-slip mechanisms, again based on the dominant sense of displacement, and are assumed to be represented by moment magnitudes of 6.71 M_W and 7.04 M_W respectively. For each of these scenario earthquakes, we used the explosion-based empirical models to predict 5-% damped PSRV spectra.

In specifying the distance to use in the ground motion calculations, we assumed hypocenters located at two different focal depths (viz. 6 km and 9 km) on the faults to provide some range of depth within the crust for the earthquake sources. Because our models essentially represent simple point sources with no effect of radiation pattern, the only effect of the focal depth differences is to alter the hypocentral distances used in the calculations. It should be noted in this regard that small differences in the assumed hypocentral distance produce relatively insignificant perturbations for the response spectra considering the other uncertainties associated with the predictions. For the normal fault scenarios, the faults were assumed to have a common dip of 57.5° with dip direction measured from field observations. The distances were then measured from the site to the hypocenter at the appropriate focal depth on each of the dipping faults. With these assumptions the hypocentral distances used for the base case normal fault scenario predictions ranged from 6.0 km to 13.3 km. For the strike-slip scenarios, the faults were assumed to be vertical; and the distances were again determined from the site to the appropriate hypocenter at each assumed focal depth on the fault. Because these faults are at fairly large horizontal distances from the Yucca Mountain site, the differences between the two assumed focal depths for the scenario earthquakes have little effect on the hypocentral distances. As a result, hypocentral distances for the Rock Valley fault scenario earthquakes are 26 km and 27 km, and hypocentral distances for the Furnace Creek fault scenario earthquakes are 51 km and 52 km.

For each of the scenario earthquakes, we calculated the PSRV spectral responses for the three empirical models described in Section 8.1 above. Thus, we generated a total of 36 response spectra for the 12 earthquake scenarios (i.e. two focal depths for each of the six faults). Figure 8.6 shows a representative prediction for the base case normal fault scenario with a magnitude of 6.4 Mw and a range of 9.1 km. This prediction corresponds to the Paintbrush Canyon fault scenario earthquake with a focal depth of 9 km. In Figure 8.6 we show comparisons of the predictions for each of the explosion-based empirical models with the prediction determined for the same scenario earthquake using the standard Geomatrix/ATC empirical model. The plot on the left shows fairly close agreement between the prediction for the equivalent explosion model and the standard Geomatrix/ATC model. At short periods, 0.05 to 0.1 seconds, and again at long periods, 0.9 to 3 seconds, the equivalent explosion model prediction lies slightly (about a factor of 1.5) above the standard Geomatrix/ATC model prediction; while at intermediate periods, 0.1 to 0.9 seconds, the two predictions overlap. The middle plot compares the standard Geomatrix/ATC empirical model prediction with the prediction using the Geomatrix/ATC model spectrum modified based on NTS explosion attenuation experience. The distance range is not much different from the reference distance used for the latter model, and as a result the two predictions are quite close. The modified

Geomatrix/ATC model prediction lies slightly above the standard model because of somewhat greater attenuation in the modified model, as discussed above. The plot on the right illustrates the steps in the process of scaling the Little Skull Mountain earthquake spectrum to the appropriate range and magnitude. Comparing the final predictions we note that the prediction based on the scaled Little Skull Mountain earthquake spectrum lies above the standard Geomatrix/ATC model prediction (by about a factor of 1.5 to 2) over the short period band, 0.05 to 0.3 seconds; while above 0.6 seconds the scaled Little Skull Mountain spectrum falls below the standard model predictions.

Figure 8.7 presents a similar set of predictions for the Furnace Creek fault scenario earthquake with a magnitude of 7.04 M_W and range of 52 km (9 km focal depth). The equivalent explosion spectrum generally agrees quite well with the standard Geomatrix/ATC spectral prediction over nearly the entire period band; maximum differences are less than a factor of about 1.5. For the modified Geomatrix/ATC model, we see in the middle plot that the predicted spectrum falls consistently below the standard model prediction by about a factor of 2. The differences are again apparently due to the stronger attenuation based on the NTS explosion experience; such differences tend to appear enhanced at the relatively large range for this scenario. Finally, the plot on the right in Figure 8.7 compares the scaled Little Skull Mountain earthquake spectrum with the standard Geomatrix/ATC model spectrum. The two predictions match very closely at short periods, 0.05 to 0.5 seconds. However, the spectral shapes are quite different; so that the scaled Little Skull Mountain prediction falls below the standard model spectrum by up to a factor of 3 at longer periods, above about 0.5 seconds.

As described elsewhere in this report, a number of physical fault rupture models were also used to provide strong ground motion predictions for the scenario earthquakes associated with the faults in the vicinity of the Yucca Mountain site. In Figure 8.8 we show a few examples of comparisons between those physical model results and the predictions developed for the explosion-based empirical models. The physical model spectra shown in each of these comparisons correspond to the median values determined from the spectral estimates derived from multiple realizations of four different physical models for each scenario. The four physical models contributing to the estimates shown here were (1) the barrier source model implemented by the University of Southern California, (2) the composite fractal source method used by the University of Nevada - Reno, (3) the stochastic method with subevents used by Pacific Engineering and Analysis, and (4) the broadband Green's function method used by Woodward-Clyde Consultants. As noted, the spectrum shown in each plot for these physical models is a median value and variations in the estimates, attributable to methodological differences and uncertainty in source parameter specification and attenuation, may be quite large, as evidenced by scatter between realizations.

The plot on the left in Figure 8.8 compares the explosion-based empirical model predictions determined for an earthquake with magnitude of 6.4 M_W at a range of 6.0 km with the prediction from the physical model. This prediction corresponds to the Paintbrush Canyon fault scenario earthquake for which we assumed a focal depth of 6 km. It should be noted that the plots in this figure correspond to 5-% damped acceleration response spectra in g's. Somewhat surprisingly the match between the spectra determined using our simple explosion-based empirical models and the median for the physical model spectrum is remarkably good. This is particularly notable considering that the estimates are for a close range site where the physical models would be expected to do a better job of accounting for near-source effects like radiation pattern which are disregarded in the explosion-based empirical models. At most periods the differences seen in the plot on the left amount to less than a factor of 2. Both the equivalent explosion and the scaled Little Skull Mountain earthquake spectra agree quite closely with the physical model prediction at short periods, 0.05 up to 0.2 seconds. Differences at longer periods are somewhat greater, particularly for the scaled Little Skull Mountain spectral prediction. However, even there it would appear that the uncertainty bounds about the median for the physical models probably envelope the explosion-based model predictions.

The middle and right-hand plots in Figure 8.8 correspond to the two strike-slip scenario earthquakes associated with the Rock Valley (6.71 M_W) and Furnace Creek (7.04 M_W) faults respectively. For these two scenarios there is more variation in the spectral prediction between our explosion-based models, and the difference between the spectra for those models and the median of the physical models is greater. The biggest differences seem to be those in the middle plot (i.e. Rock Valley scenario). There the equivalent explosion and scaled Little Skull Mountain earthquake spectrum fall below the physical model median by about a factor of 2 to 3 over a fairly broad period band, while the modified Geomatrix/ATC predictions are up to a factor of 4 lower than the physical model median. The predictions are more in agreement for the Furnace Creek scenario earthquake (shown in the right-hand figure), where maximum differences between the physical model median spectrum and the equivalent explosion and scaled Little Skull Mountain predictions are again low but only by about a factor of 2 at short periods, less than 1 second. We would suggest that the larger differences between the explosion-based and physical model predictions for the two strike-slip scenario earthquakes may be largely attributable to attenuation differences, which appear enhanced at the larger distances for these events. As noted above, the NTS explosion experience appears to indicate stronger attenuation in this region than for California. The prediction comparisons here seem to indicate that the stronger attenuation in the NTS region is not being adequately accounted for in the physical models.

8.4 Summary and Conclusions Regarding the Explosion-Based Empirical Modeling Procedures

Our objective in this element of the project has been to identify how the extensive experience with strong ground motion from NTS underground nuclear explosions might be used to assist in assessing earthquake ground motion predictions for use in design at the Yucca Mountain site. As part of these investigations, we analyzed strong ground motion observations from the 1992 Little Skull Mountain earthquake and compared those to the NTS explosion experience. Three explosion-based empirical models which take advantage of the NTS explosion experience as well as ground motion characteristics observed from the Little Skull Mountain earthquake were developed. We have applied these explosion-based empirical models to predict ground motions for the Little Skull Mountain earthquake and compared the results to observations as a test of the modeling procedures. The same models were then used to predict ground motions for several postulated scenario earthquakes which are being considered in assessing seismic design for the Yucca Mountain site.

In general, we find that the explosion-based empirical models do a fairly good job of predicting earthquake strong ground motion response spectra when compared to the Little Skull Mountain earthquake observations and to the alternative empirical and physical model predictions. With regard to specific model performance, we found that spectral predictions developed for our simple equivalent explosion model agreed surprisingly well with other prediction methods. Predictions based on the Little Skull Mountain earthquake spectral shape were generally found to be anomalously low at long periods compared to the other empirical prediction methods and to the physical model predictions; this might be associated with anomalous source depth. However, at periods below about 1 second, all three explosion-based models agree fairly well among themselves, with other empirical earthquake models, and with observations from the Little Skull Mountain earthquake, particularly at the nearer recording sites. Analyses of the 1992 Little Skull Mountain earthquake strong motion records indicate that the observed attenuation is not significantly different from that based on NTS explosion experience, so we would conclude that the explosion experience should play a role in assessing strong motion attenuation from postulated earthquakes in the region. This might be important considering that stronger attenuation in the NTS region does not appear to be properly accounted for in the physical models, particularly for more distant scenarios.

References

Bache, T. C. (1982). "Estimating the Yield of Underground Nuclear Explosions," Bull. Seism. Soc. Am. 72, pp. S131-S168.

Bennett, T. J., and J. R. Murphy (1993). "Estimation of Near-Regional Seismic Ground Motion from Underground Nuclear Explosion Tests," in Dynamic Analysis and Design Considerations for High-Level Nuclear Waste Repositories, edited by Q. A. Hossain, ASCE, New York, pp. 191-205.

Bolt, B. A. (1976). Nuclear Explosions and Earthquakes - The Parted Veil, W. H. Freeman and Company, San Francisco, CA.

Environmental Research Corporation (1974). "Prediction of Ground Motion Characteristics of Underground Nuclear Detonations," U.S. Atomic Energy Commission Nevada Operations Office Report NVO-1163-239, Las Vegas, NV.

Geomatrix (1992). "Seismic Ground Motion Studies for Major Northern California Bridges," Studies conducted in association with International Civil Engineering Consultants for Caltrans, Division of Structures, Sacramento, CA.

Houston, H., and H. Kanamori (1986). "Source Spectra of Great Earthquakes: Teleseismic Constraints on Rupture Process and Strong Motion," Bull. Seism. Soc. Am. 76, pp. 19-42.

Marshall, P. D., A. Douglas, and J. A. Hudson (1971). "Surface Waves from Underground Nuclear Explosions," Nature 234, pp. 8-9.

Murphy, J. R. (1977). "Seismic Source Functions and Magnitude Determinations for Underground Nuclear Detonations," Bull. Seism. Soc. Am. 67, pp. 135-158.

Office of Technology Assessment (1988). Seismic Verification of Nuclear Testing Treaties, OTA-ISC-361, Washington, D.C.

Phillips, J. S. (1991). "Prediction of Pseudo Relative Velocity Response Spectra at Yucca Mountain for Underground Nuclear Explosions Conducted in the Pahute Mesa Testing Area at the Nevada Test Site," Sandia Report Sand88-3032, Albuquerque, NM.

Richter, C. F. (1957). Elementary Seismology, W. H. Freeman and Company, San Francisco, CA.

Sadigh, K., C.-Y. Chang, N. A. Abrahamson, S. J. Chiou, and M. S. Power (1995). "Specification of Long-Period Ground Motions: Updated Attenuation Relationships for Rock Site Conditions and Adjustment Factors for Near-Fault Effects," in Technical Papers on Seismic Isolation, ATC-17.1, pp. 59-68.

Vortman, L. J. (1986). "Ground Motion Produced at Yucca Mountain from Pahute Mesa Underground Nuclear Explosions," Sandia Report Sand86-7006, Albuquerque, NM.

Figure Captions

Figure 8.1 Comparison of 5-% damped PSRV spectra predictions at a range of 10 km for the NTS equivalent explosion model for different moment magnitudes in the range of interest.

Figure 8.2 Comparison of standard Geomatrix/ATC 5-% damped PSRV spectral predictions with predictions produced using the Geomatrix/ATC spectral shape at 10 km scaled with distance using NTS explosion attenuation experience. Note the two predictions coincide at the nominal reference distance of 10 km.

Figure 8.3 Comparison of distance attenuation exponents and their 95-% confidence limits for NTS explosion experience and Little Skull Mountain (LSM) earthquake observations. NTS experience falls within the larger confidence limits about the LSM average (left), while LSM attenuation falls within or just above the smaller confidence limits surrounding average NTS experience (right).

Figure 8.4 Comparison of 5-% damped PSRV spectral predictions for three models with the spectrum at R = 35.7 km derived from the power law model applied to the Little Skull Mountain earthquake observations.

Figure 8.5 Comparison of 5-% damped PSRV spectral predictions for the three explosion-based empirical models with the spectra observed at the Lathrop Wells site (R = 12.9 km) for the Little Skull Mountain earthquake.

Figure 8.6 Comparison of 5-% damped PSRV spectral predictions for the base case normal scenario earthquake (Mw = 6.4) for the Yucca Mountain site at a range of 9.1 km for the equivalent explosion model (left), modified Geomatrix/ATC model (center), and Little Skull Mountain earthquake spectral shape scaled with NTS attenuation and Geomatrix/ATC magnitude dependence (right). For reference the model results are compared to similar spectral predictions based on the standard Geomatrix/ATC empirical model.

Figure 8.7 Comparison of 5-% damped PSRV spectral predictions for the Furnace Creek fault strike-slip scenario earthquake (Mw = 7.04) for the Yucca Mountain site at a range of 52 km for the equivalent explosion model (left), modified Geomatrix/ATC model (center), and Little Skull Mountain earthquake spectral shape scaled with NTS attenuation and Geomatrix/ATC magnitude dependence (right). For reference the model results are compared to similar spectral predictions based on the standard Geomatrix/ATC empirical model.

Figure 8.8 Comparison of 5-% damped acceleration response spectral predictions for the three explosion-based empirical models with the median of the spectral predictions determined from four physical models for the Solitario Canyon fault scenario earthquake (left), the Rock Valley fault scenario earthquake (center), and the Furnace Creek fault scenario earthquake (right).

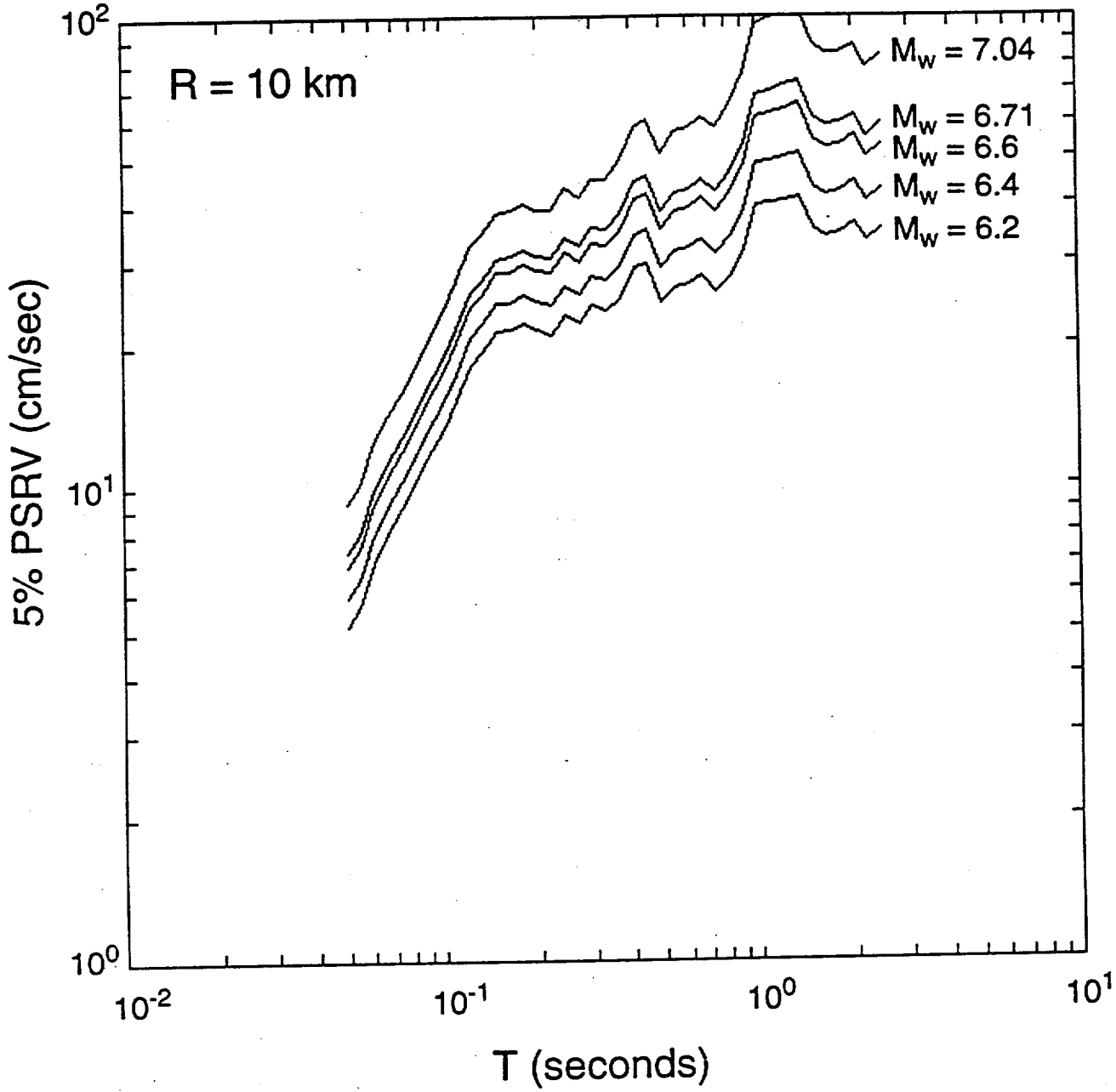
R = 10 km
M_w = 7.04
M_w = 6.71
M_w = 6.6
M_w = 6.4
M_w = 6.2
5% PSRV (cm/sec)
10^2
10^1
10^0
10^{-2}
10^{-1}
10^0
10^1
T (seconds)

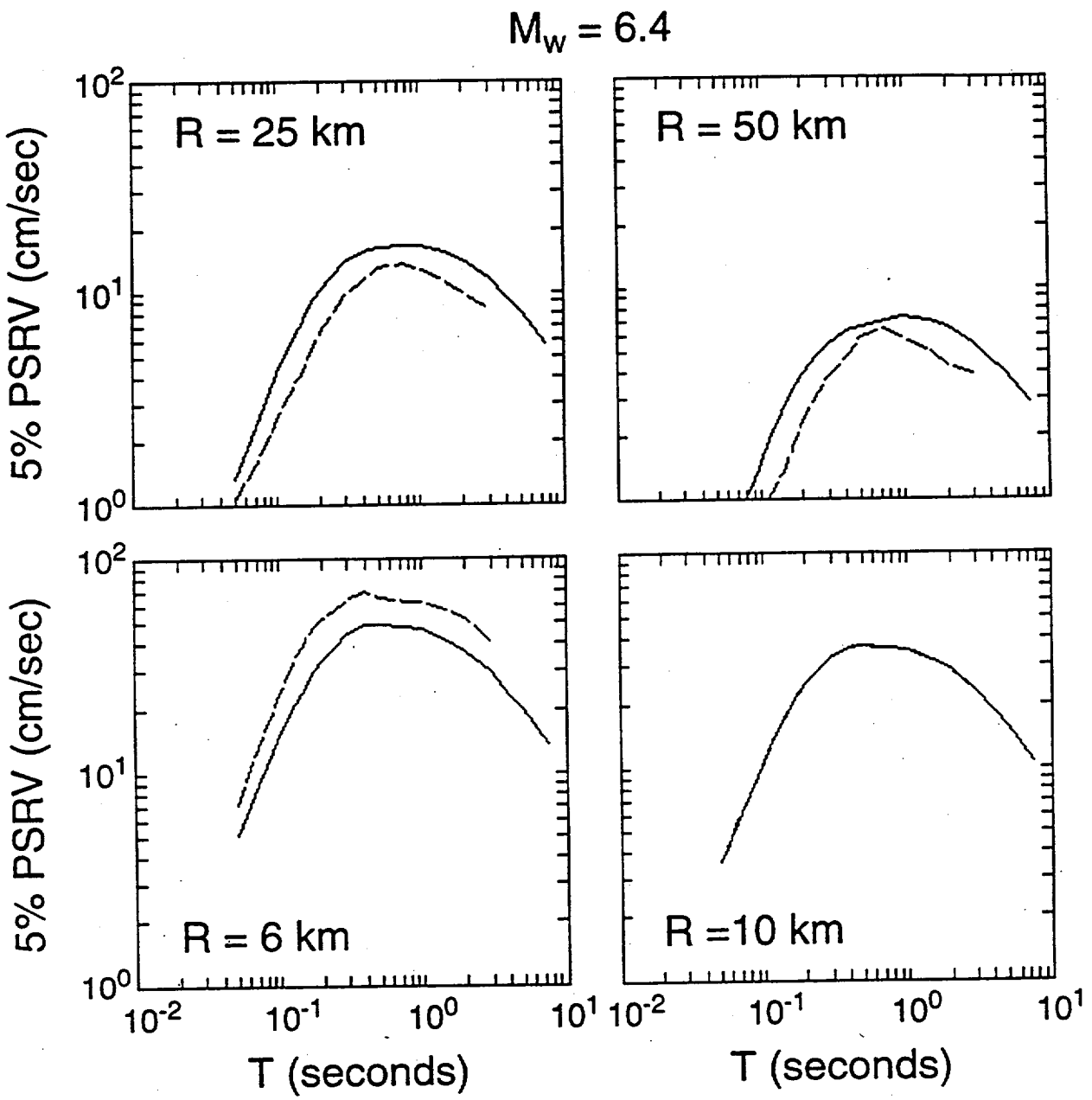
$M_w = 6.4$
R = 25 km
R = 50 km
R = 6 km
R =10 km
5% PSRV (cm/sec)
5% PSRV (cm/sec)
10^2
10^1
10^0
10^{-2}
10^{-1}
10^0
10^1
T (seconds)
T (seconds)

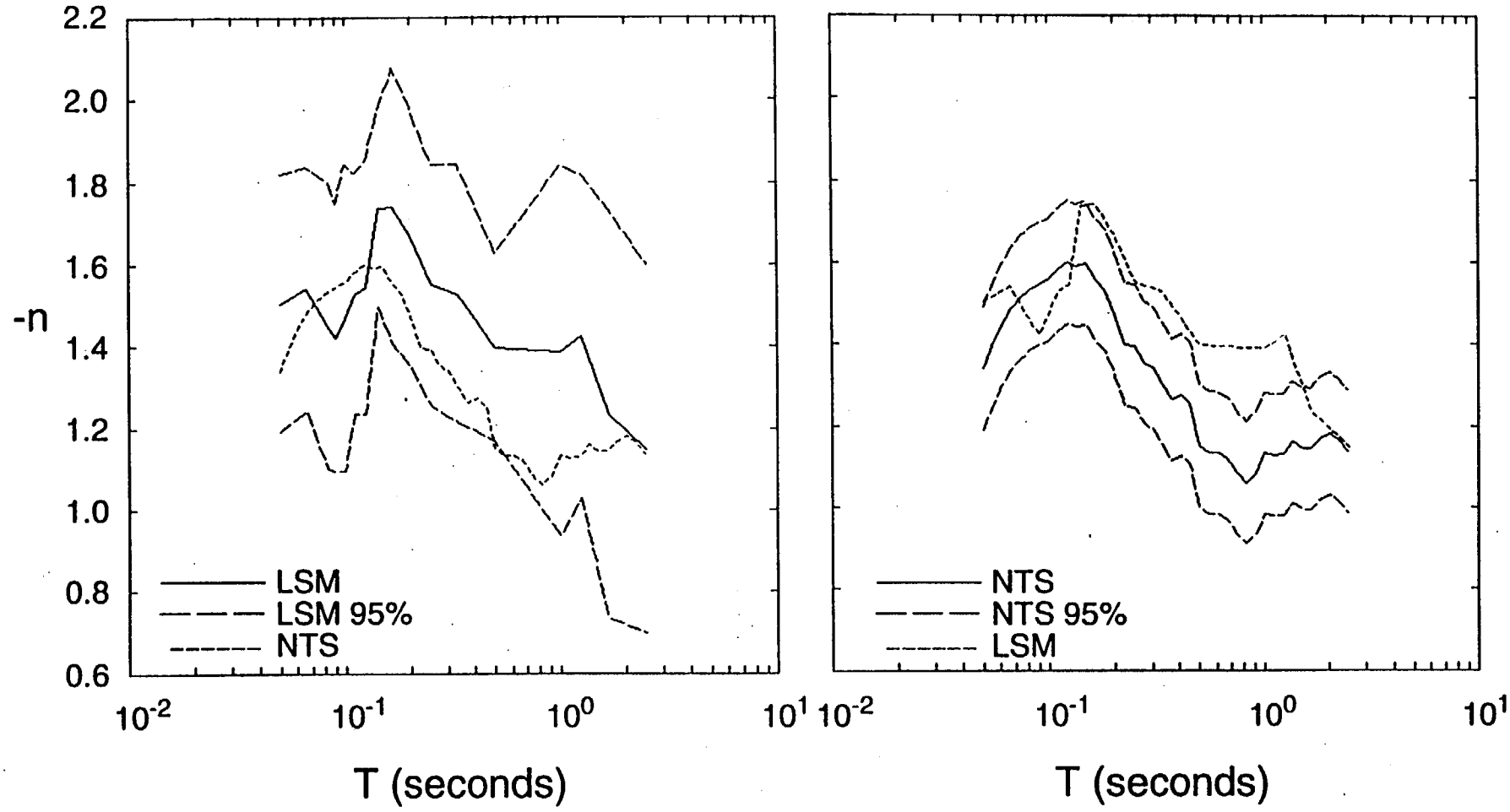
2.2
2.0
1.8
1.6
1.4
1.2
1.0
0.8
0.6
-n
LSM
LSM 95%
NTS
10^{-2}
10^{-1}
10^{0}
10^{1}
T (seconds)
NTS
NTS 95%
LSM
10^{-2}
10^{-1}
10^{0}
10^{1}
T (seconds)

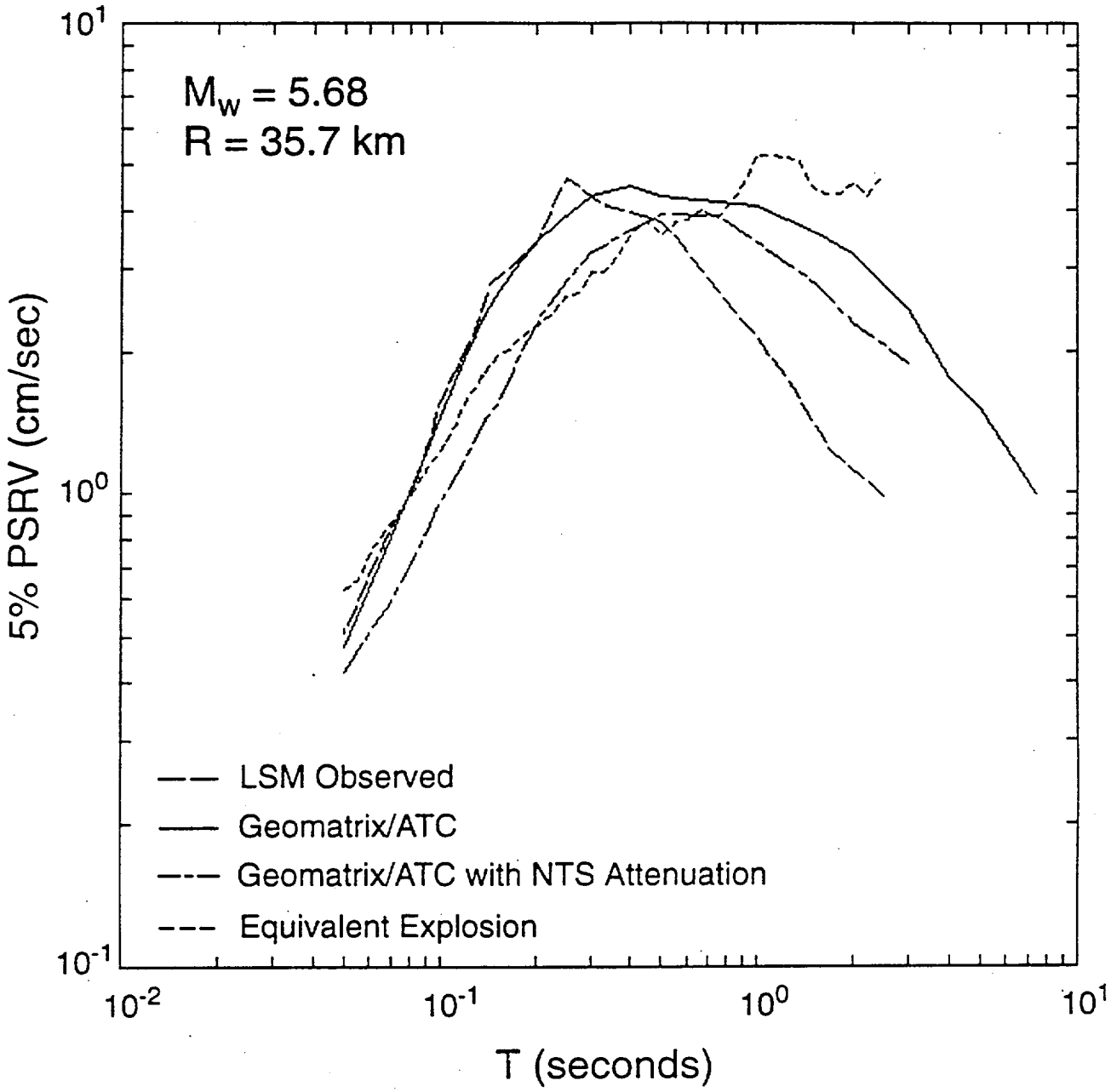
M_W = 5.68
R = 35.7 km
5% PSRV (cm/sec)
T (seconds)
LSM Observed
Geomatrix/ATC
Geomatrix/ATC with NTS Attenuation
Equivalent Explosion
10^1
10^0
10^{-1}
10^{-2}
10^{-1}
10^0
10^1

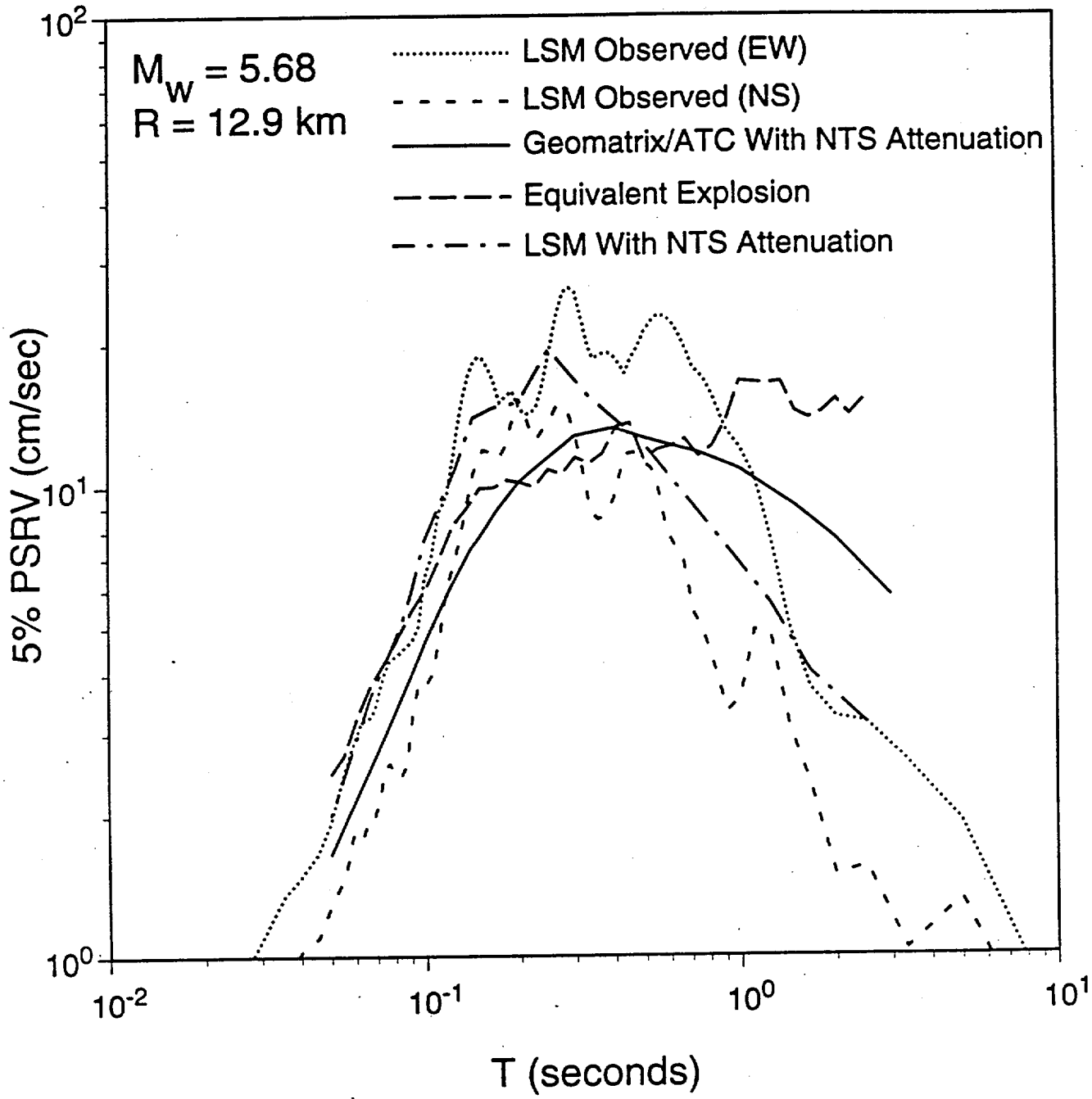
M_W = 5.68
R = 12.9 km
LSM Observed (EW)
LSM Observed (NS)
Geomatrix/ATC With NTS Attenuation
Equivalent Explosion
LSM With NTS Attenuation
5% PSRV (cm/sec)
10^2
10^1
10^0
10^{-2}
10^{-1}
10^0
10^1
T (seconds)

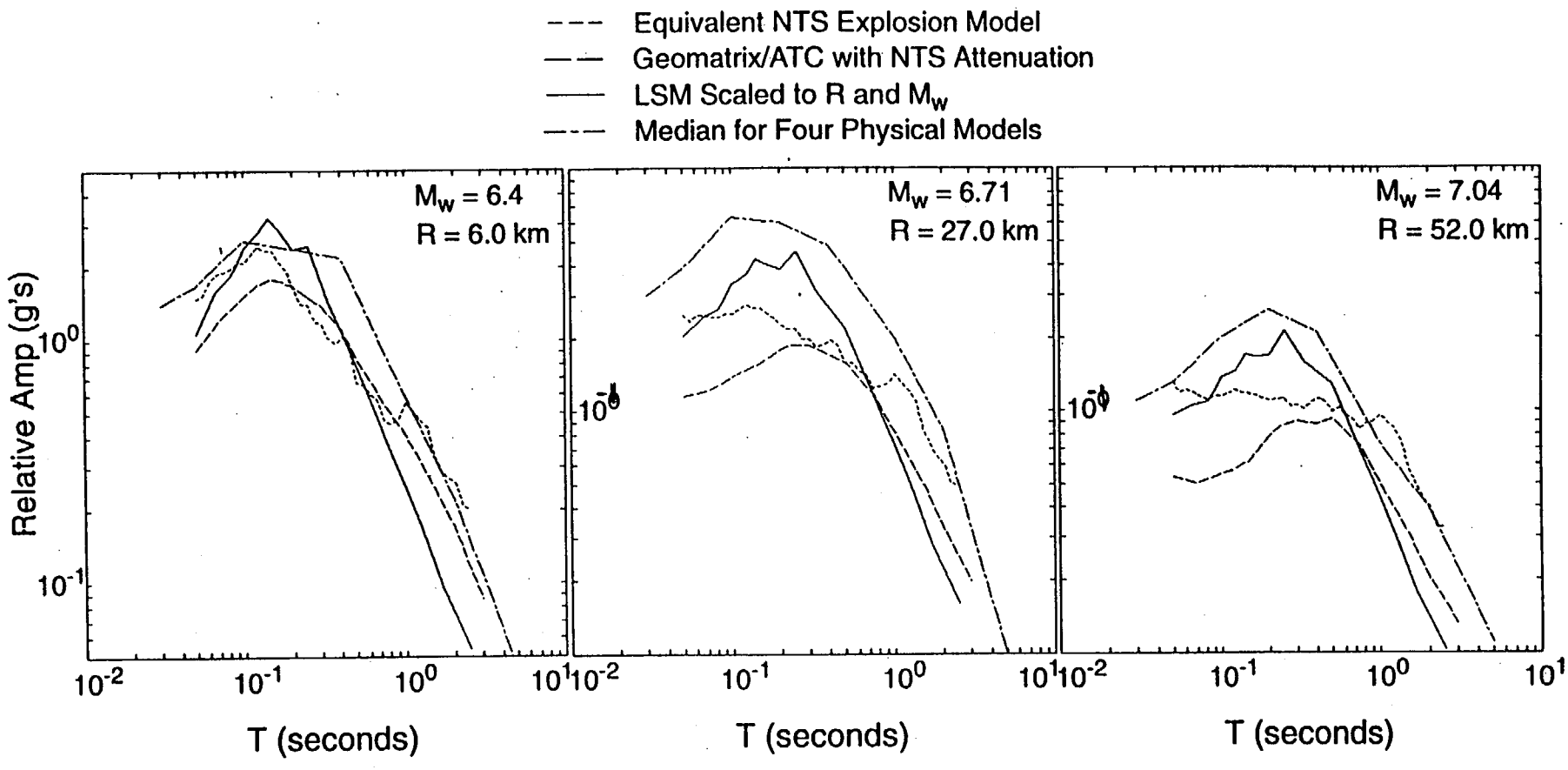
Equivalent NTS Explosion Model
Geomatrix/ATC with NTS Attenuation
LSM Scaled to R and M_w
Median for Four Physical Models
M_w = 6.4
R = 6.0 km
M_w = 6.71
R = 27.0 km
M_w = 7.04
R = 52.0 km
Relative Amp (g's)
10^0
10^{-1}
10^{-2}
10^1
T (seconds)

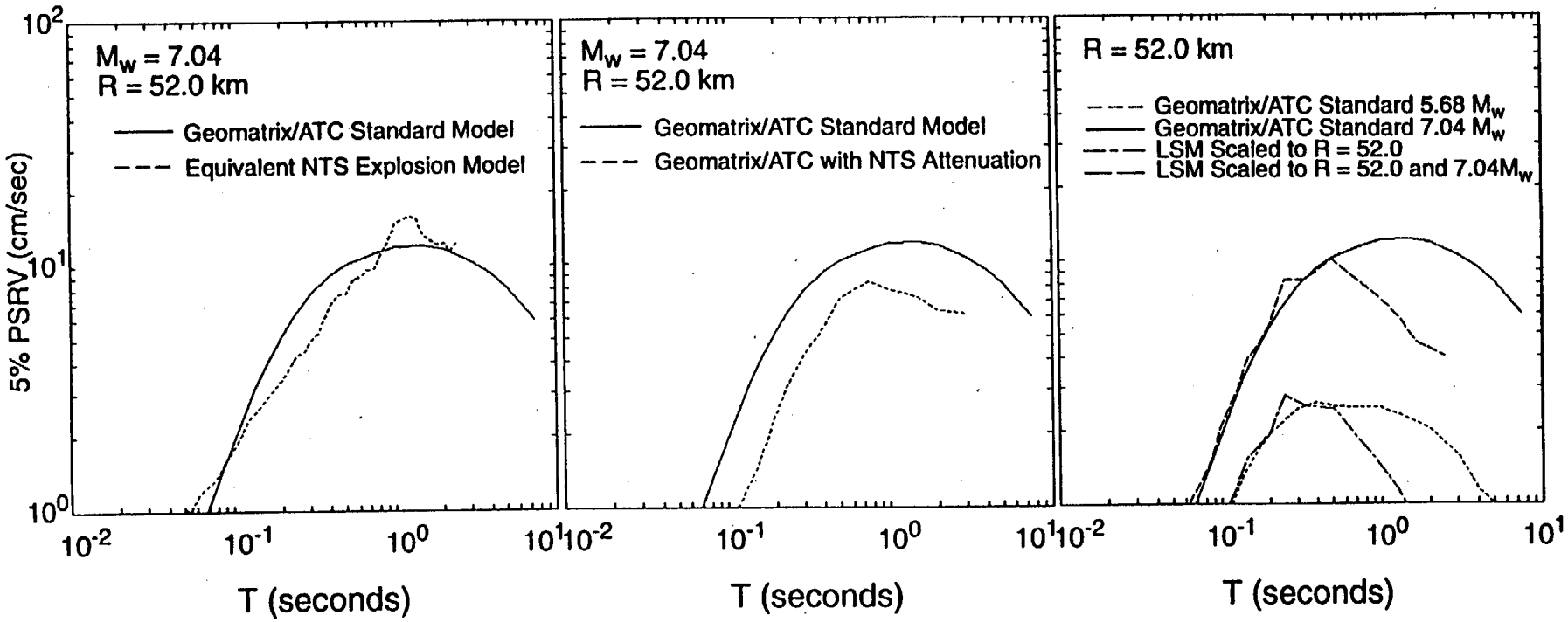
M_w = 7.04
R = 52.0 km
Geomatrix/ATC Standard Model
Equivalent NTS Explosion Model
M_w = 7.04
R = 52.0 km
Geomatrix/ATC Standard Model
Geomatrix/ATC with NTS Attenuation
R = 52.0 km
Geomatrix/ATC Standard 5.68 M_w
Geomatrix/ATC Standard 7.04 M_w
LSM Scaled to R = 52.0
LSM Scaled to R = 52.0 and 7.04M_w
5% PSRV (cm/sec)
10^2
10^1
10^0
10^{-2}
10^{-1}
10^0
10^1
T (seconds)

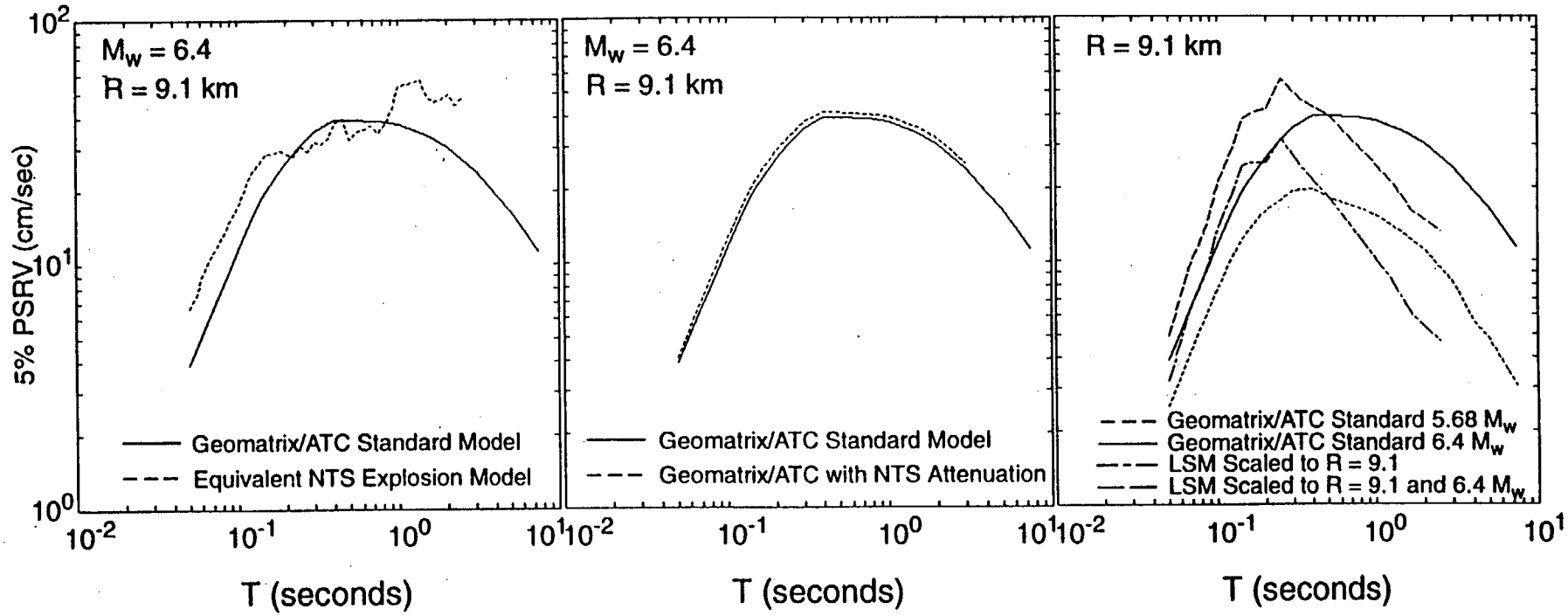
$M_W = 6.4$
R = 9.1 km
Geomatrix/ATC Standard Model
Equivalent NTS Explosion Model
$M_W = 6.4$
R = 9.1 km
Geomatrix/ATC Standard Model
Geomatrix/ATC with NTS Attenuation
R = 9.1 km
Geomatrix/ATC Standard 5.68 M_W
Geomatrix/ATC Standard 6.4 M_W
LSM Scaled to R = 9.1
LSM Scaled to R = 9.1 and 6.4 M_W
5% PSRV (cm/sec)
10^2
10^1
10^0
10^{-2}
10^{-1}
10^0
10^1
T (seconds)

5.3 Excerts from Prediction of ground motion characteristics of underground nuclear explosions

NVO-1163-239

NVO-1163-239
UC-11

PREDICTION OF GROUND MOTION CHARACTERISTICS OF UNDERGROUND NUCLEAR DETONATIONS

ENVIRONMENTAL RESEARCH CORPORATION
2769 South Highland Drive
Las Vegas, Nevada 89109

March 1974

PREPARED FOR THE U. S. ATOMIC ENERGY COMMISSION
NEVADA OPERATIONS OFFICE
UNDER CONTRACT NO. AT(29-2)-1163

5.3-2

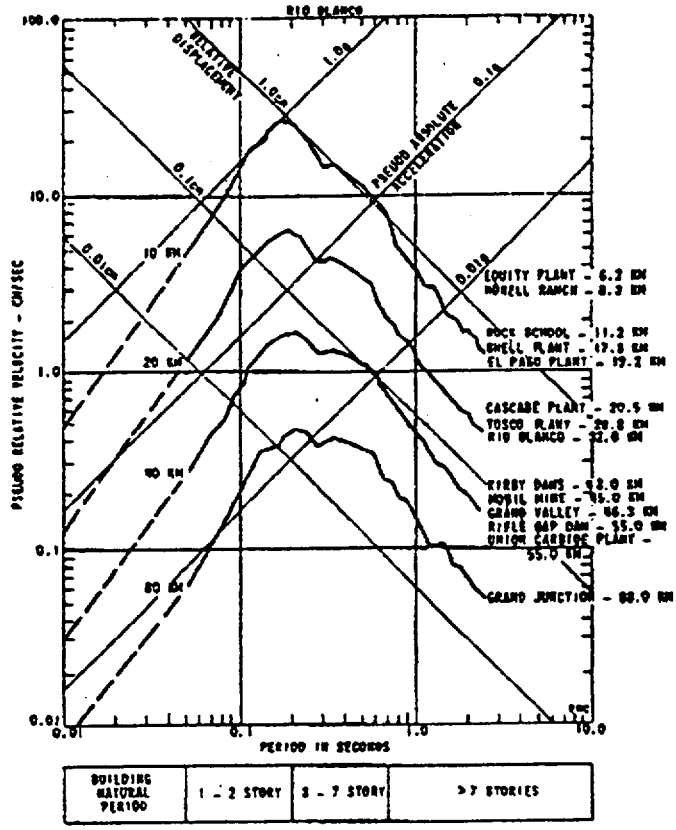

Figure 2.18. Example of Family of Predicted Mean 5% Damped PSRV Spectra, Rio Blanco Event

2.13 PREDICTION EQUATIONS

The functional relationship between mean ground motion, $\hat{M}$ (peak amplitude or spectral value at a single period) and the independent variables yield, W, and distance, R, is a power law of the form

$$\hat{M}(W, R) = AW^{B_1} R^{B_2}$$

This general equation describes the trend of the ground motion parameter with individual observations distributed in a random manner about the mean value. The distribution about the geometric mean is approximately log-normal and is characterized by the geometric standard error of estimate, σ. The amplitude coefficient, A, and the yield (B_1) and distance (B_2) scaling exponents are derived by standard statistical analyses of ground motion data.

2.13.1.3 Equation Group 3: Regression Equations for Peak Vector Motions, Pahute Mesa (Whipple and O'Brien, 1970a)

Event Area and Type of Motion	Equations: $\hat{M} = AW^{B_1} R^{B_2}$	Number of Data Points	Standard Error of Estimate
PAHUTE MESA: Acceleration: (g)	$a = 2.49 \times 10^{-1} W^{0.464} R^{-1.34}$	401	2.30
PAHUTE MESA: Velocity: (cm/sec)	$u = 6.64 \times 10^{0} W^{0.622} R^{-1.34}$	221	1.95
PAHUTE MESA: Displacement: (cm)	$d = 4.41 \times 10^{-1} W^{0.775} R^{-1.17}$	380	2.12

2.13.1.4 Equation Group 4: Average Ratio of Peak Horizontal to Resultant Vector Accelerations, Pahute Mesa Detonations

STATION	RATIO	STATION	RATIO
Mercury (Q25)	0.8	Las Vegas (SE-6)	0.7
Tonopah Church	0.6	Las Vegas (SQP)	0.9
Tonopah Motel	0.9	E-MAD	0.8
Beatty Hardrock	0.8	NRDS-1	0.8
Beatty Alluvium	0.9	Alamo Alluvium	0.8

These are applied by multiplying the appropriate equations in Groups 1, 2, 3 or 5

2.13.1.6 Equation Group 6: Regression Equations to Predict 5% Damped PSRV Spectra, Pahute Mesa Detonations (From Lynch, 1969)

Period	Amplitude Coefficient A	Yield Exponent B_1	Distance Exponent B_2	Standard Error of Estimate σ
.050	2.69E+00	.491	-1.340	3.06
.055	3.69E+00	.479	-1.395	2.87
.061	5.00E+00	.483	-1.447	2.85
.067	6.76E+00	.474	-1.486	2.84
.075	8.87E+00	.463	-1.515	2.88
.082	1.08E+01	.457	-1.533	2.85
.091	1.18E+01	.468	-1.546	2.98
.101	1.29E+01	.475	-1.558	2.96
.111	1.53E+01	.480	-1.582	2.97
.123	1.89E+01	.480	-1.600	2.98
.136	2.18E+01	.468	-1.591	3.02
.150	2.48E+01	.466	-1.597	2.98
.166	2.06E+01	.478	-1.555	2.87
.183	2.01E+01	.479	-1.533	2.84
.203	1.67E+01	.480	-1.469	2.82
.224	1.21E+01	.498	-1.399	2.82
.248	1.21E+01	.509	-1.395	2.72
.274	1.10E+01	.504	-1.354	2.65
.302	1.13E+01	.508	-1.342	2.62
.334	8.65E+00	.528	-1.303	2.66
.369	6.82E+00	.555	-1.263	2.62
.408	7.15E+00	.572	-1.276	2.62
.451	6.40E+00	.583	-1.255	2.49
.499	3.63E+00	.601	-1.150	2.54
.551	2.96E+00	.632	-1.134	2.54
.609	2.93E+00	.636	-1.134	2.59
.673	2.76E+00	.645	-1.121	2.55
.744	2.02E+00	.665	-1.085	2.54
.822	1.59E+00	.698	-1.060	2.52
.908	1.72E+00	.713	-1.083	2.54
1.004	2.08E+00	.732	-1.133	2.62
1.110	1.83E+00	.748	-1.128	2.69
1.226	1.56E+00	.771	-1.129	2.75
1.355	1.66E+00	.775	-1.160	2.74
1.498	1.61E+00	.753	-1.145	2.74
1.655	1.59E+00	.749	-1.143	2.78
1.829	1.96E+00	.732	-1.168	2.76
2.022	2.35E+00	.719	-1.181	2.72
2.234	2.37E+00	.701	-1.165	2.72
2.469	2.40E+00	.699	-1.137	2.72

Sample: 260 PSRV spectra from 11 Pahute Mesa detonations; yield range 20 to 1200 kt; distance range 4.4 to 551 km. Mean yield ~200 kt; mean distance ~100 km.

Section 6

Hybrid Empirical Model

DOCUMENTATION OF EXCEL 5.0 SPREADSHEETS FOR DEVELOPING HYBRID EMPIRICAL GROUND-MOTION ESTIMATES

Kenneth W. Campbell

EQE International, Inc.
Evergreen, Colorado

INTRODUCTION

I have developed several EXCEL 5.0 spreadsheets for calculating the various distance measures and empirical ground-motion estimates for application of the Hybrid Empirical Ground Motion Model, hereafter referred to as the Hybrid Model. These spreadsheets allow the user to add distances and ground-motion parameters for which the estimates are to be made as well as change the weights assigned to the various relationships and adjustment factors. A brief description of the spreadsheets are given below.

DESCRIPTION OF SPREADSHEETS

1. DIST_SH.XLS and DIST_DP.XLS

These spreadsheets calculate the three fault-distance measures required to estimate empirical ground motions using contemporary empirical strong-motion attenuation relationships for both shallow-focus (DIST_SH.XLS) and deep-focus (DIST_DP.XLS) earthquakes. Each spreadsheet contains three worksheets for fault dips of 90, 60, and 30 degrees. Distances for other fault dips can be calculated by simply changing the value of the fault dip on any of the worksheets or by copying an existing worksheet to a new worksheet and changing the fault dip to the desired value. Significant parameters in these spreadsheets are defined below. Only those parameters that are required to use the spreadsheets are described. All depths, widths, and distances have units of kilometers.

alpha. The dip of the fault plane measured from a horizontal plane in degrees. The dips of 90 and 60 degrees were specified by the methodology team. The dip of 30 degrees is included because there is a possibility that faults with this dip will be considered sometime in the future.

d. Depth to the center of the fault-rupture plane. This parameter is only used for shallow-focus earthquakes for which this depth is held constant for all rupture scenarios. This depth (5 km) was specified by the methodology team.

dmax. Maximum depth of fault rupture. This depth (14 km) was specified by the methodology team. For deep-focus earthquakes, the fault rupture was constrained to propagate to this depth for all earthquake scenarios, as specified by the methodology team.

dseis. Depth to the top of the seismogenic portion of the fault. The seismogenic zone of rupture is not allowed to propagate to depths shallower than this value. This

depth should be selected by the user. The value of 3 km is the minimum value recommended by Campbell (1997).

Magnitude. Moment magnitude, Mw. The values of Mw were provided by the methodology team.

Fault Width. The median estimate of the fault rupture width for the given value of moment magnitude (Mw). This width is calculated using a relationship between rupture width and magnitude developed by Wells and Coppersmith (1994), as specified by the methodology team.

Horizontal Distance. The horizontal distance from the site to the surface trace of the fault. The values of these distances were provided by the methodology team.

Rjb. The shortest distance from the site to the projection of the fault rupture plane on the surface of the earth. This is the distance measure proposed by Joyner and Boore. See Abrahamson and Shedlock (1997) for a brief description of this distance measure.

Rrup. The shortest distance from the site to the fault rupture plane. See Abrahamson and Shedlock (1997) for a brief description of this distance measure.

Rseis. The shortest distance from the site to the seismogenic part of the fault rupture plane. This is the distance measure proposed by Campbell. See Abrahamson and Shedlock (1997) for a brief description of this distance measure.

2. HYBRD_SH.XLS and HYBRD_DP.XLS

These spreadsheets calculate hybrid empirical ground-motion parameters for both shallow-focus (HYBRD_SH.XLS) and deep-focus (HYBRD_DP.XLS) earthquakes using contemporary empirical strong-motion attenuation relationships for California (except for Spudich et al., 1997) and adjustment factors for applying the California ground-motion estimates to Yucca Mountain. The adjustment factors were calculated using the band-limited white noise (BLWN) point-source stochastic simulation model with PSA, PGA, and PGV estimated from random vibration theory (RVT). A single estimate of these parameters were developed for California for each magnitude and distance of interest using model parameters developed by Walt Silva (personal communication), which he developed by calibrating these parameters to give ground-motion estimates consistent with the empirical attenuation relationship developed by Abrahamson and Silva (1997). Multiple estimates were developed for Yucca Mountain taking into account uncertainty in the median estimates of crustal attenuation (both Q_0 and (), site amplification (characterized by shear-wave velocity and density as a function of depth), and site attenuation (($_0$).

Each spreadsheet contains five worksheets. The first three worksheets give empirical estimates of ground motion for the specified ground-motion parameters, magnitudes, and horizontal distances for fault dips of 90 and 60 degrees, the latter for both the hanging wall and the foot wall of the fault plane (not the rupture plane). The fourth worksheet (Factors) gives the calculated adjustment factors and their standard deviations for the same set of ground-motion parameters, magnitudes, and distances. The fifth worksheet (Hybrid

Estimates) gives an example of the calculation of ground motions using the Hybrid Model for a single ground-motion parameter (5%-damped pseudo-absolute acceleration at 0.5 Hz) and a single value of moment magnitude (M_W = 5.0). The user can add additional ground-motion parameters, magnitudes, and distances by extending the table with the existing entries and changing the references in the cells to the appropriate cells in the other worksheets.

Significant parameters in these spreadsheets are defined below. Only those parameters that are required to use the spreadsheets are described. Parameters common to more than one worksheet are defined only once.

Empirical Estimates Worksheets (Dip=90; Dip=60, Hanging Wall; Dip=60, Foot Wall)

Attenuation Relationships. Identification of the attenuation relationships used to develop the empirical ground-motion estimates. The user can add additional relationships if desired.

Dip. The dip of the fault plane measured from a horizontal plane in degrees.

Style of Faulting (F). The style of faulting parameter F used in the attenuation relationships. The default value of 0 corresponds to strike-slip faulting. Most relationships do not include many normal-faulting earthquakes, but the authors generally recommend that F = 0 be used for normal-faulting earthquakes. This parameter should be selected by the user based on his or her opinion as to what value is appropriate for Yucca Mountain faults.

Depth to Hard Rock (D). The depth to basement (hard) rock defined by Campbell. This parameter was selected as the depth to the Yucca Mountain stratum with an S-wave velocity (V_S) of 2.9 km/sec and a P-wave velocity (V_P) of 5.0 km/sec, generally consistent with the recommendations provided by Campbell (1997), minus the depth to the stratum at which the ground-motion estimates are calculated (i.e., the stratum with V_S = 1.9 km/sec and V_P = 3.2 km/sec). This parameter is site-dependent and can be adjusted by the user as appropriate.

Mw. Moment magnitude.

Rhor. Horizontal distance to the surface trace of the fault plane. The values of these distances were specified by the methodology team.

Rjb, Rrup, Rseis. The fault-distance measures defined above. The values are those calculated in the DIST_SH.XLS and DIST_DP.XLS spreadsheets for the specified values of *Mw* and *Rhor.*

PSA. The random horizontal component of 5%-damped pseudo-absolute acceleration in g for oscillator frequencies of 0.5, 1.0, 2.0, 5.0, 10.0, and 20 Hz.

PGA. The random horizontal component of peak ground acceleration in g.

PGV. The random horizontal component of peak ground velocity in cm/sec.

Median Ground Motion Estimates. The median estimates of PSA, PGA, and PGV from the selected attenuation relationships. Only Campbell (1997) and Joyner and Boore (1988) developed attenuation relationships for PGV. Other estimates were developed by applying the median ratio of PGV to PGA from these two relationships to the median estimates of PGA from the other relationships.

Standard Errors. The standard errors (i.e., aleatory uncertainty) associated with the empirical estimates of PSA, PGA, and PGV, increased to represent the random horizontal component, if necessary, using the horizontal inter-component standard deviation calculated by Boore et al. (1997).

Subjective Weights. The weights assigned to each of the attenuation relationships. These weights must add up to 1, but can be 0 for those attenuation relationships which are not used. Equal weights were assumed for demonstration purposes only. The user should select these weights according to his or her belief that the relationship is appropriate for the specific magnitude and distance for which the estimate is being developed. Changing the weights will automatically adjust the weighted estimates in the spreadsheet.

Weighted Median. There are two sets of weighted medians, each weighted by the subjective weights assigned to the attenuation relationships: (1) the weighted median of the median ground-motion estimates, with weights applied to the logarithm of the ground-motion parameters assuming a lognormal distribution of the medians; and (2) the weighted median of the standard errors, with weights applied to the standard errors assuming a normal distribution of the standard errors.

Weighted (. There are two sets of weighted (s, each weighted by the subjective weights assigned to the attenuation relationships: (1) the weighted standard deviation of the median ground-motion estimates (i.e., epistemic modeling uncertainty), and (2) the weighted standard deviation of the standard errors. The weights are applied to the square of the standard deviations (i.e., to the variances), which is consistent with the definition of the weighted standard error in weighted regression analyses.

Adjustment Factors Worksheet (Factors)

((. Stress drop in bars. Calculations were done for a suite of stress drops so that the user can select which stress drop to use in developing the adjustment factors.

Adjustment Factors. The multiplicative adjustment factors for estimating ground-motion parameters for Yucca Mountain from those parameters estimated for California. These factors were developed using the BLWN-RVT stochastic simulation model-as described above. The median represents the median of the factors calculated from the proposed Yucca Mountain models. The (represents the standard deviation of the factors calculated from the distribution of the proposed Yucca Mountain model parameters (i.e., epistemic parametric uncertainty), assuming no uncertainty in the California model parameters. This latter assumption should be evaluated by the user. The reasons for not including any uncertainty in the California model estimates are: (1) the model parameters were

constrained by calibrating the model to the Abrahamson and Silva (1997) attenuation relationship, so modeling uncertainty that would result from calibrating these parameters to other attenuation relationships is already accounted for in the modeling uncertainty of the empirical estimates from these attenuation relationships (note that there may be a bias between the ground-motion estimates from this attenuation relationship and the weighted median of all of the attenuation relationships which has not been included); (2) the set of California parameters cannot be replaced with independent assessments of these parameters because of inter-parameter correlation, and (3) the same model is applied in both California and the Yucca Mountain regions, so presumably uncertainty in the appropriateness of the stochastic simulation model does not contribute significantly to the modeling uncertainty in the calculated adjustment factors.

Subjective Weights. The weights assigned to each of the stress drops. These weights must add up to 1, but can be 0 for those stress drops which are not used. The given weighting scheme is for demonstration purposes only. The user should select these weights according to his or her belief that the stress drop is appropriate for earthquakes in the Yucca Mountain region. Note that the stress drop used for California earthquakes in the development of the adjustment factors was 59 bars, so appropriate median stress drops for earthquakes in the Yucca Mountain region should be selected relative to this value (i.e., whether the median stress drop is higher or lower than the median stress drop for California earthquakes). Changing the weights will automatically adjust the weighted estimates in the spreadsheet.

Weighted Median. There are two sets of weighted medians, each weighted by the subjective weights assigned to the stress drops: (1) the weighted median of the median adjustment factors, with weights applied to the logarithm of the ground-motion parameters assuming a lognormal distribution of the medians; and (2) the weighted median of the standard deviation of the adjustment factors, with weights applied to the standard deviations assuming a normal distribution of the standard deviations.

Weighted (. There are two sets of weighted (s, each weighted by the subjective weights assigned to the stress drops: (1) the weighted standard deviation of the median adjustment factors (i.e., epistemic parametric uncertainty), and (2) the weighted standard deviation of the standard deviations of the adjustment factors. The weights are applied to the square of the standard deviations (i.e., to the variances), which is consistent with the definition of the weighted standard error in weighted regression analyses. If the user believes that epistemic modeling uncertainty should be included in the California BLWN-RVT estimates, this uncertainty should be included in the estimate of the standard deviation of the median adjustment factors.

<u>Example Hybrid Estimates Worksheet (Hybrid Estimates)</u>

Median. The weighted median empirical ground-motion estimate times the weighted median adjustment factor for the given ground-motion parameter, magnitude, and horizontal distance. Estimates for only one ground-motion parameter and magnitude are given as an example. The user should extend this table to include all other ground-motion parameters, magnitudes, and horizontal distances of interest.

(. The standard deviations of the empirical ground-motion estimates (aleatory uncertainty), of the hybrid empirical estimates (epistemic uncertainty), and of the aleatory and epistemic standard deviations (() for the given ground-motion parameter, magnitude, and horizontal distance. All of the standard deviations are given in terms of the natural logarithm (log base e). The epistemic uncertainty includes modeling uncertainty in the median estimates of the empirical ground motions from the attenuation relationships, parametric uncertainty in the median stress drop for the Yucca Mountain region, and parametric uncertainty in the median adjustment factors for a given stress drop. The standard deviation of (includes the standard deviations of the weighted standard deviations of the empirical ground-motion estimates from the attenuation relationships and of the adjustment factors.